

Intravital imaging reveals neutrophils interact with cancer cells to form neutrophil extracellular traps *in vivo*

Juwon Park^{1,2}, Robert W Wysocki^{1,3}, Miriam R Fein^{1,3}, Mikala Egeblad¹

¹Cold Spring Harbor Laboratory, Cold Spring Harbor, NY 11724, USA. ²Tropical Medicine, Medical Microbiology and Pharmacology, John A. Burns School of Medicine, University of Hawaii at Manoa, HI 96823, USA. ³Graduate Program in Genetics, Stony Brook University, Stony Brook, NY 11794, USA.

Intravital microscopy (IVM) serves as an imaging tool to study physiological and pathological process at the cellular resolution. Studies on metastasis heavily rely on the traditional end-point measurement, but this information cannot address the dynamic aspect of the metastatic process. IVM with transgenic mouse lines expressing fluorescent proteins (FPs) provides insight as to how cancer cells interact with their surrounding environments, including fibroblasts, endothelial cells, and immune cells. This study aims to investigate the role of neutrophils in breast cancer metastasis, particularly within the lung, one of the metastatic sites for the breast cancer. A custom-made bass thoracic window was placed to the lung from 4T1-mCherry-injected lysozyme 2 (LysM)-EGFP mice to visualize neutrophils. Given that neutrophils form neutrophil extracellular traps (NETs), NET forming cells were visualized by labeling with DAPI and neutrophil elastase dye to detect and quantify NETs in the lung when cancer cells seed. We found that metastatic cancer cells stimulate neutrophils to form NETs in *in vivo* even in the absence of infection. Furthermore, blockage of NETs with DNase-I coated nanoparticles markedly reduced lung metastasis in metastatic 4T1 mouse model. This study provided *in vivo* evidence that cancer cells hijack neutrophils' defense mechanism to promote metastasis in the lung.

Light-driven biomass reforming and hydrogen production

Jungki Ryu^{1,2,3*}

¹School of Energy and Chemical Engineering, ²Graduate School of Carbon Neutrality, and ³Emergent Hydrogen Technology R&D Center, Ulsan National Institute of Science and Technology (UNIST), Ulsan 44919, Republic of Korea. *Email:

jryu@unist.ac.kr

Artificial photosynthesis is a promising technology for the efficient use of unlimited but intermittent solar energy. In principle, various chemicals can be produced in a sustainable manner through a series of photoelectrochemical reactions using water as a cheap and clean source of electrons. However, oxidation of water is a challenging task and acts as a bottleneck for the practical application of artificial photosynthesis technologies due to its slow kinetics and energy-intensive nature. In this presentation, we report novel photo(electro)catalytic systems for the efficient solar hydrogen production with simultaneous production of value-added chemicals via reforming of biomass. We found that certain catalytic electron mediators can depolymerize biomass to readily extract electrons and protons while selectively producing value-added chemicals via depolymerization. By utilizing electron mediators and biomass for anodic reactions for photo(electro)catalytic systems, we can produce hydrogen and valuable chemicals simultaneously under simulated sunlight irradiation. This approach allows efficient (photo)electrochemical production of hydrogen and brings additional economic benefits from byproducts.

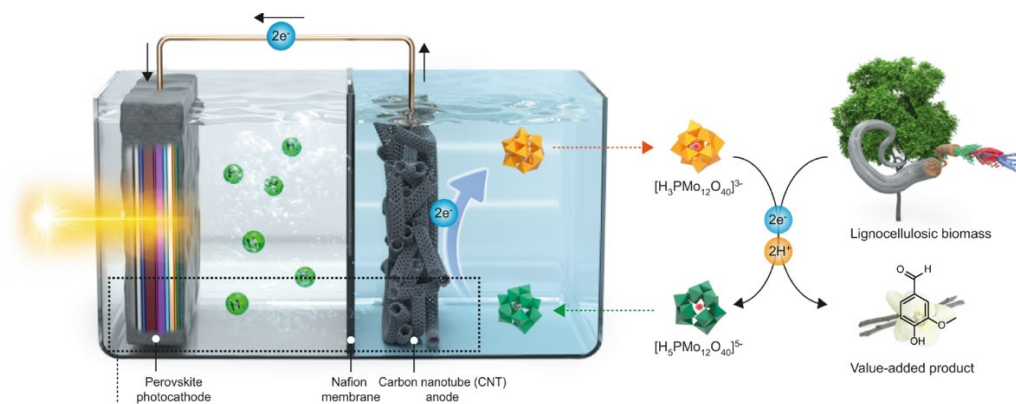


Fig. 1: Schematic illustration of biomass depolymerization combined with (photo)electrochemical hydrogen production.

References

- [1] H. Oh et al., Phosphomolybdic acid as a catalyst for oxidative valorization of biomass and its application as an alternative electron source. *ACS Catal.* **2020**, *10*, 2060-2068.
- [2] Y. Choi et al., Bias-free solar hydrogen production at 19.8 mA cm^{-2} using perovskite photocathode and lignocellulosic biomass. *Nat. Commun.* **2022**, *13*, 5709.
- [3] S.-J. Yim et al., Modular flow reactors for valorization of kraft lignin and low-voltage hydrogen production. *Adv. Sci.* **2022**, *9*, 2204170.

Biography

Jungki Ryu is an Associate Professor at the Ulsan National Institute of Science and Technology (UNIST), South Korea. He received his B.S. and Ph.D. in Materials Science and Engineering from Yonsei University in 2006 and from the Korea Advanced Institute of Science and Technology (KAIST) in 2011. After postdoc research at the Massachusetts Institute of Technology, he joined the UNIST School of Energy and Chemical Engineering in 2014. His research interests include electrocatalysis for energy conversion, solar fuel production, biomass utilization, and electrochemical waste refinery.

Transdermal Photomedicine Using Various Upconverting Nanomaterials

Ki Su Kim

*School of Chemical Engineering, College of Engineering, Pusan National University
2 Busandaehak-ro 63beon-gil, Geumjeong-gu, Busan, 46241, Republic of Korea
kisukim@pusan.ac.kr*

A variety of drug delivery systems have been investigated for high therapeutic efficacy via easy administration. Among them, transdermal delivery is presented as an attractive alternative to needle-based drug delivery because of patient preferences. Although transdermal microneedles are less invasive promising alternatives, needle - free topical delivery without involving physical damage to the natural skin barrier is still sought after as it can further reduce needle - induced anxiety and is simple to administer. However, this long-standing goal has been elusive since the intact skin is impermeable to most macromolecules. Here, we show an efficient, noninvasive transdermal delivery using Hyaluronic acid (HA) derivatives as carrier. In addition, we present the recent results of non-invasive transdermal photomedicine using various organic/inorganic upconverting nanomaterials with HA. As the upconversion nanoparticle (UCNP) can be served as small sized visible-light source, we successfully demonstrated the facilitated photomedicine application including photochemical tissue bonding and antibacterial therapy. These platform technologies might be successfully applied for the development of various futuristic nanomedicines.

Plasmonic sensing with quantum light

Changhyoup Lee

*Korea Research Institute of Standards and Science
E-mail address: changhyoup.lee@kriss.re.kr*

Plasmonic platforms are well known to offer great advantages in sensing with extraordinary sensitivity, but started to reach their fundamental limit, called the shot noise limit, which originated from the Poisson photon number distribution of an illuminating laser. Recently, many theoretical and experimental studies have suggested to use quantum light in a way that reduces the noise further below the shot noise limit in plasmonic sensing, consequently beating the the fundamental classical limit. In this talk, we introduce quantum plasmonic sensing using quantum light and discuss how the sensitivity with sub-shot noise limit is obtained. For this purpose, we review recent works that have focused on integrating quantum sensing techniques with conventional plasmonic sensors, opening up a new route for improving the performance of plasmonic sensors.

[1] Changhyoup Lee, Benjamin Lawrie, Raphael Pooser, Kwang-Geol Lee, Carsten Rockstuhl, and Mark Tame, Chem. Rev. **121**, 8, 4743–4804 (2021)

SERS Nanosensor for Monitoring Plant Health

Dae Hong Jeong

Seoul National University

jeongdh@snu.ac.kr

When under stress, plants release molecules to activate their defense system [1,2]. Detecting these stress-related molecules offers the possibility to address stress conditions and prevent the development of diseases. However, detecting endogenous signaling molecules in living plants remains challenging due to low concentrations of these analytes and interference with other compounds.

Here we demonstrate a SERS-based nanosensor for the real-time detection of multiple stress-related endogenous molecules in living plants. The nanosensor particles are consisted of corrugated Ag nanoshell on silica nanosphere of *ca.* 200 nm modified by a water-soluble cationic polymer poly(diallyldimethylammonium chloride) (PDDA), which can interact with multiple plant signaling molecules and are optically active in the near-infrared region (785 nm) to avoid interferences from plant autofluorescence. We measured a SERS enhancement factor of 2.9×10^7 and signal-to-noise ratio of up to 64 with an acquisition time of ~ 100 ms. To show quantitative multiplex detection, we adopted a binding model to interpret the SERS intensities of two different analytes bound to the SERS hot spot of the nanoprobe. Under either an abiotic or biotic stress, our optical nanosensors can successfully monitor salicylic acid, extracellular adenosine triphosphate, cruciferous phytoalexin, and glutathione in *Nasturtium officinale*, *Triticum aestivum* L., and *Hordeum vulgare* L., all stress-related molecules indicating the possible onset of a plant disease [3]. We believe that plasmonic nanosensor platforms can enable early diagnosis of stress, contributing to a timely disease management of plants.

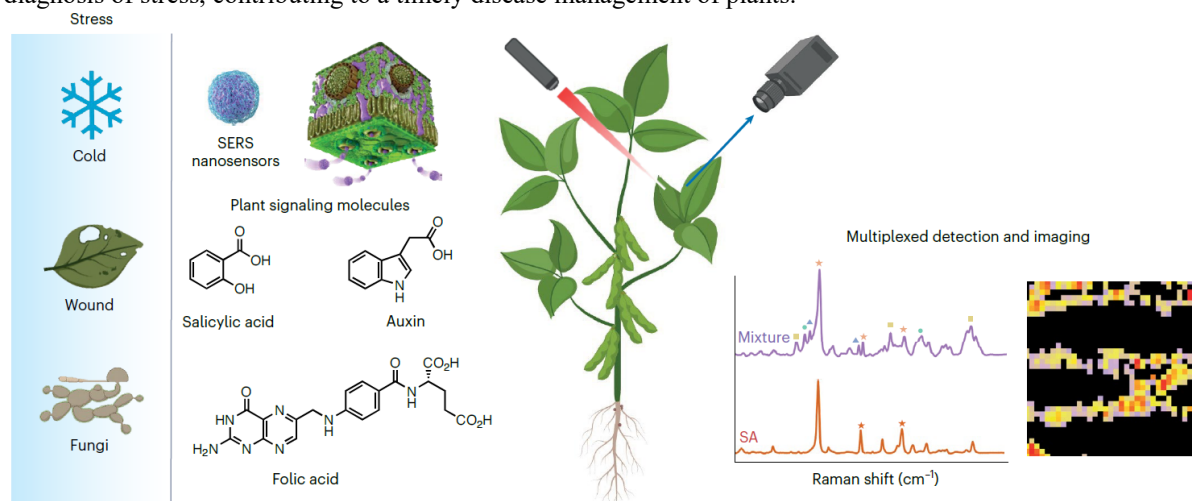


Fig. 1. Monitoring scheme of plant signaling molecules. (Left) Measurement strategy. (Right) SERS spectra of molecules and intensity map.

References

- [1] A. Koornneef, & C. M. Pieterse, *Plant Physiol.* **146**, 839–844 (2008).
- [2] C. M. Pieterse, A. Leon-Reyes, A., S. Van der Ent, S. C. M. Van Wees, *Nat. Chem. Biol.* **5**, 308–316 (2009).
- [3] W. K. Son, Y. S. Choi, Y. W. Han, D. W. Shin, K. M., J. Shin, M. J. Lee, H. Son, D. H. Jeong & S.-Y. Kwak, *Nat. Nanotechnol.* **18**, 205–216 (2023). <https://doi.org/10.1038/s41565-022-01274-2>

Flexible Control of Gold Nanorod Arrangements on Polymer Brush Substrates

Hideyuki MITOMO

Hokkaido University, Research Institute for Electronic Science
E-mail address: mitomo@es.hokudai.ac.jp

Abstract: Gold nanorods (AuNRs) have great potential for various applications due to their useful localized surface plasmon resonance (LSPR) properties. For the effective use of their longitudinal LSPR, control of their arrangement, such as orientation and assembly/disassembly state, is important. To actively tune their arrangements, we have immobilized them onto the polymer brush substrates as a soft template. As a result, we succeeded in preparation of vertically (uniformly) oriented AuNR array. Further, active control of their orientation and assembly/disassembly in the polymer brushes was also realized by changes in solution environment.

Gold nanoparticles (AuNPs) have attracted attentions in various research fields due to their useful optical properties, known as Localized Surface Plasmon Resonance (LSPR). Rod-shaped gold nanoparticles (gold nanorods: AuNRs) show two LSPR modes due to their anisotropy; one is transverse LSPR (T-LSPR) at 520-550 nm, and the other one is longitudinal LSPR (L-LSPR) in the near-infrared region (Fig. 1 top). As this L-LSPR is quite strong and sensitive, an effective use of this is important for applications. Then, how we can control this L-LSPR? We can tune their peak wavelength by assembly/disassembly. In the case of spherical AuNPs, assembly formation cause red-shift of the plasmon peak (Fig. 1 bottom). On the other hand, side-by-side assembly of AuNRs cause blue-shift of L-LSPR. Further, the L-LSPR in AuNRs show significant angle dependence to the incident light on their intensity. Thus, control of their arrangements can be the way to achieve it. In this talk, I will introduce our approach to actively control AuNR arrangements using polymer brushes as a scaffold (Fig. 2)[1].

First, we prepared polymer brushes composed of DNA, which is an anionic polymer, and attached cationic AuNRs onto them via electrostatic interaction. Moderate interaction between AuNR and DNA provided vertically aligned AuNR arrays [2,3]. By changing solution pH, AuNR orientation was reversibly tuned via their interaction changes (vertical at pH 7 to tilted at pH 4) [4]. Not only by pH, but salt concentration changes allow active AuNR orientation changes. Interestingly, the mechanism of AuNR orientation changes by pH and salt conc. changes is different, indicating great potential on their control by various ways. Next, we newly prepared thermo-responsive AuNRs by applying alkyl-terminated OEG-derivatives for surface modification [5]. Our AuNRs preferably form side-by-side assembly on heating in solution. To apply this thermo-responsive AuNRs for the polymer brush system, we modified AuNR surfaces with the mixture of our thermo-responsive ligands and cationic ligands, and then attached them onto DNA brush substrates. AuNRs showed reversible assembly and disassembly on temperature changes, although they were immobilized in DNA brush layers.

Our AuNR arrays on polymer brush substrates can be actively tunable plasmonic substrates.

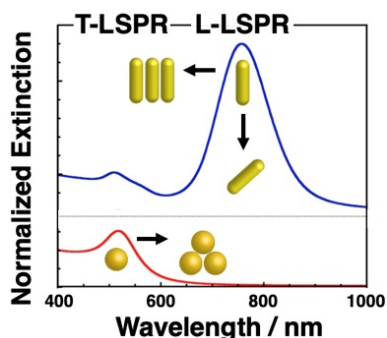


Fig. 1 Extinction spectra of AuNPs and AuNRs

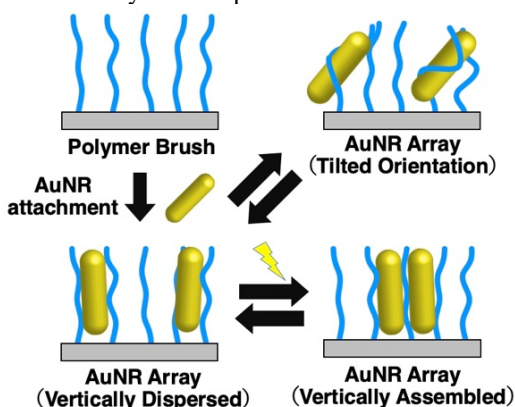


Fig. 2 Schematic illustration of flexibly configurable AuNR arrays

- [1] S. Nakamura, H. Mitomo*, K. Ijiro*, *Chemistry Letters*, **50**, 361-370 (2021).
- [2] S. Nakamura, H. Mitomo*, K. Ijiro*, et al, *ACS Omega*, **2**, 2208-2213 (2017).
- [3] S. Nakamura, H. Mitomo*, K. Ijiro*, et al, *Langmuir*, **36**, 3590-3599 (2020).
- [4] Y. Sekizawa, H. Mitomo*, K. Ijiro*, et al, *Nanoscale Advances*, **2**, 3798-3803 (2020).
- [5] R. Iida, H. Mitomo*, K. Ijiro*, et al, *Small*, **14**, 1704230 (2018).

White-nanolight-source through plasmon nanofocusing for background-free nanoimaging

Prabhat Verma

*Department of Applied Physics, Osaka University, Suita 565-0871, Osaka, Japan
E-mail address: verma@ap.eng.osaka-u.ac.jp*

Abstract: Plasmon nanofocusing is an alternate technique to confine light field at the apex of a metalized nanotip for invoking tip-enhanced Raman scattering, where plasmons are excited by illuminating a plasmon coupler located far from the apex of the tip. This allows one to measure background-free near-field and TERS signals. Unlike plasmon-resonance-based confinement, the confinement of light in plasmon nanofocusing is wavelength-independent. Therefore, by using plasmon nanofocusing, one can confine all wavelengths simultaneously, or in other words, create a white nanolight at the tip apex for multi-color nanoimaging and other applications.

Plasmonically enhanced spectroscopies, such as surface-enhanced Raman spectroscopy (SERS) and tip-enhanced Raman spectroscopy (TERS), have been well utilized for both, sensing tiny amounts of specific molecules and imaging samples at the nanoscale [1–5]. The most important phenomenon in such measurements is the selective enhancement of the Raman signal from the nanometric volume of a sample, which makes it possible to study a sample at extremely high spatial resolution and at a very low concentration. For this purpose, perfect tuning of plasmon resonance wavelength is required. This is achieved by illuminating a plasmonic nanoantenna, such as the apex of a metallic nanotip in TERS or metallic nanoparticles in SERS, with a diffraction-limited focused laser beam. This results in the creation of a nanolight-source in the close vicinity of the antenna through the resonant oscillation of localized surface plasmons. Since the resonance condition is achieved only for a very narrow wavelength range that matches the plasmon resonance for a chosen antenna, the nanolight-source also has a narrow wavelength range. In addition to creating a nanolight-source in this process, one also receives an unwanted background scattering that originates from the diffraction-limited illumination of the sample. In some cases, one would like to have fast wavelength switching or even multiple wavelengths at the nanolight-source without changing the antenna. Also, one would like to avoid unwanted background scattering.

Plasmon nanofocusing [6–8], which is not based on the plasmon resonance, is an alternative method for creating a nanolight-source at the tip apex. It is a phenomenon in which plasmons are excited near the broader end of a tapered or conical metallic tip, which then propagate towards the apex of the tip and slow down by adiabatically compressing their energies and eventually stop near the apex, where all energy is converted to light creating a strong light field localized at the nanometrically sharp apex of the tip. Here plasmons are excited by coupling propagating photons with plasmons via a grating that works as the plasmon coupler. As the plasmon coupler and the apex of the tip are physically separated by a reasonably large distance of about 5–8 μm , the illuminating light does not fall on the sample, avoiding the unwanted background scattering by preventing direct illumination of the sample with incident light. In addition, because one can create a nanolight-source through the propagation of plasmons rather than the localized resonance, it works over an extremely wide wavelength range from UV to near-IR. However, the plasmon coupler, which is grating, can efficiently couple only a narrow wavelength range and imposes a restriction on the wavelength range of the nanolight-source. This can be overcome if a suitable coupler is designed that couples a broad wavelength range, or in other words, the white light. We found that, if properly designed, a single slit can work as an efficient plasmon coupler for white light, ultimately creating a white-nanolight-source. We have recently proposed the generation of a white-nanolight-source through broadband plasmon nanofocusing and successfully exploited it for super-resolution spectral optical imaging, which has exhibited great potential for broadband plasmon nanofocusing not only for optical imaging but also for diverse scientific fields as a novel tiny light source. In this talk, we will discuss how to create a white-nanolight-source and utilize it in various interesting applications.

- [1] P. Verma, Chem. Rev. **117**, 6447-6466 (2017).
- [2] P. Verma, T. Ichimura, T. Yano, Y. Saito, and S. Kawata, Laser Photon. Rev. **4**, 548-561 (2010).
- [3] T. Yano, P. Verma, Y. Saito, T. Ichimura, and S. Kawata, Nature Photon. **3**, 473-477 (2009).
- [4] T. Yano, T. Ichimura, S. Kuwahara, F. H'Dhili, K. Uetsuki, Y. Okuno, P. Verma, and S. Kawata, Nature Communications **4**, 2592 (2013).
- [5] R. Kato, T. Moriyama, T. Umakoshi, T. Yano, and P. Verma, Science Adv. **8**, eabo4021 (2022).
- [6] T. Umakoshi, Y. Saito, and P. Verma, Nanoscale **8**, 5634-5640 (2016).
- [7] T. Umakoshi, M. Tanaka, Y. Saito, and P. Verma, Science Adv. **6**, eaba4179 (2020).
- [8] K. Taguchi, T. Umakoshi, S. Inoue, and P. Verma, J. Phys. Chem. C **125**, 6378-6386 (2021).

Near-field spectroscopy and control of excitons in 2D van der Waals heterostructures

Vasily Kravtsov

*School of Physics and Engineering, ITMO University, Saint Petersburg 197101, Russia
E-mail address: vasily.kravtsov@metalab.ifmo.ru*

Abstract: We study exciton physics in monolayer transition metal dichalcogenides (TMDs) and heterostructures at room temperature with two different implementations of near-field optical spectroscopy. We demonstrate that tip-enhanced photoluminescence (TEPL) spectroscopy enables nano-imaging and optical control of intra- and inter-layer excitons in TMD heterobilayers, while Fourier-plane microscopy combined with evanescent wave coupling provides access to exciton polaritons in TMD-based subwavelength waveguides.

1. Introduction

Atomically thin TMDs are direct band gap semiconductors that host excitons with large binding energies and sizeable exciton-exciton interaction strength. When stacked into heterostructures, these materials acquire many unique optical properties associated with the interlayer coupling and formation of new excitonic and polaritonic states. Near-field spectroscopy provides an indispensable tool for studying such states, as well as their coupling, dynamics, and control. We employ two complementary approaches to perform near-field spectroscopy on TMD-based structures: TEPL spectroscopy and Fourier-plane microscopy with evanescent wave coupling.

2. Results and discussion

We perform TEPL spectroscopy of intra- and interlayer excitons in TMD heterobilayers placed on a gold substrate (Fig. 1a). The composition of the layers is selected in such a way that the inter- and intralayer excitonic resonances overlap with the enhancement band of the tip-sample gap plasmon resonance [1]. In the experiment, we demonstrate nano-imaging of interlayer exciton PL intensity, peak position, and linewidth. Further, we control the tip-enhanced interlayer exciton PL spectrum via tip-sample distance, GPa-scale pressure, and excitation power, revealing a new regime of interlayer trion formation [2].

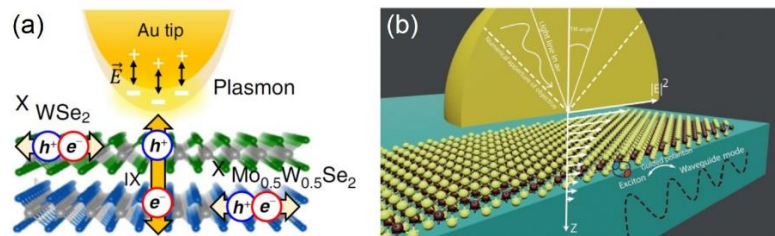


Fig. 1. (a) Tip-enhanced photoluminescence spectroscopy of TMD heterobilayers. (b) Fourier-plane microscopy of strongly coupled excitons in TMD-based waveguides with evanescent wave coupling through a high-index solid immersion lens.

To obtain access to non-radiating exciton-polariton states in TMD-based waveguides, we perform Fourier-plane microscopy with evanescent wave coupling [3] using a high index solid immersion lens (Fig. 1b). We study two systems supporting waveguide polaritons at room temperature: (i) monolayer WS₂ integrated with 90 nm thick Ta₂O₅ waveguide and (ii) monolayer WS₂ encapsulated in 100 nm thick hexagonal boron nitride. We demonstrate that both systems reach the strong light-matter coupling regime at room temperature, measure the polariton dispersions, and demonstrate nonlinear polariton-polariton interaction. Our results provide a powerful platform for studying room-temperature exciton and polariton physics in 2D van der Waals semiconductors.

3. References

- [1] Y. Koo, H. Lee, T. Ivanova, R. Savelev, M. Petrov, V. Kravtsov, and K.-D. Park, ACS Nano **17**, 4854-4861 (2023).
- [2] Y. Koo, H. Lee, T. Ivanova, A. Kefayati, V. Perebeinos, E. Khestanova, V. Kravtsov, and K.-D. Park, Light Sci. Appl. **12**, 59 (2023).
- [3] D. V. Permyakov, V. I. Kondratiev, D. A. Pidgayko, I. S. Sinev, and A. K. Samusev, JETP Lett. **113**, 780-786 (2021).

Nanocavity-integrated van der Waals heterobilayers for nano-excitonic transistor

Yeonjeong Koo, Hyeongwoo Lee, Tatyana Ivanova, Roman Savelev, Mihail Petrov, Vasily Kravtsov, and
Kyoung-Duck Park

*Department of Physics, Pohang University of Science and Technology (POSTECH), Pohang, 37673, Republic of Korea,
School of Physics and Engineering, ITMO University, Saint Petersburg, 197101, Russia,
E-mail address: vasily.kravtsov@metalab.ifmo.ru, parklab@postech.ac.kr*

Abstract: We present a new approach towards nano-excitonic transistors in 25 nm² area of WSe₂/Mo_{0.5}W_{0.5}Se₂ heterobilayers through adaptive tip-enhanced photoluminescence modulation of intra-/inter-layer excitons. We suggest a simple theoretical model describing the underlying adaptive TEPL modulation mechanism, which relies on the additional spatial degree of freedom provided by the presence of the plasmonic tip.

1. Introduction

An optical transistor is a fundamental building block for realizing optical computing, which can resolve the problem of exponentially growing computational workloads [1]. In comparison to a conventional electronic transistor, the photon-based transistor can dramatically increase the speed of information processing while reducing ohmic losses. However, direct *on-and-off* and *in-and-out* processes of light are hard to modulate due to the intrinsically non-interacting nature of photons. Furthermore, diffraction limits the optical mode volume ($\approx \lambda/2$) and prevents further device miniaturization. Hence, exploiting light-matter interactions at the nanoscale through optically controllable quasiparticles is highly desirable for the development of the optical transistor.

Here, we present a new approach for creating an ultrathin 2-bit nano-excitonic transistor using photoluminescence (PL) of intralayer excitons (X) and interlayer excitons (IX) in a WSe₂/Mo_{0.5}W_{0.5}Se₂ heterobilayer. To amplify and selectively modulate PL responses of X and IX in ~ 25 nm² area, we employ an adaptive tip-enhanced PL (*a*-TEPL) modulation technique with the near-field wavefront shaping [2]. This fundamental concept of a 2-bit nano-excitonic transistor can be applied for further development of ultracompact optical computing and communication devices. In addition, the ability to read-out optical data within ~ 25 nm² of surface area can be useful for high-density optical memory, i.e., nano-ray disc, which can innovatively improve the data capacity of a blu-ray disc up to $\sim 7,200$ -fold.

2. Result and Discussion

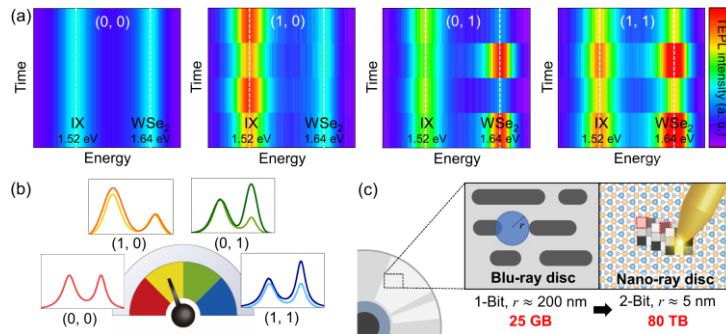


Fig. 1. (a) Demonstration of the fully-optically modulated *a*-TEPL spectra of IX and X_{WSe₂} emissions displaying the data units of a 2-bit nano-excitonic transistor, (0, 0), (1, 0), (0, 1), and (1, 1). (b) Illustration of a two-optical bit processing using four different data units from (a). (c) Illustration of the nano-ray disc using a 2-bit nano-excitonic transistor with significantly increased data capacity compared to a conventional blu-ray disc.

As shown in Fig. 1(a), we can selectively modulate the TEPL emission of X and IX, especially achieving a 2-bit transistor through a full-optical control. The underlying mechanism comes from a deterministic manipulation of tip-localized surface plasmon (tip-LSP) characteristics to improve plasmon-IX or plasmon-X coupling strength through a spatial phase control of the excitation beam [3]. This non-invasive and totally reversible engineering strategy provides a potential to heterobilayers as a future opto-electronic communication platform which has the higher bit-rate and energy efficiency than the conventional bias-based computing and engineering device.

3. References

- [1] A. V. Zasedatelev, A. V. Baranikov, D. Urbonas, F. Scafirimuto, U. Scherf, T. Stöferle, R. F. Mahrt, and P. G. Lagoudakis, *Nature Photonics*, **13**, 378 (2019).
- [2] D. Y. Lee, C. Park, J. Choi, Y. Koo, M. Kang, M. S. Jeong, M. B. Raschke, and K.-D. Park, *Nature Communications*, **12**, 3465 (2021).
- [3] I. Vellekoop and A. Mosk, *Optics Communications*, **281**, 3071 (2008).

Anomalous Phonon Softening of Wrinkled Monolayer WSe₂

**Dong Hyeon Kim(a), (b), Byeong Geun Jeong(a), (b), Sung Hyuk Kim(a), (b), Hyeong Chan Suh (b),
Jaekak Yoo(a), (c), Yo Seob Won(a), Tae Hoon Kim (b), Seung Mi Lee(c),
Ki Kang Kim(a)*, Mun Seok Jeong(b)***

(a) *Department of energy science, Sungkyunkwan University, Suwon, Korea*

(b) *Department of Physics, Hanyang University, Seoul, Korea*

(c) *Korea Research Institute of Standard and Science, Daejeon, Korea*

*e-mail of corresponding author: mjeong@hanyang.ac.kr

The excellent optical and electrical properties of transition metal dichalcogenides (TMDc) induce tremendous studies about the TMDc intrinsic characteristics and applications. In advance, many researchers applied the strain on TMDc to control the quasiparticles actively. Applied strain can tune the level of valence band maximum, conduction band minimum, the lattice vibration properties, etc. Tip-enhanced optical spectroscopy which includes both Raman scattering and photoluminescence can reveal the nanoscale strain-induced properties and apply the strain to the sample to track the appearances. However, there is a lack of lattice vibration studies with strain at the nanoscale regime which could be a strong insight to understand the born nature of materials.

Here we present the atypical phonon softening of tungsten diselenide (WSe₂) wrinkle which has a linear correlation with inherent strain. The powerful tip-enhanced Raman spectroscopy brought out the unnormal phonon properties at the nanoscale level and moreover propose a new strain indicator for TMDc at the nanoscale level.

Quantum plasmonic applications

Mark Tame

*Stellenbosch University, South Africa
E-mail address: mstame@sun.ac.za*

Abstract: Integrated photonic systems provide an attractive platform for quantum state engineering. Dielectric materials are often used to construct complex optical circuitry in this setting, but plasmonic materials can provide a way to confine light to much smaller scales, which enables more compact devices and the enhancement of light-matter coupling. This can in principle be used to build single-photon sources and switches, both of which are important for quantum technologies. Unfortunately, the confinement of light using plasmonics comes at the expense of significant loss. Fortunately, recent studies have shown that with careful engineering one can overcome loss and even exploit it for realising quantum applications at the nanoscale. I will talk about some of these applications, many of which have been experimentally demonstrated, including quantum sensing, quantum random number generation, and the production and distillation of entanglement.

Large-Scale Zero-Static Power Programmable Quantum Photonic Processor

Sangyoon Han

Dept. of Robotics and Mechatronics Engineering, Daegu Gyeongbuk Institute of Science and Technology, Daegu 42988, Republic of Korea
E-mail address: s.han@dgist.ac.kr

Abstract: We have been developing low power programmable silicon photonic MEMS for linear optical quantum computing. A large-scale programmable photonic circuit based on zero-static power MEMS-tunable coupler and -phase shifter will be introduced.

1. Introduction

The concept of programmable photonic circuits has been studied and developed extensively in the last few years. It has shown great potential in cutting-edge applications, including machine learning, quantum computing, radio frequency (RF) signal processing, and hardware accelerators. For the scalable quantum computing applications, it is desirable to have low optical loss, small footprint, and low operating electrical power [1]. Most of the quantum photonic processors today are based on the thermo-optic tuning or electro-optic tuning [2]. The thermo-optic tuner requires high operating power and therefore it is impossible to operate them in cryogenic environments. In addition, the thermal crosstalk between the tuner impedes increasing integration density of the processors. The electro-optic tuning requires less energy; however, the long length of their phase shifters make it difficult to scale the processors.

On the other hand, the MEMS-based tuning mechanism has shown its potential to implement large-scale photonic circuits by demonstrating large-scale photonic switches [3]. The large scalability of the technology originates from its tuning mechanism that allows moving optical building blocks using an extremely small amount of power. By moving optical elements, large index contrast can be created, and therefore large optical effect follows. The electrostatic actuator creating the movements is just a simple variable capacitor that consumes electrical power only when the state of the elements is changing. Our team has been developing various MEMS-tunable photonic processors for power-efficient and low-loss photonic circuits. We have demonstrated programmable photonic processors directly applicable to classical and quantum photonics applications using the MEMS-tunable elements. In this talk, we will show our recent progress on MEMS-based programmable photonic circuits and their perspective on large-scale photonic quantum circuits on chip.

2. Results

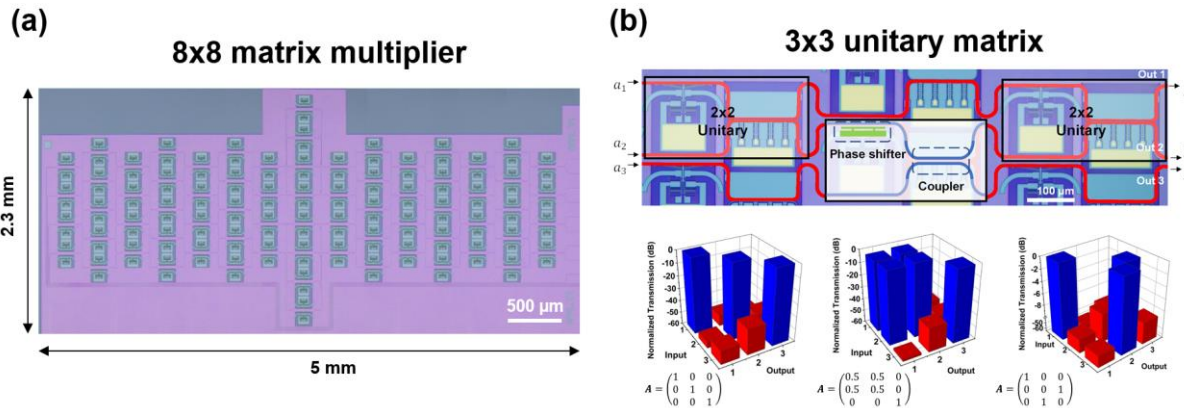


Fig. 1 (a) 8×8 optical matrix multiplier implemented on silicon photonic MEMS. (b) 3×3 unitary matrix multiplier and its operation results.

Figure 1 shows linear quantum photonic processors implemented on silicon photonic MEMS platform. The processors are implemented based on electrostatic MEMS-tunable couplers and -phase shifters. The electrostatic actuators used to actuate the coupler and the phase shifter consume nearly zero-static power which is required to hold the elements in particular states. For tuning, they only require less than few tens of picojoule at maximum. The insertion loss of a phase shifter is less than 0.15 dB. Fig. 1(a) and (b) show the 8×8 optical matrix multiplier and the 3×3 optical unitary matrix multiplier. The unitary matrix multiplier allows us to operate 3×3 unitary operations between 3 optical modes.

3. References

- [1] J. L. O'Brien, "Optical Quantum Computing," *Science*, vol. 318, 2007
- [2] W. Bogaerts *et al.*, "Programmable photonic circuits," *Nature*, vol. 586, no. 7828, pp. 207–216, 2020
- [3] T. J. Seok, K. Kwon, J. Henriksson, J. Luo, and M. C. Wu, "Wafer-scale silicon photonic switches beyond die size limit," *Optica*, vol. 6, no. 4, p. 490, 2019.

Quantum photonic sources based on nanophotonic structures

Xi-Feng Ren

University of Science and Technology of China, China

Integrated quantum photonics has attracted intensive attention due to the compactness, scalability, and stability. Quantum photonic source, especially an on-chip entangled photon source, is a basic device for realizing quantum photonic integrated circuits (QPICs). I will introduce our recent works about quantum photonic sources based on nanophotonic structures, such as 2D materials, metalens array, microcavity, nanowaveguide, etc.

Photosensitizing materials and platforms for light-triggered modulation of Alzheimer's β -amyloid self-assembly

Byung Il Lee, Ph.D.

Amyloid Solution

E-mail address: bilee@amyloidsolution.com

Abstract: The accumulation of β -amyloid ($A\beta$) peptides in an abnormal manner is a representative feature of Alzheimer's disease, which is one of the most common types of age-related dementia worldwide. Despite a lack of clarity on the exact mechanism of neuronal loss and cognitive decline in AD, the idea that $A\beta$ aggregation plays a crucial role in its pathology has received significant support from various in vitro and in vivo studies. In this respect, searching and developing therapeutic agents that can regulate $A\beta$ aggregation is considered as an attractive option to treat AD. This talk will outline the attempts to employ light energy to intervene the self-assembly of $A\beta$ peptides by generating oxidative stress by photosensitizers such as natural or synthetic dyes, light-responsive nanomaterials, and photoelectrochemical platforms. The mechanism behind photodynamic reactions reducing $A\beta$ aggregation and the issue of creating oxidative stress, which has been long considered harmful, will be discussed, highlighting the positive impact of oxidative stress created by photosensitizers in suppressing $A\beta$ -triggered neurotoxicity. Furthermore, the recent study to apply the photo-induced treatment in mouse model will also be presented.

Acceleration of antigen-antibody reaction by optical force for detecting biological nanomaterials

Takuya Iida^{*1,2}, Kana Fujiwara^{1,2,3}, Yumiko Takagi^{1,2}, Shota Hamatani^{1,2,3},
Mamoru Tamura^{2,4}, Shiho Tokonami^{2,3}

¹ Graduate School of Science, Osaka Metropolitan University

² Research Institute for Light-induced Acceleration System (RILACS), Osaka Metropolitan University

³ Graduate School of Engineering, Osaka Metropolitan University

⁴ Graduate School of Engineering Science, Osaka University

E-mail address: t-iida@omu.ac.jp

Abstract: We have investigated a mechanism of accelerating the antigen-antibody reaction with the optical force under fluidic pressure in narrow microchannel. Remarkably, we demonstrated the selective detection of several thousands of biological nanoparticles and several tens attogram proteins in sub-microliter liquid sample, where 1-2 orders higher sensitivity and ultrafast specific detection only by 3-5 minutes can be realized. The obtained results will innovate the biological nanophotonics and the early diagnosis of various diseases.

1. Introduction

Liquid biopsy detecting biological nanomaterials (proteins and nucleic acids etc.) is expected to be used for the early diagnosis of various diseases such as cancer [1], infectious diseases such as the COVID-19 [2] and so on, where antigen-antibody reaction has been used for the selective detection of various types of proteins. Conventional enzyme immunoassay methods use spontaneous antigen-antibody reactions requiring incubation time for 1 to 2 hours waiting for the target protein to bind to the modified antibody on the substrate by chance and multiple washing processes. On the other hand, optical condensation techniques have been proposed for the detection of biological micro-objects and nano-objects such as bacterial cells and molecules guiding them to the detection site by the synergetic effect of light-induced force and photothermal convection [3]. Here, paying attention to this technique, we have proposed a new principle of light-induced acceleration of antigen-antibody reactions to detect trace amounts of proteins and biological nanoparticles (extracellular vesicle (EV) etc.) secreted from biological cells [4,5] at the solid-liquid interface by increasing the probability of collisions between target molecules and probe particles mediated by optical pressure and fluidic pressure in a microchannel (Fig.1).

2. Method

Introducing target biological nanomaterials (proteins or EVs) and antibody-modified polymer beads with a diameter of 2 μm into a microchannel (width: 100 μm , height: 100 μm), where a laser of several hundred mW was defocused with the spot size of about 70 μm comparable to the width of a microchannel. Based on this system, we performed the detection of CD63/CD9 fusion protein and EVs derived from cancer cells. Also, we performed model calculations assuming the optical force and fluidic pressure.

3. Results and Discussion

Since the size of each micro bead is in the Mie regime, the strong scattering force pushed the beads to the bottom of the microchannel leading to the accumulation of antibody-modified beads and target proteins without causing thermal damage in a laser spot mediated by pressure-driven flow. Target proteins ranging from 46.5 ag to 750 ag were successfully detected in a 300 nL sample without any pretreatment after only 3 minutes of laser irradiation. This result means that is about 100 times higher sensitivity and ultra-fast specific detection of attogram-level proteins in a sample volume less than 1/300 of conventional protein detection methods such as ELISA (~100 μL) requiring several hours for detection due to multiple processes such as incubation and washing. Also, we have selectively detected EVs as nanoparticles from cancer cells within 5 minutes by our developed method. These results will promote the development of biological nanophotonics, and the construction of an innovative platform for high-throughput bioanalysis through the control of diverse biochemical reactions leading to early diagnosis of various diseases such as cancer, dementia, and microbial infections.

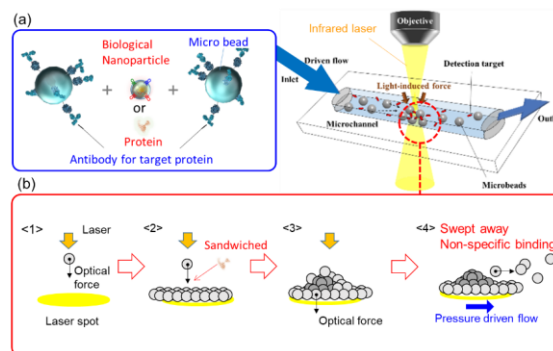


Fig.1 Schematic image of light-induced acceleration of antigen-antibody reaction under the fluidic pressure in a microchannel.

[1] E. Crowley, F. Nicolantonio, F. Loupakis, et al. *Nat. Rev. Clin. Oncol.* **10**, 472 (2013).

[2] A. Stukalov, V. Girault, V. Grass, et al. *Nature* **594**, 246 (2021).

[3] T. Iida, *Readout: Horiba technical reports* **55**, 11, (2021).

[4] T. Iida, S. Hamatani, Y. Takagi, K. Fujiwara, M. Tamura, S. Tokonami, *Commun. Biol.* **5**, 1053 (2022).

[5] K. Fujiwara, Y. Takagi, M. Tamura, I. Nakase, S. Tokonami, T. Iida, under review (2023).

Strong coupling between plasmonic nanostructures and 2D semiconductors

Hong Wei

*Institute of Physics, Chinese Academy of Sciences, Beijing 100190, China
E-mail address: weihong@iphy.ac.cn*

Abstract: The strong coupling between excitons and single plasmonic nanocavities enables plexcitonic states in nanoscale systems at room temperature. Here we demonstrate the strong coupling of surface plasmon modes of metal nanowires and excitons in monolayer semiconductors, with Rabi splitting manifested in both scattering and photoluminescence spectra. By utilizing the propagation properties of surface plasmons on the nanowires, the photoluminescence emitted through the scattering of plasmon-exciton hybrid modes is extracted. The analytically calculated scattering and photoluminescence spectra well reproduce the experimental results. These findings unify the scattering and photoluminescence spectra in the plexcitonic system and eliminate the ambiguities of photoluminescence emission, shedding new light on understanding the rich spectral phenomena in the plasmon-exciton strong coupling regime.

When the coherent energy exchange rate between an exciton and an optical cavity is faster than their average dissipation rate, the strong coupling is achieved with exciton polariton states formed. In recent years, the strong coupling of plasmonic nanocavities and excitons has attracted intense interest because surface plasmons possess highly confined electromagnetic field with ultrasmall mode volume [1,2]. This unique property of surface plasmons leads to larger coupling strength and allows for the observation of strong coupling at room temperature at single nanoparticle level and even single exciton level.

In this talk, I will present our research on the strong coupling between single silver nanowires and monolayer WSe₂ [3,4]. Because of the long propagation length of surface plasmons on silver nanowires, the excitation and collection regions can be spatially separated, which is utilized to extract the photoluminescence emitted through the scattering of plasmon-exciton hybrid modes. It is found that the photoluminescence and scattering light share the same spectral profiles resulting from strong coupling. The analytical calculation results agree with the experimental data. These results clarify the correlative scattering and photoluminescence processes and offer new perspective on the spectral responses of plasmon-exciton strong coupling systems.

References

- [1] X. H. Yan, and H. Wei, *Nanoscale* **12**, 9708-9716 (2020).
- [2] H. Wei, X. H. Yan, Y. J. Niu, Q. Li, Z. L. Jia, and H. X. Xu, *Adv. Funct. Mater.* **31**, 2100889 (2021).
- [3] Y. J. Niu, H. X. Xu, and H. Wei, *Phys. Rev. Lett.* **128**, 167402 (2022).
- [4] Y. J. Niu, L. Gao, H. X. Xu, and H. Wei, *Nanophotonics* **12**, 735-742 (2023).

Plasmonics in Metal Nanoparticles

Jeong-Eun Park

Department of Chemistry, GIST, Gwangju 61005, Korea
E-mail address: parkje@gist.ac.kr

Plasmonics utilize light-matter interaction at a dimension smaller than the wavelength of light. Due to their flexible shapes and geometries, metal-based plasmonic materials can be a reliable tool for obtaining desired plasmonic near- and far-field properties. In this talk, I will first introduce the highly controlled synthesis of gold nanoparticles [1, 2]. From their uniform structures and strong plasmonic effect, we achieved reproducible surface-enhanced Raman scattering signals and the highest metal photoluminescence quantum yield. In the second part, I will present collective nanoparticle-emitter hybrid systems. When nanoparticles are periodically arranged in two dimensions, diffractive coupling of plasmon modes from each nanoparticle generates surface lattice resonances [3]. By integrating plasmonic lattices with perovskites, we investigated unique optical feedback for lasing and ultrafast dynamics of strongly coupled perovskites [4, 5].

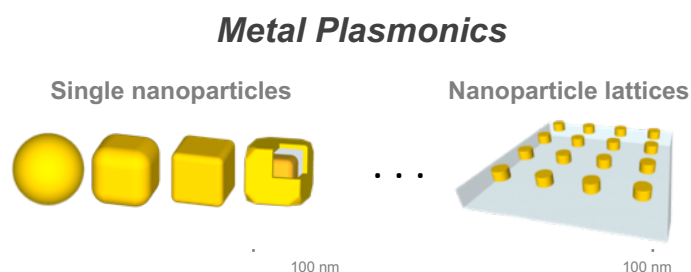


Fig. 1. Plasmonic metal nanoparticle systems in various morphologies

- [1] Park, J. E.; Kim, S.; Son, J.; Lee, Y.; Nam, J. M. *Nano Lett.* **16**, 7962-7967 (2016).
- [2] Park, J. E.[†]; Lee, Y.[†]; Nam, J. M. *Nano Lett.* **18**, 7419-7419 (2018).
- [3] Guan, J.; Park, J. E.; Deng, S. K.; Tan, M. J.H.; Hu, J.; Odom, T. W. *Chem. Rev.* **122**, 15177-15203 (2022).
- [4] Park, J. E.; López-Arteaga, R.; Sample, A. D.; Cherqui, C. R.; Spanopoulos, I.; Guan, J.; Kanatzidis, M.; Schatz, G. C.; Weiss, E. A.; Odom, T. W. *ACS Nano* **16**, 3917-3925 (2022).
- [5] Tan, M. J.H.[†]; Park, J. E.[†]; Freire-Fernández, F.; Guan, J.; Juarez, X. G.; Odom, T. W. *Adv. Mater.* **34**, 202203999 (2022).

Interlayer Excitons in Various Heterostructures

Jinsoo Joo¹, Taek Joon Kim¹, Sang-hun Lee¹, Jun Young Kim¹, Jeongyong Kim²

¹Department of Physics, Korea University, Seoul, South Korea

²Department of Energy Science, Sungkyunkwan University, Suwon, South Korea

E-mail address: jjoo@korea.ac.kr

Heterostructures (HSs) using transition metal dichalcogenides (TMDs), organic semiconductors, perovskites, and quantum-dots (QDs) are promising platforms for exciton-based advanced photonics and optoelectronics. The photoinduced charge transfer (CT) in type-II energy band alignment plays an important role for the formation of interlayer excitons (IXs) at various HSs.

In this study, various HSs were fabricated consisting of perovskite MAPbI₃, CdSe-ZnS core-shell QDs, WS₂ TMDs, PbI₂, and organic donor/acceptor molecules. Distinctive IX emission at far-red region ($\lambda_{em} = 873$ nm) was observed for the perovskite MAPbI₃/CdSe-ZnS-QDs HS (Fig. 1a and 1b) modulating energy band alignment through the diameter of QDs [1]. The photoinduced CT of the MAPbI₃/CdSe-ZnS-QDs HSs was clearly observed for the insertion of thin h-BN layer and for thin ZnS shell barrier of QDs. The photodetectors using the MAPbI₃/CdSe-ZnS-QDs HS were successfully performed with incident irradiation of far-red region (Fig. 1c). The intense and broad PL emission of IX of the HS using monolayer WS₂ and multilayer PbI₂ was also observed in visible light region at 675-700 nm at low temperatures [2]. The drastic decrease in PL intensity of the WS₂/PbI₂ HS indicates the occurrence of CT with type-II band alignment. The characteristics of IXs of the WS₂/PbI₂ and MAPbI₃/CdSe-ZnS-QDs HSs are compared to those of the intermolecular CT excitons (i.e., exciplexes) in the HS consisting of organic donor (D) and acceptor (A) molecules. The electroluminescence of D-A bilayer organic light emitting diodes was blue-shifted due to the orthogonal formation of dipoles of exciplexes compared to that of Frenkel excitons of pristine molecules. For IXs (including exciplexes) of various HSs studied here, PL peaks were blue-shifted with increasing excitation power, originating from the screening effect of Coulomb repulsive interaction between dipole-aligned IXs. The lifetime of IXs of the HSs was considerably longer than that of pristine excitons. Back focal plane imaging suggests that the directions of dipole moments of the IXs at the interfaces are relatively out-of-plane compared to those of intralayer excitons.

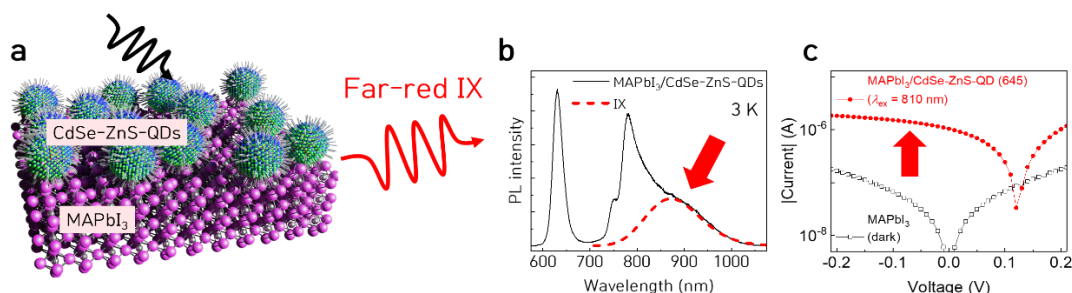


Fig. 1. (a) Schematic illustration of MAPbI₃/CdSe-ZnS-QD heterostructure (HS). (b) PL spectra of the MAPbI₃/CdSe-ZnS-QD HS (black curve) and the far-red IX related signal (red dashed curve). (c) Current-voltage (*I*-*V*) curve of the MAPbI₃-based photodetectors.

[1] T. J. Kim, S. Lee, E. Lee, C. Seo, J. Kim, and J. Joo, Adv. Sci. in press, doi.org/10.1002/advs.202207653, (2023).

[2] J. Y. Kim, T. J. Kim, S. Lee, E. Lee, J. Kim, and J. Joo, ACS Appl. Nano Mater. 5, 11167-11175 (2022).

Visualizing charge dynamics with shot noise STM

Doohee Cho

Department of Physics, Yonsei University, Seoul, 03722, Republic of Korea
E-mail address: dooheecho@yonsei.ac.kr

Abstract: Scanning Tunneling Microscope (STM) has become an essential tool for exploring the local electronic structure of correlated electron systems. However, its limited time resolution has prevented the acquisition of valuable information about the dynamics of electric charge transport. Shot noise, the temporal fluctuation of current due to the granularity of charges, is present in all STM measurements. Still, the relationship between shot noise and electronic properties is not well-understood. In this work, we have combined a STM with a MHz amplifier that includes niobium inductors and a high-mobility electron transistor to achieve shot noise measurements at the atomic scale. This new technique has revealed unexpected charge dynamics in a cuprate high-temperature superconductor, a disordered superconducting TiN film. These findings provide new insights into understanding the electronic correlation properties hidden in time-averaged transport measurements of exotic quantum materials.

1. Introduction

The conventional STM has limitations due to the low-pass filter formed by the high tunnelling junction resistance and the stray capacitance of the long coaxial cable, which limits its bandwidth to about 1 kHz. However, within this bandwidth, the shot noise associated with the discreteness of the charge carriers is much weaker than the mechanical vibrations and $1/f$ noise. The shot noise is essential in understanding charge dynamics in the tunnelling junction, but conventional STM cannot access it. To study the charge dynamics, we developed the hf -amplifier, which comprises a superconducting Nb inductor and a high-mobility electron transistor (Fig. 1a). This new technique enables us to measure current fluctuations with atomic resolution at MHz atomic resolution [1].

2. Results

We employed the shot noise STM to investigate the unconventional superconductors. We found several unusual features that are hidden in the time-averaged tunnelling spectra. In a cuprate high-temperature superconductor, we discovered the noisy centres driven by charge trapping with polaron formation in the insulating layers capping the metallic hole-doped cuprate [3]. The shot noise enhancement can be caused by the correlated quasiparticle tunnelling into the superconducting gap via Andreev reflection (Fig. 1b). It can be another ideal tool to prove the existence of paired electrons instead of the spectral gap. Our shot noise spectra obtained in the normal(superconductor)-insulator-superconductor junction clearly shows the noise enhancement driven by the double electron tunnelling. In a disordered superconductor, we found a novel quantum state with paired electrons without a superconducting gap [3].

3. Figures

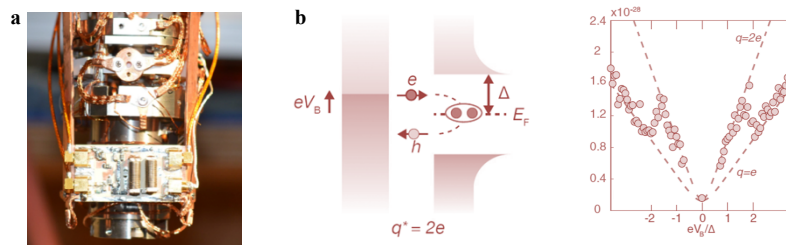


Fig. 1 a. A hf -amplifier for shot noise STM. **b.** The shot noise enhancement driven by Andreev reflection.

4. References

- [1] K. M. Bastiaans et al., Review of Scientific Instruments 89, 093709 (2018).
- [2] K. M. Bastiaans et al., Nature Physics 14, 1183 (2018).
- [3] K. M. Bastiaans et al., Phys. Rev. B 100, 104506 (2019).
- [4] K. M. Bastiaans et al., Science 374, 608 (2021).

Optical Spectroscopic Investigations of Wafer-scale Atomically Thin Materials

Jae-Ung Lee

*Department of Physics, Ajou University, Gyeonggi-do 16499, Korea
E-mail address: jaeunglee@ajou.ac.kr*

Atomically thin materials have unique optical properties originating from its dimensional nature. Controlling and characterizing the optical properties of such materials is necessary to realize desired optical functionality. Wafer-scale monolayer atomically thin films can be grown by metal-organic chemical vapor deposition (MOCVD). It has the advantage of precisely controlling the amount of the injected precursors, which can realize the scalable few-atom-thick materials. Not only the scalability, but it also opens the unique opportunity to tune the optical properties during growth. I will present the optical spectroscopic study of the MOCVD-grown atomically thin materials toward emerging optical functionalities in this presentation.

Exciton Dynamics in Transitional Metal Dichalcogenides by Tip-enhanced Cavity Spectroscopy (TECS)

Hyuntae Kim

Park Systems Corporation, KANC 4F, Iui-Dong 906-10, Suwon, 16229, Republic of Korea
E-mail address: ht.kim@parksystems.com

Abstract: Since the exciton modes in two-dimensional (2D) transition metal dichalcogenides (TMDCs) have been experimentally and theoretically studied due to their interesting behaviors. The hybrid structure of noble metal nanoparticles (NPs) with TMDCs has been introduced to enhance the light-matter interaction caused by plasmon-exciton couplings. The techniques for enhancing the optical response are based on the local EM field confinements on a metallic nanostructure referred to as the localized surface plasmon resonance (LSPR).

In this presentation, I will introduce the tip-enhanced photoluminescence (TEPL) and cavity spectroscopy (TECS) techniques for highly enhancing optical responses and suggest the intertwined mechanism of plasmon-exciton couplings in each exciton mode on the hybrid structure of the monolayer molybdenum disulfides (MoS_2) and non-centrosymmetric AuNP. Here, I will also summarize the emission of strain-induced localized excitons (X_L) mode, which could not be observed at room temperature due to the low binding energy. Furthermore, the correlation between the optical responses and electrical characteristics is analyzed by Kelvin probe force microscopy (KPFM).

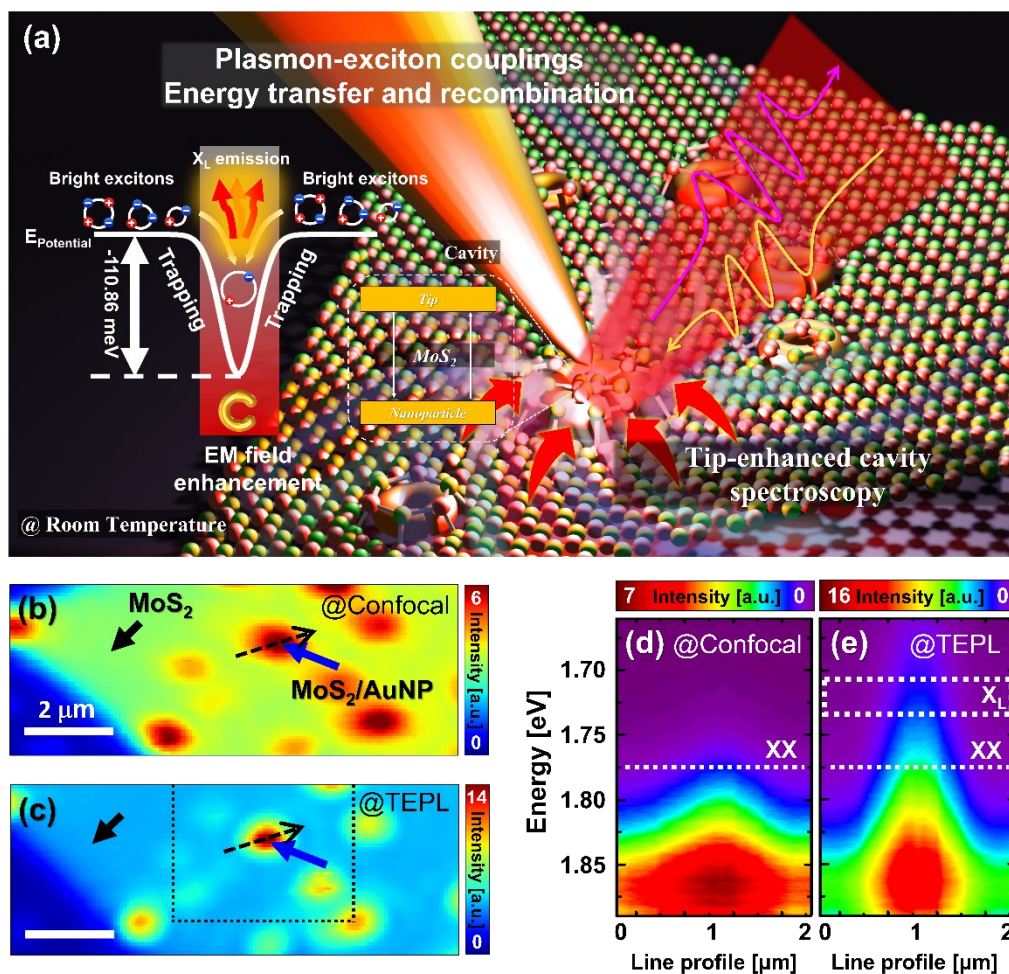


Figure 1. (a) The schematics of plasmon-exciton coupling mechanism. (b) Confocal PL and (c) TEPL mapping image. Hyper-spectral mapping image of (d) confocal PL and (e) TEPL.

Nonlocal response theory of tip-enhanced photoluminescence of a single molecule

Y. Tomoshige¹, M. Tamura^{1,2}, T. Yokoyama¹, H. Ishihara¹

¹Graduate School of Engineering and Science, Osaka University, Japan

²Research Institute for Light-induced Acceleration System, Osaka Metropolitan University, Japan

E-mail address: tomoshige.y@opt.mp.es.osaka-u.ac.jp

Abstract: Tip-enhanced photoluminescence (TEPL) is a microscopy technique enabling to excite a sample locally and obtains optical information at the nanoscale. We have developed the theory incorporating nonlocal response to calculate TEPL of a single molecule in a self-consistent way. This theory can describe the optical response including the large radiative shift due to the strong interaction between the localized surface plasmons and molecules. We have obtained the photoluminescence map of the phthalocyanine molecule depending on the conditions of incident light.

Tip-enhanced photoluminescence (TEPL) based on scanning probe microscopy enables to excite a sample locally and obtains optical information at the nanoscale. Imada et al. combined a narrow-line tunable laser with a scanning tunneling microscope and achieved selective excitation and precise characterization of the individual state of a single phthalocyanine molecule with the high space-energy resolution resulting from measuring the photoluminescence spectrum [1].

In this study, we propose the theory of TEPL based on the nonlocal response theory and input-output theory [2]. We self-consistently determine the molecular polarization expressed by the nonlocal susceptibility and the electric field expressed by the Green's function. Compared with the previous study on the theory of TEPL [3], we treat the Green's function with a dependency of frequency, and hence, we can correctly discuss the photoluminescence spectrum even in the situation where the resonance level of the molecule shifts or splits due to the strong coupling between the gap plasmons sustained at the metal probe tip and the molecule.

Figure 1(a) shows the schematic model of TEPL calculation. The phthalocyanine molecule was located in the cavity structure constructed by the silver probe tip with minute protrusion and the silver substrate. With the fixed configuration of the molecule, we assumed two cases varying the configuration of incident light and detector position as shown in Figure 1(b). In the case 1, the propagating direction of incident light and the position of detector were configured in the yz plane with the elevation angle 30° , whereas in the case 2, they were in the xz plane. In the either case, the incident light was p-polarization. Figures (c) and (d) show the calculated result of photoluminescence intensity map as a function of the probe tip position for optically allowed transitions. The energy of incident light was set to each transition energy of the molecule while the same energy of photoluminescence light was calculated. The intensity map reflects the distribution of transition dipole selectivity excited by incident light. Also, the effect of the nonlocality emerges especially in the case of optically forbidden transition with several nodes inside the molecule.

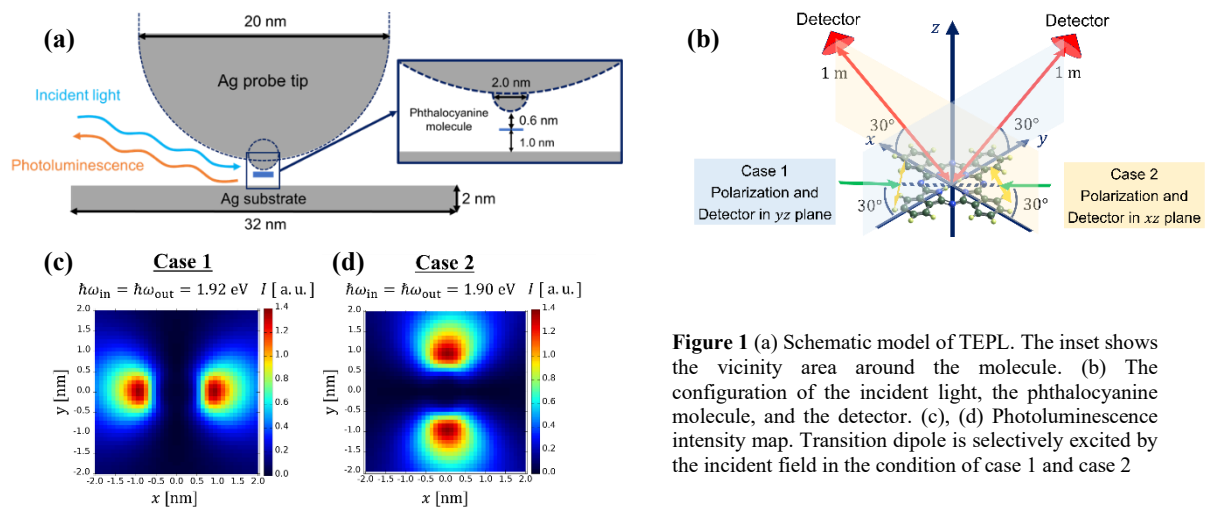


Figure 1 (a) Schematic model of TEPL. The inset shows the vicinity area around the molecule. (b) The configuration of the incident light, the phthalocyanine molecule, and the detector. (c), (d) Photoluminescence intensity map. Transition dipole is selectively excited by the incident field in the condition of case 1 and case 2

[1] Imada, H., Imai-Imada, M., Miwa, K. *et al.*, Science **373**, 95 (2021).

[2] Matsuda, T., Yokoshi, N., and Ishihara, H., Physical Review B **93**, 155418 (2016).

[3] Lyu, S., Zhang, Y., Zhang, Y., Chang, K., Zheng, G., and Wang, L., The Journal of Physical Chemistry C **126**, 11129 (2022).

Quantum sensing and imaging based on solid-state spin qubits in diamond

Donghun Lee^{1),†}

¹⁾ *Department of Physics, Korea University, South Korea*

[†]donghun@korea.ac.kr

Abstract

Nitrogen-vacancy (NV) centers are point defects in diamond and solid-state spin qubits that can probe magnetic field with high sensitivity and high spatial resolution. In this presentation, we will introduce the working principle and examples of sensing and imaging magnetic field with the diamond NV centers. We will focus on three imaging experiments based on the NV centers but with different image scale from nanometers to millimeters. First, the NV center is combined with a scanning probe microscope to map out stray field from magnetic materials and current flows in 2D materials at nanometer scale. Second, ensemble of NV centers is combined with a wide field-of-view optical microscope to image magnetic nanowires and magnetic structures at micrometer scale. Finally, we make a portable magnetometer based on the NV ensemble and image stray field from disk magnets and superconductors at millimeter scale using a 2D motorized translation stage.

Keywords: magnetic sensor, diamond NV center, quantum sensing

Decision Making by Quantum and Near-Field Light

Makoto Naruse¹, Kazuharu Uchiyama², Kingo Uchida³, and Hirokazu Hori²

¹ Dept. Information Physics and Computing, Graduate School of Information Science and Technology, The University of Tokyo, 7-3-1 Bunkyo-ku, Tokyo, 113-8656, Japan

² University of Yamanashi, 4-3-11 Takeda, Kofu, Yamanashi, 400-8511, Japan

³ Ryukoku University, 1-5 Yokotani, Oe-cho, Seta, Otsu, Shiga, 520-2194, Japan

E-mail address: makoto_naruse@ipc.i.u-tokyo.ac.jp

Abstract: We demonstrate that entanglement and quantum interference are useful for social decision-making, whereby the expected value regards maximizing social benefits and ensuring fairness among individuals. Furthermore, complex spatiotemporal light correlations induced in the subwavelength scale become precious resources for problem-solving. We demonstrate an order recognition algorithm driven by versatile optical near-field patterns produced within photochromic materials.

Optics and photonics have been extensively explored for information processing across various applications, with a special focus on machine learning [1]. Reinforcement Learning (RL) stands as an essential branch at the research frontier [2]. RL has become a critical component in information and communication technology, finding applications from resource allocation in wireless communications to search functions in artificial intelligence. These applications often require considering dynamically changing uncertainties. In this paper, we review our research on the efficient physical implementation or acceleration of RL using both quantum and near-field light [3]. Our discussion begins with an exploration of multi-armed bandit (MAB) problems, where the objective is to maximize the cumulative rewards in uncertain reward environments. These problems present challenging trade-offs known as the exploration-exploitation dilemma. We outline the principle of resolving MAB problems by leveraging the wave-particle duality of single photons. In this approach, the probabilistic characteristics of single light quanta are utilized for exploration [4]. This principle is then transformed into ultrafast laser chaos. Here, the irregular oscillations of chaotic time series offer rapid and scalable decision-making capabilities [5].

While the primary aim of solving multi-armed bandit (MAB) problems is to identify the best arm – that is, the choice yielding the highest reward – recognizing the order can also be pivotal in certain applications. Narisawa *et al.* enhanced chaos-based bandit solvers with the concept of a confidence interval, leading to the successful implementation of order recognition [6]. Meanwhile, recent advancements in nano-optics have opened up new pathways toward computing functionalities. Nakagomi *et al.* developed a complex nanoscale structure within photochromic nanocrystals autonomously, facilitated by local optical excitation via optical near-fields [7]. By utilizing such complex nanostructures, the generation of Schubert polynomials was achieved [8]. Moreover, Uchiyama *et al.* recently demonstrated order recognition based on near-field photon statistics observed from the photochromic nanocrystals [9]. It is worth emphasizing that the spatial correlation inherent in the nanocrystals, brought about through optical near-fields, accelerated the ability for order recognition compared to uniformly distributed pseudorandom numbers [9].

The problem escalates in complexity when multiple players are involved, leading to what is termed as the Competitive Multi-Armed Bandit (CMAB) problem. In this scenario, the expected value is directed towards maximizing societal benefits and ensuring fairness among individuals. We have both theoretically and experimentally demonstrated that entangled photons can resolve the CMAB problem in two-player, two-armed situations [10]. Expanding this solution to address general CMAB problems involving multiple players [11] and multiple arms [12] presents a significant and intriguing challenge. Amakasu *et al.* have demonstrated the use of photon's orbital angular momentum to scale the number of arms, while also employing the quantum interference effect to physically ensure the avoidance of decision conflicts [12,13].

- [1] K. Kitayama, M. Notomi, M. Naruse, K. Inoue, S. Kawakami, A. Uchida, APL Photonics **4**, 090901 (2019).
- [2] R. S. Sutton and A. G. Barto, Reinforcement learning: An introduction. Cambridge, MA: MIT press (1998).
- [3] M. Naruse, *et al.* IEEE J. Sel. Top. in Quantum Electron. **26**, 7700210, (2020).
- [4] M. Naruse, M. Berthel, A. Drezet, S. Huant, M. Aono, H. Hori, S.-J. Kim, Sci. Rep. **5**, 13253 (2015).
- [5] M. Naruse, Y. Terashima, A. Uchida, S. -J. Kim, Sci. Rep. **7**, 8772 (2017).
- [6] N. Narisawa, N. Chauvet, M. Hasegawa, M. Naruse, Sci. Rep. **11**, 4459 (2021).
- [7] R. Nakagomi, K. Uchiyama, H. Suzui, E. Hatano, K. Uchida, M. Naruse, H. Hori, Sci. Rep. **8**, 14468 (2018).
- [8] K. Uchiyama, H. Suzui, R. Nakagomi, H. Saigo, K. Uchida, M. Naruse, H. Hori, Sci. Rep. **10**, 2710 (2020).
- [9] K. Uchiyama, S. Nakajima, H. Suzui, N. Chauvet, H. Saigo, R. Horisaki, K. Uchida, M. Naruse, H. Hori, Sci. Rep. **12**, 19008 (2022).
- [10] N. Chauvet, *et al.* Sci. Rep. **9**, 12229 (2019).
- [11] N. Chauvet, G. Bachelier, S. Huant, H. Saigo, H. Hori, and M. Naruse, Sci. Rep. **10**, 20420 (2020).
- [12] T. Amakasu, N. Chauvet, G. Bachelier, S. Huant, R. Horisaki, M. Naruse, Sci. Rep. **11**, 21117 (2021).
- [13] H. Shinkawa, N. Chauvet, A. Röhm, T. Mihana, R. Horisaki, G. Bachelier, M. Naruse, Phys. Rev. Appl. **18**, 064018 (2022).

Azimuth Angle-Dependent Exciton-Polariton Dispersions of One-Dimensional CsPbBr₃ Microcavity

Hyeonjong Jeong¹, Hyeon-Seo Choi¹, Jung-Gue Park², Jang-Won Kang², and Chang-Hee Cho^{1*}

¹Department of Physics and Chemistry
Daegu Gyeongbuk Institute of Science and Technology (DGIST)
Daegu 42988, South Korea

²Department of Semiconductor and Applied Physics
Mokpo National University
Muan 58554, South Korea

*E-mail: chcho@dgist.ac.kr

Abstract: When the excitons in the semiconductors are strongly coupled with cavity photons, new quantum states can be formed, the exciton-polaritons. In the case of the conventional planar microcavity, photons are confined just along the out-of-plane direction of the cavity by distributed Bragg reflector mirrors. Using a one-dimensional microcavity, however, photons could get another in-plane confinement effect due to the refractive index difference at the lateral end facets. Here, we measured continuously varying exciton-polariton energy-momentum dispersions by manipulating the azimuth angle of the CsPbBr₃ microwire cavity to the spectrometer slit at room temperature. When the slit and cavity are parallel, general exciton-polariton dispersion with anti-crossing behavior is shown. Adjusting the azimuth angle from parallel to perpendicular, the exciton-polariton dispersion changes into several discrete branches with reduced curvature. Finally, curvature-less dispersions are formed at a completely perpendicular state. These results can provide an alternative route for realizing the dispersion-convertible polaritonic devices operating at room temperature utilizing one-dimensional microcavities.

Optimization of Nitride MXene Synthesis

Afrizal Lathiful Fadli, Anir S. Sharbirin, and Jeongyong Kim

Department of Energy Science, Sungkyunkwan University, Suwon 16419, Republic of Korea. †

E-mail address: j.kim@skku.edu

Abstract: MXenes are fascinating materials with two-dimensional (2D) transition metals containing carbide, nitrides, and carbon nitride. MXenes have been investigated intensively in numerous applications, such as biomedical engineering, sensing, energy storage, and photothermal therapy.[¹] Nitride MXenes are considered as prominent candidates that provide unique optical properties, electronic conductivities and an abundant functional surface group with O, F, or OH than carbide MXenes.[²] In addition, hydrogen fluoride (HF) is a chemical that is widely used for producing MXenes, but the highly reactive etchant could destroy the structure of MXene during the etching process, especially for nitride MXenes [³] which hence increases the difficulties of handling nitride MXene synthesis. In this study, we explore the different etching methods of MXene from Ti_2AlN as the main precursor. The quality of resultant powders of Ti_2N MXene were confirmed by the Raman spectroscopy and XRD pattern. We then investigated the morphology of Ti_2N MXene by SEM and TEM. Our work could provide a more approachable method of synthesizing nitride MXene.

References

- [1] Anasori, B., Lukatskaya, M. R. & Gogotsi, Y., *Nat. Rev. Mater.* **2**, 1–17 (2017).
- [2] Urbankowski, P., Anasori, B., Makaryan, T., Er, M., Kota, S., Walsh, P.L., Zhao, M., Shenoy, V.B., Barsouma, M.W., Gogotsi, Y., *Nanoscale* **8**, 11385 (2016).
- [3] Zhang, L., Song W., Liu H., Ding H., Yan Y.,¹, Chen R., *A Review. Processes* **10**, 1744 (2022).

On-chip chalcogenide glass resonators and waveguides for mid-infrared applications

Hansuek Lee^{a,b}, Daewon Suk^b, Kiyoungh Ko^a, Soobong Park^a, Dohyeong Kim^a, Seong Cheol Lee^a,
Kwang-Hoon Ko^c, Fabian Rotermund^a, Duk-Yong Choi^d

^a Department of Physics, Korea Advance Institute of Science and Technology

^b Graduate School of Nanoscience and Technology, Korea Advance Institute of Science and Technology

^c Laser Application Research Team, Korea Atomic Energy Research Institute, Daejeon 34057, South Korea

^d Department of Quantum Science and Technology, Research School of Physics, Australian National University, Canberra, Australia

E-mail address: hansuek@kaist.ac.kr

Abstract: We discuss the recent advancement of nonlinear optical sources based on on-chip chalcogenide waveguides and resonators with extremely low loss, as well as their applications in the mid-infrared wavelength region.

1. Introduction

Chalcogenide glasses have attracted great attention due to their extraordinarily low material absorption in the mid-infrared wavelength range, in addition to their high nonlinearity and photorefractive effect. Here, we present a method for fabricating on-chip chalcogenide waveguides and resonators with extremely low optical loss. The loss was reduced to the level of the inherent material absorption by introducing a method for forming a light-guiding geometry on a chip by depositing a core material without a following etching process. The applications of these chalcogenide optical components are presented such as Brillouin lasing process and supercontinuum generation in the mid-infrared.

2. Device design, fabrications, and optical characteristics

Chalcogenide glasses are of significant interest due to their high mid-IR transparency and nonlinearity [1]. However, their irregular nanostructure, which results from differences in stoichiometry and bond structures, can result in nanoscale roughness when etched due to nonuniformity in the local etch rate [2]. To address this problem, a universal method has been created that enables the definition of light-guiding structures on a chip with extremely smooth surfaces without etching the core. This is accomplished by depositing chalcogenide glass on a silica platform structure with a trapezoidal cross-section, where the top-flat region of the deposited chalcogenide serves as the core that confines light. Using this method, ring resonators with optical Q-factors greater than 10^7 have been fabricated successfully. The waveguide loss attained from the Q-factor was comparable to the state-of-the-art optical fibers made from the same material [3].

3. Applications – Brillouin lasers

By matching the free spectral range to the Brillouin phonon frequency, the Brillouin lasing process was observed in the near-IR with a threshold that was approximately one hundred times lower than previous chalcogenide devices because of the enhanced Q-factor [3]. We will also present the recent observation of the Brillouin scattering process in the mid-IR.

4. Applications – Supercontinuum and molecular sensing

By designing waveguide dispersion to support ultra-wide spectrum broadening, efficient supercontinuum generation was observed in the near-infrared and mid-infrared regions [4]. We resolved the absorption spectra of the fundamental vibration state of carbon dioxide and carbon monoxide molecules and quantitatively measure the gas pressure by the cepstrum analysis method.

5. Discussions

In the presentation, we will discuss the exciting potential applications of nonlinear mid-infrared optical sources based on on-chip chalcogenide high-Q resonators and low-loss waveguides. By exploiting the unique characteristics of chalcogenide glasses, such as their high mid-infrared transparency and high nonlinearity, it is possible to create optical devices with unprecedented precision and sensitivity.

[1] Eggleton, B. J., Luther-Davies, B. & Richardson, K., *Nature Photonics* **5**, 141 (2011)

[2] Choi, D. Y., Madden, S., Rode, A., Wang, R. & Luther-Davies, B., *Journal of Applied Physics* **102**, 083532 (2007)

[3] Dae-Gon Kim, Sangyoon Han, Joonhyuk Hwang, In Hwan Do, Dongin Jeong, Ji-Hun Lim, Yong-Hoon Lee, Muhan Choi, Yong-Hee Lee, Duk-Yong Choi, Hansuek Lee, *Nature Communications* **11**, 5933 (2020)

[4] Joonhyuk Hwang, Dae-gon Kim, Sangyoon Han, Dongin Jeong, Yong-Hee Lee, Duk-Yong Choi, Hansuek Lee, *Optics Letters* **46**, 2413 (2021)

Parallel Information Processing and Computation using Optical Frequency Combs

Myoung-Gyun Suh

Physics & Informatics Laboratories, NTT Research, Inc., Sunnyvale, CA 94085, USA
E-mail address: mgsuh@ntt-research.com

Abstract: We introduce a parallel optical matrix-vector multiplier employing mixed space-frequency multiplexing of optical frequency combs. With spatial multiplexing and hyperspectral encoding, this modular, scalable, and programmable system can enable future optical information processing beyond Peta OPS.

The recent advancement of machine learning has revolutionized numerous industries, resulting in a surge in demand for matrix-vector multiplication (MVM) operations, essential for various algorithms, particularly in deep learning and large-scale optimization. This growing computational requirement challenges traditional von Neumann computing architectures, prompting researchers to explore alternate approaches like in-memory computing [1]. In-memory computing addresses the performance bottleneck by incorporating non-volatile memory elements within the processor, enabling efficient data reuse, reduced power consumption, and highly parallel computations. Simultaneously, there is increasing interest in using optics for energy efficient MVM. Although optical MVM systems have been demonstrated [2, 3], developing a highly parallel, precise, programmable, and scalable optical computing system remains a challenge. We propose an optical computing system incorporating these features, inspired by parallel information processing schemes in spectroscopy [4], imaging [5], and display. The demonstrated MVM system employs mixed space-frequency multiplexing of optical frequency combs [5, 6] and Spatial Light Modulators (SLMs) [7,8] for highly parallel optical information processing due to their precision and scalability. The SLM serves as programmable optical memory for fixed matrix operations, like combinatorial optimization problem solvers, and as a parallel optical modulator for varying matrix operations. In the system, 45 GHz-spaced comb lines are generated via cascaded electro-optical modulation of a continuous-wave laser at the optical C-band, and input vector elements (x_i) are encoded in comb line intensities using line-by-line waveshaping [8]. Comb lines are spatially separated by two gratings, elongated, fanned out vertically by a cylindrical concave lens, and focused on the SLM, encoding matrix elements (M_{ij}) as attenuation weights. A beam splitter (BS) captures the optical matrix on a 2D short-wavelength infrared (SWIR) camera. Lastly, the matrix is summed horizontally and detected by a line-SWIR camera, completing the MVM or multiply-accumulate (MAC) operation. We analyzed error distribution for each MAC value with a unit input vector and 2-bit matrix, attributing errors to comb line intensity fluctuations and accumulated detector noise. Optical summation is expected to improve precision by enhancing the signal-to-noise ratio at detector pixels.

Our optical MVM multiplier leverages advances in SLM and optical frequency comb technologies. Utilizing frequency, space, and time multiplexing, the system maximizes computational speed and throughput. The system is also highly scalable with spatial and frequency multiplexing, and scalable SLM display technology. In addition, matrix-matrix multiplication is also possible in a similar architecture when a Virtually Imaged Phased Array (VIPA) is used with gratings, allowing hyperspectral encoding for higher throughput. Furthermore, spatial multiplexing using 2D arrays of optical components can enable scaling of the physical system. Importantly, the modular nature of our system, with well-defined roles for critical components, allows for independent improvements of components and improved overall system performance. With spatial multiplexing and hyperspectral encoding in addition to advances in component technologies, such an architecture can enable future optical information processing systems beyond Peta operations per second (OPS).

References

- [1] A. Sebastian, M. Le Gallo, R. Khaddam-Aljameh, and E. Eleftheriou, "Memory devices and applications for in-memory computing," *Nat. nanotechnology* 15, 529–544 (2020).
- [2] J. Feldmann, N. Youngblood, M. Karpov, H. Gehring, X. Li, M. Stappers, M. Le Gallo, X. Fu, A. Lukashchuk, A. S. Raja et al., "Parallel convolutional processing using an integrated photonic tensor core," *Nature* 589, 52–58 (2021).
- [3] T. Wang, S.-Y. Ma, L. G. Wright, T. Onodera, B. C. Richard, and P. L. McMahon, "An optical neural network using less than 1 photon per multiplication," *Nat. Commun.* 13, 123 (2022).
- [4] S. A. Diddams, L. Hollberg, and V. Mbele, "Molecular fingerprinting with the resolved modes of a femtosecond laser frequency comb," *Nature* 445, 627–630 (2007).
- [5] C. Bao, M.-G. Suh, and K. Vahala, "Microresonator soliton dual-comb imaging," *Optica* 6, 1110–1116 (2019).
- [6] E. Hase, T. Minamikawa, T. Mizuno, S. Miyamoto, R. Ichikawa, Y.-D. Hsieh, K. Shibuya, K. Sato, Y. Nakajima, A. Asahara et al., "Scan-less confocal phase imaging based on dual-comb microscopy," *Optica* 5, 634–643 (2018).
- [7] U. Efron, *Spatial light modulator technology: materials, devices, and applications*, vol. 47 (CRC press, 1994).
- [8] A. M. Weiner, "Femtosecond pulse shaping using spatial light modulators," *Rev. scientific instruments* 71, 1929–1960 (2000).

Extremely broadband topological waveguide coupler based on odd-number Su-Schrieffer-Heeger chains

Yu Sung Choi¹, Youngsun Choi¹, Jae Woong Yoon¹

*Department of physics, Hanyang University, Seoul 04763, Korea
yoonjw@hanyang.ac.kr*

Abstract: A basic model of topological insulators, the Su-Schrieffer-Heeger (SSH) model, has been applied in various photonic systems for novel optical effects and related applications. Here, we show that odd-numbered SSH chains enable extremely broadband waveguide couplers. A special feature of odd-numbered SSH chain is that there is always a zero-energy localized state regardless of its bulk topological invariant. We utilize this unique feature in adiabatic photonic waveguide systems for spectrally robust optical power dividers or combiners as opposed to the conventional, wavelength-dependent interferometric components such as directional couplers and multimode interference couplers. We demonstrate broadband edge-to-edge and 1×N couplers with their power balance persisting over the entire optical telecommunications bands. We provide detailed theory, experimental results, and remaining challenges.

The topological energy transfer mechanism has been extensively studied in the field of solid-state physics and has been applied to optics [1]. In particular, quantized charge transport is protected by the topological invariants, which enables robust energy and signal transport against coupling-induced perturbations [2,3]. In this paper, we analyze the energy band and properties of the Su-Schrieffer-Heeger (SSH) chain with the odd number of atomic sites. In the conventional even-sized SSH model, the zero-energy state, *i.e.*, the topological edge state, depends on relative strengths of inter-cell c_1 and intra-cell c_2 coupling constants. In contrast, in the odd-numbered SSH chain, edge states always exist regardless of the coupling strength between sites. This property provides remarkable advantages in terms of robustness of the energy transfer against parametric changes.

We analyze the band structure of an SSH chain with an odd number of sites as a function of the coupling strength, comparing it to the case of the conventional model. As shown in Fig. 1, we confirm that in the case of an SSH chain with the odd number of sites, there always exists a zero-energy state independent of the coupling strength. In particular, we demonstrate that the case of $c_1 = c_2$ results in the wave function being uniformly present only on the odd-numbered sites. These characteristics provide an edge-to-edge energy transport, as it enables the transport without passing through the canonical conduction-band states.

We propose an optical waveguide array based on an odd-numbered SSH model. As shown in Fig 2, we design such a waveguide array on the standard silicon-on-insulator platform. The selected structural parameters for the optical wavelength correspond to a core height and width of 260 nm and 400 nm, respectively, at an operating wavelength of 1,550 nm. The spacing between adjacent optical wavelengths is in the range of 50 to 550 nm. To obtain edge-to-edge optical power transfer, we adjust the distance between adjacent optical waveguides in accordance with adiabatic conditions and the propagation direction of light. When the design of the output section of a waveguide array sets the spacing between all waveguides to be the same, output wave is uniformly distributed to every waveguide at the odd-number sites. Figures 3(a) and 3(b) show the operation of a directional coupler and a 1-to-N splitter, respectively.

In conventional waveguide couplers, the coupling coefficient depends on the wavelength due to its reliance on interference. In contrast, as shown in Fig 4, our topological waveguide coupler exhibits considerably weaker wavelength dependence, enabling broadband operation over the entire optical telecommunication bands. We expect that the topological waveguide is applicable to various photonic components including optical signal dividers, combiners, resonant filters, optical comb generators, and many others wherever the broadband stable coupling is desired.

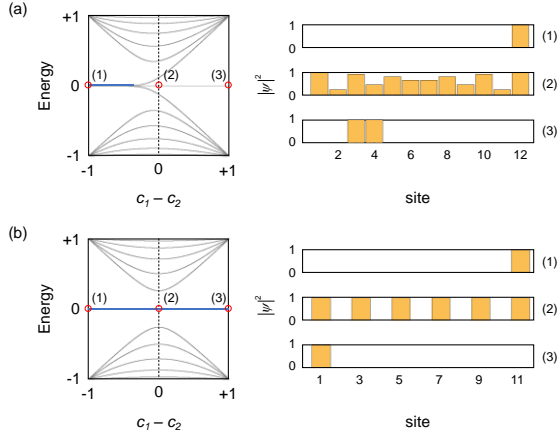


Fig. 1. Band structure of (a) even and (b) odd-number SSH chain

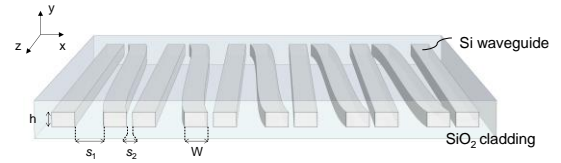


Fig. 2. Schematic of topological waveguide coupler

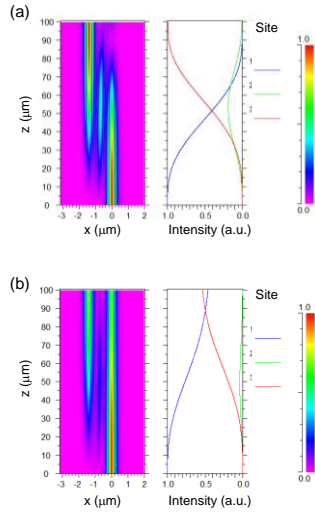


Fig. 3. BPM calculation for (a) directional coupler, (b) splitter.

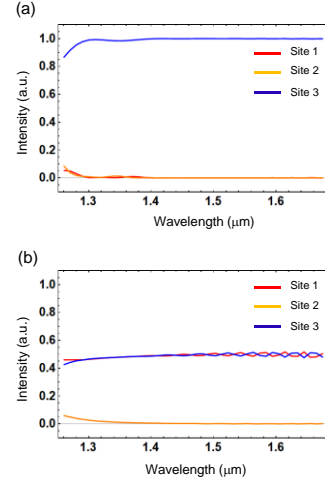


Fig. 4. Broadband operation over the entire optical telecommunication bands.

References

- [1] Nakajima, Shuta, et al. "Topological Thouless pumping of ultracold fermions." *Nature Physics* 12.4 (2016): 296-300.
- [2] Thouless, D. J. "Quantization of particle transport." *Physical Review B* 27.10 (1983).
- [3] Liu, Weijie, et al. "Observation of edge-to-edge topological transport in a photonic lattice." *Physical Review A* 105.6 (2022).

Nonreciprocal fiber-optic amplifier enabled by encircling-an-EP emulation and gain saturation nonlinearity.

Seung Han Shin, Yu Sung Choi, and Jae Woong Yoon

Department of Physic. Hanyang university
jwoon@hanyang.ac.kr

Abstract: Optical nonreciprocity is required in many optical systems for signal stabilization, laser protection, non-destructive probing. Here, we experimentally demonstrate a nonreciprocal fiber-optic amplifier enabled by encircling-an-exceptional-point emulation and gain-saturation nonlinearity. We realize the proposed system by combining optical attenuators, Erbium-doped fiber amplifiers (EDFA), and 2×2 couplers. We obtain remarkably high nonreciprocal transmission ratio > 20 dB persisting over the entire gain band from 1,530 to 1,560 nm at moderate input power conditions from 0.1 to 1 mW.

Breaking the time-reversal symmetry in optical transmission has been studied for a long time because of its importance in fundamental study and applications. Previously, the optical nonreciprocity by means of stationary components is mainly based on magneto-optic crystals or asymmetric nonlinear resonators. Unfortunately, they have limitations such as integration incompatibility or narrow operation band. In order to obtain broadband optical nonreciprocity in integration-compatible manners, various approaches have been proposed so far. Dynamically encircling an exceptional point (EP) combined with optical nonlinearity [1] is one out of many different approaches. Realizing such a system, there are several difficulties such as simultaneous real and imaginary potential distributions and combining it with certain available optical nonlinearity. Here, we propose a nonlinear 2×2 fiber-optic coupler that produces the effect of the nonlinear encircling-an-EP process by using simple off-the-shelf optical components as demonstrated in Fig. 1. Although our system is not realized on an integrated optics platform, it demonstrates an experimental proof of the concept.

In order to avoid potential complications for the dynamically encircling an EP while obtaining the desired identical effect, we employ an emulating fiber-optic system originally suggested in [2] and combine it with native gain-saturation nonlinearity in Erbium-doped-fiber amplifiers (EDFA). Through this system, as shown in Fig. 2, we experimentally confirm the desired mode switching action and nonreciprocal optical transmission. Importantly, the competition between unsaturated loss and saturated gain results in highly robust performance against wavelength change. The experimental result in Fig. 3 demonstrates nonreciprocal transmission ratio (NTR) as high as 30 dB, 20-dB bandwidth ~ 30 nm (= gain bandwidth), and moderate input optical power range from 0.1 to 1 mW.

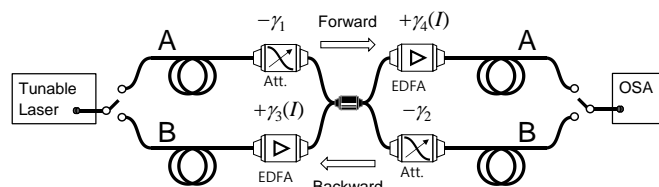


Fig.1. 2×2 fiber-optic coupler

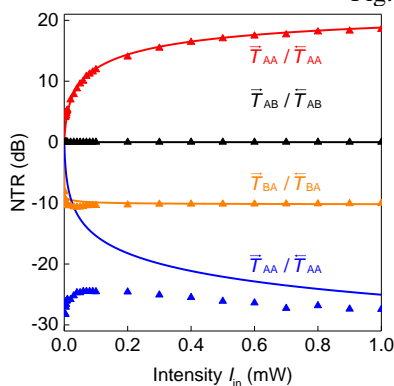


Fig. 2. Nonreciprocal transmission ratio by input intensity

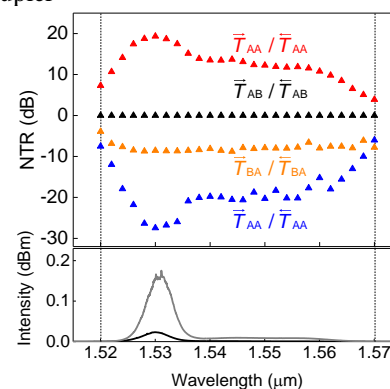


Fig. 3. Nonreciprocal transmission ratio by wavelength and EDFA emission spectrum

- [1] Choi, Youngsun, et al. "Extremely broadband, on-chip optical nonreciprocity enabled by mimicking nonlinear anti-adiabatic quantum jumps near exceptional points." *Nature Communications* 8.1 (2017): 14154.
[2] Khurgin, J. B., et al. "Emulating exceptional-point encirclements using imperfect (leaky) photonic components: asymmetric mode-switching and omni-polarizer action." *Optica* 8.4 (2021).

One-step Optical Quantification of DNA Loading on Gold Nanoparticles

Jaewon Lee¹ and Seungwoo Lee^{1,2,3,4*}

¹KU-KIST Graduate School of Converging Science and Technology, ²Department of Integrative Energy Engineering, ³Department of Biomicrosystem Technology, and ⁴KU Photonics Center, Korea University, Seoul 02841, Republic of Korea
E-mail address: seungwoo@korea.ac.kr

Abstract: The conventional methods used to quantify DNA loading on gold nanoparticles (Au NPs) involve physical detachment of DNA from Au NPs, which is time-consuming and unreliable. Here, we proposed an optical alternative that uses effective medium theory and molecular dynamics (MD) simulation in combination with the absorption spectra measurements of DNA-Au NPs. This approach enables non-invasive, rapid, and reliable quantification of DNA loading on Au NPs, which can facilitate the use of DNA-Au NPs as a versatile tool for both experts and newcomers.

DNA-coated gold (Au) colloidal nanoparticles (hereafter abbreviated as DNA-Au NPs) have become the spearhead in the rapid advancement of nanotechnology due to their exotic ability to control the self-assembled geometry and site-specific functionality. These properties have enabled their wide range of applications in sensing, therapeutics, and molecular imaging [1]. However, their immediate and translational use has been limited by the necessity of quantifying DNA loading on Au NPs, which significantly affect their functionalities in self-assembly, target delivery, and sensing capacity. Although there has been a consistent search for the reliable quantifying method, most of the quantifying protocols are heavily rely on just one approach: physical detachment/segregation of DNA from Au NPs and quantifying their amount, which can be time-consuming and unreliable [2].

In this work, we propose a non-invasive and rapid method to quantify DNA loading on Au NPs by merely measuring visible absorption spectra of DNA-Au NPs [3]. Herein, we utilized the simple fact that the DNA shell layer on Au NPs can be considered as a homogeneous medium with effective permittivity (ϵ), which induce the localized surface plasmon resonance (LSPR) peak shift of Au NPs. More specifically, the LSPR peak shift can be used to determine DNA loading density on Au NPs by (i) constructing a combinatorial library of effective ϵ and DNA shell thickness as a function of DNA density through effective medium theory and MD simulation, (ii) theoretically calculating LSPR peak shift, and (iii) matching these results with the experimental LSPR peak shifts. Once the combinatorial libraries and theoretically calculated LSPR peak shifts are established, the end user can get information on DNA loading density by only measuring LSPR peak shift. Therefore, our method significantly simplifies the quantification procedures compared to conventional methods.

To verify the proposed approach, we prepared DNA-Au NPs and quantified the DNA loading density upon varying sodium ion (Na^+) concentration, size of NPs, and length of DNA. Indeed, the optically measured DNA loading density increased with Na^+ concentration and decreased with the size of NPs and length of DNA, matching well with the conventional quantification (Fig. 1a). We further tested the reliability of the optical method by assessing quantification reproducibility between researchers with different levels of experience. It turned out that the optical approach led to the highly consistent quantification results among the researchers, unlike the conventional counterparts (Fig. 1b). Taken together, we demonstrated that the optical method presented here enables non-invasive and rapid quantification of DNA loading on Au NPs with high reliability and accuracy. Benefitting from its simplicity and versatility, we anticipate that this framework will addresses the gap in analytical integrity between the beginners and experts.

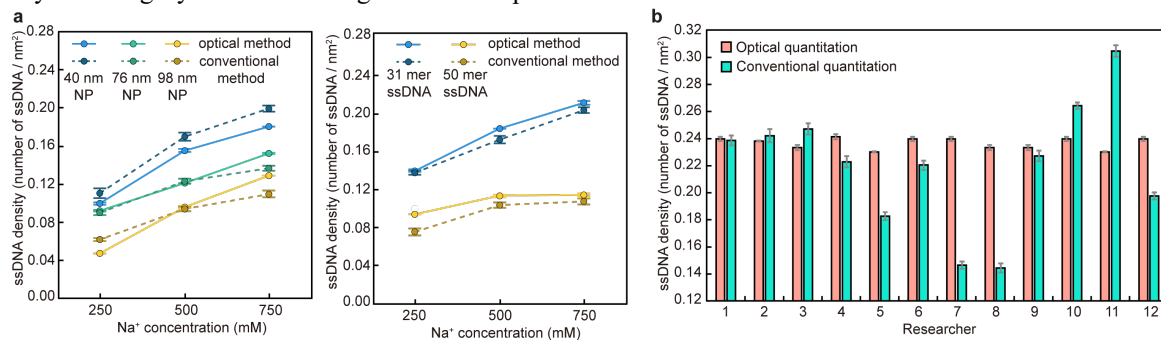


Fig 1. (a) Optically quantified DNA loading density with varying Na^+ concentration, NP size, and DNA length. (b) Quantified DNA loading density using optical (red bars) and conventional (green bars) method by researchers with different levels of experience.

- [1] H. Xin, B. Namgung, and L. P. Lee, *Nat. Rev. Mater.* **3**, 228-243 (2018).
[2] B. Liu, and J. Liu, *Anal. Methods.* **9**, 2633-2643 (2017).
[3] J. Lee, and S. Lee, *Anal. Chem.* **95**, 1856-1866 (2023).

Rapid inverse design of metasurfaces for all optical image processing

N. Priscilla^a, L. Wesemann^a, S. Sulejman^a, L. Clark^b, T.J. Davis^a and A. Roberts^a

^aARC Centre of Excellence for Transformative Meta-Optical Systems, School of Physics, The University of Melbourne, VIC 3010, Australia

^bSchool of Physics, The University of Melbourne, VIC 3010, Australia

Author e-mail address: npriscilla@student.unimelb.edu.au

Abstract: Metasurfaces with potential applications in image processing and real-time phase imaging with a large numerical aperture and high contrast are generated through rapid inverse design via a mode matching technique.

1. Introduction

The manipulation of light on the nanoscale has become possible through the structuring and fabrication of novel materials. This technology has led to miniaturization of optical systems with one emerging example in real-time image processing. Nanostructures in these applications have optical responses that enable access to and alteration of the spatial information carried by an optical field or image. However, designing metasurfaces with multiple degrees of freedom using full-field solvers such as the finite element method (FEM) can be time-consuming and computationally expensive. To address this issue, we use a rapid optimization method for metasurface design that couples a modal matching technique (MMT) in the monomode approximation with an optimization algorithm. The MMT is a quasi-analytic model initially developed for calculating the optical response of perfectly electrically conducting frequency selective surfaces [1,2]. Although the MMT sacrifices precision compared with full-field approaches, it can determine the broad optical characteristics of a device orders of magnitude faster which can then be fine-tuned using a full field solver.

2. Results

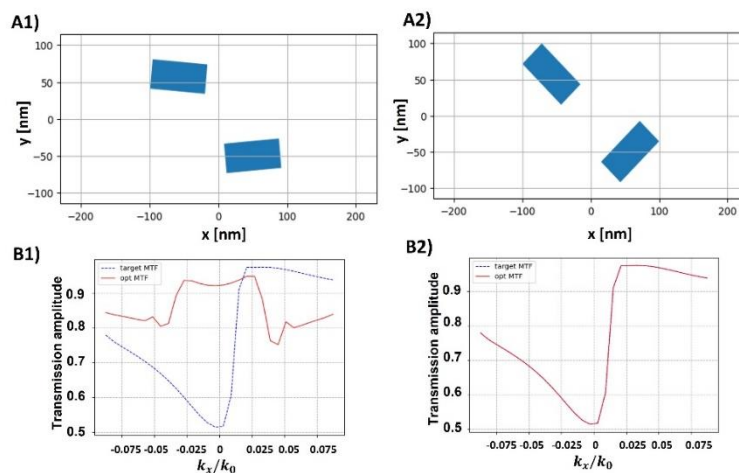


Fig. 1. Initial (A1) and optimised (A2) unit cell designs with their respective optical transfer functions in (B).

The metasurface designs produced by the MMT involve the arbitrary placement of two or more plasmonic nanorods in a unit cell, setting a target optical response, and adjustments of certain geometrical parameters, such as rod sizes, orientation and periodicity of the unit cell. We tested the capability of this algorithm by using a device design with a known asymmetrical optical response [3]. Initially, two silver rods were placed in the unit cell (Fig. 1ai) and a target modulation transfer function is given. The result replicates the design of the spin orbit structure with precise matching of the transfer function.

Using this optimization algorithm, several device designs that exhibit a linear optical transfer function with high numerical aperture (> 0.3) and high contrast were generated and will be presented. The application of the devices to phase contrast imaging is demonstrated alongside preliminary experimental results. These metasurfaces have potential for applications in bioimaging and remote sensing, without the need for bulky or expensive components.

4. References

- [1] C. Chen, IEEE Transactions on Antennas and Propagation, Vol. AP-18, 5 (1970).
- [2] D. H. Dawes, R. C. McPhedran and B. Whitbourne, Appl. Opt., 28(16), 3498-3510 (1989).
- [3] L. Wesemann, J. Rickett, T. J. Davis, and A. Roberts, ACS Photonics 9 (5), 1803-1807 (2022)

Adaptive-Tunable Nanogap-Enhanced Raman Scattering

Taeyoung Moon[†], Bamadev Das[‡], Huitae Joo[†], Yeonjeong Koo[†], Mingu Kang[†],
Hyeongwoo Lee[†], Sunghwan Kim[‡], Yung Doug Suh^{*,†,§}, Dai-Sik Kim^{*,‡}, and Kyoung-Duck Park^{*,†}

Author affiliations

[†] Department of Physics, Pohang University of Science and Technology (POSTECH), Pohang 37673, Republic of Korea

[‡] Department of Physics and Quantum Photonics Institute, Ulsan National Institute of Science and Technology (UNIST), Ulsan 44919, Republic of Korea

[¶] Department of Chemistry & School of Energy and Chemical Engineering, Ulsan National Institute of Science and Technology (UNIST), Ulsan, 44919 Republic of Korea

[§] Center for Multidimensional Carbon Materials (CMCM), Institute for Basic Science (IBS), Ulsan 44919, Republic of Korea
E-mail address: ydsuh@unist.ac.kr, daisikkim@unist.ac.kr, parklab@postech.ac.kr

Abstract: Nanogap-enhanced Raman scattering (NERS) enables sensitive observations of the chemical properties of various materials. However, due to narrow and not tunable GP resonance at static gap-plasmonic structures, broad-spectral NERS analysis has not been demonstrated. In this work, we present an adaptive-tunable NERS platform to selectively enhance and modulate different vibrational modes via active flexible Au nanogap, with adaptive optical control. This study provides a flexible nanogap platform for observing and controlling the enhanced chemical responses of various materials with dynamic tunability.

1. Introduction

Plasmon-enhanced Raman scattering enables high-speed, label-free, and biomedical sensing through quantitative analysis of Raman fingerprints [1]. Specifically, gap-plasmonic structures produce greater Raman enhancement compared to that of single-antenna type plasmonic structures. However, most NERS platforms have a narrow spectral range of gap plasmon (GP) resonance with a fixed photon energy due to their static structures. Thus, the spectral range of plasmon-enhanced Raman scattering is significantly restricted. This study presents a tunable NERS platform via a flexible 1D plasmonic nanogap, facilitating the selective enhancement of different Raman spectral regions of chemical molecules. We demonstrate tunable NERS spectra of brilliant cresyl blue (BCB) molecules, selectively enhancing different Raman spectral regions by the tunability of GP resonance ($\sim 1200 \text{ cm}^{-1}$) through engineering gap width. We present an adaptive NERS (a-NERS) approach to additionally increase the NERS enhancement factor by up to $\sim 150 \%$.

2. Results and discussion

Fig. 1.(a) illustrates the resonance tunable NERS experiment. We fabricated an active flexible Au nanogap device based on a PET substrate and placed BCB molecules into the nanogap using spin-coating and rinsing methods. Moreover, this gap-tunable platform provides resonance tuning of GP, that is, the GP resonance (λ_{GP}) is redshifted when gap width (w_{gap}) decreases. Thus, frequency-selective NERS sensing is reversible. We perform a tunable NERS sensing experiment for the BCB molecules by changing the GP resonance. Fig. 1.(b) shows the measured NERS spectra at $w_{\text{gap}} = 42 \text{ nm}$ (blue) and $w_{\text{gap}} = 26 \text{ nm}$ (red). When we set $w_{\text{gap}} = 42 \text{ nm}$, the GP resonance near the Raman mode of $\sim 584 \text{ cm}^{-1}$ emerged and the Raman intensity in the corresponding spectral region highly enhanced. When we switch the GP resonance to $\sim 1600 \text{ cm}^{-1}$ by decreasing w_{gap} to 26 nm , the Raman modes near the $\sim 1600 \text{ cm}^{-1}$ highly enhanced with a decreasing Raman signal of the $\sim 584 \text{ cm}^{-1}$ mode. Fig. 1.(c) shows the adaptive NERS (a-NERS) spectrum of the BCB molecules at $w_{\text{gap}} = 42 \text{ nm}$. The a-NERS intensity of the target peak ($\nu \approx 584 \text{ cm}^{-1}$) is $\sim 150 \%$, enhanced with the optimal PM (top) compared to the normal NERS intensity with linearly polarized excitation (bottom).

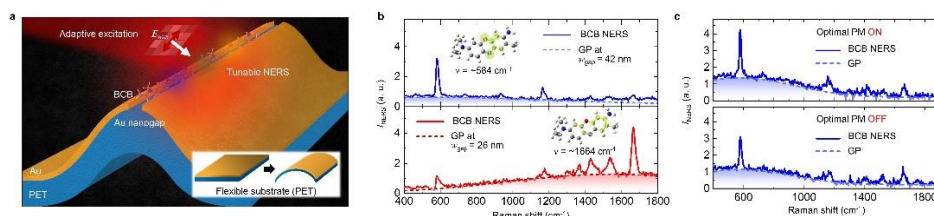


Fig. 1. Flexible Au nanogap for tunable 1D NERS applications. (a) Schematic illustration of tunable NERS sensing for BCB molecules using a flexible Au nanogap, in combination with adaptive excitation wavefront shaping. (b) Measured NERS spectra of BCB molecules (solid line) at $w_{\text{gap}} = 42 \text{ nm}$ and $w_{\text{gap}} = 26 \text{ nm}$ of the flexible nanogap. The background board spectra (dashed line) show the corresponding response of GP resonance. (c) Adaptive NERS (a-NERS) spectra exhibiting an additional NERS enhancement through the wavefront shaping using a SLM.

Gap-Plasmon-Enhanced Broadband Photodetection in a Plasmonic Superconducting Photon Detector

Jing-Wei Yang¹, Feng-Yang Tasi^{1,2}, Tzu-Yu Peng^{1,2}, Jia-Wern Chen¹, Yu-Jung Lu^{1,2,3*}

¹Research Center for Applied Sciences, Academia Sinica, Taipei 11529, Taiwan

²Graduate Institute of Applied Physics, National Taiwan University, Taipei 10617, Taiwan

³Department of Physics, National Taiwan University, Taipei 10617, Taiwan

Author e-mail address: possibleantony@gmail.com

Abstract: We designed and demonstrated a superconducting NbN microwire photon detector with gap plasmon resonance-enhanced photodetection. FDTD calculation results show the mode profile with a gap plasmon resonance at 532 nm, and the optical field strongly confined in a 5-nm thick Al_2O_3 layer sandwiched between Ag nanoparticle and NbN microwire; the local field-induced heating can destroy the Cooper pairs and further improve the detection efficiency. We further demonstrate broadband photodetection ranging from 400 nm to 637 nm with wavelength-independent high detection efficiency by designing different sizes of Ag nanoparticles.

Introduction

Superconducting nanowire single-photon detectors (SNSPDs) have been widely studied in recent decades because their intrinsic detection efficiency is higher than those with microwires. However, the nanofabrication of large-area nanowire superconducting photodetectors is challenging. For example, a superconducting wire with narrower width performs a higher detection efficiency than a wider wire, but it may have a smaller detection area, polarization-dependent detection, and its critical temperature is suppressed at the same time. To overcome this predicament, we designed and demonstrated a superconducting NbN microwire photon detector with gap plasmon resonance enhanced photodetection. FDTD calculation results show the mode profile with a gap plasmon resonance at 532 nm, and the optical field strongly confined in a 5-nm thick Al_2O_3 layer sandwiched between Ag nanoparticle (with 40 nm long and 30 nm thick) and NbN microwire, the local field induced heating can destroy the Cooper pairs and further improve the detection efficiency. We further demonstrate broadband photodetection with wavelength-independent high detection efficiency by designing different sizes of Ag nanoparticles with various gap plasmon resonant wavelengths. Hence, we can enhance the photoresponse of the detector for a wide visible range from 400 nm to 637 nm with a minimum detectable power of 0.1 nW. In the end, we will discuss the advantages of the designed plasmonic NbN microwire photon detector, including polarization independence, low kinetic inductance, large active area, and high photoresponse in the visible light region.

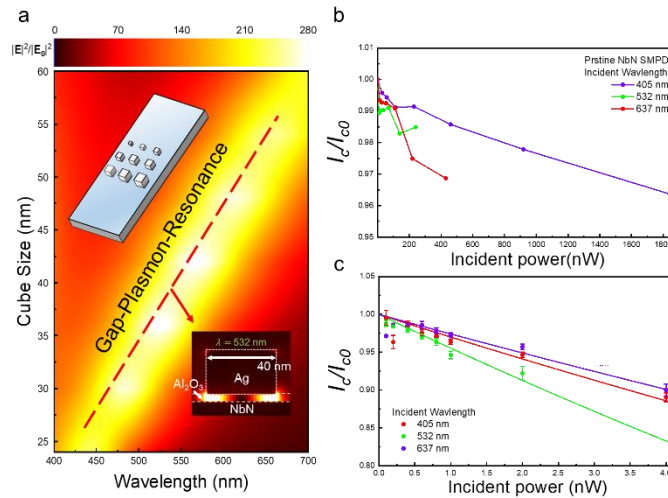


Fig. 1: **a.** The color map of numerically calculated $|E|^2/|E_0|^2$ spectra as a function of the size of the Ag nanoparticles. **b.** The measured critical current difference of pristine NbN SSPD with incident light of 405 nm, 532 nm and 637 nm. **c.** The measured critical current difference (dots) of GPR-enhanced SMPD with incident light of 405 nm, 532 nm and 637 nm. The solid lines were calculated by hot-belt model.

Tip-enhanced Raman spectroscopy for nanoscale resolving the electronic properties and chemical activities

Huishu Feng, Tengxiang Huang, Xiang Wang, Bin Ren*

Department of Chemistry, Xiamen University, Xiamen 361005, China

E-mail address: bren@xmu.edu.cn

Abstract: Tip-enhanced Raman spectroscopy (TERS), which combines scanning probe microscopy and plasmon-enhanced Raman spectroscopy, is capable of simultaneously obtaining the topographical and Raman fingerprint information at nanometer spatial resolution. Such a spatial resolution will allow the identification of the local physicochemical properties of different sites on the nanocatalysts without bothering the averaged effect in ensemble measurements, which makes it possible to disentangle the electronic effect and geometric effect with the change of the size. We visualized the size-specific electronic, geometric and catalytic properties of the different sites located on the individual Pd nanocatalyst by real-space TERS imaging with 3 nm spatial resolution. We further developed electrochemical tip-enhanced Raman spectroscopy (EC-TERS) for in situ monitoring the geometric and electronic evolution of individual active sites of MoS₂ during hydrogen evolution reaction (HER) and revealed the progressive generation of active sites during the electrochemical activation and reaction processes. These discoveries offer new insights into our understanding of the active site and its dynamics during electrocatalytic processes.

Sub-nanometer Resolved Single-Molecule Optical Imaging

Zhen-Chao Dong

Hefei National Research Center for Physical Sciences at the Microscale, University of Science and Technology of China, Hefei, China
E-mail address: zcdong@ustc.edu.cn

Aspirations for reaching atomic resolution with light have been a major force in shaping nano-optics, whereby a central challenge is to achieve highly localized optical fields. The plasmonic nanocavity defined by the coinage-metal tip and substrate in a scanning tunneling microscope (STM) can provide highly confined and dramatically enhanced electromagnetic fields upon proper tuning of plasmonic resonance, which can modify both the excitation and emission of a single molecule inside the nanocavity and produce intriguing new optoelectronic phenomena. In this talk, I shall demonstrate two recent STM-based phenomena related to single-molecule optical spectroscopy. The first is single-molecule Raman scattering [1]. The spatial resolution of tip enhanced Raman spectroscopy (TERS) has been further driven down to the Angstrom scale at the single-bond level [2,3]. Such a capability not only yields a new methodology called scanning Raman picoscopy for structural reconstruction [3] and tracking bond breaking and forming of surface reactions [4,5], but also enables to clarify the chemical enhancement mechanism in TERS through well-controlled local contact environments [6,7]. The second phenomenon is single-molecule electroluminescence. Through managements over molecular quenching and energy level alignment, we demonstrate clear single-molecule electroluminescence and even single-photon emission [8]. Furthermore, by precisely controlling intermolecular distances, we can not only demonstrate coherent dipole–dipole coupling in homodimers [9], but also reveal intriguing transitions from incoherent hopping-like Forster energy transfer to coherent wavelike electronic energy transfer in donor–acceptor heterodimers [10]. In addition, the wavelike quantum-coherent transfer channel is found three times more efficient than the incoherent channel in a one-step transfer process, highlighting the advantage of coherent channels in electronic energy transfer processes in large molecular networks. Our results provide new routes to optical imaging, spectroscopy and engineering of light–matter interactions and intermolecular coupling at the sub-nanometer scale.

- [1] R. Zhang, Y. Zhang, Z. C. Dong*, S. Jiang, C. Zhang, L. G. Chen, L. Zhang, Y. Liao, J. Aizpurua, Y. Luo, J. L. Yang, and J. G. Hou*, *Nature* **498**, 82–85 (2013).
- [2] J. Lee*, K. T. Crampton, N. Tallarida and V. A. Apkarian*, *Nature* **568**, 78–82 (2019).
- [3] Y. Zhang, B. Yang, A. Ghafoor, Y. Zhang, Y. F. Zhang, R. P. Wang, J. L. Yang, Y. Luo*, Z. C. Dong* and J. G. Hou*, *Natl. Sci. Rev.* **6**, 1169–1175 (2019).
- [4] J. Y. Xu, X. Zhu, S. J. Tan*, Y. Zhang, B. Li, Y. Z. Tian, H. Shan, X. F. Cui, A. D. Zhao, Z. C. Dong, J. L. Yang, Y. Luo, B. Wang*, and J. G. Hou*, *Science* **371**, 818 (2021).
- [5] R. P. Wang, B. Yang, Q. Fu, Y. Zhang*, R. Zhu, X. R., Dong, Y. Zhang, B. Wang, J. L. Yang, Y. Luo, Z. C. Dong*, and J. G. Hou*, *J. Phys. Chem. Lett.* **12**, 1961–1968 (2021).
- [6] B. Yang, G. Chen, A. Ghafoor, Y. F. Zhang, Y. Zhang, Y. Zhang*, Y. Luo, J. L. Yang, V. Sandoghdar, J. Aizpurua, Z. C. Dong* and J. G. Hou*, *Nat. Photonics* **14**, 693–699 (2020).
- [7] B. Yang, G. Chen, A. Ghafoor, Y. F. Zhang, X. B. Zhang, H. Hang, X. R. Dong, R. P. Wang, Y. Zhang, Y. Zhang, and Z. C. Dong*, *Angew. Chem. Int. Ed.* (2023), e202218799. doi.org/10.1002/anie.202218799.
- [8] L. Zhang, Y. J. Yu, L. G. Chen, Y. Luo, B. Yang, F. F. Kong, G. Chen, Y. Zhang*, Q. Zhang, Y. Luo, J. L. Yang, Z. C. Dong* and J. G. Hou*, *Nat. Commun.* **8**, 580 (2017).
- [9] Y. Zhang, Y. Luo, Y. Zhang, Y. J. Yu, Y. M. Kuang, L. Zhang, Q. S. Meng, Y. Luo, J. L. Yang, Z. C. Dong* and J. G. Hou*, *Nature* **531**, 623–627 (2016).
- [10] F. F. Kong, X. J. Tian, Y. Zhang*, Y. Zhang, G. Chen, Y. J. Yu, S. H. Jing, H. Y. Gao, Y. Luo, J. L. Yang, Z. C. Dong* and J. G. Hou*, *Nat. Nanotechnol.* **35**, 713–719 (2022).

2-Dimensional and 3-Dimensional Hot Nanoparticles for near-field focusing

Sungho Park

Sungkyunkwan University, Korea

Surface plasmonics of nanomaterials has been one of the major research themes in nanoscience. The control of size and shape of corresponding nanoparticles is necessary to fully utilize their optical behavior for further applications, like biosensing, catalysis, and energy conversion. Here we successfully synthesized a new class of nanomaterials, 2-dimensional and/or 3-dimensional nanoframes with high uniformity through wet-chemistry. The synthetic strategy comprised serial reactions, which is executable on-demand, involving site-selective growth of Pt on the rim of Au nanoparticles, subsequent etching of Au, followed by regrowth of Au on the Pt rim, if the last structures are Au nanoframes. We will show how one can synthesize a variety of nanoparticles with rational synthetic steps. The resultant product exhibited unprecedented strong near-field focusing originating from nanogaps. In summary, we will discuss how one can rationally design and synthesize complex “hot nanoparticles” for maximizing near-field focusing.

Magnetic Topological Photonic Crystals

Baile Zhang^{1,2}

¹*Division of Physics and Applied Physics, School of Physical and Mathematical Sciences,
Nanyang Technological University, Singapore 637371, Singapore*

²*Centre for Disruptive Photonic Technologies, Nanyang Technological University, Singapore 637371, Singapore
E-mail address: blzhang@ntu.edu.sg*

Abstract: Over a decade ago, topological photonics came into existence with the discovery of the first photonic topological insulator, which comprised a two-dimensional (2D) periodic lattice of gyromagnetic rods, or a magnetic photonic crystal, with a topological band gap characterized by the Chern number. Despite the significant progress made in the field of topological photonics in recent years, the potential of magnetic photonic crystals has not been fully explored. On the other hand, the magnetic photonic crystals do provide a unique platform with broken time reversal symmetry, which is able to demonstrate a few interesting phenomena that are difficult in other platforms. In this talk, we present some of our recent works about the generalization of Chern-type bulk boundary correspondence: (1) from the Hermitian regime to the non-Hermitian regime, and (2) from edge states to surface states. The former involves the incorporation of two winding numbers with the Chern number in order to characterize the interaction between point-gap topology and line-gap topology. The latter requires the generalization of a scalar Chern number to a Chern vector that consists of three Chern numbers.

The field of topological photonics [1] investigates a novel class of photonic states that exhibit topological protection, similar to the behavior of electrons in topological quantum matter. This field began a decade ago with the realization of the first photonic topological insulator, a periodic lattice of gyromagnetic rods or a magnetic photonic crystal [2]. This achievement marked the first demonstration of the Chern insulator phase [3], even before its condensed-matter realization [4], highlighting the benefits of using photonic crystals for demonstrating challenging physics.

Despite its long history, the Chern-type bulk-boundary correspondence was established for Hermitian systems, without considering non-Hermitian topology, a newly developed topological description for non-Hermitian systems [5]. In a non-Hermitian system, the complex eigenenergy can form two types of band gaps: line gaps and point gaps [5]. While the line-gap topology can be inherited from the Hermitian counterpart, the point-gap topology is unique to non-Hermitian systems. A typical consequence of point-gap topology is the recently discovered non-Hermitian skin effect [6], where an extensive number of bulk states can be localized towards a boundary. However, the interaction between point-gap topology and line-gap topology is difficult to explore in experiment. We will discuss the design and demonstration of skin effect of Chern-number-protected chiral edge states, in the platform of a magnetic topological photonic crystal.

The generalization of topological insulators from 2D to 3D was a remarkable breakthrough in topological physics, upgrading topological states from edge states to surface states [7,8]. However, the realization of their photonic analogues in 3D, known as 3D photonic topological insulators, remains extremely challenging, with only a few realizations to date [9]. Recent studies in condensed matter systems have offered new avenues for exploration in magnetic topological insulators and magnetic topological semimetals. It is thus of particular interest to explore the potential of 3D magnetic topological photonic crystals. We will discuss the design and demonstration of a 3D magnetic topological photonic crystals [10].

References

- [1] T. Ozawa, H. M. Price, A. Amo, N. Goldman, M. Hafezi, L. Lu, M. C. Rechtsman, D. Schuster, J. Simon, O. Zilberberg and I. Carusotto, "Topological Photonics," *Rev. Mod. Phys.* 91, 015006 (2019).
- [2] Z. Wang, Y. D. Chong, J. D. Joannopoulos and M. Soljacic, "Observation of Unidirectional Backscattering-Immune Topological Electromagnetic States," *Nature* 461, 772 (2009).
- [3] F. D. Haldane, "Model for a quantum Hall effect without Landau levels: condensed-matter realization of the 'parity anomaly'," *Phys. Rev. Lett.* 61, 2015 (1988).
- [4] C.-Z. Chang, J. Zhang, X. Feng, J. Shen, Z. Zhang, M. Guo, K. Li, Y. Ou, P. Wei, L.-L. Wang, Z.-Q. Ji, Y. Feng, S. Ji, X. Chen, J. Jia, X. Dai, Z. Fang, S.-C. Zhang, K. He, Y. Wang, L. Lu, X.-C. Ma, and Q.-K. Xue, "Experimental observation of the quantum anomalous Hall effect in a magnetic topological insulator," *Science* 340, 167 (2013).
- [5] E. J. Bergholtz, J. C. Budich, and F. K. Kunst, "Exceptional topology of non-Hermitian systems," *Rev. Mod. Phys.* 93, 015005 (2021).
- [6] X. Zhang, T. Zhang, M.-H. Lu, and Y.-F. Chen, "A review on non-Hermitian skin effect," *Adv. Phys.* X 7, 2109431 (2022).
- [7] M. Z. Hasan and C. L. Kane, "Colloquium: topological insulators," *Rev. Mod. Phys.* 82, 3045 (2010).
- [8] X. L. Qi and S. C. Zhang, "Topological insulators and superconductors," *Rev. Mod. Phys.* 83, 1057 (2011).
- [9] Y. Yang, Z. Gao, H. Xue, L. Zhang, M. He, Z. Yang, R. Singh, Y. Chong, B. Zhang, and H. Chen, "Realization of a three-dimensional photonic topological insulator," *Nature* 565, 622, (2019).

[10] G.-G. Liu, Z. Gao, Q. Wang, X. Xi, Y.-H. Hu, M. Wang, C. Liu, X. Lin, L. Deng, S. A. Yang, P. Zhou, Y. Yang, Y. Chong, and B. Zhang, “Topological Chern vectors in three-dimensional photonic crystals,” *Nature* 609, 925 (2022).

Nonlinearity enabled higher-order exceptional point

Meng Xiao

Wuhan University, China

The role of nonlinearity on topology has been investigated extensively in Hermitian systems, while nonlinearity has only been used as a tuning knob in a PT-symmetric non-Hermitian system. Here, this talk shows that nonlinearity plays a crucial role in the topological classification of a non-Hermitian system. We provide a simple and intuitive example by demonstrating with both theory and circuit experiments an exceptional nexus (EX), a higher-order exceptional point with a hybrid topological invariant (HTI), within only two coupled resonators with the aid of nonlinear gain. The anisotropic critical behavior of the eigenspectra is verified with experiments. Our findings lead to advances in understanding the peculiar features of nonlinear non-Hermitian systems, possibly opening new avenues for applications.

Exceptional Points in Lossy Media for Deep Wave Penetration and Flat Radiation

Sangsik Kim

Korea Advanced Institute of Science and Technology, Korea

Wave propagation in lossy media is typically characterized by exponential intensity decay. However, recent research has linked exceptional point (EP) singularities in non-Hermitian systems to unconventional wave propagation. In this talk, we will present our recent discovery and demonstration on EPs-led exponential-decay-free wave propagation in a uniform lossy medium. A nanostructured photonic slab waveguide with EPs is used to observe up to 400-waves of deep wave propagation with a uniformly distributed energy loss. This unconventional wave propagation was analyzed by coupled-mode theory and electromagnetic simulations, confirming its relation to EPs. These results hold true across other physical waves and have immediate applications for generating large, uniform, and surface-normal free-space plane waves directly from photonic chips.

Minimal-Gain-Printed On-Demand Si-Integrable Continuous-Wave Nanolasers

Min-Woo Kim¹, Byoung Jun Park², Myung-Ki Kim², You-Shin No^{1,*}

¹Department of Physics, Konkuk University, Republic of Korea

²KU-KIST Graduate School of Converging Science & Technology, Korea University, Republic of Korea

Email address of corresponding author: ysno@konkuk.ac.kr

Abstract: A rapidly increasing demand for fast-bandwidth, low-power consumption and more compact miniaturization has unprecedentedly challenged the conventional limits of Si-based optical integration, and thus required key optical components to be as small as the operational wavelength or sometimes smaller than the physical limit of optics. However, despite the substantial progress being made in Si-based light modulation and detection and their large-scale, cost-effective, monolithic device integration technology, the realization of small, efficient, and reliable high-quality light sources, for example, continuous-wave (CW) III-V semiconductor nanolasers on Si at room temperature has remained a formidable challenge. We report on a new concept of on-demand Si-integrable nanolaser capable of operating under continuous-wave conditions at room temperature.

With the aid of advanced compound epitaxial techniques capable of realizing rich optical gain structures, e.g., multi-quantum-wells (MQWs), the integration of III-V materials on a Si platform has been considered as one of the most feasible and promising solutions for a laser-on-Si. Numerous approaches relying on flip-chip method, adhesive wafer-bonding via thermosetting polymer, and die-to-die/wafer bonding combined with low temperature plasma-assisted processes have successfully realized the III-V microlasers on Si substrate, demonstrating the hybrid and/or evanescent coupling to Si waveguides (WG). However, apart from the limitations of the rugged flip-chip process resulting in imprecise/inaccurate alignments and the inefficient use of III-V materials in the heterogeneous/hybrid wafer-bonding technique, the development of a thermally stable, low-power, and non-cryogenic continuous-wave (CW) Si-integrable nanolaser with a device footprint of \sim few μm^3 has long been a formidable challenge due to the several levels of fundamental and technical issues. Here, we report on a new concept of on-demand minimal-gain-printed Si nanolaser. A smartly designed minimal III-V semiconductor optical gain structure in conjunction with an individually addressable and highly precise on-demand gain-printing technique addresses both fundamental and technological issues, demonstrating a superior spectral stability in the pulsed conditions and thus even allowing a stable CW operation with a low-threshold of $\sim 50 \mu\text{W}$. A simple demonstration of the laser-on-waveguide represents a full-fledged merit of the on-demand gain-printing and the integrated Si nanolaser and thus exhibits its potential of wide and ubiquitous adoption in Si photonics and photonic integrated circuit (PIC) communities.

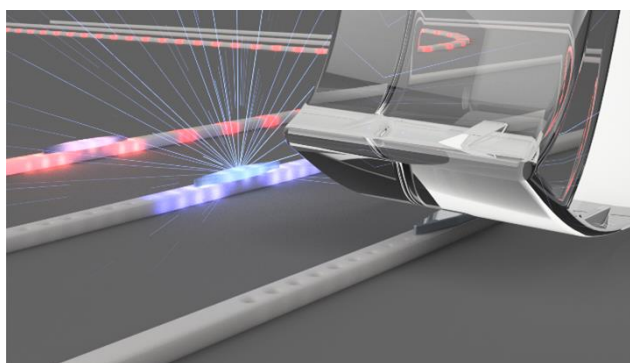


Fig. 1. A schematic showing minimal-gain-printed Si-integrable nanolaser.

4. References

- [1] B.-J. Min et al., Electrically driven on-chip transferrable micro-LEDs, Appl. Phys. Lett., 121, 21107, (2022).
- [2] M.-W. Kim, et al., All-Graphene-Contact Electrically Pumped On-Demand Transferrable Nanowire Source, Nano Lett., 22, 1316-1323, (2022).
- [3] S.-W. Park, On-Chip Transferrable Microdisk Lasers, ACS Photon., 7, 3313-3320 (2020).

Nanostructural Optical Antennas for Functional Devices

Zhaogang Dong^{1,2,*}

¹Institute of Materials Research and Engineering, A*STAR (Agency for Science, Technology and Research), 2 Fusionopolis Way, #08-03 Innovis, 138634 Singapore

²Department of Materials Science and Engineering, National University of Singapore, 9 Engineering Drive 1, 117575, Singapore
E-mail address: dongz@imre.a-star.edu.sg

Abstract: In this talk, we present our recent work on the nanostructural optical antennas for functional devices, such as mix nanoantenna array for fluorescence enhancements, imaging of the inaccessible bound-states-in-the-continuum (BIC) mode, quasi-BIC resonance for enhancing cathodoluminescence (CL) emission, the highly saturated red color pixels, color-sensitive miniaturized detectors, tunable color pixels, as well as the plasmonic resonances of Si nanostructures at ultra-violet (UV).

Nanostructural optical antennas have enabled the strong light-matter interactions, where the structural resonances are either based on plasmonics or dielectric Mie resonances. In this talk, we present our recent work on the nanostructural optical antennas for functional devices, such as mix nanoantenna array for fluorescence enhancements [1], imaging of the inaccessible bound-states-in-the-continuum (BIC) mode [2], quasi-BIC resonance for enhancing cathodoluminescence (CL) emission [2], the highly saturated red color pixels [3], color-sensitive miniaturized detectors [4], tunable color pixels [5, 6], as well as the plasmonic resonances of Si nanostructures at ultra-violet (UV) [7].

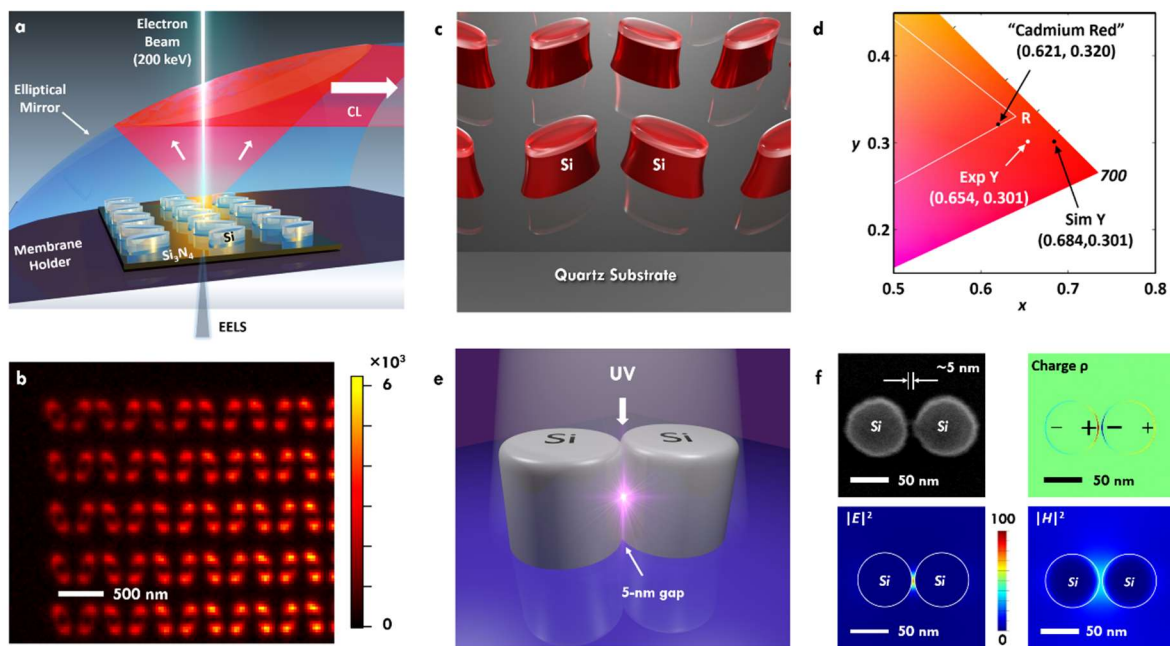


Figure 1. Nanostructural Si optical antennas. (a) Schematic illustration on probing the inaccessible BIC mode on a transmission electron microscope (TEM) setup via electron energy loss spectroscopy (EELS) and CL emission. (b) Spatial mapping of CL emission showing the coherent interaction length of quasi-BIC resonance and CL enhancements. (c) Schematic illustration on Si nanostructures with quasi-BIC resonance to achieve the highly saturated red color pixels. (d) CIE 1931 chromaticity diagram to show the high color saturation as achieved by the quasi-BIC resonance. (e) Schematic illustration of Si plasmonics at UV. (f) Scanning electron micrograph (SEM) image of Si dimer with ~5 nm gaps and the simulated optical field distributions.

References

- [1] Z. Dong, S. Gorelik, R. Paniagua-Domínguez, J. Yik, J. Ho, F. Tjioharsono, E. Lassalle, S. D. Rezaei, D. C. J. Neo, P. Bai, A. I. Kuznetsov and J. K. W. Yang, *Nano Lett.* **21**, 4853-4860 (2021).
- [2] Z. Dong, Z. Mahfoud, R. Paniagua-Domínguez, H. Wang, A. I. Fernández-Domínguez, S. Gorelik, S. T. Ha, F. Tjioharsono, A. I. Kuznetsov, M. Bosman and J. K. W. Yang, *Light: Science & Applications* **11**, 20 (2022).
- [3] Z. Dong, L. Jin, S. D. Rezaei, H. Wang, Y. Chen, F. Tjioharsono, J. Ho, S. Gorelik, R. J. H. Ng, Q. Ruan, C.-W. Qiu and J. K. W. Yang, *Science Advances* **8**, eabm4512 (2022).

- [4] J. Ho, Z. Dong, H. S. Leong, J. Zhang, F. Tjiptoharsono, S. D. Rezaei, K. C. H. Goh, M. Wu, S. Li, J. Chee, C. P. Y. Wong, A. I. Kuznetsov, and J. K.W. Yang, *Science Advances* **8**, eadd3868 (2022).
- [5] S. Zhang, J. Zhang, W. P. Goh, Y. Liu, F. Tjiptoharsono, H. Y. L. Lee, C. Jiang, J. Ding, J. K.W. Yang, and Z. Dong, *Nanophotonics* (2023). <https://doi.org/10.1515/nanoph-2022-0646>
- [6] L. Lu, Z. Dong, F. Tjiptoharsono, R. J. H. Ng, H. Wang, S. D. Rezaei, Y. Wang, H. S. Leong, P. C. Lim, J. K.W. Yang, and R. E. Simpson, *ACS Nano* **15**, 19722-19732 (2021).
- [7] Z. Dong, T. Wang, X. Chi, J. Ho, C. Tserkezis, S. L. K. Yap, A. Rusydi, F. Tjiptoharsono, D. Thian, N. A. Mortensen and J. K. W. Yang, *Nano Lett.* **19**, 8040-8048 (2019).

Effects of particle randomness on photonic band gap size in self-assembled colloidal crystals

Duanduan Wan

*School of Physics and Technology, Wuhan University, Wuhan 430072, China
E-mail address: ddwan@whu.edu.cn*

Abstract: Using computer simulations, we explore how thermal noise-induced randomness in a self-assembled photonic crystal affects its photonic band gaps (PBGs). We consider a two-dimensional photonic crystal composed of a self-assembled array of parallel dielectric hard rods of infinite length with circular or square cross section. We find that PBGs can exist over a large range of intermediate packing densities and the largest band gap does not always appear at the highest packing density studied. Remarkably, for rods with square cross section at intermediate packing densities, the transverse magnetic (TM) band gap of the self-assembled (i.e., thermal) system can be larger than that of identical rods arranged in a perfect square lattice. By considering hollow rods, we find the band gap of transverse electric (TE) modes can be substantially increased while that of TM modes show no obvious improvement over solid rods. We further investigate how PBGs are influenced solely by positional or orientational randomness of particles. Our study suggests that particle shape and internal structure can be used to engineer the PBG of a self-assembled system despite the positional and orientational randomness arising from thermal noise.

References

- [1] D. Wan and S. C. Glotzer, Phys. Rev. Lett. **126**, 208002 (2021)
- [2] Z. Qin, T. Liu, and D. Wan, arXiv:2302.01812 (2023)

All-optical control of high-purity trions in nanoscale waveguide

Hyeonwoo Lee¹, Yeonjeong Koo¹, Shailabh Kumar^{2,3}, Yunjo Jeong⁴, Dong Gwon Heo⁵, Soo Ho Choi⁶, Huitae Joo¹, Mingyu Kang¹, Radwanul H. Siddique^{2,3}, Ki Kang Kim^{6,7}, Hong Seok Lee⁵, Sangmin An⁵, Hyuck Choo^{2,8*} and Kyoung-Duck Park^{1*}

¹Department of Physics, Pohang University of Science and Technology (POSTECH), Pohang 37673, Republic of Korea.

²Department of Medical Engineering, California Institute of Technology (Caltech), Pasadena, CA 91125, USA.

³Meta Vision Lab, Samsung Advanced Institute of Technology (SAIT), Pasadena, CA 91101, USA.

⁴Institute of Advanced Composite Materials, Korea Institute of Science and Technology, Jeonbuk 55324, Republic of Korea.

⁵Department of Physics, Research Institute of Physics and Chemistry, Jeonbuk National University, Jeonju 54896, Republic of Korea.

⁶Center for Integrated Nanostructure Physics, Institute for Basic Science (IBS), Suwon 16419, Republic of Korea.

⁷Department of Energy Science, Sungkyunkwan University (SKKU), Suwon 16419, Republic of Korea.

⁸Advanced Sensor Lab, Device Research Center, Samsung Advanced Institute of Technology (SAIT), Suwon 16678, Republic of Korea.

E-mail address: parklab@postech.ac.kr

Abstract: Generating high-purity localized trion, dynamic exciton-trion interconversion, and spatial controllability in 2D semiconductors under ambient conditions are a quantum leap to realize the trion-based excitonic devices. Here, we present all-optical control of excitonic conversion dynamics in MoS₂ monolayer under ambient conditions by exploiting the propagating surface plasmon polariton (SPP) in the nano-gap based metal-insulator-metal (MIM) waveguide device.

1. Introduction

The spatial control of excitonic quasiparticles in two-dimensional (2D) semiconductors has been extensively studied for the development of various exciton-based optoelectronic devices, especially facilitating intermedium of the electronic system and optical system, as well as highly efficient light-harvesting devices. Recently, with n-type TMD MLs under a similar strain gradient geometry, the excess electrons are funneled together with X₀ and converted to trions (X⁻) via an exciton-to-trion conversion process [1]. The efficiency of this exciton-to-trion conversion can reach 100% in a WS₂ ML suspended on a microhole-based strain gradient. Given the characteristics of X⁻, particularly the high-efficiency generation and reactivity to the external electric field, the exciton-to-trion conversion can be a promising alternative to the inefficient funneling process of X₀.

Here, we present a versatile method for the all-optical control of trion behavior in MoS₂ ML, including complete exciton-to-trion conversion and localization, dynamic exciton-trion interconversion, and spatial modulation of trions at ambient conditions. In our device, the nanogap geometry of the lateral plasmonic metal-insulator-metal (MIM) waveguide induces a 1D nanoscale strain gradient in the suspended MoS₂ ML. The induced nanoscale strain gradient significantly increases the funneling efficiency, thus confining X₀ to the nanogap center. The plasmon-induced hot electron generation process enables the injection of electrons from Au to the MoS₂ ML. These extra electrons are funneled toward the nanogap center and locally increase the electron density, stimulating additional exciton-to-trion conversion in the nanoscale region, i.e., the nanoscale generation of radiative X⁻ emission. Furthermore, we employ adaptive wavefront shaping using a spatial light modulator (SLM) to dynamically manipulate the SPP mode of the waveguide, which in turn spatially modulates the exciton-to-trion conversion region.

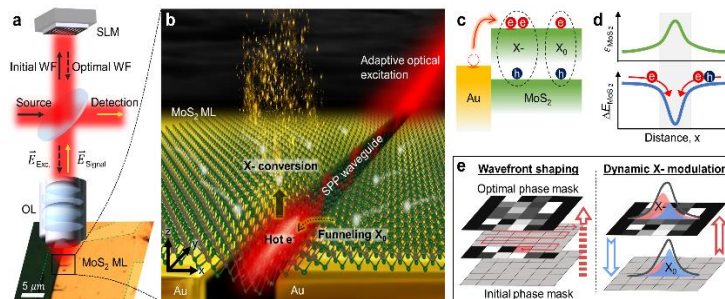


Fig. 1. (a) Schematic illustration of the waveguide device combined with SLM for adaptive wavefront shaping. (b) Detailed view of the waveguide device to facilitate the nanoscale trion conversion. (c) The illustration of the hot electron injection from the Au nano-gap to the MoS₂ ML. (d) The strain and corresponding bandgap diagram of MoS₂ ML. (e) The adaptive wavefront shaping by SLM to find an optimal phase mask (left) and dynamic modulation of the optimal phase mask (right).

2. References

[1] Harats, M. G. et al. "Dynamics and efficient conversion of excitons to trions in non-uniformly strained monolayer WS₂", *Nat. Photon.* **14**, 324-329 (2020).

High-quality optical vortices generation and near-perfect absorption via inverse design

Munseong Bae¹, Svetlana V. Boriskina², Haejun Chung¹.

¹Department of Electronic Engineering, Hanyang University, Seoul, 04763, South Korea,

²Department of Mechanical Engineering, Massachusetts Institute of Technology, Cambridge, MA 02139, USA,
munseong97@hanyang.ac.kr, sborisk@mit.edu, haejun@hanyang.ac.kr

Abstract: Optical vortex (OV) offers a new sensing and optical communication application strategy. Nevertheless, there is no standardized OV generation method. In this abstract, we suggest a grating structure designed by inverse design and shows high-quality Optical vortices (90% purity) generation and Near-Perfect (NP) absorption (97.846%) via finite-difference time-domain (FDTD) simulation.

Introduction

OV has a rapidly changing phase with high energy flow (Orbital angular momentum) centered by zero electromagnetic field point. OV also can be demonstrated by topological charge calculated from phase accumulation in the closed loop. Based on these characteristics, OV is applied in a broad area, such as sensing [1], optical communication in free space [2], and polarization control [1]. Despite these potentials, no standardized OV generation method [3]. In this abstract, we suggest a grating structure designed by inverse design [4,5] and show high-quality OVs generation and NP absorption of the thin film with FDTD simulation. Inverse design is the state-of-the-art optimization algorithm focused on the design of nanoscale optical devices with Figure of Merit (FoM) including electric field (E-field) vector. Inverse design calculates the E-field from front propagation. After substituting the material arrangement with the light source, the adjoint field is calculated from backpropagation using reciprocity. Derivative of FoM can be calculated from these two fields.

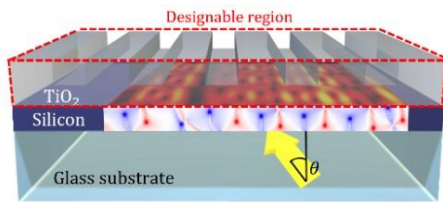


Fig. 1. Schematic showing a structure in which optimized grating layer (TiO₂) and thin film (Silicon) are on a substrate (Glass). When the 775nm band planewave with incidence angle θ propagates from the bottom (from substrate) to the top (to thin film), OVs are generated nearby thin film with high absorption.

Method

MEEP is used as FDTD solver for inverse design and simulation. Fig.1 shows the simulation setting that propagation of 775nm wavelength planewave with incidence angle θ from the substrate (1.3 μ m Glass) to thin film (100nm Silicon) with optimized structure (500nm TiO₂). FoM for optimization maximizes the E-field intensity of thin film with 0° of θ . The designed structure has 1.5 μ m periodicity. The Aspect ratio is set as 10 for fabrication. The

optimized structure shows NP absorption (97.8%). Polarity and quality of OV evaluated from Eq.1.

$$\Gamma = \oint_0^{2\pi} \mathbf{a}_\phi \cdot \mathbf{S}(\phi, \mathbf{r}) \cdot d\phi. \quad (\text{Eq. 1})$$

\mathbf{S} is Poynting vector (cross product of E, H field), \mathbf{a}_ϕ is cylindrical $\hat{\phi}$ unit vector, \mathbf{r} is radius and Γ is quality of OV. Fig.2 shows the optimized structure, E-flux intensity, and Γ distribution nearby thin film.

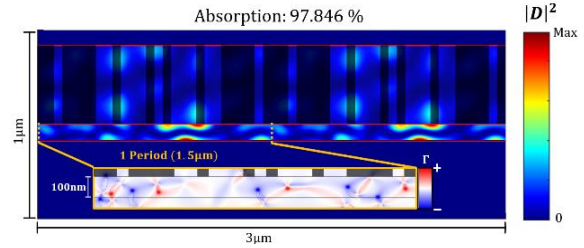


Fig. 2. E-flux and Γ (subplot) distribution nearby silicon thin film with optimized structure. There is a high electric flux inside the thin film. The Γ distribution in the subplot shows that high-quality OVs cause NP absorption of the thin film.

Result

Fig.2 demonstrates that the grating structure designed by inverse design can show NP absorption (97.846%) and generate high-quality OVs. Especially the minimum purity of OV was 90%, and with an 80° range (-40~40°) of θ , the optimized structure shows a minimum of 1800% absorption improvement compared to single pass (w/o TiO₂ layer) absorption. Furthermore, we can tune the OV in a nanoscale with a more specifically designed FoM for inverse design. Which can lead us to new opportunities for OV applications.

References

- [1] Sakotic, Zarko, et al. "Topological scattering singularities and embedded eigenstates for polarization control and sensing applications." *Photonics Research* 9.7 (2021): 1310-1323.
- [2] Xie, Zhenwei, et al. "Ultra-broadband on-chip twisted light emitter for optical communications." *Light: Science & Applications* 7.4 (2018): 18001-18001.
- [3] Kim, Dongha, et al. "Spontaneous generation and active manipulation of real-space optical vortices." *Nature* 611.7934 (2022): 48-54.
- [4] Chung, Haejun & Owen D. Miller. "High-NA achromatic metalenses by inverse design." *Opt Exp* 28.5 (2020): 6945-6965.
- [5] Chung, Haejun & Owen D. Miller. "Tunable metasurface inverse design for 80% switching efficiencies and 144 angular deflection." *Acs Photonics* 7.8 (2020): 2236-2243.

Inverse design of metaphotonics for multicolor and 3D holography

Sunae So^{1,*}

*1 Department of Electro-Mechanical Systems Engineering, Korea University, Sejong,
30019, Republic of Korea)*

** E-mail : sunaeso@korea.ac.kr*

Metaphotonics has enabled the realization of advanced optical technologies with ultra-thin devices, but the design of metaphotonics for desired optical properties remains a challenge. In this presentation, we propose an inverse design method for designing single-cell metasurfaces with tailored optical properties for multicolor and 3D holography [1]. Our approach leverages a gradient-descent optimization method to encode multiple pieces of holographic information into a single phase profile, demonstrating the state-of-the-art data capacity of a single-cell metasurface. Specifically, we design and experimentally demonstrate both multiplane RGB color and 3D holography using low-loss materials of TiO₂. Our work provides an effective and systematic approach for designing metaphotonics with desired optical properties, and has potential applications in various areas, including imaging, sensing, and communication. The proposed inverse design method using single-cell metasurfaces could pave the way for the development of next-generation optical devices with enhanced performance and functionality.

[1] S. So, J. Kim, T. Badloe, C. Lee, Y. Yang, H. Kang, J. Rho, Adv. Mat. **35**, 2208520 (2023)

Phase imaging using polarization-sensitive dielectric metasurfaces

Shaban B. Sulejman^{1,*}, Lukas Wesemann¹, Wendy S. L. Lee^{1,2}, Kenneth B. Crozier^{1,2} and Ann Roberts¹

¹ARC Centre of Excellence for Transformative Meta-Optical Systems, School of Physics, The University of Melbourne, Victoria 3010, Australia

²ARC Centre of Excellence for Transformative Meta-Optical Systems, Department of Electrical and Electronic Engineering, The University of Melbourne, Victoria 3010, Australia
E-mail address: sulejmans@unimelb.edu.au

Abstract: Dielectric metasurfaces are sub-wavelength structures that can exhibit Mie resonances. Here, progress towards phase imaging using a silicon-based metasurface is presented, which possesses the potential for ultra-compact biological imaging.

1. Introduction

Probing light-matter interactions on the nanoscale has led to various technological developments, such as telecommunications and ultra-sensitive cameras. Conventional imaging sensors capture the intensity, spectral, and in some cases, the polarization information of light, but cannot sense the phase. Transparent samples often impart only phase shifts onto light transmitted through them, therefore requiring phase contrast imaging for their visualization. Common techniques include Zernike [1] and differential interference contrast [2] microscopy, but these can be limited by complex configurations and cost.

Metasurfaces are ultra-thin devices that provide a miniaturized approach to phase imaging through all-optical image processing. They can transform phase gradients of wavefields into intensity changes enabled by an angular-dispersive transmission. For example, Wesemann et al. [3] visualized phase with a switchable contrast using a spin-orbit coupling enabled metasurface. Here, a silicon-based, polarization-sensitive device capable of phase visualization will be presented.

2. Results

The device (Fig. 1) supports waveguide-coupled Mie resonances within a square lattice of nanoantennas on a waveguiding layer to convert phase into intensities for *p*-polarized light. Experiments visualizing phase profiles of a sine grating introduced by a spatial light modulator are shown in Fig. 1(c) at a wavelength of 920 nm. It has an enhanced contrast compared to the relatively featureless reference image (Fig. 1(b)) obtained without the metasurface. Moreover, the contrast generated is comparable to that obtained in differential interference contrast microscopy.

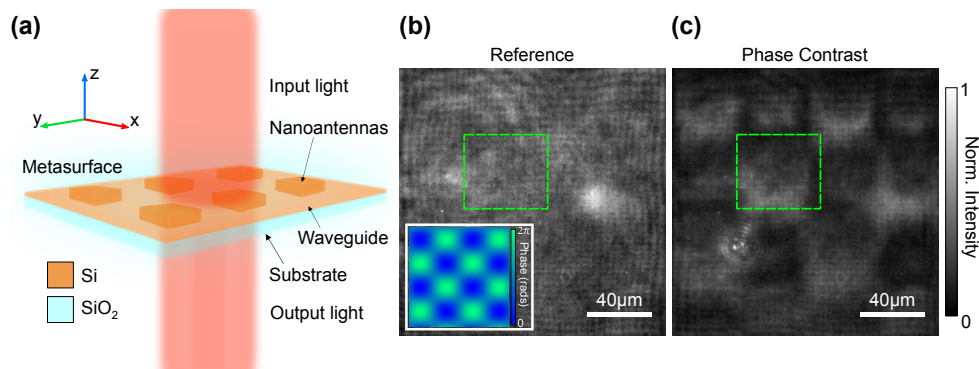


Fig. 1: The metasurface (a) produced the phase image (c) of phase profiles of a sine grating (inset of (b)). A reference image taken without the metasurface is given in (b) for comparison.

3. Conclusion

In conclusion, real-time phase imaging was performed with a silicon-based metasurface in the near-infrared. This work demonstrates the potential in biomedical applications such as ultra-compact biological imaging.

References

- [1] F. Zernike, *Physica* **9**, 686-698 (1942).
- [2] W. Lang, Nomarski differential interference-contrast microscopy, Carl Zeiss (1982).
- [3] L. Wesemann, J. Rickett, T. J. Davis and A. Roberts, *ACS Photonics* **9**, 1803-1807 (2022).

Large field of view, large area and broadband achromatic mid-infrared metalens

Yen-Chun Chen, Chen-Yi Yu, Wei-Lun Hsu and Chih-Ming Wang*

Department of Optics and Photonics, National Central University, Taoyuan, 32001, Taiwan.

* cmwang@cc.ncu.edu.tw

Abstract: We proposed a design of a small total track mid-infrared meta-optics device with a large field of view. The diameter of this metalens is 5.75 mm. In our design, the metalens' doughnut-shaped meta-atoms are designed to eliminate the chromatic aberration for wavelengths of 8 μm , 9.6 μm , 12 μm , and 14 μm . Our metalens provides a 90° large field of view. This metalens is fabricated by an i-line stepper, which has mass-production advantages and is low-cost. In the future, mid-infrared metalens has excellent potential for use in thermal detection and imaging.

1. Introduction

For optical imaging systems, metalens with chromatic aberration-free, large dimensions, and wide field of view (FOV) are benefits for providing high-quality images. Although that the chromatic aberration can be eliminated by controlling the group delay of meta-atoms. The group delay is also limited the maximum diameter of a metalens. Therefore, designing a chromatic aberration-free metalens with a large diameter is very challenging [1]. In this work, we designed a metalens with large-area, chromatic aberration free, and wide FOV for mid-infrared (MIR) wavelength operation. This metalens shows great potential for applications in fire detection, optical inspection, and temperature sensing [2].

2. Design and Results

Fig.1(a) presents the ray tracing of the optimized meta-optics system, consisting of an aperture and metalens with diameters of 2.65 mm and 5.750 mm, respectively. The phase distribution of the metalens are designed based on even polynomials. We further optimized the phase distribution to eliminate the chromatic aberration for wavelengths 8 μm , 9.6 μm , 12 μm , and 14 μm . Moreover, the modulation transfer function (MTF) is shown in Fig.1(b). The cutoff frequencies of 90° FOV are 16.7 lp/mm, 17.0 lp/mm, 16.3 lp/mm, and 15.7 lp/mm for 8 μm , 9.6 μm , 12 μm , and 14 μm , respectively.

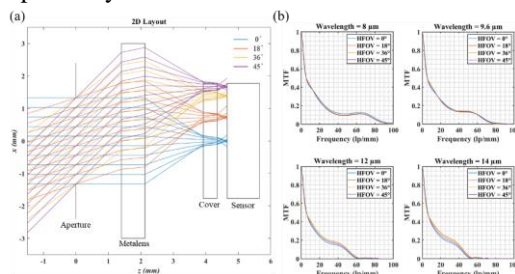


Fig.1 (a) Schematic ray trace of the propose optical system, the blue, orange, yellow and purple line representing 0°, 18°, 36° and 45° half field of view (HFOV), respectively. (b) The calculated MTF of 0°, 18°, 36° and 45° HFOV in this system.

The doughnut-shape meta-atoms are chosen to design the metalens, which the i-line stepper lithography process can pattern. The SEM image of the MIR metalens is shown in Fig. 2. As we observed, doughnut-shaped structures are fairly patterned by i-line stepper.

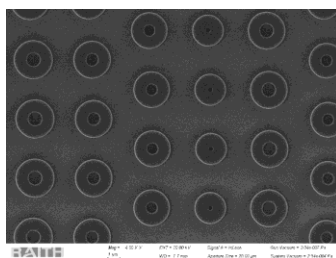


Fig.2 The SEM image of metalens with doughnut-shaped meta-atom.

3. References

- [1] Shrestha, S., Overvig, A.C., Lu, M. et al., "Broadband achromatic dielectric metalenses." *Light Sci Appl* 7, 85 (2018).
- [2] Uocheng et al., "Long Wavelength Infrared Imaging under Ambient Thermal Radiation via All-Silicon Metalens." *Optical Materials Express*. 11 (2021).

Single-molecule Near-field Spectroscopy with STM

Yousoo Kim

The University of Tokyo, RIKEN

E-mail address: ykim@riken.jp

When irradiated on a nanoscale metal structure, light can be squeezed in an extremely small region of several nm, far beyond the diffraction limit (several 100 nm) of visible light due to the localized surface plasmon (LSP) resonance. We have achieved spectroscopic measurements and controlled photochemical reactions of individual molecules that are spatially fixed on solid surfaces at low temperatures by using the tiny light (near-field light, NFL) localized between a metal probe of a scanning tunneling microscope (STM) and a metal substrate. The LSP has a characteristic interaction with matter, especially a single molecule. The STM is a versatile and powerful tool for investigating and controlling the chemistry of individual molecules on solid surfaces. We developed an optical STM technology that combines the STM with light irradiation and detection technologies for our own purpose [1], which allows us to apply the NFL to explore novel chemical reactions and spectroscopy based on the interaction between the NFL and electronic/vibrational quantum states of a single molecule at the STM junction. We have developed single-molecule emission and absorption (Fig. 1(a)) spectroscopy [1] using the interaction between the NFL and a molecule, in which the NFL participates in the exciton formation in a target molecule [2]. Combining the emission and absorption spectroscopies, we visualized fluorescence resonance energy transfer between two different molecules [3]. We have also explored the detailed mechanism of single-molecule chemical dynamics induced by the NFL (Fig. 1(b)) [4]. We also applied the NFL to measure tip-enhanced resonance Raman spectra of a single molecule (Fig. 1(c)) [5]. Furthermore, we achieved an ultrahigh-energy resolution photoluminescence measurement of a single molecule using a tunable excitation laser (Fig. 1(d)) [6]. These optical setups enable a real-space measurement of photocurrent pathways at a single molecule (Fig. 1(e)) [7].

In this talk, I will discuss recent issues focusing on single-molecule spectroscopy based on the excitation of molecular quantum states by NFL at the STM junction.

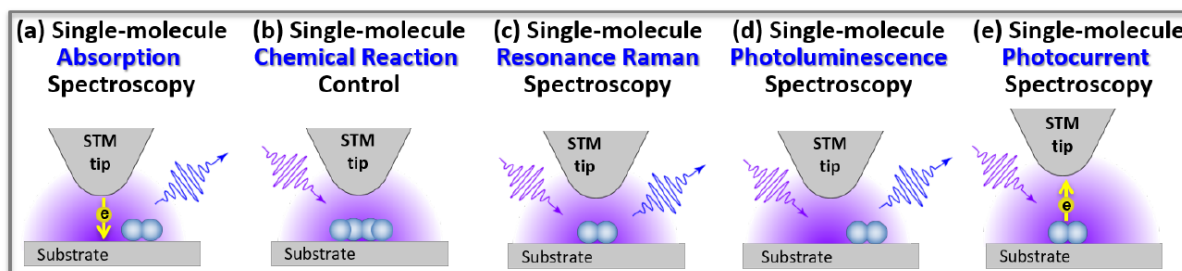


Fig. 1. Single-molecule chemistry and spectroscopy technologies that we have developed using near-field light. (a) Single-molecule absorption spectroscopy, (b) Single-molecule chemical reaction (plasmon chemistry), (c) Single-molecule resonance tip-enhanced Raman spectroscopy, (d) Single-molecule photoluminescence spectroscopy, and (e) Single-molecule photocurrent spectroscopy.

References

- [1] H. Imada, K. Miwa, M. Imai-Imada, S. Kawahara, K. Kimura, Y. Kim, *Phys. Rev. Lett.* **119**, 013901 (2017).
- [2] K. Kimura, K. Miwa, H. Imada, M. Imai-Imada, S. Kawahara, J. Takeya, M. Kawai, M. Galperin, Y. Kim, *Nature* **570**, 210 (2019).
- [3] H. Imada, K. Miwa, M. Imai-Imada, S. Kawahara, K. Kimura, Y. Kim, *Nature* **538**, 364 (2016).
- [4] E. Kazuma, J. Jung, H. Ueba, M. Trenary, Y. Kim, *Science* **360**, 521 (2018).
- [5] R.B. Jaculbia, H. Imada, K. Miwa, T. Iwasa, M. Takenaka, B. Yang, E. Kazuma, N. Hayazawa, T. Taketsugu, Y. Kim, *Nature Nanotech.* **15**, 105 (2020).
- [6] H. Imada, M. Imai-Imada, K. Miwa, H. Yamane, T. Iwasa, Y. Tanaka, N. Toriumi, K. Kimura, N. Yokoshi, A. Muranaka, M. Uchiyama, T. Taketsugu, Y.K. Kato, H. Ishihara, Y. Kim, *Science* **373**, 95 (2021).
- [7] M. Imai-Imada, H. Imada, K. Miwa, Y. Tanaka, K. Kimura, I. Zoh, R.B. Jaculbia, H. Yoshino, A. Muranaka, M. Uchiyama, Y. Kim, *Nature* **603**, 829 (2022).

Revealing the Local Band Structures of Sharp WS_2/MoS_2 Heterojunction and Graded $\text{W}_x\text{Mo}_{1-x}\text{S}_2$ Alloy by Near-Field Optical Imaging

Po-Wen Tang¹, He-Chun Chou¹, Shiue-Yuan Shiau², Xin-Quan Zhang³, Yi-Hsien Lee³, and Chi Chen^{1*}

¹ Research Center for Applied Sciences, Academia Sinica, Taipei, 115, Taiwan

² Physics Division, National Center for Theoretical Sciences, Taipei, 106, Taiwan

³ Department of Materials Science and Engineering, National Tsing-Hua University, Hsinchu, 300, Taiwan

E-mail: chenchi@gate.sinica.edu.tw

With the development of various chemical vapor deposition (CVD) methods [1], many artificial 2D semiconductors have been synthesized, which increase the chances of forming disrupted interfaces and non-periodic or small-sized systems (defects and grain boundaries). All such systems create local electronic band structures within a finite scale, which cannot be readily explained by solid-state band theory nor be probed easily by confocal microscopes and macroscopic transport.

In this study, we investigated abrupt heterojunctions and graded alloys between two transition metal dichalcogenides (TMD), which involve non-periodic band structures and require high spatial resolution. We employed near-field photoluminescence (NF-PL) imaging to study the atomically sharp 1D interfaces between WS_2 and MoS_2 (Fig. 1b). With an optical resolution of 68 nm, a 105 nm-wide region for quenched PL was confirmed using NF-PL imaging [2]. Our NF-PL imaging resolved the narrowest quenching width and sharpest strain mapping because of the superior spatial resolution and stability of our home-built SNOM [3].

We further developed a near-field broadband absorption (or transmittance, NF-tr) imaging method to overcome the limitations of NF-PL for low-quantum-yield materials. The NF-tr technique provides abbreviation-free and nanoscale-resolution imaging capability of the entire conduction band over highly lateral inhomogeneity. We utilized NF-tr microscopy to investigate the varying bandgap and bowing factor of a single-layered $\text{W}_x\text{Mo}_{1-x}\text{S}_2$ alloy [4]. For the bilayer $\text{W}_x\text{Mo}_{1-x}\text{S}_2$ alloy, the energy contour maps present the bandgap evolution in the alloy and reveal bilayer coupling between the top and bottom layers (Fig. 1c). We can conclude that the bottom layer has an alloy nature, whereas the top layer is composed of pure WS_2 . High-spatial-resolution spectral capability is essential for analyzing compositional and location-dependent bandgap evolutions.

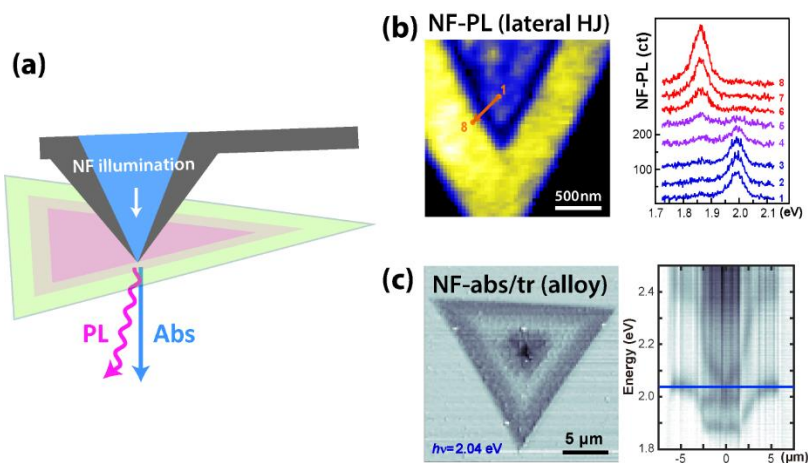


Fig. 1 (a) Schematics of the near-field absorption/transmittance (NF-abs/tr) and near-field photoluminescence (NF-PL) measurements. (b) NF-PL imaging and spectra of the lateral heterojunction. (c) NF-tr spectroscopic imaging and band structure of the graded alloy.

[1] K.-C. Chiu and Y.-H. Lee *et al.*, *Adv. Mater.* 30, 1704796 (2018)

[2] H.-C. Chou and C. Chen *et al.*, *Nanoscale* 14, 6323 (2022)

[3] J.-R. Yu and C. Chen *et al.*, *Rev. Sci. Instrum.* 91, 073703 (2020)

[4] P.-W. Tang and C. Chen *et al.*, *ACS Nano*, 16, 5, 7503 (2022)

Selective Mapping of Tip-launched Near-field Scattering of Surface Plasmon Polaritons for Retrieving Dispersion Relation in Silver Nano Flakes

Hwi Je Woo

Sungkyunkwan University (SKKU), Suwon, Korea
E-mail hjwoo.aron@gmail.com

Scattering-type near-field scanning optical microscopy (s-NSOM) has been beneficial for observing various nano-optical phenomena by overcoming the spatial resolution diffraction limit, creating optical dispersion, and investigating optoelectronic systems. We used s-NSOM on mono-crystalline silver nano flakes to selectively decompose tip-launched surface plasmon polariton (SPP) signals and suppress the undesired geometrical effects arising from the silver nano flakes and s-NSOM tips. Comparing each Fourier transform analysis data from all the edges of silver nano flakes, we successfully identified the momentum of tip-launched SPPs. We have conducted energy spectral measurements on mono-crystalline silver nano flakes and applied on geometry-independent factor: tip-launched SPP. We neglected the additional complex contribution from various shapes of the nano flakes in the visible-near infrared regime. These experimentally obtained momentums of SPPs have a good agreement with analytical calculations. We observed that propagation of SPP increases with a decrease in excitation energy even without additional destructive fabrications on the surface, although the surface quality of silver nano flakes is affected by dirt and oxidation. This study provides a precise interpretation of the experimental studies on the various polariton studies using s-NSOM.

Enhancing precise nanophotonic dark-field microscopy with low-loss substrate

Yongdeok Cho¹, Ji-Hyeok Huh¹, Minh Thang Nguyen¹, Hayun Ahn¹, Nayeoun Kim¹, Young-Seok Kim^{3*}, and Seungwoo Lee^{1,2,4,5*}

¹KU-KIST Graduate School of Converging Science and Technology, Korea University, Seoul 02841, Republic of Korea

²Department of Biomicrosystem Technology, Korea University, Seoul 02841, Republic of Korea

³Display Research Center, Korea Electronic Technology Institute (KETI), Gyeonggi-do 13509, Republic of Korea

⁴Department of Integrative Energy Engineering (College of Engineering) and KU Photonics Center, Korea University, Seoul 02841, Republic of Korea

⁵Center for Opto-Electronic Materials and Devices, Post-Silicon Semiconductor Institute, Korea Institute of Science and Technology (KIST), Seoul 02792, Republic of Korea

E-mail address: seungwoo@korea.ac.kr; vis4freedom@keti.re.kr

Abstract: Conventional substrates can induce a lossy feature that prevents the accurate measurement of the intrinsic optical properties of nanoparticles. In this study, we present a method to overcome this issue by using a 20-nanometer thickness nanomembrane as the substrate. The intrinsic optical properties of gold and selenium colloids were measured using optical microscopy, and the results were compared to those obtained using a conventional substrate. The use of the nanomembrane eliminated the substrate-induced lossy feature and allowed for the accurate measurement of the nanoparticles' optical properties. Our findings demonstrate the importance of considering the substrate effect on the measurement of nanoparticles' intrinsic optical properties and provide a solution to overcome this issue.

Nanophotonic, the study of light at the nanoscale, has emerged as a promising field with a wide range of applications in areas such as sensing, imaging, and optical device [1]. To fully exploit the potential of nanophotonic, it is crucial to accurately measure the optical properties of nanoscale materials and structures. However, conventional substrates such as glass, or TEM grid used in the measurements can often induce a lossy feature that interferes with the intrinsic optical properties of the nanomaterials, leading to inaccurate measurements. To address this technical challenge, we utilize an ultra-low-loss thin formvar nanomembrane on a grid (FNoG), which has a thickness of approximately 20 nm.

FNoG's low-loss nature allows for accurate measurements of the optical properties and scattering of nanomaterials. Gold colloids, which exhibit plasmon resonant behavior, can be significantly impacted by the choice of substrate. Compared to other substrates, FNoG demonstrates the highest scattering signal for the ED feature of gold colloids. We also compared the scattering signal of a metamolecule inspired by the ring-inclusion motif [2] self-assembled heptamer gold cluster on various substrates. The results revealed that the magnetic resonance from the heptamer cluster showed the highest scattering efficiency when measured on FNoG. In addition, FNoG can be further useful when measuring the high index colloids. Selenium with refractive index of 2.9~3.1 are one of a candidate among high index materials that could exhibit electric dipole and magnetic dipole simultaneously [3]. Especially when higher mode like magnetic quadrupole is observed, it is likely that the scattering signal can be reduced due to lossy feature of substrate. Indeed, the magnetic quadrupole is highly concentrated toward the outside surface of colloids which is vulnerable to face directly to substrate. To reduce any lossy feature of magnetic quadrupole, we had demonstrated that selenium colloids could preserve one's optical characteristics using FNoG.

Using FNoG as a substrate provides multiple benefits for the measurement of colloidal samples. Its low-loss nature results in higher scattering efficiency, and it preserves the optical characteristics of the samples. The results of our study demonstrate the potential of FNoG as a versatile platform for optical characterization, while also highlighting the significant impact of substrate choice on the accuracy of measurements in the field of nanophotonic [4].

[1] Hatice Altug, Sang-Hyun Oh, Stefan A. Maier, and Jiri Homola, "advances and applications of nanophotonic biosensor," *Nature Nanotechnology* **17**, 5-16 (2022).

[2] A. Alu, A. Salandrino, N. Engheta, "Negative effective permeability and left-handed materials at optical frequencies," *Opt. Express* **14**, 1557-1567 (2006)

[3] Yongdeok Cho, Ji-Hyeok Huh, Kwangjin Kim, and Seungwoo Lee, "Scalable, Highly Uniform, and Robust Colloidal Mie Resonators for All-Dielectric Soft Meta-Optics," *Adv. Opt. Mater.* **7**, 181167. (2019)

[4] Thang Minh Nguyen, Yongdeok Cho, Ji-Hyeok Huh, Hayun Ahn, Nayeoun Kim, Kyung Hun Rho, Jaewon Lee, Min Kwon, Sung Hun Park, ChaeEon Kim, Kwangjin Kim, Young-Seok Kim, and Seungwoo Lee, "Ultralow-Loss Substrate for Nanophotonic Dark-Field Microscopy," *Nano Lett.* **23**, 4, 1546-1554 (2023).

Unlocking the Potential of Far-Field Optical Microscopy in Nanoworld

Seok-Cheol Hong

*Center for Molecular Spectroscopy and Dynamics, Institute for Basic Science, Seoul 02841, Korea
Department of Physics, Korea University, Seoul 02841, Korea*

hongsc@korea.ac.kr

Abstract: Optical microscopy is not only the extension of our visual sensation towards finer length scales but also the driving force for scientific revolutions. Scattering-based ordinary far-field optical microscopy has long been routinely used in biological as well as physical sciences for its simplicity, full commercialization, and decent performance. Recent innovations based on simple classical ideas have, however, elevated such visual means to sensitive imaging methods. In particular, interferometric scattering microscopy (iSCAT) as a non-fluorescent, label-free imaging tool, enables remarkable sensitivity to scattering matter and therefore permits extremely short acquisition period for signal detection, supporting unprecedentedly fast optical imaging. In this talk, we briefly overview our recent achievements with the method for sensitive and fast visualization of nanoparticles and biological cells, highlighting fast and high-throughput tracking of unlabeled nanoparticles and label-free, long-term imaging of nano-scale cargos inside a living cell.

1. Introduction

Scientists aim to uncover the fundamental principles behind various phenomena by examining their constituents and the interactions between them. Consequently, observing the microscopic world is crucial in most natural sciences, as it often reveals fascinating microscale phenomena that differ from those observed at the macroscale. Research in the microscopic realm has faced challenges due to the optical diffraction limit, leading to a reliance on near-field microscopes. However, the recent emergence of fluorescence-based super-resolution microscope technology has enabled investigations beyond the Abbe limit through far-field imaging. Despite this advancement, researchers continue to explore alternative methods due to the limitations of fluorescence technology.

2. Results and Conclusion

The recent development of interferometric scattering microscopy (iSCAT) as a non-fluorescent imaging technique, has allowed for the high-sensitivity detection of nanoparticles and high-speed and long-term observation of various nano-objects. This has opened the door to acquiring rich dynamic information from extensive imaging data. In this talk, I will present our research on nanoparticle and intracellular cargo transport, utilizing iSCAT.

Our research has made it possible to track the movement of nanoparticles, enabling direct determination of particle size, material properties, and concentration. By tracking multiple intracellular vesicles in real-time, we have gained insights into their transportation over time and reconstructed the underlying cytoskeletal network, which provides the vesicles' path, with super resolution by pinpointing the vesicles' positions at every moment. This work represents the first implementation of single-molecule localization microscopy (SMLM) in scattering microscopy.

Our work is expected to significantly advance the field by allowing far-field optical microscopy to provide non-invasive, long-term observations of nanoparticles and cellular nanostructures without relying on fluorescence.

Super-resolution imaging in space and time domain with extreme lights

Changyong Song

*Department of Physics, POSTECH, Pohang 37673, Korea
E-mail address: (cysong@postech.ac.kr)*

Abstract: Continued developments of new light sources keep adding new modalities to experimental probes with improved performance in investigating material systems. Advent of intense femtosecond X-ray laser has reshaped this race by opening the window to view physical phenomena in femtosecond temporal and nanoscale spatial domain. Much has remained unknown in such an extreme space-time domain so far. Kinetic reactions in strong nonequilibrium condition are largely unexplored, which stimulates strong research interest in revealing the reaction dynamics of individual atoms prompted by photo-depleted electrons. However, research activities on ultrafast atomic dynamics have been limited by the challenges in resolving involved irreversible processes. By newly developing single-pulse time-resolved imaging technique using femtosecond X-ray laser pulses, we established a path to directly image irreversible kinetic reactions in materials at several tens of femtoseconds temporal and several nanometer spatial resolutions. Detailed atomic scale dynamics accompanied during the irreversible solid-to-liquid phase transition in gold nanoparticles was uncovered to understand ultrafast energy transfer process from photon-to-ions. Recent progress in single-pulse ultrafast imaging with achievements including the establishment of comprehensive atomic-scale picture describing the heterogeneous progression of melting will be introduced.

References

- [1] Y. Ihm, *et al.*, *Nat. Commun.* **10**:2411 (2019).
- [2] C. Jung, *et al.*, *Science Advances* **7**:eabj8552 (2021).
- [3] J. Shin, *et al.*, *Nano Letters* **23**:1481 (2023).

Tackling background noise problem in stimulated emission depletion nanoscopy

Jong-Chan Lee^{a,b}

^a Department of New Biology, Daegu Gyeongbuk Institute of Science and Technology, Daegu, Republic of Korea

^b New Biology Research Center, Daegu Gyeongbuk Institute of Science and Technology, Daegu, Republic of Korea

E-mail address: jcleee@dgist.ac.kr

Abstract: Stimulated emission depletion (STED) super-resolution microscopy (or nanoscopy) offers significant enhancement of optical resolution compared to conventional optical microscopy. Here, we report simple and easy-to-implement methods to tackle the background noise problem in STED nanoscopy.

1. Introduction

Stimulated emission depletion (STED) super-resolution microscopy (or nanoscopy) offers significant enhancement of optical resolution compared to conventional microscopy [1]. To achieve resolution beyond the diffraction-limit, STED nanoscopy uses orders of magnitude (roughly $\sim 10^5$) more photons than the conventional confocal microscopy. Those additional ‘STED’ photons, which are designed to deplete the fluorescence at the periphery of focus, can induce unintended background noise. Increased low spatial frequency background noise decreases the signal-to-background ratio (SBR) and deteriorates the image quality by masking the high spatial frequency, super-resolved signal.

2. Result

Here, we report a simple and easy-to-implement method, which we call polarization switching STED (psSTED), that can efficiently suppress the low spatial frequency background appearing in STED images [2]. In psSTED, we switch the STED beam polarization between two different circularly polarized states to record a regular STED image and a background noise image. A simple, unambiguous subtraction process between these two images accomplishes a background-free super-resolved image. With both simulation and experimentation, we demonstrate psSTED works universally for different STED conditions. Finally, we compare the performance of psSTED with other state-of-the-art background subtraction methods and highlight its capability of efficient background suppression with a much simpler hardware implementation.

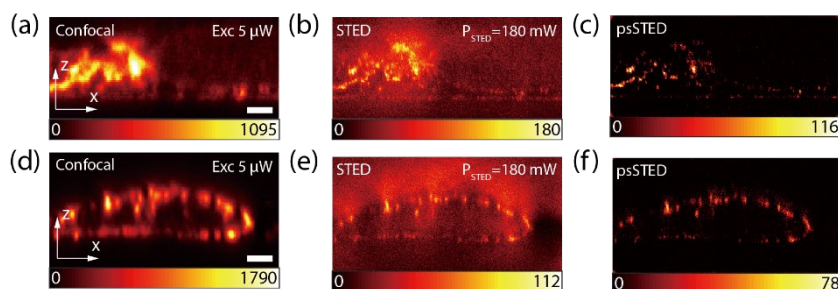


Figure 1. Background noise problem in STED and significant background reduction by psSTED. Scale bar: 2 μm. (a) Confocal, (b) conventional STED, (c) psSTED images of microtubules in a 3T3 cell labelled with SiR-tubulin. (d) Confocal, (e) conventional STED, (f) psSTED images of actin filaments in a LN229 cell labelled with SiR-actin

3. References

- [1] Rittweger, E., Han, K. Y., Irvine, S. E., Eggeling, C. & Hell, S. W. “STED microscopy reveals crystal colour centres with nanometric resolution,” *Nat. Photonics* **3**, 144–147 (2009).
- [2] J.-C. Lee, Y. Ma, K. Y. Han, T. Ha, “Background-free STED nanoscopy by polarization switching,” *ACS Photonics* **6**, 1789 (2019).

Light-induced phenomena in condensed matter system from *ab initio* approach

Dongbin Shin

Department of Physics and Photon Science, Gwangju Institute of Science and Technology (GIST), Gwangju 61005, Republic of Korea

E-mail address: dshin@gist.ac.kr

Abstract: Light-induced phase transitions in condensed matter systems have attracted significant attention due to their potential applications and unprecedented physical phenomena. Recent studies have demonstrated light-induced topological phase transitions in materials such as WTe_2 and ZrTe_5 [1-2], which have been explained by lattice dynamics caused by excited electronic structures [3]. Additionally, light-induced ferroelectric transitions are observed in quantum paraelectric SrTiO_3 through mid-infrared and terahertz lights [4-5], with theoretical evidence suggesting the unique properties of the quantum paraelectric phase is the origin of this terahertz field-induced ferroelectricity [6]. This talk will provide an overview of recent studies on light-induced phase transitions in condensed matter systems including light-induced ferroelectricity in SrTiO_3 , light-induced topological phase transition in HgTe , and cavity-induced topological phase transition in WTe_2 , focusing on the microscopic mechanisms behind these transitions from an *ab initio* approach.

- [1] Sie, E. J. et al. An ultrafast symmetry switch in a Weyl semimetal. *Nature* 565, 61–66 (2019).
- [2] Vaswani, C. et al. Light-Driven Raman Coherence as a Nonthermal Route to Ultrafast Topology Switching in a Dirac Semimetal. *Phys Rev X* 10, 021013 (2020).
- [3] Guan, M.-X., Wang, E., You, P.-W., Sun, J.-T. & Meng, S. Manipulating Weyl quasiparticles by orbital-selective photoexcitation in WTe_2 . *Nat Commun* 12, 1885 (2021).
- [4] Nova, T. F., Disa, A. S., Fechner, M. & Cavalleri, A. Metastable ferroelectricity in optically strained SrTiO_3 . *Science* 364, 1075–1079 (2019).
- [5] Li, X. et al. Terahertz field-induced ferroelectricity in quantum paraelectric SrTiO_3 . *Science* 364, 1079–1082 (2019).
- [6] Shin, D. et al. Simulating Terahertz Field-Induced Ferroelectricity in Quantum Paraelectric SrTiO_3 . *Phys Rev Lett* 129, 167401 (2022).

Spin wavepackets in the Kagome ferromagnet Fe₃Sn₂: propagation and precursors

Changmin Lee

Hanyang University, Korea

The propagation of spin waves in magnetically ordered systems has emerged as a potential means to shuttle quantum information over large distances. Conventionally, the arrival time of a spin wavepacket at a distance, d , is assumed to be determined by its group velocity, vg . Here we report time-resolved optical measurements of wavepacket propagation in the Kagome ferromagnet Fe₃Sn₂ that demonstrate the arrival of spin information at times significantly less than d/vg . We show that this spin wave "precursor" originates from the interaction of light with the unusual spectrum of magnetostatic modes in Fe₃Sn₂. Related effects may have far-reaching consequences toward realizing long-range, ultrafast spin wave transport in both ferromagnetic and antiferromagnetic systems.

Direct Imaging of Ultrafast Charge Carriers Dynamics in Semiconductor Thin Films

Jooyoung Sung

Daegu Gyeongbuk Institute of Science and Technology, Korea

Carrier transport dynamics in solid-state semiconductors play a pivotal role in achieving high device performance. A deep understanding of how charge carriers transport in bulk/thin semiconductors will shed light on developing next-generation semiconductors. However, the observation of true charge carrier transport has hardly been reported due to limitations in time- and space-resolved techniques. In brief, space-resolved spectroscopy techniques, such as TEM, SEM, and various types of optical microscopy, offer excellent spatial resolving power but with poor time resolution. On the other hand, time-resolved spectroscopy techniques, such as TAS, TRPL, etc., have good time-resolving capabilities but lack good spatial resolution. This necessitates a new type of integrated time- and space-resolved technique. In this talk, I will first introduce a new type of time- and space-resolved spectroscopy technique called transient absorption microscopy (TAM), which offers dual capabilities: femtosecond time resolution and nanometer-scale spatial resolution. I will then discuss the application of TAM to perovskite thin films, which exhibit ballistic transport of non-equilibrium charge carriers with transport lengths of up to 150 nm. I will further explore how the non-equilibrium charge carrier dynamics are influenced by the nanoscale chemical heterogeneity, as revealed by fs-microscopic measurements on alloyed perovskite thin films.

Ultra-broadband high efficiency polarization beam splitter metagratings using integrated resonant unit elements into metasurface designs

Hui-Hsin Hsiao

Department of Engineering Science and Ocean Engineering, National Taiwan University
E-mail address: hhsiao@ntu.edu.tw

Abstract: We have developed a broadband high efficiency polarized beam splitting (PBS) metagrating based on integrated resonant units (IRUs) to simultaneously enable polarization analysis, spectral dispersion, and spatial imaging in the near infrared (NIR). A PBS metagrating with a diameter of 60 mm is the key technology component of the High-resolution Multiple-species Atmospheric Profiler in the NIR (HiMAP-NIR). HiMAP-NIR will enable the aerosol profiling in the planetary boundary layer (PBL, surface-2 km) by simultaneously measuring four spatial-spectral-polarimetric images from 680 to 780 nm. Through detailed optimization of hybridized resonant modes in IRUs, the PBS metagrating shows a diffraction efficiency of 70% (or better) for all four linear-polarized incident light and polarization contrasts between orthogonal states are 0.996 (or better) from 680 to 780 nm. It meets the stringent performance required by the HiMAP-NIR exploiting a new paradigm for the broad application of metasurfaces.

1. Introduction

Metasurfaces have opened a whole new paradigm for controlling electromagnetic waves in unprecedented ways, intriguing various novel optical effects and applications. A variety of polarization-multiplexing metadevices such as polarization-dependent beam splitters [1], meta-polarimetry [2], and full-Stokes polarization cameras [3] have been developed for versatile applications. Several pioneering works utilized integrated resonant units (IRUs) designs, which combine multi-nanorod configuration into one unit cell, to successfully tailor phase dispersion and efficiency enhancement for circular-polarized light over a continuous broad spectral range [4].

In this work, we developed a broadband high efficiency polarized beam splitting (PBS) metagrating based on IRU designs to simultaneously enable polarization analysis, spectral dispersion, and spatial imaging for four linear polarization states (0° , 90° , 45° , and 135°) (Fig. 1a). Through the near-field coupling of multiple nanobricks, the hybridized mode in IRUs achieve a broadband reflection efficiency enhancement and retain the required phase value with a linear and smooth phase dispersion for the co-polarized light [5]. Both the simulated and measured optical performance of the IRU-based PBS metagrating exhibit an ultra-broadband efficiency enhancement from $\lambda = 600$ nm to 1000 nm outperforming their single-rod counterparts (Fig. 1b), which reaches $\sim 70\%$ entire the NIR oxygen bands, a polarization contrast greater than 0.996 for the four LP states. An IRU-based PBS metagrating with a diameter of 60 mm has been fabricated and will be integrated into the HiMAP-NIR instrument. Our findings establish a robust basis for building up ultrabroadband high efficiency metadevices and foster the applications of versatile metadevices.

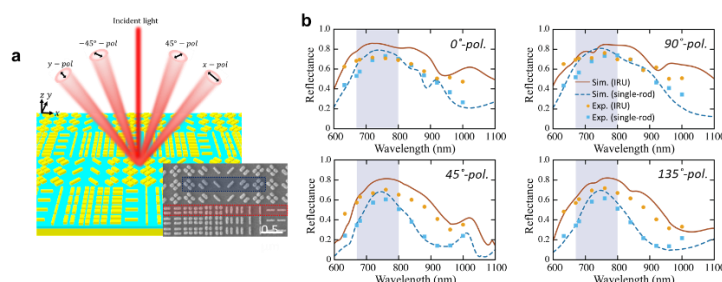


Fig. 1. (a) The schematic view and the SEM images of the PBS metagratings. (b) Simulated and measured efficiency for four linear-polarized light.

References

- [1] Y. Deng, C. Wu, C. Meng, S. I. Bozhevolnyi, and F. Ding, ACS Nano 15, 18532 (2021).
- [2] A. Pors, M. G. Nielsen, and S. I. Bozhevolnyi, Optica 2, 716 (2015).
- [3] N. A. Rubin, G. D'Aversa, P. Chevalier, Z. Shi, W. T. Chen, and F. Capasso, Science 365, eaax1839 (2019).
- [4] H.-H. Hsiao, Y. H. Chen, R. J. Lin, P. C. Wu, S. Wang, B. H. Chen, and D. P. Tsai, Advanced Optical Materials 6, 1800031 (2018).
- [5] H.-H. Hsiao*, R. E. Muller*, J. P. McGuire, D. J. Nemchick, C.-H. Shen, G. v. Harten, M. Rud, W. R. Johnson, A. D. Nordman, Y.-H. Wu, D. W. Wilson, Y.-P. Chiou, M. Choi, J. J. Hyon, and D. Fu*, Advanced Science 9, 2201227 (2022).

Design, fabrication, and application of metasurface/metalens based on dielectric waveguide

Kentaro Iwami

Department of Mechanical Systems Engineering and Department of Bio-Functions and Systems Science,
Tokyo University of Agriculture and Technology, 2-24-16 Nakacho, Koganei, Tokyo 184-8588 Japan
E-mail address: k_iwami@cc.tut.ac.jp

Abstract: Dielectric metasurfaces as phase lattices have attracted attention for their high transmittance and diffraction efficiency, and have been adopted to control wavefront, polarization, and deflection of light. Their applications range from lenses, structured illuminations, holographies, and combined micro-optical elements. In this study, we introduce our recent results including metalenses, holographic movies based on a cinematographic approach, and prism-quarter waveplate combined metasurface.

1. Rotational varifocal moiré metalens

We have investigated a variety of varifocal metalens [1, 2], line-focusing metalens [3], etc. Fig. 1 shows a schematic illustration of a rotational varifocal moiré metalens. The focal length can be varied over a wide range from negative to positive by the mutual rotation of the two lenses. We fabricated the lenses at wavelengths of 900 nm and 633 nm using amorphous and crystalline silicon as materials, respectively.

2. Metasurface holographic movie based on a cinematographic approach

Monochromatic and multicolor holographic movies with multiple frames and wide viewing angles have been achieved based on a cinematographic approach [4-6]. Fig. 2 shows holographic images reconstructed from metasurface holograms made of silicon nitride which shows high transmittance in the whole visible region. A 3-D movie consisting of multiple frames was reproduced by a cinematograph method that sequentially illuminates each frame image while the substrate is driven by the stage.

3. Multifunctional metasurface

Fig. 3 shows the multifunctional metasurface that combines a collimator lens, a quarter waveplate, and a prism. We report on an experimental result of a prism-quarter waveplate combined metasurface made of hydrogenated amorphous silicon (a-Si:H) for a miniaturized reflection-type optical gas cell [7]. Such metasurfaces and gas cells should be useful for miniaturizing various optical devices including chip-scale atomic clocks and micro spectrometers. the next line.

4. Conclusion

Dielectric metasurfaces have enabled various functionalities that were previously impossible. It is expected that applications using these metasurfaces will expand further in the future.

- [1] K. Iwami, C. Ogawa, T. Nagase, and S. Ikezawa, Opt. Express **28**, 35602 (2020).
- [2] C. Ogawa, S. Nakamura, T. Aso, S. Ikezawa, and K. Iwami, Nanophotonics **11** 1941 (2022).
- [3] S. Ikezawa, R. Yamada, K. Takaki, C. Ogawa, and K. Iwami, IEEE Sens. J., **22** 14851 (2022).
- [4] R. Izumi, S. Ikezawa, and K. Iwami, Opt. Express **28** 23761–23770 (2020).
- [5] N. Yamada, H. Saito, S. Ikezawa, and K. Iwami, Opt. Express **30** 17591 (2022).
- [6] M. Yamaguchi, H. Saito, S. Ikezawa, and K. Iwami, Proc. IEEE MEMS 2023, T73-h (2023).
- [7] P. Pruthongs, K. Aoki, S. Ikezawa, M. Hara, and K. Iwami, Proc. Transducers 2023, W2B.02 (2023).

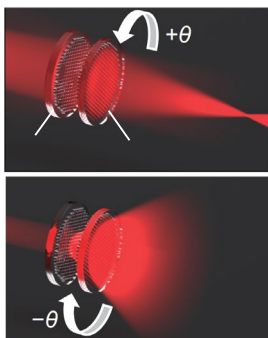


Fig. 1 Rotational varifocal moiré metalens.

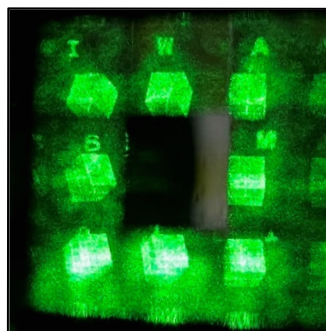


Fig. 2 Multiframe metasurface holography for cinematograph

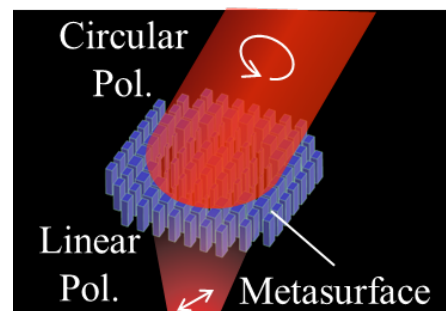


Fig. 3 Multifunctional metasurface for micro optical integration

Meta-lenses from Visible to Vacuum UV Light

Mu Ku Chen^{a,b,c,*}, Xiaoyuan Liu^a, Jingcheng Zhang^a, Jin Yao^a, and Din Ping Tsai^{a,b,c}

^a Department of Electrical Engineering, City University of Hong Kong, Kowloon, Hong Kong 999077.

^b Centre for Biosystems, Neuroscience, and Nanotechnology, City University of Hong Kong, Kowloon, Hong Kong 999077.

^c The State Key Laboratory of Terahertz and Millimeter Waves, City University of Hong Kong, Kowloon, Hong Kong 999077.

E-mail address: mkchen@cityu.edu.hk

Abstract: Meta-lens is an emerging optical device composed of artificial nanostructures that can freely manipulate the phase, polarization, and amplitude of light. We demonstrate various meta-lens applications of optical imaging, advanced sensing, and vacuum UV light generation. The design, application, and experimental verification of meta-device applications are reported in this talk.

Introduction

Meta-lens, an emerging optical device, is composed of artificial nanostructures. Meta-device can freely manipulate the phase, polarization, and amplitude of light. Meta-lenses show excellent performance and novel applications to meet optical demands. The fascinating advantages of meta-lenses are their new properties, lighter weight, small size, high efficiency, better performance, broadband operation, lower energy consumption, data volume reduction, and CMOS compatibility for mass production. In this talk, we demonstrate various meta-device applications of optical imaging, advanced sensing, and vacuum UV light generation, including the design, application, and experimental verification of meta-device applications. We developed the meta-lens for achromatic full-color imaging[1], light field imaging[2], depth sensing[3], edge detection[4], drone camera[5], varifocal bio-imaging[6], underwater stereo vision[7], VUV light generation[8] etc.

We inspired and learned from nature to develop the meta-lens array for advanced imaging and sensing[1-4]. A 60×60 broadband achromatic optical meta-lens array is designed and fabricated for working in the whole visible range. We developed the meta-lens array-based light field imaging system for digital focusing, full-color imaging, depth sensing for static and dynamic objects(Figure 1 (A)), and 1D to 3D edge detection (Figure 1 (B)). The achromatic meta-lens array can collect high-dimensional light field information of objects in the scene.

Following the Moiré technique, a variable focus dielectric meta-lens is designed and implemented for high-contrast optical sectioning fluorescence microscopy at the visible spectral region[6]. In Figure 1(C), we demonstrated telecentric imaging equipped with variable focus meta-lens, which performs high-contrast multi-plane fluorescence imaging for ex-vivo mice intestine tissue samples.

We demonstrate a metalens that both generates, by second-harmonic generation, and simultaneously focuses the generated VUV light. The metalens consists of 150-nm-thick zinc oxide (ZnO) nanoresonators that convert 394 nm light into focused 197-nm radiation, producing a spot $1.7 \mu\text{m}$ in diameter with a 21-fold power density enhancement as compared to the wavefront at the metalens surface.

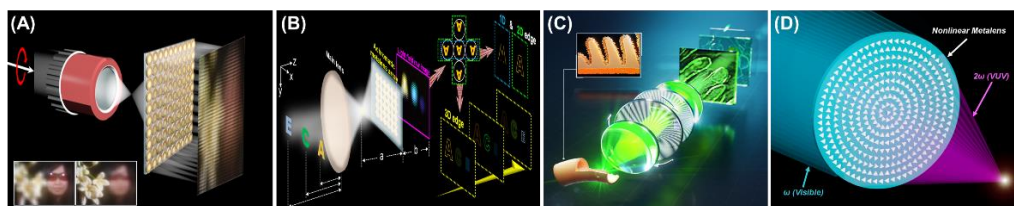


Figure 1 Meta-device applications. (A) Light field imaging, (B) edge detection, (C) varifocal bio-imaging, and (D) VUV light generation.

Our achievements show the importance of optical meta-devices for next-generation optical imaging and sensing. We believe this is an important milestone of the research on advanced meta-devices and opens up an avenue for future applications of optical devices in micro-robotic vision, unmanned-vehicle sensing, virtual and augmented reality, drones, and miniature personal security systems.

References

- [1] Wang, S. M. *et al.* A broadband achromatic metalens in the visible. *Nat. Nanotechnol.* **13**, 227-232, (2018).
- [2] Chen, M. K. *et al.* Optical meta-devices: advances and applications. *Jpn. J. Appl. Phys.* **58**, 8, (2019).
- [3] Lin, R. J. *et al.* Achromatic metalens array for full-colour light-field imaging. *Nat. Nanotechnol.* **14**, 227+, (2019).
- [4] Chen, M. K. *et al.* Edge detection with meta-lens: from one dimension to three dimensions. *Nanophotonics*, (2021).
- [5] Chen, M. K. *et al.* Meta-Lens in the Sky. *IEEE Access* **10**, 46552-46557, (2022).
- [6] Luo, Y. *et al.* Varifocal metalens for optical sectioning fluorescence microscopy. *Nano Lett.* **21**, 5133-5142, (2021).
- [7] Liu, X. *et al.* Underwater Binocular Meta-lens. *ACS Photonics*, (2023).
- [8] Tseng, M. L. *et al.* Vacuum ultraviolet nonlinear metalens. *Science advances* **8**, eabn5644, (2022).

Meta-lens for Intelligent Land, Underwater, and Aerial Imaging

Xiaoyuan Liu¹, Mu Ku Chen^{1,2,3}, Cheng Hung Chu⁴, Jingcheng Zhang¹, Borui Leng¹,
Takeshi Yamaguchi⁴, Takuo Tanaka^{4,5,6}, and Din Ping Tsai^{1,2,3}

¹Department of Electrical Engineering, City University of Hong Kong, Kowloon, Hong Kong 999077

²Centre for Biosystems, Neuroscience, and Nanotechnology, City University of Hong Kong, Kowloon, Hong Kong 999077

³The State Key Laboratory of Terahertz and Millimeter Waves, City University of Hong Kong, Kowloon, Hong Kong 999077

⁴Innovative Photon Manipulation Research Team, RIKEN Center for Advanced Photonics, Saitama 351-0198, Japan

⁵Metamaterial Laboratory, RIKEN Cluster for Pioneering Research, Saitama 351-0198, Japan

⁶Institute of Post-LED Photonics, Tokushima University, Tokushima 770-8506, Japan

E-mail address: xliu499-c@my.cityu.edu.hk

Abstract: We demonstrated a series of intelligent imaging systems based on meta-lens for land, underwater, and aerial application scenarios. Monocular, binocular, and multilocular meta-lenses were specially designed and fabricated for aerial, underwater, and land imaging and sensing applications, respectively. With deep-learning support, intelligent and real-time sensing results were realized.

1. Introduction

Meta-lens is a planar optical device that can control the wavefronts of light via subwavelength nano-antennas. [1-4] Nano-antennas of various structures can provide all kinds of modulation of phase, amplitude, polarization, etc., for a wide range of applications. Traditional optical imaging systems usually consist of a group of lenses to correct spherical or chromatic aberration, which are bulky. When using more than one camera, there will be a set of complex data transformations to calibrate the whole imaging system. Meta-lenses are more flexible to match various scientific and technical application scenarios than the traditional optical lens, especially in space-constrained and fragile environments, such as drones, autonomous driving, and micro-submarines.

2. Land, Underwater, and Aerial Imaging

Due to the limited and specific light field information obtained by single-lens imaging, an intelligent and compact depth-sensing meta-device is proposed for autonomous land driving, as shown in Fig. 1(a). With the support of deep learning, the array of 3600 achromatic metalenses integrates the functions of light field imaging and structured light imaging, which is suitable for different scenes at all light levels. For the exploration of the aquatic environment, a novel GaN binocular meta-lens is specifically designed and fabricated to demonstrate underwater stereo vision (see Fig. 1(b)). Proposed underwater binocular meta-lens stereo vision can realize real-time depth imaging with neural networks. The intrinsic superhydrophobicity of nanostructured GaN meta-lens enables its anti-adhesion, stain-resistant, and self-cleaning functions. For the demands of compact, miniaturized, portable, lightweight, and low energy consumption, we demonstrate a GaN-based polarization-independent metalens camera on a drone, as shown in Fig. 1(c). The meta-lens can realize aerial photography and landing assistance for drones and reduce the weight burden to prolong flight time. Meta-lens will significantly benefit future imaging and sensing applications in aerial, land, and underwater environments.

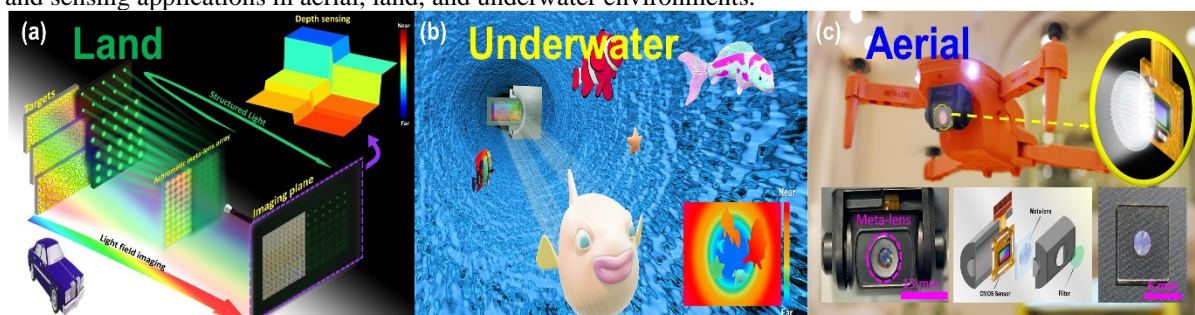


Fig. 1. Applications of meta-lenses. (a) Autonomous vehicles on land. (b) Submarine robot in the ocean. (c) Drone in the sky.

3. References

- [1] M. K. Chen, C. H. Chu, X. Liu, J. Zhang, L. Sun, J. Yao, Y. Fan, Y. Liang, T. Yamaguchi, T. Tanaka, D. P. Tsai, "Meta-Lens in the Sky," IEEE Access **10**, 46552-46557 (2022).
- [2] M. K. Chen, X. Liu, Y. Sun, D. P. Tsai, "Artificial Intelligence in Meta-optics," Chem. Rev. **122**(19), 15356-15413 (2022).
- [3] M. K. Chen, X. Liu, Y. Wu, J. Zhang, J. Yuan, Z. Zhang, D. P. Tsai, "A Meta-Device for Intelligent Depth Perception," Adv. Mater., 2107465 (2022).
- [4] X. Liu, M. K. Chen, C. H. Chu, J. Zhang, B. Leng, T. Yamaguchi, T. Tanaka, D. P. Tsai, "Underwater Binocular Meta-lens," ACS Photonics, doi.org/10.1021/acsp Photonics.2c01667 (2023).

Meta-lenses for Future Communication Systems

Jing Cheng Zhang, Mu Ku Chen, Xiaoyuan Liu and Din Ping Tsai

Department of Electrical Engineering, City University of Hong Kong, Kowloon, Hong Kong SAR, China

E-mail address: jzhang2442-c@my.cityu.edu.hk

Abstract: 6G communication technology targets improved signal strength concentration and directivity, which can be achieved using meta-lenses in the terahertz band. Our study focuses on varifocal meta-devices that control terahertz beam direction and coverage area, enabling secure and highly directed 6G communication with adjustable transmission direction. With their cost-effectiveness, meta-lenses are well-suited for large-scale deployment in 6G communication systems, wireless power transfer, zoom imaging, and remote sensing.

1. Introduction to main text format and page layout

Rotary metasurface technology could enhance the 6G wireless communication systems by providing tunable terahertz beam steering capabilities in arbitrary 2D or 3D space [1]. While conventional THz systems use bulky and heavy dielectric lenses and reflectors to collimate and focus waves, planar metasurfaces can manipulate wavefronts with sub-wavelength resolution using artificial meta-antennas [2]. Varifocal meta-devices, such as achromatic meta-lens [3], can be integrated with liquid crystal layers or other materials to achieve beam steering and projection. However, existing methods have limitations in controlling the radiation direction and coverage area of beams in THz bands without excessive active components. Rotary metasurface technology can overcome these limitations and increase directivity, security, and flexibility in future 6G applications.

2. Results and discussion

Figures 1a-1k present the manipulation of Airy beam focal spots in 2D and 3D space. In 2D, sixteen points from different radii were experimentally demonstrated, and their predicted and measured results were shown in Figures 1b-1c. As depicted in the insert, the focal spots were directed to any point in the 2D focal plane. In the x-z plane, Figures 1d-1e illustrate the numerically predicted and measured Airy beams. Additionally, Figures 1f-1k show the regulation of focal spots in the entire space using meta-lenses, where the focal length can be tailored between 40 mm to 60 mm. The experimental results for such focal planes are shown in Figures 1f-1h, with an insert depicting the nearby solid black points. The numerical and experimental results in the x-z plane for focal lengths of 40 mm, 50 mm, and 60 mm are shown in Figures 1i-1k.

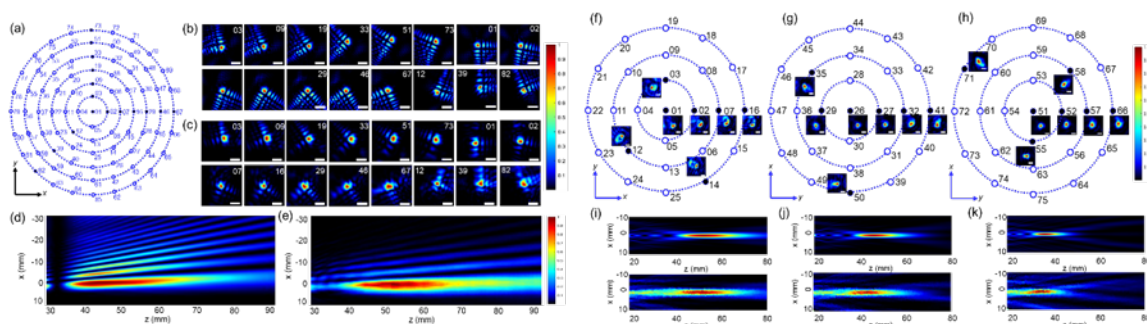


Fig. 1. Experimental demonstration of the performance of the varifocal meta-lens system

3. Results and discussion

Our compact tunable meta-devices, designed with synthetic phase profiles and fabricated using 3D printing, demonstrate the complete manipulation of the THz beam's propagation direction and coverage area. The doublet meta-device can steer Airy beams in a 2D plane, offering signal transmission stability and security. In contrast, the triplet meta-device can focus THz waves to arbitrary positions in 3D space without requiring additional space. This dynamic control enables 6G communication systems to deliver highly concentrated signals to specific users/detectors, providing secure, flexible, high directivity, and high signal concentration.

4. References

- [1] Gros J B, Popov V, Odit M A, et al. A reconfigurable intelligent surface at mmWave based on a binary phase tunable metasurface[J]. IEEE Open Journal of the Communications Society, 2021, 2: 1055-1064.
- [2] Zhu S Y, Wu G B, Pang S W, et al. Compact terahertz dielectric folded metasurface[J]. Advanced Optical Materials, 2022, 10(3): 2101663.
- [3] Wang S, Wu P C, Su V C, et al. A broadband achromatic metalens in the visible[J]. Nature Nanotechnology, 2018, 13(3): 227-232.

Stacking-specific plasmonic responses and structural changes of few-layer graphene revealed by IR near-field microscopy

*Zee Hwan Kim**

Department of Chemistry, Seoul National University, Seoul 08826, Korea

In this talk, I will present two studies on few-layer graphene (FLG) employing IR scattering-type near-field optical microscopy (IR-sSNOM). First, I will show how the stacking-orders in trilayer graphene (TLG) influences the propagation and reflection of IR surface plasmon polaritons (SPPs). We found that the near-field spectra and SPP-wavelengths for Bernal (ABA) and rhombohedral (ABC) stacking domains of TLG exhibit significant stacking-dependent behaviors that can be fully explained by the stacking-specific intraband optical conductivities. This conductivity difference also explains the observed SPP-reflection at the ABA-ABC domain boundaries. However, we discovered that some of the ABC-edges of TLG exhibit anomalous reflection that cannot be accounted for by the SPP-reflection at the idealized discontinuity in conductivity. Instead, this finding strongly suggests a strongly absorbing ABC-edge state. Second, I will show that bilayer graphene (BLG) can reversibly capture CO₂ gas between the graphene layer, which transforms the tightly stacked AB-like BLG into two nearly uncoupled single-layer graphenes. Such CO₂-loading in FLG may provide a new means to capture and store anthropogenic CO₂ and also provide a means to tune the interlayer electronic coupling in few-layer graphene.

Mid-infrared image polaritons in van der Waals crystals

Min Seok Jang

*School of Electrical Engineering, KAIST
E-mail address: jang.minseok@kaist.ac.kr*

Abstract: Polaritons in two-dimensional materials have been attracting enormous research interest due to their deep-subwavelength field-confinement enabling strong light matter interactions. In this presentation, I introduce a new class of polaritonic modes – image polaritons - that appear when a polaritonic material is in close proximity to a highly conductive metal, so that the polaritonic mode couples with its mirror image. The image polaritons constitute an appealing nanophotonic platform, providing an unparalleled degree of optical field compression into nanometric volumes while exhibiting lower normalized propagation loss compared to conventional van der Waals polaritons on nonmetallic substrates. I will cover three different mid-infrared image polaritons in van der Waals Crystals: image plasmons in graphene and image phonon polaritons in h-BN and α -MoO₃.

Control of multi-step vibrational excitation using ultrafast infrared plasmonics

Satoshi Ashihara

Institute of Industrial Science, The University of Tokyo
ashihara@iis.u-tokyo.ac.jp

Abstract: A marriage of ultrafast lasers and plasmonics in the mid-infrared range achieves strong interaction of a mid-infrared photon and a molecular vibration in a short time scale. It enables ultrasensitive nonlinear vibrational spectroscopy and efficient multi-quantum vibrational excitation, opening a possibility of bond-selective chemistry at metal surfaces.

Ultrashort mid-infrared (mid-IR) laser pulses offer great potential for nonlinear vibrational spectroscopy [1] and active control of chemical reactions at electronic ground states [2–6]. Deposition of sufficient vibrational energy into a specific chemical bond via vibrational ladder climbing (VLC) is useful for active control over molecular processes at electronic ground states because strong excitation of key reagent vibrations should directly contribute to chemical reactions.

Surface plasmons in the mid-IR range can provide a new platform for nonlinear vibrational spectroscopy and vibrational quantum control. Plasmonics takes advantage of the coupling of light to metal electrons, enabling subwavelength localization and strong field enhancements and enhanced light–matter interactions. In the mid-IR range, the plasmonic field enhancement may play a key role in accelerating VLC to enable sufficient energy deposition on a timescale faster than vibrational relaxation.

In recent years, we have studied temporal responses of surface plasmons on noble metals in the mid-IR range [7,8] and applied them to nonlinear vibrational spectroscopy [9, 10], and vibration-mediated reaction control [11]. In particular, plasmonic near-fields of chirped mid-IR pulses strongly driven molecular vibrations and thereby realized bond-breaking of condensed-phase molecules [11].

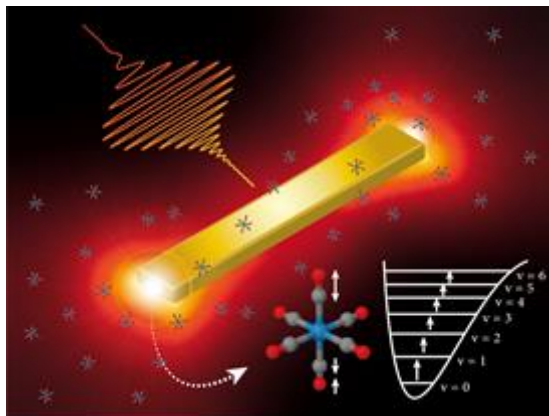


Fig. 1 Plasmonic near-field enhancement of chirped mid-infrared pulses and its application to efficient vibrational ladder climbing [11].

References

- [1] P. Hamm, M.T. Zanni, Concepts and Methods of 2D Infrared Spectroscopy (Cambridge University Press, 2011).
- [2] J.C. Polanyi, Acc. Chem. Res. **5**, 161 (1972).
- [3] M. Artamonov, T.S. Ho, H. Rabitz, Chem. Phys. **328**, 147 (2006).
- [4] C. Gollub, M. Kowalewski, S. Thallmair, R. de Vivie-Riedle, Phys. Chem. Chem. Phys. **12**, 15780 (2010).
- [5] M. Delor, S. A. Archer, T. Keane, A. J. H. M. Meijer, I. V. Sazanovich, G. M. Greetham, M. Towrie, J. A. Weinstein, Nat. Chem. **9**, 1099 (2017).
- [6] T. Stensitzki, Y. Yang, V. Kozich, A. A. Ahmed, F. Kössl, O. Kühn, K. Heyne, Nat. Chem. **10**, 126 (2018).
- [7] F. Kusa, S. Ashihara, J. Appl. Phys. **116**, 153103 (2014).
- [8] F. Kusa, K.E. Echternkamp, G. Herink, C. Ropers, S. Ashihara, AIP Adv. **5**, 077138 (2015).
- [9] F. Kusa, I. Morichika, A. Takegami, S. Ashihara, Opt. Express **25**, 12896 (2017).
- [10] I. Morichika, F. Kusa, A. Takegami, A. Sakurai, S. Ashihara, J. Phys. Chem. C **121**, 11643 (2017).
- [11] I. Morichika, K. Murata, A. Sakurai, K. Ishii, S. Ashihara, Nat. Commun. **10**, 3893 (2019).

Moiré excitons and correlated states in 2D materials

Hyeonjun Baek

Department of Physics, Sogang University, Seoul, Korea

E-mail address: hjbaek@sogang.ac.kr
.kr

Van der Waals heterostructures can be designed to confine electrons and holes in unique ways. One remarkable approach is to vertically stack two atomically thin layers of transition metal dichalcogenide (TMD) semiconductors. The relative twist or lattice mismatch between the two layers leads to moiré pattern formation, which modulates the electronic band structure according to the atomic registry. Single-particle wave packets can be trapped in the moiré-induced potential pockets with three-fold symmetry, leading to the formation of trapped interlayer excitons and correlated states. In this talk, I will explain photoluminescence emission of moiré confined excitons in MoSe₂/WSe₂. Interesting properties of moiré excitons like antibunching, large Stark shift, and doping dependence will be presented. Furthermore, correlated states, such as Mott insulating states and Wigner crystals, observed from moiré heterostructures will be presented.

Monolayer Semiconductors with High Luminescence Efficiency

Hyungjin Kim

Department of Materials Science and Engineering, Yonsei University, 50 Yonsei-ro, Seodaemun-gu, Seoul 03722, South Korea
E-mail address: hyungjin.kim@yonsei.ac.kr

Abstract: Two-dimensional (2D) transition metal dichalcogenide (TMDC) monolayers such as MoS_2 , WS_2 , and WSe_2 have aroused significant attention among researchers over past years due to their unique properties which possess the promise for future optoelectronic applications. Atomically thin TMDC monolayers exhibit the tunability of their properties through electric field and strain as well as the capability to achieve van der Waals heterostructures free of lattice mismatch. While these advantages enable their application for various optoelectronic devices including light-emitting diodes (LEDs) and photodetectors, one of the main constraints for their implementation in practical applications is the low photoluminescence (PL) quantum yield (QY), which is reported in the range of 0.01 to 6% at room temperature. PL QY is a key figure of merit in optoelectronic applications because it directly determines the maximum efficiency that the device can achieve.

In this work, 2D TMDC monolayers with high optoelectronic quality were demonstrated in both mechanically exfoliated and synthesized samples through proper material processing [1, 2]. Moreover, we achieved near-unity PL QY in monolayers at all exciton densities, which paves the way for developing LEDs that will retain high efficiency at all brightness [3].

- [1] M. Amani, D.-H. Lien, D. Kiriya, J. Xiao, A. Azcatl, J. Noh, S. R. Madhvapathy, R. Addou, S. K. C., M. Dubey, K. Cho, R. M. Wallace, S.-C. Lee, J.-H. He, J. W. Ager III, X. Zhang, E. Yablonovitch, A. Javey, *Science* **350**, 1065 (2015).
- [2] D.-H. Lien, S. Z. Uddin, M. Yeh, M. Amani, H. Kim, J. W. Ager III, E. Yablonovitch, and A. Javey, *Science* **364**, 468 (2019).
- [3] H. Kim, S. Z. Uddin, N. Higashitarumizu, E. Rabani, A. Javey, *Science* **373**, 448 (2021).

Transition Metal Dichalcogenides (TMDs)-based Photodetector: Performance Enhanced by Chemical Doping Technique

Dong-Ho Kang

*School of Electrical Engineering and Computer Science (EECS), Gwangju Institute of Science and Technology (GIST)
E-mail address: donghokang@gist.ac.kr*

Abstract: Chemical doping plays an essential role in nanophotonics, particularly in improving the performance of TMD photodetector by suppressing the recombination rate of photocarriers in the channel layer. In this talk, we introduce our doping studies performed on several TMD devices (e.g., MoS₂, WSe₂, ReS₂, and ReSe₂) by meticulously analyzing key performance factors such as photoresponsivity, detectivity, and rising/decaying time. Our studies explain the fundamental mechanisms underlying the significance of doping techniques in enhancing the performance of TMD photodetectors. In addition, we introduce the intrinsic limitations of doping techniques and propose diverse solutions.

Two-dimensional (2D) semiconducting materials, also known as transition metal dichalcogenides (TMDs), have recently attracted many attentions as a nanoscale channel material for future flexible, wearable, and transparent electronic/optoelectronic device[1-2] due to their superior physical[3], electrical[4], and optical properties[5]. In particular, TMDs are the best materials for optoelectronic applications (e.g., photodetectors and solar cells due to their tunable energy bandgap properties, which can be controlled by changing their number of layers (from 1.8 to 1.2 eV), and their excellent quantum efficiency. However, the high contact resistance due to the van der Waals gap between TMD and metal layer is an inevitable limitation that hinders the performance of TMD-based applications. Meanwhile, the development of doping techniques for 2D TMDs is required to reduce the metal–semiconductor (M-S) contact resistance and also to lower the recombination rate of carriers, which should lead to improved performance of TMD-based electronic and optoelectronic devices.

In this talk, we introduce our recently reported high-performance TMD photodetector techniques based on several n- and p-type doping techniques using octadecyltrichlorosilane (OTS)[6], 3-aminopropyltriethoxysilane (APTES)[7], triphenylphosphine (PPh₃)[8], and hydrochloric acid (HCl)[9]. Furthermore, the photoluminescence studies for n- and p-type doping effects on TMD are discussed to elucidate the mechanism of doping and its impact on key performance factors including photoreponsivity, detectivity, and rising/decaying time. Lastly, we introduce our recent progress on high-performance 2D photodetector for polarization-sensitivity and synaptic application.

- [1] S. Das, R. Gulotty, A. V. Sumant, A. Roelofs, Nano Lett. **14**, 2861 (2014).
- [2] J. Pu, Y. Yomogida, K.-K. Liu, L.-J. Li, Y. Iwasa, T. Takenobu, Nano Lett. **8**, 4013 (2012).
- [3] K. F. Mak, C. Lee, J. Hone, J. Shan, T. F. Heinz, Phys. Rev. Lett. **105**, 136805 (2010)
- [4] A. Splendiani, L. Sun, Y. Zhang, T. Li, J. Kim, C.-Y. Chim, G. Galli, F. Wang, Nano Lett. **10**, 1271 (2010).
- [5] H. Wang, L. Yu, Y.-H. Lee, Y. Shi, A. Hsu, M. L. Chin, L.-J. Li, M. Dubey, J. Kong, T. Palacios, Nano Lett. **9**, 4674 (2012).
- [6] D.-H. Kang, J. Shim, S. K. Jang, J. Jeon, M. H. Jeon, G. Y. Yeom, W.-S. Jung, Y. H. Jang, S. Lee, J.-H. Park, ACS Nano **9**, 1099-1107 (2015)
- [7] D.-H. Kang, M.-S. Kim, J. Shim, J. Jeon, H.-Y. Park, W.-S. Jung, H.-Y. Yu, C.-H. Pang, S. Lee, J.-H. Park, Adv. Funct. Mater. **25**, 4219-4227 (2015)
- [8] S.-H. Jo, D.-H. Kang, J. Shim, J. Jeon, M. H. Jeon, G. Yoo, J. Kim, J. Lee, G. Y. Yeom, S. Lee, H.-Y. Yu, C. Choi, J.-H. Park, Adv. Mater. **28**, 4824-4831 (2016)
- [9] J. Kim, K. Heo, D.-H. Kang, C. Shin, S. Lee, H.-Y. Yu, J.-H. Park, Adv. Sci. **6**, 1901225 (2019).

Ultrafast photo-induced dynamics in 2D materials with low in-plane symmetry

Jiacheng Song, Sung Bok Seo, Sang Ho Suk and Sangwan Sim*

School of Electrical Engineering, Hanyang University, Ansan, 15588 South Korea

E-mail address: swsim@hanyang.ac.kr

Abstract: We discuss the transient optical modulation and carrier diffusion dynamics of low symmetric 2D materials, including ReS_2 and ZrTe_5 , studied by ultrafast pump-probe spectroscopy. Their strong polarization-dependent ultrafast photo-induced dynamics will be discussed.

1. Introduction

The low-symmetrical 2D materials, such as black phosphorus, ReS_2 , GeSe , and SnSe , possess in-plane crystal anisotropy, opening up new avenues for developing advanced optical, electrical, and thermal devices. Their optical anisotropy provides a path for creating highly polarized light detectors, emitters, and optical information devices. In recent years, ultrafast tuning of the anisotropic optical characteristics in these materials has gained interest due to its potential for high-speed polarization-controlled optical devices. Furthermore, the unique quasi-1D dynamics of photocarriers with orientation-dependent mobilities and diffusivities displayed in ultrafast spatiotemporal dynamics is crucial information for advancing the anisotropic device technologies.

2. Results

We will discuss the anisotropic, transient optical modulation and carrier diffusion of low symmetrical 2D materials, including ReS_2 and ZrTe_5 , studied using ultrafast pump-probe spectroscopy [1-2]. Our focus will be on their strong polarization-dependent ultrafast photo-induced dynamics, offering ample opportunities for ultrafast modulation applications. The orientation-dependent ultrafast carrier diffusion observed by spatiotemporal scanning pump-probe microscopy will also be covered.

[1] S. B. Seo, S. Nah, M. Sajjad, N. Singh, Y. Shin, Y. Kim, J. Kim, S. Sim, *Phys. Rev. Applied* 18, 014010 (2022)

[2] S. B. Seo, S. Nah, M. Sajjad, J. Song, N. Singh, S.H. Suk, H. Baik, S. Kim, G.-J. Kim, J.-I. Kim, and S. Sim, *Adv. Opt. Mater.* 3, 2201544 (2023)

Ultrafast Field-Induced Nonlinear Optics

Bong Joo Kang

Division of Advanced Materials, Korea Research Institute of Chemical Technology (KRICT), Daejeon 34114, Republic of Korea
E-mail address: bj.kang@kRICT.re.kr

Abstract: We report ultrafast field-induced nonlinear effects in solid-state and liquid-state materials. These observations broaden our understanding of strong field-matter interaction, paving the way for exploring novel nonlinear phenomena and developing ultrafast devices.

The control and characterization of material properties through electromagnetic waves have attracted significant research interest for various applications. In particular, electromagnetic waves in THz frequency allow us to directly observe numerous fundamental modes of quasiparticles in different phases. In recent decades, phase-stable THz sources with sufficiently strong electric fields have been developed by employing various techniques [1]. Owing to such technical progress, the scope of research has expanded from basic phenomena to diverse applications, paving the way for exploring novel nonlinear phenomena and developing ultrafast devices.

This talk is dealing with our recent efforts to efficiently generate table-top THz sources and the related nonlinear optics, especially ultrafast field-induced phenomena in solid-state and liquid-state materials. Ultrafast THz radiation can be regarded as a quasi-DC electric field owing to its unique position in the electromagnetic spectrum. This ultrafast quasi-DC field can accelerate electrons or distort potential barriers, leading to impact ionization, Zener tunneling, quantum tunneling between the nanometer-scale gap, and Stark effect with sub-picosecond time resolutions [2,3]. Such investigations open previously inaccessible perspectives and broaden our understanding, thus help us contribute substantially to the field of ultrafast nonlinear optics and their applications in material sciences.

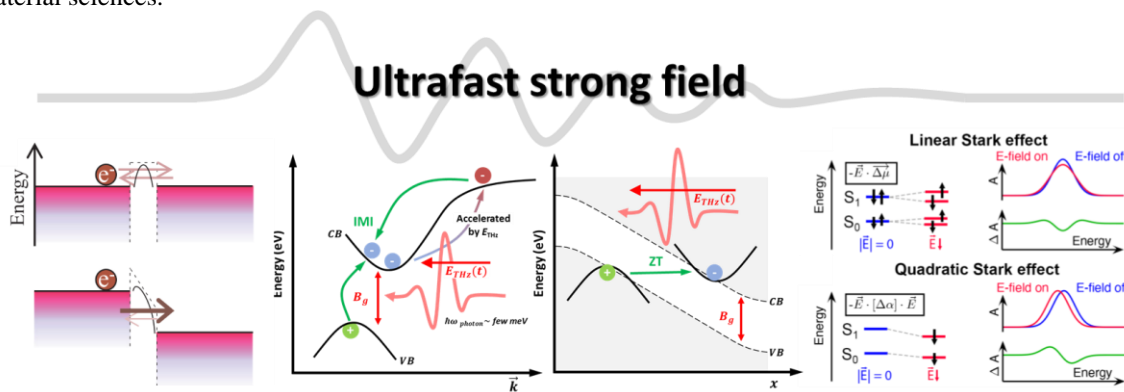


Fig. 1. Ultrafast field-induced nonlinear phenomena such as quantum tunneling between the nanometer-scale gap, impact ionization, Zener tunneling, and linear/quadratic Stark effect.

- [1] S.-J. Kim*, B. J. Kang*, U. Puc*, W. T. Kim, M. Jasbinsek†, F. Rotermund†, O.-P. Kwon†, Adv. Opt. Mater. **9**, 2101019 (2021).
- [2] Y.-M. Bahk*, B. J. Kang*, Y. S. Kim, J.-Y. Kim, W. T. Kim, T. Y. Kim, T. Kang, J. Rhie, S. Han, C.-H. Park, F. Rotermund†, D.-S. Kim†, Phys. Rev. Lett. **115**, 125501(2015).
- [3] B. J. Kang, D. Rohrbach, F. D. J. Brunner, S. Bagiante, H. Sigg, T. Feurer, Nano Lett. **22**, 2016 (2022).

Ultrafast control of topological surface and bulk charge transport through hypersonic vibrational coherence

Tae Gwan Park and Fabian Rotermund

Department of Physics, Korea Advanced Institute of Science and Technology (KAIST), Daejeon 34141, Republic of Korea
E-mail address: tgpark1160@kaist.ac.kr

Abstract: Control of topological invariants is essential to construct a topological on/off switching device such as a transistor, a fundamental part of electronic applications. Although topological phases can be changed by tensile stress, the mechanical strain has been constrained by the formation of in-plane cracks. To overcome this limitation, we use photoinduced strain to selectively generate the longitudinal direction and demonstrate the topological phase switching by employing ultrafast optical and THz spectroscopy. The suppression of surface-bulk coupling, enabling by the photoinduced strain waves, allows for selective transport control in topological surface and bulk states across the transition. These observations offer crucial information for possible topological switching applications with time-varying protocols at room temperature.

Introduction

Bi_2Se_3 offers novel platforms for specific uses including spintronics and quantum information processing at ambient temperature thanks to its symmetry-protected topological surface states (TSS) and bulk states (BS) with a large bulk gap [1]. Control of topological invariants enables the implementation of a topological on/off switching device such as a transistor, one of the fundamental components of upcoming applications. For the purpose of trying to make such a reversible transition, a mechanical strain has been used [2]. However, it indicates a limit in operating speed and is accompanied by in-plane cracks prior to such transitions in Bi_2Se_3 . Recently, light-driven phononic transition and strain have been considered as an efficient way to control the topological invariants in ultrafast and time-varying schemes [3]. Nonetheless, the light-driven transition and its transport characteristics during the topological phase change in Bi_2Se_3 , which are crucial for developing topological switching devices, have not been studied.

Results

In this work, we use light to change the topological phases of Bi_2Se_3 by applying a tensile strain along the out-of-plane direction (Fig. 1a). The temporal evolution of photoinduced strain waves and simultaneous transport characteristics are monitored by near-IR ($\Delta R/R_0$) and THz ($-\Delta E/E_0$) probe lights as shown in Fig. 1b. Although experiments were conducted ambient temperature far above the Debye temperature where surface-bulk scattering predominates, the strain-dependent THz conductance shows the bipolar response from TSS and BS transports (Fig. 1c). By allowing backscattering in symmetry-protected TSS above photoinduced strain of around 5%, the transport lifetime in the TSS channel abruptly decreased, while the bulk conductance is significantly enhanced about 9 times by band shrinks and gap-closing. The method demonstrated in the present work shows that the light-driven strain is a powerful source for ultrafast switching the topological invariants and controlling the transport characteristics at hypersonic frequencies and room temperature. In the presentation, power-dependent excitation and coherent modulation by lattice vibrations will be discussed with DFT calculation results.

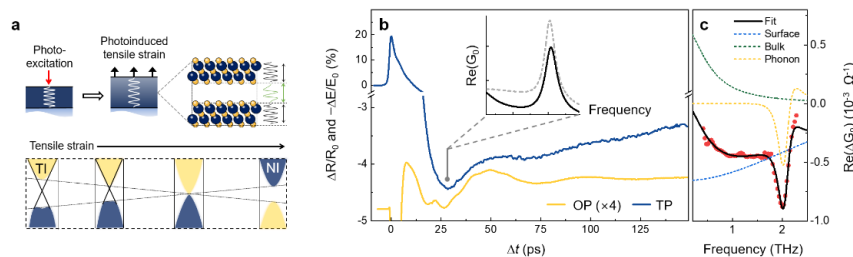


Fig. 1. (a) Schematic of photoinduced strain, which alters topological phases in Bi_2Se_3 . (b) Temporal evolution in photoexcited dynamics, measured with optical probe (OP, $\Delta R/R_0$) and THz probe (TP, $-\Delta E/E_0$) pulses with $F_{\text{pump}} = 2.3 \text{ mJ/cm}^2$. The inset indicates the real part of THz conductance at a selected time delay ($\Delta t = 25 \text{ ps}$) with equilibrium conductance (gray). (c). Differential THz conductance of Bi_2Se_3 recorded at $\Delta t = 25 \text{ ps}$, which corresponds to the maximum expansion of lattice. The black line indicates the fitting curve based on the Drude model fit.

References

- [1] M. Z. Hasan and C. L. Kane, *Rev. Mod. Phys.* **82**, 3045 (2010).
- [2] C. Lin et al., *Nat. Mater.* **20**, 1093 (2021).
- [3] E. J. Sie et al., *Nature* **565**, 61 (2019).

Active control of THz polarization states by graphene metasurfaces

Teun-Teun Kim

*Department of Semiconductor Physics, University of Ulsan, Ulsan, 44610, Republic of Korea
E-mail address: ttkim@ulsan*

Abstract: Manipulation of polarization states of electromagnetic waves can be realized by anisotropy of birefringent materials. However, in the terahertz regime, relatively small anisotropy of naturally existing transparent materials has impeded the miniaturization of optical components or devices. Here, we demonstrate an active control of polarization states by different designs of graphene metasurfaces with chirality, anisotropy or non-Hermiticity. Continuous control of polarization states may provide a wide range of opportunities for the development of compact THz polarization devices and polarization-sensitive THz technology.

Polarization of electromagnetic waves plays a vital role in numerous fields because the responses of materials and devices to electromagnetic waves typically rely on their polarization states. Effective control of polarization states is crucial for the development of complex optical systems. However, at THz frequencies, controlling polarization states is limited by the lack of naturally occurring materials with strong chirality and birefringence, as well as the absence of high-performance polarization devices. Although metasurfaces have been proposed to manipulate polarization states, most metasurface-based polarization devices are passive. Recently, researchers have demonstrated dynamic control of polarization states using various tuning methods. However, integrating graphene into metasurfaces would be attractive because of its extreme thinness and the ability to control its conductivity through electric gating with low gate voltages. In this presentation, we will discuss recent research on metasurface designs that exhibit exceptional polarization properties. We will demonstrate how hybrid material systems, comprising artificially constructed meta-atoms and an atomically thin graphene layer, enable gate-induced switching and linear modulation of polarization states [1-4]. Unlike intrinsic properties of composite materials, well-designed metasurfaces offer extensive capabilities for developing high-performance and integrated optical devices that surpass traditional bulk optical elements.

- [1] Kim, T.-T. et al. "Optical Activity Enhanced by Strong Inter-molecular Coupling in Planar Chiral Metamaterials," *Sci. Rep.* 4, 5864 (2014).
- [2] Kim, T.-T. et al. "Electrical access to critical coupling of circularly polarized waves in graphene chiral metamaterials," *Sci Adv* 3, 1701377 (2017).
- [3] Beak, S. et al. "Non-Hermitian chiral degeneracy of gated graphene metasurfaces," *arXiv:2208.10675* (2012).
- [4] Park, H. et al. "Electrically tunable THz graphene metasurface wave retarders," *Nanophotonics*, under review

Ultra-stable terahertz synthesizer referenced to a high-finesse optical cavity

Young-Jin Kim*, Dong-Chel Shin, Guseon Kang, Jae-Yoon Kim, Heesuk Jang, and Seung-Woo Kim*

Department of Mechanical Engineering, Korea Advanced Institute of Science and Technology

Author e-mail address: yj.kim@kaist.ac.kr

Abstract: A terahertz synthesizer is devised to transfer the stability of a high-finesse optical cavity for the terahertz domain, achieving an instability of 3×10^{-15} at a 1-s averaging.

1. Introduction

Extremely stable and precise terahertz-frequency synthesizers will expedite emerging terahertz applications of molecular spectroscopy, probing metamaterials, terahertz radar, and next-generation 6G wireless communication. In this study, we demonstrate an ultra-stable continuous-wave terahertz synthesizer via frequency mixing of two comb lines from an optical frequency comb. The terahertz synthesizer inherits the exceptional stability of the mother frequency comb stabilized to a high-finesse optical cavity with a fractional frequency instability of 10^{-15} .

2. Experimental design and results

Figure 1a illustrates the system configuration describing how the terahertz synthesizer devised in this study generates terahertz frequencies referenced to a high-finesse optical cavity. First, an optical frequency comb from an Er-doped fiber oscillator (source comb) is stabilized to a high-finesse optical cavity, resulting in short-term frequency stability of $\Delta f/f \approx 10^{-15}$ at 1 s averaging [1]. Then, a pair of comb lines, ν_1 and ν_2 , are extracted from the source comb through wavelength-division multiplexing (WDM) combining a fiber Fabry-Perot (FFP) filter and a fiber Bragg grating (FBG) filter. Then, the optical injection locking method is applied to amplify the extracted comb lines through stimulated emissions in distributed feedback laser diodes (DFB LD) without degrading the stability and linewidth inherited from the source comb [2]. Being incident into a photomixer, the two comb lines are converted to terahertz waves with a frequency of intensity modulation by the interfering comb lines, i.e., $f_t = |\nu_1 - \nu_2| = n_t f_r$ where f_t and n_t is the terahertz frequency and an integer.

The radiated terahertz waves are detected in a photoconductive antenna (PCA) with the aid of another frequency comb (Comb#2). To coherently detect the terahertz waves, Comb#2 is adjusted to yield a slightly different repetition rate of $f_r + \Delta f_r$, and phase-locked to the comb lines ν_1 and ν_2 . The pulse train of Comb#2 is made incident to the PCA such that the excitations of electron-hole pairs are periodically generated, forming a terahertz comb, $f_{t, \text{comb}} = n(f_r + \Delta f_r)$. The terahertz comb produced by Comb#2 allows for the heterodyne detection of the terahertz waves, yielding a heterodyne frequency $f_t - f_{t, \text{comb}} = n_t \Delta f_r$ which is then evaluated for determining the exact terahertz frequency and the frequency stability.

Figure 1b depicts the linewidths of the terahertz frequencies obtained by performing a fast Fourier transformation (FFT) of the acquired signal for 500 s. All the frequencies of 0.10 THz, 0.66 THz, and 1.05 THz show 2 mHz linewidth, which corresponds to the FFT resolution limit. Also, the frequency instability at 0.66 THz approaches 3×10^{-15} at a 1-s averaging. By incorporating one of the state-of-the-art optical clocks [3], the absolute sub-mHz linewidths may be realized, although not implemented here in the current version of the hardware system. Moreover, our terahertz synthesizer allows for arbitrary frequency control without loosening the source comb stabilization. As shown in figure 1c, one comb line is hopped to the next comb line while the other comb line remains fixed. Specifically, the DFB LD for the injection-locking of ν_1 is set on a programmed current control sequence so that the injection-locking operational window is shifted consecutively in steps of 100 MHz repetition rate. To validate the tunability of our synthesizer, a scanning sequence with the W-letter pattern over a 1.0 GHz range with 10 stopovers of 10 s duration per each is performed (Figure 1d).

Physics Informed Deep Learning Enabled Inverse Design in Terahertz Nano-photonics

Hyoung-Taek Lee, Jeonghoon Kim, and Hyeong-Ryeol Park*

Department of Physics, Ulsan National Institute of Science and Technology, Ulsan, Republic of Korea
E-mail address: nano@unist.ac.kr

Abstract: In this study, the inverse design method combining the deep Q-learning and the modal expansion methods, is used to design a fast optimization of terahertz nanophotonic device. Here, the terahertz nanophotonic device is loop nano-gaped structure, and this structure is promising for strong field enhancement application such as sensing and nonlinear optical effect. Our method is about 2,400,000 times faster than the inverse design method using simulation methods.

1. Introduction

In the field of photonics, the inverse design method using the reinforcement learning method of artificial intelligence is used to design the optimal structure for the desired application [1]. The inverse design method is mainly used by applying simulation.

In the inverse design method that performs tens of thousands of calculations, it is not too much to apply computational simulation because the shape, period, and thickness of the thin film have a size comparable to the wavelength in the case of the visible or infrared region. In the case of nanophotonic devices for terahertz region, the time required for computational simulation increases exponentially because the nanometer gap area is 1/10,000 times smaller than the wavelength. If inverse design is carried out in this simulation method, it will take more than several years to calculate one device.

To solve this problem, the inverse design method based on deep Q learning combined with modal expansion method is used to obtain optimized structural designs of terahertz nanophotonic device [2]. With our inverse design method based on the analytical solution, computational resources can be significantly reduced, making it an alternative to the numerical simulation-based inverse design, which was unfeasible due to the mass computation time.

2. Results

Using modal expansion, an analytical solution for the rectangular nanoloop structure, it takes about 0.36 seconds for one calculation. The desired structure is designed using the inverse design method combined with this analytical solution. To verify this, finite element method simulation is also performed using wave optics module in COMSOL MULTIPHYSICS software.

Using our inverse design method, a device with a 2 nm gap with an enhancement of about 30,000 at 0.14THz was found. Furthermore, we experimentally and numerically double-check that our device exceeds the existing maximum enhancement of 25,000 at 0.075 THz [3], despite the doubled gap size and higher resonance frequency. It shows more than twice the performance of the device with the same gap size that has already been reported [3].

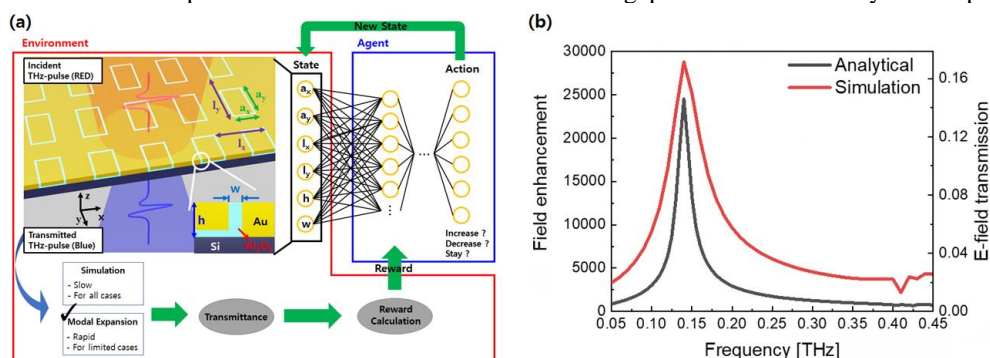


Fig. 1. (a) THz-nanophotonic device design with deep Q-learning method. (b) Analytical and simulation results for inverse designed terahertz nanophotonic device using our method.

[1] S. Molesky, Z. Lin, A. Y. Piggott, W. L. Jin, J. Vuckovic, A. W. Rodriguez, "Inverse design in nanophotonics" Nat. Photonics **12**(11), 659-670 (2018).

[2] Jeeyoon Jeong, Dai-Sik Kim and Hyeong-Ryeol Park, "Beyond-hot-spot absorption enhancement on top of terahertz nanotrenches", Nanophotonics, **11**(13), 3159-3167 (2022).

[3] Xiaoshu Chen*, Hyeong-Ryeol Park*, Matthew Pelton, Xianji Piao, Nathan C. Lindquist, Hyungsoon Im, Yun Jung Kim, Jae Sung Ahn, Kwang Jun Ahn, Namkyoo Park, Dai-Sik Kim and Sang-Hyun Oh, "Atomic layer lithography of wafer-scale nanogap arrays for extreme confinement of electromagnetic waves" Nat. Commun. **4**, 2361 (2013).

Full quantum control of terahertz electromagnetic waves in a nanometric tunnel junction.

Gangseon Ji,¹ Jae Deock Jeon,² Seonhye Eom,¹ Sang Woon Lee,² Hyeong-Ryeol Park,^{1,*}

1. Department of Physics, Ulsan National Institute of Science and Technology (UNIST), Ulsan 44919, Republic of Korea.

2. Department of Physics and Department of Energy Systems Research, Ajou University, Suwon 16499, Republic of Korea.

*E-mail address: nano@unist.ac.kr

Abstract: The terahertz range has gained increasing attention in the field of 6G communication, highlighting the importance of modulating and controlling electromagnetic waves. In this study, we demonstrate reversible control of terahertz electromagnetic waves using quantum tunneling in an Au/6 nm TiO₂/Au tunnel junction. With an onset field of tunneling as low as 0.5 V/nm, full quantum control of terahertz electromagnetic waves can be achieved without the risk of damage caused by joule heating. This low-voltage operating quantum tunnel junction opens up new opportunities for potential applications, such as in the development of field-effect transistors and terahertz detectors.

1. Introduction

Subwavelength confinement in a nanometer-scale gap regime plays an important role in engineering the optical response and improving light-matter interaction in a local area. But for the sub-10 nm level, quantum tunneling becomes prominent at terahertz frequencies when the field amplitude of the gap is applied to a few V/nm [1], much earlier than for visible light where sub-nanometer gaps are required for tunneling effects [2]. Tunneled electrons hinder the accumulation of electrons on the metal surface, reducing the confinement of terahertz waves and leading to a nonlinear decrease in transmission. But, increasing the incident terahertz field strength results in a decrease in the width of tunnel barrier, leading to prominent electron tunneling phenomena, but causing damage to the metal-insulator-metal (MIM) junction due to high voltage-induced optical joule heating $P = \int \sigma E^2 dV$. Here, we demonstrate the low voltage operating ring-shaped quantum tunnel junction (Au/6 nmTiO₂/Au) with Schottky barrier 1 eV, enabling the terahertz electromagnetic wave control in a reversible manner.

2. Result

We generate intense terahertz pulse using pulse front tilting method in LN crystal. Intense terahertz pulse is enhanced up to 1.2 V/nm in metallic nanogap structure when field strength is 38 kV/cm, changing the potential barrier shape as shown in Fig. 1 (a) and (b). We observe the nonlinear response of a quantum tunnel junction, with electron tunneling starting above the 0.5 V/nm regime. The transmission of the quantum tunnel junction reduced to 70% with 1.2 V/nm in the gap (Fig. 1 (c)), which showed well-matched results with the theoretical quantum-corrected model (black line) [3] shown in Figure 1(d). In Fig. 1 (e), we show that the device can operate sustainably without damage caused by joule heating, because low-voltage operating is possible.

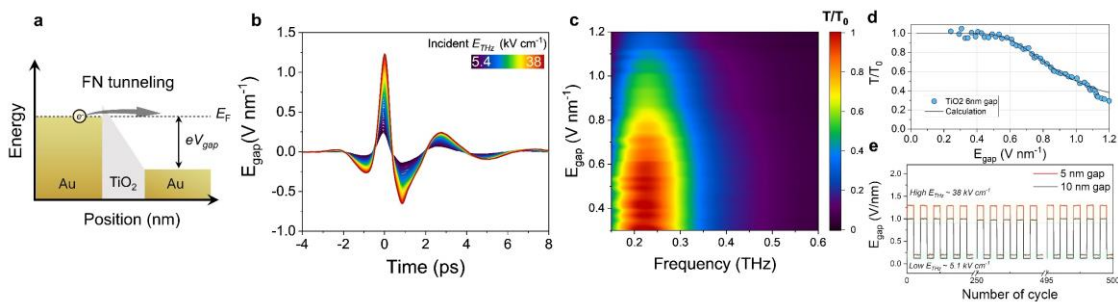


Fig. 1. (a) Schematic diagram of Fowler-Nordheim tunneling in Au/TiO₂/Au structure. (b) Electric field across the gap in 6 nm TiO₂ nanogap. (c) Corresponding transmittance spectra. (d) Terahertz transmittance at resonance frequency as a function of electric field across the gap E_{gap} . (e) Reversible control of quantum tunnel junction with 5 and 10 nm gap width.

3. References

- [1] Joon-yeon Kim, Bong Joo Kang, Joohyun Park, Young-Mi Bahk, Won Tae Kim, Jiyeah Rhie, Hyeongtag Jeon, Fabian Rotermund, and Dai-sik Kim, *Nano Lett.* **15**, 6683-6688 (2015).
- [2] Kevin J. Savage, Matthew M. Hawkeye, Rubén Esteban, Andrei G. Borisov, Javier Aizpurua and Jeremy J. Baumberg, *Nature* **491**, 574-577 (2012).
- [3] Ruben Esteban, Andrei G. Borisov, Peter Nordlander and Javier Aizpurua, *Nat. commun.* **3**, 825 (2012).

Terahertz virus detection on two-dimensional optical hotspots in gold nanogaps.

Gangseon Ji,¹ Hwan Sik Kim,² Seong Ho Cha,² Hyung-Taek Lee,¹ Hye Ju Kim,² Sang Woon Lee,² Kwang Jun Ahn,² Kyoung-Ho Kim,³ Yeong Hwan Ahn,² and Hyeon-Ryeol Park.^{1,*}

1. Department of Physics, Ulsan National Institute of Science and Technology (UNIST), Ulsan 44919, Republic of Korea.

2. Department of Physics and Department of Energy Systems Research, Ajou University, Suwon 16499, Republic of Korea.

3. Department of Physics, Research Institute for Nanoscale Science and Technology, Chungbuk National University, Cheongju 28644, Republic of Korea.

*E-mail address: nano@unist.ac.kr

Abstract: The rapid detection of viruses with low densities is a pressing issue in the field of virology, as early identification can help contain outbreaks and mitigate their impact. In this context, virus detection at terahertz frequency has emerged as a promising technology due to its ability to provide fast, non-destructive, and ultra-small, label-free analysis. Here, we present the ultrasensitive virus detection method using two dimensional optical hotspots in gold nanogap sensor. By tightly attaching virus particles to optical hotspots, the sensitivity of the system is enhanced twofold, resulting in exceptional responsiveness to even subtle changes in the local refractive index by gap plasmon.

1. Introduction

The COVID-19 pandemic has emphasized the significance of detecting biomolecules, including viruses, proteins, and DNA [1]. While PCR tests are highly accurate, they are time-consuming, while antigen tests require a large number of virus particles for positive results. Light-based detection methods such as terahertz sensing are fast and non-destructive [2], but the size mismatch between viruses and terahertz wavelengths is challenging. To address this, terahertz metamaterials have been proposed, but reducing gap size with standard lithography techniques is difficult.

2. Result

To overcome this issue, we utilize atomic layer lithography to create gold nanogaps with a 20 nm gap width as shown in Fig. 1 (a) [3]. Field enhancement of gold nanogap show 580-fold at resonance frequency, two-dimensional optical hotspots on these nanogaps can detect the PRD1 bacteria virus (Fig.1 (b)), which is 60 nm thick, resulting in a redshift of resonance frequency due to the change in the local index near the optical hotspots. We clearly observe the resonance shift of the etched nanogap enhanced twofold compared to unetched nanogap as shown in Fig 1. (d). This is attributed to the tight adhesion of virus particles in a bridge-like configuration in the vicinity of the gap, which can induce a substantial modulation in the local refractive index. Through COMSOL simulations, it has been demonstrated that even with fewer than 100 viruses, a significant resonance shift can be induced.

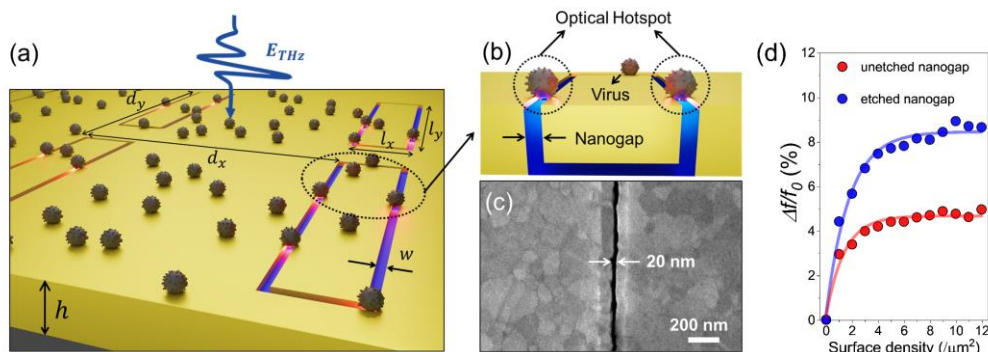


Fig. 1. (a) Schematic diagram of virus coated on nanogap array and (b) enlarged figure at two-dimensional optical hotspots (c) FE-SEM image of 20 nm thick gold nanogap (d) Terahertz resonance change at resonance frequency as a function of surface density.

3. References

- [1] I. Smyrlaki, M. Ekman, A. Lentini, N. R. de Sousa, N. Papanicolaou, M. Vondracek, J. Aarum, H. Safari, S. Muradrasoli, A. G. Rothfuchs, J. Albert, B. Hogberg, B. Reinius, Nat. Commun. **11**, 4812 (2020).
- [2] S. J. Park, S. H. Cha, G. A. Shin, Y. H. Ahn, Biomed. Opt. Express **8**, 3551 (2017).
- [3] X. S. Chen, H. R. Park, M. Pelton, X. J. Piao, N. C. Lindquist, H. Im, Y. J. Kim, J. S. Ahn, K. J. Ahn, N. Park, D. S. Kim, S. H. Oh, Nat. Commun. **4**, 2361 (2013).

Infrared photo-induced force microscopy for quantitative molecular spectro-nanoscopy

Sung Park

*Molecular Vista, San Jose, CA 95119 USA
sung@molecularvista.com*

Abstract: While quantitative elemental mapping at nanoscale (~ 1 to 10 nm) has been available for many years via EDX in transmission electron microscopy, the best quantitative molecular mapping has been limited to a spatial resolution of ~ 200 nm for ToF-SIMS. With optical spectroscopy, even though tip-enhanced Raman spectroscopy (TERS) has demonstrated single-molecule sensitivity on an isolated molecule, mapping of 2D and 3D materials with nanoscale spatial resolution has proven to be difficult due to the large far-field contribution. In this talk, a non-destructive quantitative molecular spectroscopy/mapping technique called infrared photo-induced force microscopy (IR PiFM) is introduced. It combines IR spectroscopy with atomic force microscopy to provide both structural imaging and IR spectro-nanoscopy with sub-5 nm spatial resolution and single-molecule-level sensitivity. PiF-IR spectra on homogeneous samples agree with their bulk FTIR spectra extremely well even though PiF-IR's sampling volume is at least billion times less. On samples with nanoscale heterogeneity, whether chemical or structural (such as crystallinity) in nature, PiF-IR spectra reflect the local chemical bonding environments. Examples from various organic, inorganic, and biological samples will be presented to showcase the capabilities of IR PiFM.

Pushing the Detection Limit of Infrared Photoinduced Force Microscopy

Jian Li

State Key lab of Analytical Chemistry for Life Science, School of Chemistry and Chemical Engineering, Nanjing University, 210023 Nanjing, China
E-mail address: jianli@nju.edu.cn

Abstract: Infrared photoinduced force microscopy (IR-PiFM) provides unique vibrational information of samples with nanoscale resolution, which has been widely used in optics, polymer science and biosciences. However, the detection limit of IR-PiFM is limited by the weak light-matter interaction of ultrathin samples. Thus, for interfacial studies, promotion of sensitivity is highly desired. Here, we have summarized our recent processes of IR-PiFM performed on ultrathin sample with promoted sensitivity, including the experimental set-ups for solid/gas interface and solid/liquid interfaces analysis and the related applications.

With the modulation of Van der Waals force in between AFM tip and samples by tip enhanced photothermal expansion (Shown in Figure 1), infrared photoinduced force microscopy (IR-PiFM) allows for the precise chemical identification of samples with sub-5 nm spatial resolution[1]. Further applying IR-PiFM for interfacial chemical analysis requires a sensitivity up to molecular monolayer level, which is difficult to be achieved owing to the ultrathin sample thickness that leads to much-reduced photothermal expansion.

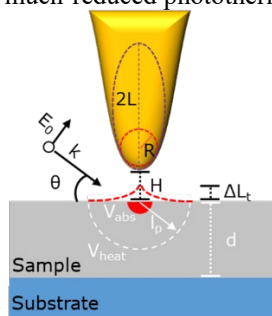


Figure 1. Schematic illustration of the photothermal expansion below an illuminated tip.

A possible way to increase the photothermal expansion is to locally improve the E field. In the past 5 years, we have proposed several configurations successfully promoting the sensitivity of IR-PiFM to monolayer level, including the tip-metal gap and tip-antenna configuration (Figure 2). Detection of ~hundreds chemical bonds has been proved in ambient air and liquid environment, exhibiting broad spectral and imaging applications ranging of plasmonic antenna, organic molecular monolayer, polymer, protein and DNA samples[2-5]. Specifically, the proposed method successfully illustrated the anisotropic growth mechanism of nanoparticles mediated by the facet-specifically adsorbed surfactants[6].

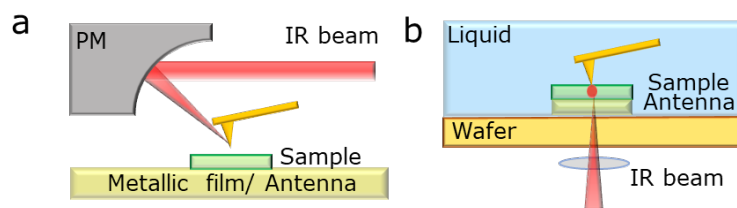


Figure 2. Schematic illustration of the tip-metal gap and tip-antenna configuration applied in air and liquid environments.

References

- [1] D. Nowak, W. Morrison, H. Wickramasinghe, J. Jahng, E. Potma, L. Wan, R. Ruiz, T. Albrecht, K. Schmidt, J. Frommer and D. Sanders, *Sci. Adv.* **2**, e150157(2016).
- [2] J. Li, J. Pang, Z. Yan, J. Jahng, J. Li, W. Morrison, J. Liang, Q. Zhang, and X. Xia, *CCS Chem.* **3**, 2717-2726(2021).
- [3] J. Li, J. Li, Z. Yan, X. Ding and X. Xia, *J. Phys. Chem. Lett.* **12**, 10255-10261(2021).
- [4] J. Li, J. Jahng, J. Pang, W. Morrison, J. Li, E. Lee, J. Xu, H. Chen and X. Xia, *J. Phys. Chem. Lett.* **11**, 1697-1701(2020).
- [5] J. Li, Z. Yan, J. Li, Z. Wang, W. Morrison and X. Xia, *Nanoscale* **11**, 18543-18549(2019).
- [6] J. Li, Q. Shen, J. Li, J. Liang, K. Wang, and X. Xia, *J. Phys. Chem. Lett.* **11**, 8322-8328(2020).

1.3 μm Ultrashort Pulse Generation in Praseodymium Doped Fiber Laser using Zinc Phosphate Mode-Locker

Harith Ahmad, Bilal Nizamani and Muhamad Zharif Samion

¹Photonics Research Centre, Universiti Malaya, 50603 Kuala Lumpur, Malaysia

E-mail: harith@um.edu.my

The development of fiber lasers at 1.3 μm , also known as O-band, has recently attracted substantial interest from researchers due to the availability of rare-earth doped fibers at this regime. The O-band signal propagation in optical fibers has zero dispersion, which applies to upstream broadband communication systems. Among many compositions of fluoride glasses, $\text{ZrF}_4\text{-BaF}_2\text{-LaF}_3\text{-AlF}_3\text{-NaF}$ (ZBLAN) fiber is commonly used as a host for Pr^{3+} ions, which is a heavy metal fluoride glass that has a wide transparency window and low phonon energy. This work achieved the mode-locked laser at 1301 nm using praseodymium (Pr^{3+}) doped fluoride fiber as the gain medium and zinc phosphate-coated arc-shaped fiber as the mode-locker. Zinc phosphate is a non-toxic metal phosphate comprising zinc, phosphorus, and oxygen. Nonlinear optical properties were also studied for zinc phosphate-coated arc-shaped fiber where the linear absorption was 3.3 dB at 1.3 μm , and modulation depth was obtained as 18%. Ultrashort pulses of 452 fs duration were generated with a repetition rate and signal-to-noise ratio (SNR) of 0.4 MHz and 50 dB, respectively.

Ultrafast Thulium-Doped Fiber Laser with Zinc Oxide Nanorods

Saturable Absorber

M. Z. Samion, M. F. Ismail, S.A Reduan, M. K. A. Zaini, L. Bayang, H. Ahmad

Photonics Research Centre, Universiti Malaya, 50603 Kuala Lumpur Malaysia

Email: zarifzf@um.edu.my

Pulsed fiber lasers operating in the 2.0-micron wavelength region have recently attracted substantial interest due to their potential applications in laser ablation, spectroscopy, and in medicine. Lasing in the 2.0-micron region can be realized through the use of thulium-doped fibers (TDFs) as the gain medium, which emits across a wide spectral range of 1.7–2.0-micron and is particularly desirable for spectroscopy or sensing applications as it coincides with the absorption lines of carbon dioxide (CO₂) gas and water (H₂O). Passive pulse generation in fiber lasers can be obtained through a number of techniques, with the most common being the use of saturable absorbers (SAs) in the laser cavity. In this regard, various nanomaterials such as carbon nanotubes, graphene, topological insulators (TIs), and black phosphorus have all been demonstrated to successfully generate stable pulsed outputs. Recently, transition metal oxides (TMOs) have also received substantial attention as SA candidates due to their large optical nonlinearity, exceptional thermal and chemical stability and mechanical strength. TMOs have also demonstrated semi-conductive properties and a size-dependent bandgap, making these materials highly favourable for optoelectronic applications. Of the many TMOs, zinc oxide (ZnO) is a highly attractive alternative to complement other SA materials due to its high third order nonlinear coefficient and its ultrafast carrier dynamics. In this work, a mode-locked TDF laser (TDFL) using ZnO based SA is proposed and demonstrated. The incorporation of the ZnO based SA into the cavity and the use of the TDF as the gain medium allow for mode-locking operation to be realised in the 2.0-micron wavelength region. The proposed laser would have potential uses for a variety of sensing and spectroscopic applications, in particular for biological and medical applications in the ‘eye-safe’ 2.0-micron wavelength region.

Preparation of Highly Stable Core-Shell Perovskite QDs through Alkali-Metal Doping and Ligand Passivation

Chang-Lyoul Lee*

*Advanced Photonics Research Institute (APRI), Gwangju Institute of Science and Technology (GIST)
Gwangju, Republic of Korea
E-mail address: vsepr@gist.ac.kr*

Abstract: Highly stable perovskite QDs have been realized by combination of alkali metal doping, core-shell structure and ligand passivation.

Halide perovskite quantum dots (PQDs) are emerging as next-generation emissive materials due to their outstanding optoelectronic properties such as high PLQY, color purity with narrow bandwidth. However, they have poor structural instabilities, being easily decomposed or degraded by external energies such as moisture, oxygen, and heat. Perovskite QDs with highly structural stabilities were realized by (1) surface passivation, (2) core-shell structure and (3) metal doping. These methods significantly enhanced structural stabilities of perovskite QDs by minimizing ligand dissociation and defect generation. In this work, R, G, B CsPbX₃ perovskite QDs with high PLQY and structural stabilities are developed by combination of anion exchanges, core-shell structure and alkali metal doping.

Unraveling the Origin of Spectral Instability of Perovskite Light-emitting Diodes and Pioneering Deep-blue Emissive Quasi-2D Perovskites

Dong Ha Kim

Ewha Womans University, Korea

Quasi-2D layered perovskites have recently attracted enormous interest as light emitters due to their outstanding photophysical and electrical properties. Due to their inherent quantum confinement and reduced dielectric screening, layered perovskites offer strong exciton binding energy and subsequent stable excitonic medium even at the room temperature. Mixed halide perovskites, however, suffer from significant spectral instability which obstructs their utilization for the light-emitting diodes. We found that the different activation energies required for directional ion hopping lead to the redistribution of anions during the device operation and suggested that the dominant red emission is ascribed to the thermodynamically favorable selective hole injection. Next, solution-processed quasi-2D perovskites contain multiple quantum wells and often exhibit a broad width distribution. To overcome these limitations, it is important to control quantum well dispersity. Modulation of film formation kinetics has paved the way for developing deep-blue emissive quasi-2D perovskites. Inhomogeneity of solution-processed quasi-2D perovskites results in the charge funneling into the smallest bandgap components, which hinders deep-blue emission and accelerates Auger recombination. We introduce a universal synthetic strategy to narrow the width distribution of perovskite quantum wells.

High-lying excitons and excitonic quantum interference in 2D semiconductors

Kai-Qiang Lin

State Key Laboratory of Physical Chemistry of Solid Surfaces, College of Chemistry and Chemical Engineering, Xiamen University, 361005 Xiamen, China.

Kaiqiang.lin@xmu.edu.cn

Two dimensional semiconductors such as transition-metal dichalcogenide (TMDC) monolayers show a wealth of exciton physics. We present the existence of a novel excitonic species, the high-lying exciton (HX), in TMDC monolayers with almost twice the energy of the band-edge A-exciton but with a linewidth as narrow as that of band-edge excitons. The HX is populated through momentum-selective optical excitation in the K-valleys, and is identified experimentally in upconverted photoluminescence and theoretically in *ab initio* GW-BSE calculations. These calculations show that the HX is comprised of electrons of negative effective mass. The coincidence of such high-lying excitonic species at around twice the energy of band-edge excitons gives rise to a well-defined excitonic three-level system, which enables quantum-interference phenomenon revealed in optical second-harmonic generation. We show that the temporal dynamics in such a three-level system can be probed through time-resolved sum-frequency generation and four-wave mixing. The HXs can also be tuned over a wide range by twisting and Stark effect in bilayer WSe₂, which gives control over the excitonic quantum interference and the corresponding optical nonlinearities. Finally, we show how an electrical gate can be used to tune excitonic quantum interference in a monolayer TMDC transistor device by forming trions.

Hetero Interlayer Exciton in Far-Red Range from Perovskite-MAPbI₃/CdSe-ZnS-QD Hybrids

Taek Joon Kim¹, Sang-hun Lee¹, Jinsoo Joo^{1,*}, Jeongyong Kim²

¹Department of Physics, Korea University, Seoul, South Korea

²Department of Energy Science, Sungkyunkwan University, Suwon, South Korea

E-mail address: jjoo@korea.ac.kr, tj_kim@korea.ac.kr

Hetero interlayer excitons (HIXs) have attracted considerable attention because of intrinsic long lifetime and diffusion length that are applicable to advanced photovoltaics, light emitting diodes, and quantum information processing. In this work, hybrid system (HS) with methylammonium lead iodide (MAPbI₃) perovskite and CdSe-ZnS quantum-dot (CdSe-ZnS-QD) was fabricated using anti-solvent method for MAPbI₃ and drop-casting for CdSe-ZnS-QD. Energy bands of the MAPbI₃/CdSe-ZnS-QD HS (Fig. 1a) were aligned in the staggered type (type-II), confirmed by ultraviolet photoelectron, absorption, and photoluminescence (PL) spectra [1].

Emission energy of the HIX of the MAPbI₃/CdSe-ZnS-QD HS was observed at 1.42 eV (= 873 nm; far-red range) from PL spectra measured at 3 K (Fig. 1b). From time-resolved PL (tr-PL) spectra at 3 K, lifetime of the HIX was estimated approximately 5.68 μ s (Fig. 1c), which was extremely longer than that of the CdSe-ZnS-QD (\approx 0.715 ns). PL peak of the HIX of the HS was blue-shifted with increasing incident laser power whereas that of intralayer excitons (MAPbI₃ and CdSe-ZnS-QD) was almost constant. These results indicate that the dipoles of the HIXs were strongly repulsed each other owing to their well-aligned moments, which was confirmed through back focal plane imaging. Interestingly, the peak of the HIX was blue-shifted near the phase transition temperature (at 90 K) of MAPbI₃, affected by the shift of energy band of the MAPbI₃ during structural phase transition.

To investigate HIX-based optoelectronic application, MAPbI₃/CdSe-ZnS-QD photodetector was fabricated. Photocurrent and detectivity were enhanced after CdSe-ZnS-QD hybridization with far-red light-irradiation with extremely low-voltage operation (Fig. 1d). These results indicate that the photo-induced far-red HIXs were dissociated and contributed to performance of the photodetector, suggesting new-type of excitonic devices based on the far-red HIXs.

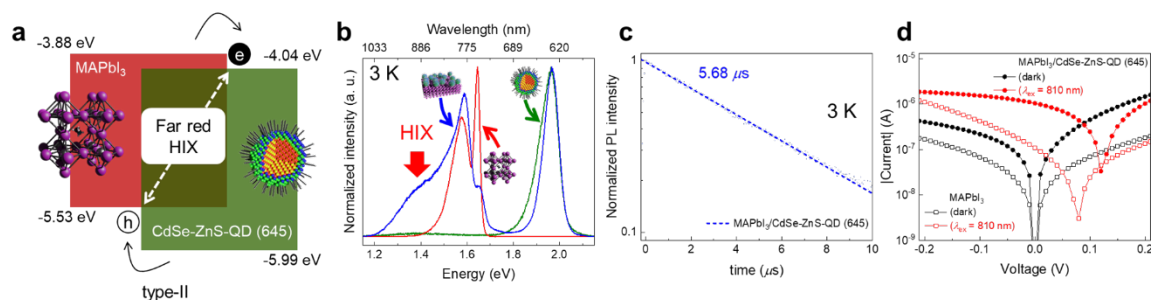


Fig. 1. (a) Energy band alignment of MAPbI₃/CdSe-ZnS-QD HS. (b) Normalized PL spectra of the CdSe-ZnS-QD (green), MAPbI₃ (red), and MAPbI₃/CdSe-ZnS-QD HS (blue) at 3 K. (c) tr-PL spectrum of the HIX of MAPbI₃/CdSe-ZnS-QD HS at 3 K. (d) Current-voltage characteristic curves of pristine MAPbI₃ (open markers) and MAPbI₃/CdSe-ZnS-QD HS (solid markers) photodetectors in dark (black) and 810-nm light-irradiation condition (red).

Exploring the Correlation between Phonon and Excited Exciton in WSe₂ Monolayer: A Novel Approach using eXplainable Artificial Intelligence and Density Functional Theory

Jaekak Yoo^{1,2,†}, Youngwoo Cho³, Soo Ho Choi¹, Ki Kang Kim¹, Seong Chu Lim¹, Seung Mi Lee², Jaegul Choo³, Mun Seok Jeong⁴

¹ Department of Energy Science, Sungkyunkwan University, Suwon 16419, Republic of Korea

² Korea Research Institute of Standards and Science, Daejeon 34113, Republic of Korea

³ Kim Jaechul Graduate School of Artificial Intelligence, Korea Advanced Institute of Science and Technology, Daejeon 34141, Republic of Korea

⁴ Department of Physics, Hanyang University, Seoul 04763, Republic of Korea

E-mail address: yoo.jk1025@gmail.com

Abstract: The emergence of deep learning applications in scientific research has enabled a more comprehensive explanation of non-linear phenomena through the processing of massive amounts of data by deep neural networks. The interpretation methods, also known as explainable artificial intelligence, provide advanced scientific insights to human users. However, the interpreted results obtained through explainable artificial intelligence require external validation processes, as the interpretation often provides implied rather than explicit results. To address this issue, we propose the use of quantum mechanical calculations as an independent cross-validation method. This approach bridges the results obtained from explainable artificial intelligence and theoretical calculations, leading to reliable and comprehensive scientific discoveries. Our work not only describes validated novel physical findings but also presents an advanced platform for researchers to gain an enhanced understanding of nature.

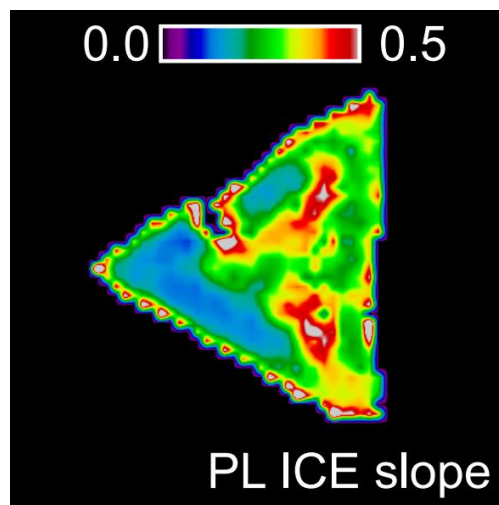


Figure 1. Interpretation of Deep Learning Model

Nano-electromechanically tunable resonant dielectric metasurfaces

Hyoungchan Kwon

Korea Institute of Science and Technology, Korea

Optical dielectric metasurfaces have shown great advances in the last two decades and become promising candidates for next-generation free-space optical elements. In addition to their compatibility with scalable semiconductor fabrication technology, metasurfaces have provided new and efficient ways to actively manipulate diverse characteristics of light. In this talk, we demonstrate nano-electromechanically tunable resonant dielectric metasurfaces as a general platform for novel reconfigurable free-space optical elements. First, we show different types of the phase and amplitude modulators. While one utilizes resonant guided-modes, the other is based on the high-Q asymmetric Mie resonances. Such devices achieve large phase modulation, small pixel-size, and electrical control of diffraction. Besides, we demonstrate tuning of circular-polarization dependent optical responses in dielectric chiral metasurfaces. Realizing wavelength-scale pixel size, low driving voltage, and large modulation simultaneously, these works pave the ways for the metasurfaces' application to the next-generation spatial light modulators.

Extreme Nanophotonics Based on Surface Polaritons in Two-Dimensional Materials

In-Ho Lee

Post-silicon Semiconductor Institute, Korea Institute of Science and Technology, Seoul, Korea.
E-mail address: inholee87@kist.re.kr

Abstract: In the field of nanophotonics that employs two-dimensional materials, a major obstacle is the weak interaction between light and matter due to the mismatch in size between the thickness of the material and the wavelength of light in free space. However, we have successfully demonstrated a way to couple incident radiation to surface polaritons in two-dimensional materials with almost perfect efficiency. This high level of efficiency was achieved by using a two-stage polariton coupling mechanism, a photon-recycling device architecture, and a fabrication process that ensures an atomically smooth interface between the substrate and graphene. Our findings offer promising prospects for the development of nanophotonic devices that rely on two-dimensional materials and achieve high levels of optical efficiency.

1. Introduction

Extensive research has been conducted on two-dimensional (2D) materials, as they offer potential for various nanophotonic applications, including photodetectors, metasurfaces, and biochemical sensors. However, the primary challenge in this field is the weak light-matter interaction, which severely limits the efficiency of 2D material-based nanophotonic devices. To address this issue, researchers have attempted to combine 2D materials with various photonic devices, including silicon waveguides [1], microcavities [2], and plasmonic antennas [3]. However, due to the mismatch between the optical modes of these devices and the 2D material layer, the enhancement of light-matter interaction has been limited. Surface polaritons in 2D materials, which result from the strong coupling of photons with electrons, phonons, and excitons, can overcome this limitation due to their extremely confined fields. However, the strong field confinement leads to a significant momentum mismatch with incident radiation.

This presentation introduces a coupling mechanism that overcomes this extreme momentum mismatch. Using a new resonator scheme based on this mechanism, it was possible to excite graphene plasmons, one of widely known surface polaritons, with near-perfect coupling efficiency, despite their extreme confinement.

2. Result and Discussion

Our graphene resonator is different from conventional graphene plasmon resonators that use an array of two-dimensional material ribbons. Instead, our resonator uses an unpatterned two-dimensional material layer along with an array of metallic ribbons, as shown in Fig. 1(a). By exciting graphene plasmons at the edges of the metallic ribbons, they can constructively interfere and drastically improve the coupling of incoming radiation to the graphene plasmons. The absorption spectra of our polaritonic resonators are displayed in Figure 1(b). These resonators employ a design in which the plasmon momentum is determined by the gap size (g) between a continuous graphene sheet and an array of metallic antennas that excite graphene plasmons. Interestingly, the absorption efficiencies on resonance for the four resonators are approximately 90%, regardless of the gap size. The maximum efficiency of 94% is achieved when $g = 8$ nm. Moreover, the absorption efficiencies remain nearly constant as the gap size is reduced, suggesting that our coupling mechanism is able to overcome the extreme momentum mismatch with a light source.

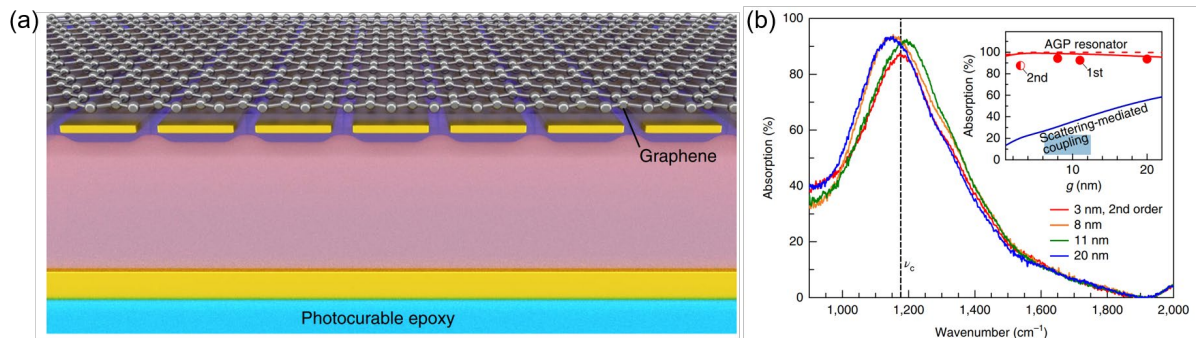


Fig. 1. (a) Schematic illustration of the proposed polaritonic resonator. (b) Absorption spectra of graphene plasmon resonators. The inset shows the absorption on resonance as a function of the gap size between a continuous graphene layer and an array of metallic antenna [4].

3. Acknowledgement

This work was supported by the National Research Foundation of Korea (NRF) grant funded by the Ministry of Science and ICT (No. RS-2023-00211359).

4. References

- [1] M. Liu et al., “A graphene-based broadband optical modulator”, *Nature* 474, 64–67 (2011).
- [2] M. Furch et al., “Microcavity-integrated graphene photodetector”, *Nano Lett.* 12, 2773-2777 (2012).
- [3] Z. Fang et al., “Graphene-antenna sandwich photodetector”, *Nano Lett.* 12, 3808-3813 (2012).
- [4] I.-H. Lee et al., “Graphene acoustic plasmon resonator for ultrasensitive infrared spectroscopy”, *Nat. Nanotechnol.* 14, 313-319 (2019).

Optical Performance and Limitation of Pixelated Metalens

Chen-Yi Yu, Qui-Chun Zeng, Yen-Chun Chen, Wei-Lun Hsu, and Chih-Ming Wang*

Department of Optics and photonics, National Central University, Taiwan

E-mail address: cmwang@dop.ncu.edu.tw

Abstract: In this study, we utilized the Rayleigh-Sommerfeld diffraction (RSD) theory to evaluate the optical performance of metalens with varying unit cell sizes. The corresponding focusing efficiency, focal spot size, and modulation transfer function (MTF) are analyzed. In addition, we proposed a hybrid arrangement of metalens to improve the resolution at high spatial frequency.

1. Method

We use the RSD theory to calculate the focusing efficiency of metalens. The Strehl ratio represents the focusing efficiency and is shown in Fig. 1(a). The focal spot size is defined as the diameter of the first dark ring of the Airy disk and is shown in Fig. 1(b). Fig. 1(c) shows the MTF of the metalens with varying meta-atom's sizes. All the meta-atom's sizes (x label of Fig. 1) are normalized to the operating wavelength. Conventionally, people utilize Nyquist spatial frequency as a criterion to decide the up-limited size of meta-atoms [2]. In Fig. 1, we respectively denoted the 1x Nyquist frequency and 2x Nyquist frequency by circle and triangle symbols for reference. It is found that for analyzing the spot size and MTF, the Nyquist sampling theory works well for designing the meta-atom size. However, there is a significant weakness in the Strehl ratio. Under the 1x Nyquist frequency, the corresponding Strehl ratio is lower than 0.6. According to our calculation results, one must choose 2x Nyquist frequency (denoted by triangle symbols) for a diffraction-limited metalens. Therefore, we conclude that the meta-atom's size of a diffraction-limited metalens should be smaller than Λ_g/λ and 2x Nyquist frequency, which is denoted by the shading area.

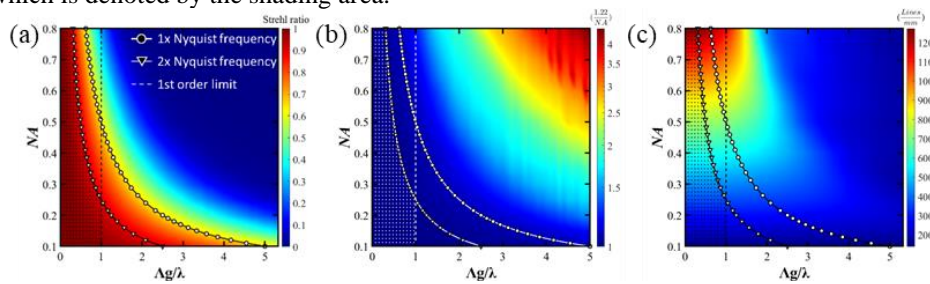


Fig. 1 (a) Strehl ratio, (b) spot size and (c) MTF as a function of NA and Λ_g/λ . Where Λ_g/λ is normalized by the operating wavelength.

2. Result

We design three metalenses with a working wavelength of 0.94 μm , diameter of 100 μm , and NA of 0.447 based on three different meta-atom arrangements. The meta-atom's periodicity of the first arrangement is 0.4 μm , corresponding to 2x Nyquist frequency. The periodicity of the second one is 0.8 μm , corresponding to 1x Nyquist frequency. The third one is a metalens with hybrid meta-atoms. The period at the inner diameter (radius < 25 μm) and outer diameter (radius > 25 μm) of metalens are 0.8 μm and 0.4 μm , respectively. The SEM image of the third case is shown in Fig. 2(a). The result of Figure 2(b) is as expected, where the 1x Nyquist frequency has tiny impact on MTF and spot size. Nevertheless, it is not sufficient for the Strehl ratio, resulting in a decreasing efficiency. Compared to the first and second metalens, the third has mediocre efficiency but a higher resolution in high spatial frequency (SP) MTF, effectively improving the image quality because the third metalens can simultaneously limit high and low-frequency components. Thus, imaging quality is improved by enhancing the MTF in high SP.

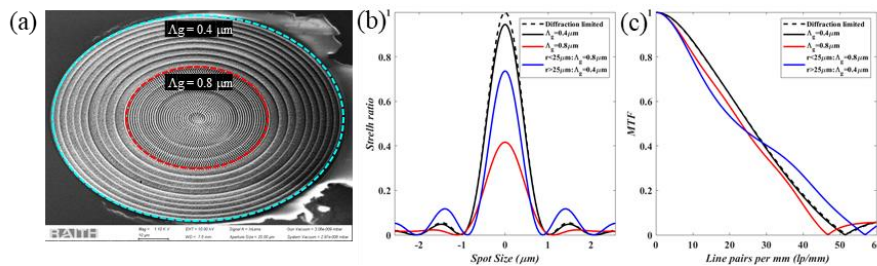


Fig. 2 (a) SEM image of hybrid design of metalens. (b) Strehl ratio and (c) MTF of three designs.

3. References

- [1] Hu, Y., Wang, Z., Wang, X. et al., "Efficient full-path optical calculation of scalar and vector diffraction using the Bluestein method" Light Sci Appl 9, 119 (2020).
- [2] M. Khorasaninejad and F. Capasso, "Metalenses: versatile multifunctional photonic components," Science, vol. 358, p. 1146 (2017).

Metasurface-based Polarization Light Sorting

Wei-Lun Hsu¹, Chun-Yuan Wang², Qiu-Chun Zeng¹, Yen-Chun Chen¹, and Chih-Ming Wang^{1,*}

¹Department of Optics and Photonics, National Central University, Taoyuan, 32001, Taiwan.

²VisEra Technologies Company Limited, Hsinchu, 30078, Taiwan

*cmwang@cc.ncu.edu.tw

Abstract: We proposed a metasurface-based polarization light sorting device. This metasurface provided opposite phase distributions for x-polarized and y-polarized light, which can split the x and y-polarization light to different positions on a complementary metal-oxide-semiconductor (CMOS) sensor. Measurement scattering intensity at different orders showed that the intensity of x-polarization is eight times higher than y-polarization at +1 order. In the future, metasurface-based can potentially be applied as automotive safety components.

1. Introduction

In the past two decades, polarization information has been used in many research fields, such as medicine [1], remote sensing [2], and earth science [3]. In recent years, consumers have paid more attention to the safety assistance function of the automobile. The components of polarized information provide helpful information for the safety assistance of the automobile. For example, water's surface reflects specific polarization of light, which can be used to identify road conditions. However, the standard polarization light sorting components are usually designed by the polarizers [4,5]. Half of the light intensity will be lost when light passes through the polarizers. Therefore, developing a polarization light sorting component by metasurface can reduce light loss [6].

2. Results

Figure 1(a) shows the schematic of the polarization light sorting, which consists of a metasurface and a CMOS sensor. By arranging the dimension of the meta-atom in the x and y-direction, this metasurface provided opposite phase distributions for x-polarized and y-polarized light. The x and y-polarization lights are split to different positions of the CMOS sensor after passing through the metasurface. Figure 1(b) presents the SEM image of the proposed structure. The dimension of the meta-atom is between 128 nm and 263 nm. Figure 1(c) shows the measurement intensity versus scattering order of x and y-polarization light. In our design, the x and y-polarization split to +1 and -1 order, respectively. At -1 order, the intensity of y-polarization is almost two times higher than x-polarization. Moreover, the x-polarization's intensity is eight times stronger than the y-polarization at +1 order. We further measured the near-field spectra of the metasurface. The ratio of x to y-polarization at desired positions is 1.6 at wavelength 670 nm and 1.2 from wavelength 450 nm to 800 nm.

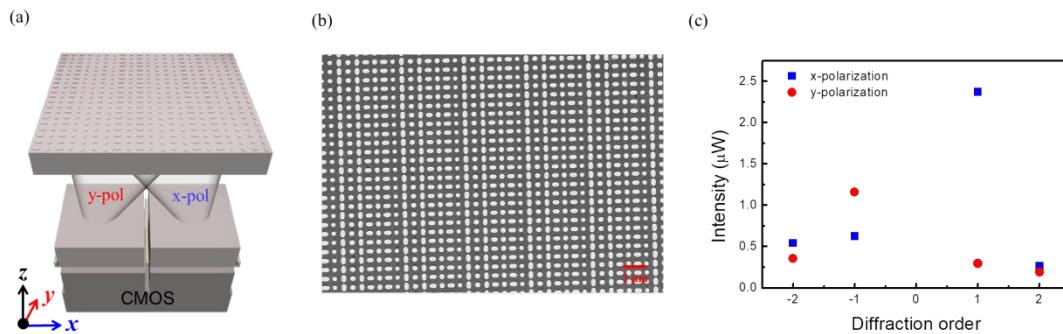


Fig. 1. (a) The polarization light sorting schematic comprises a metasurface and CMOS sensor. The x and y-polarization lights are respectively split at different positions of the CMOS sensor. (b) The SEM image of the metasurface. (c) The measured intensity of x and y-polarization at different diffraction orders.

3. References

- [1] S. N. Tukimin, S. B. Karman, M. Y. Ahmad and W. S. Wan Kamarul Zaman, "Polarized Light-Based Cancer Cell Detection Techniques: A Review," *IEEE Sensors Journal* 19, 9010-9025 (2019).
- [2] J. Scott Tyo, Dennis L. Goldstein, David B. Chenault, and Joseph A. Shaw, "Review of passive imaging polarimetry for remote sensing applications," *Appl. Opt.* **45**, 5453-5469 (2006).
- [3] M. Sterzik, S. Bagnulo, and E. Palle, "Biosignatures as revealed by spectropolarimetry of Earthshine," *Nature* **483**, 64-66 (2012).
- [4] C. Guan et al., "Integrated Real-Time Polarization Image Sensor Based on UV-NIL and Calibration Method," *IEEE Sensors Journal* **22**, 3157-3163 (2022).
- [5] Viktor Gruev, Jan Van der Spiegel, and Nader Engheta, "Dual-tier thin film polymer polarization imaging sensor," *Opt. Express* 18, 19292-19303 (2010).
- [6] K.-H. Chang et al., "Axicon metalens for broadband light harvesting" *Nanophotonics* (2023).

Interrogating the optical magnetism of structured light through subtle optical forces

Jinwei Zeng^{1,2*}, Mohammad Albooyeh^{2,3}, Mohsen Rajaei², Abid Anjum Sifat², Eric O. Potma⁴, H. Kumar Wickramasinghe², Filippo Capolino².

¹Wuhan National Laboratory for Optoelectronics and School of Optical and Electronic Information, Huazhong University of Science and Technology, Wuhan, Hubei, 430074, China.

²Department of Electric Engineering and Computer Science, University of California Irvine, Irvine, CA, 92697, USA

³Mobix Labs Inc., 15420 Laguna Canyon, Irvine, California 92618, USA

⁴Department of Chemistry, University of California Irvine, Irvine, CA, 92697, USA
zengjinwei@hust.edu.cn

Abstract: Optical magnetism describes matter's response to the magnetic field of light, which is typically weak in nature. However, efficient exploitation of the optical magnetism can be the important foundation to make the future advanced opto-magnetic devices such as high-speed magnetic storage or high-resolution magnetic imaging. In this work, we investigate the optical magnetism through direct detection of the photo-induced magnetic force on a magnetic nanoprobe magnetically excited by structured light. The detected force maps exhibit excellent resolution and signal-to-noise ratio, which can serve as the foundation of future dense high-speed opto-magnetic devices.

The magnetic force of light, defined as the dipolar Lorentz force exerted on a magnetic dipole, holds promise for investigating for optical magnetism of matters. The localization nature of the Lorentz force on a nanoprobe allows for effective nearfield detection while simultaneously suppressing farfield interference. However, due to the typically weaker magnetic response of common materials compared to their electric counterparts, the optical detection of the magnetic force of light remains challenging.

In this study, we propose a novel approach to detect the magnetic force effectively by designing a specialized light-matter interaction system. Our approach involves using an azimuthally polarized beam (APB), which exhibits a maximum longitudinal magnetic field and a vanishing electric field at the beam axis. The APB interacts with a dielectric nano-scatterer with aligned axes, leveraging Mie resonance to excite an exclusive magnetic dipole. When this dipole approaches a certain surface, it generates an image dipole and induces a magnetic force between them. Consequently, the magnetic dipole functions as a magnetic probe, enabling exclusive detection of the magnetic force without the influence of the electric counterpart, as shown in Fig. 1.

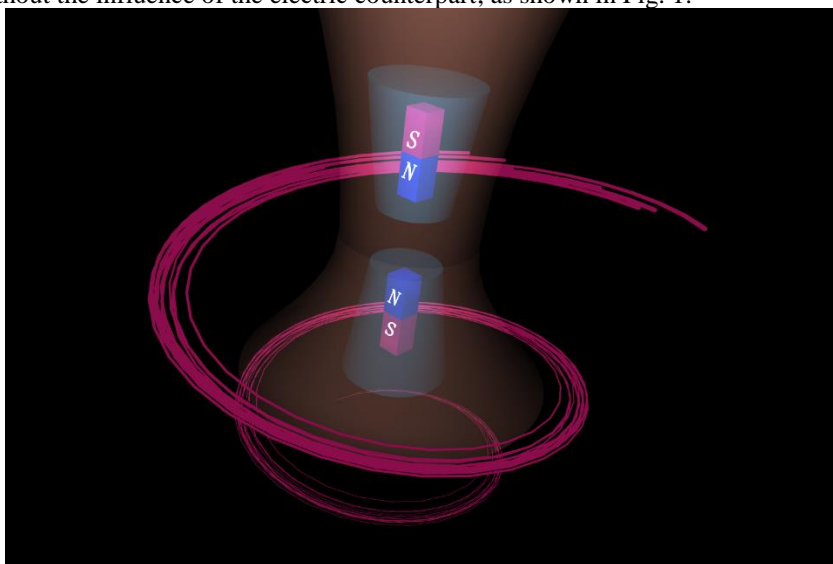


Fig. 1. The schematics of two magnetic dipoles excited by the incident APB, while the magnetic force can be induced between the two dipoles.

Based on this concept, we measure the photoinduced magnetic force by the instrument photoinduced force microscopy (PiFM) produced by Molecular Vista. Notably, the force maps revealed a solid center for the magnetic probe and a donut-shaped pattern for the electric probe. This significant finding signifies the successful and efficient direct detection of the magnetic force at the beam axis. Overall, the utilization of the PiFM instrument in conjunction with the specialized truncated-cone probe and APB illumination enabled us to precisely measure and observe the photoinduced magnetic force [1].

4. References

[1] J. Zeng, M. Albooyeh, M. Rajaei, A. Sift, E. Potma, H. Wickramasinghe, F. Capolino, *Sci. Adv.* 8, eadd0233 (2022).

Nanospectroscopy of Optical Force

Junsuke Yamanishi¹, Tsukasa Torimoto², Hajime Ishihara³, Hiromi Okamoto¹, and Yasuhiro Sugawara⁴

Author affiliations: ¹Institute for Molecular Science, National Institutes of Natural Sciences, Okazaki, Aichi, Japan. ²Department of Materials Chemistry, Graduate School of Engineering, Nagoya University, Chikusa-ku, Nagoya, Aichi, Japan. ³Department of Materials Engineering Science, Osaka University, Toyonaka, Osaka, Japan. ⁴Department of Applied Physics, Osaka University, Suita, Osaka, Japan.
E-mail address: yamanishi@ims.ac.jp

Abstract: Photoinduced force microscopy is a promising scanning probe microscopy that observes the optical properties of materials at the nanoscale. In this study, we propose a method to separately measure the contribution of optical force and that of photothermal expansion of the tip and the sample. Using this measurement technique, we succeeded in observing quantum dots in ultra-high vacuum with a spatial resolution on the single-nanometer scale.

Optical force is explained by the law of conservation of momentum between light and matter and has been utilized in applications such as optical trapping and laser cooling. Photoinduced force microscopy (PiFM) is a promising technology for detecting optical force which has been developed recently based on atomic force microscopy [1, 2]. PiFM observes the interaction between light and matter through the motion of the probe tip. The physical origin of the measured quantity can be classified into two categories: the optical force acting on the probe tip and the photothermal expansion due to the absorption of light by the probe and the sample [3, 4].

We proposed a method called the heterodyne-FM technique, which separates the effects of optical force and photothermal expansion, enabling us to measure pure optical force on a nanoscale [5]. Furthermore, we realized nanospectroscopy of optical force under ultrahigh vacuum [6]. We observed a single quantum dot composed of different components: nanorods and nano-ellipsoids. Since these components have different absorption spectra as shown in Fig. 1(a), PiFM is expected to exhibit different optical forces at each component. The imaging results show that the dumbbell shaped quantum dot in AFM image (Fig. 1(b)) and strong optical force at the edge part of the quantum dot in a PiFM image when wavelength of the incident light is 660nm (Fig. 1(c)). On the other hand, when the wavelength of the incident light was 520 nm, it was confirmed that an almost homogeneous optical force was generated on the quantum dot (Fig. 1(d)). These results are consistent with theoretical simulations and indicate that spectroscopic features of the PiFM responses of the quantum dot has been observed. Furthermore, the spatial resolution achieved was higher than 1 nm [6]. In this presentation, we will also present results from recent applied measurements of photoinduced force microscopy.

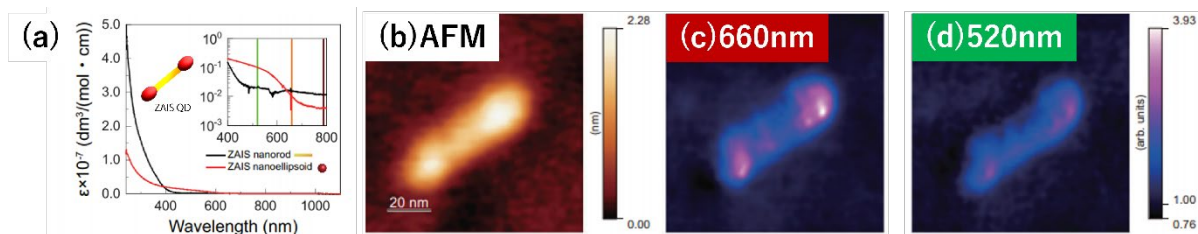


Fig. 1. Photoinduced force microscopy measurement. (a) Absorption spectra of the observed quantum dots. Black and red curves are the spectra of the nanorod and the nano-ellipsoid, respectively. (b) AFM image of the quantum dot. (c, d) PiFM images observed with the incident light at 660 nm and 520 nm, respectively.

References

- [1] I. Rajapaksa, K. Uenal, and H. K. Wickramasinghe, *Appl. Phys. Lett.* **97**, 073121 (2010).
- [2] J. Jahng, J. Brocious, D. A. Fishman, F. Huang, X. Li, V. Ananth Tamma, H. K. Wickramasinghe, and E. O. Potma, *Phys. Rev. B* **90**, 155417 (2014).
- [3] B. T. O'Callahan, J. Yan, F. Menges, E. A. Muller, and M. B. Raschke, *Nano Lett.*, **18**, 5499–5505 (2018).
- [4] J. Jahng, E. O. Potma, and E. S. Lee, *Anal. Chem.* **90**, 11054 (2018).
- [5] J. Yamanishi, Y. Naitoh, Y. J. Li, and Y. Sugawara, *Phys. Rev. Applied* **9**, 024031 (2018).
- [6] J. Yamanishi, H. Yamane, Y. Naitoh, Y. J. Li, N. Yokoshi, T. Kameyama, S. Koyama, T. Torimoto H. Ishihara, and Y. Sugawara, *Nat. Commun.*, **12**, 3865 (2021).

Photo-induced dipole force and thermal force for spectroscopic nanoimaging

Junghoon Jahng

Hyperspectral Nano-imaging Lab, Korea Research Institute of Standards and Science, Daejeon, 34113, South Korea

E-mail address: phyjjh@kriss.re.kr

Photo-induced force microscopy (PiFM) is a scan probe technique that offers images with spectroscopic contrast at a spatial resolution in the nanometer range. PiFM utilizes the non-propagating, enhanced near field at the apex of a sharp tip to locally induce a polarization in the sample, which in turn produces an additional force acting on the cantilevered tip. This photo-induced force, though in the pN range or less, can be extracted from the oscillation properties of the cantilever, thus enabling the generation of photo-induced force maps. Since its inception in 2010, the PiFM technique has grown into a useful nano-spectroscopic tool that has expanded its reach in terms of imaging capabilities and applications. In this talk, we discuss the physical origin of the PiFM signal, highlighting the contributions from dipole–dipole forces as well as forces that derive from photo-thermal processes.

Development of highly efficient light-emitting devices with a wide wavelength range using plasmonics and nanophotonics

Koichi Okamoto

*Department of Physics and Electronics, Osaka Metropolitan University
E-mail address: Okamoto@omu.ac.jp*

Abstract: Plasmonics improves the luminous efficiency of materials, making it applicable to high-efficiency light-emitting devices like LEDs. To achieve practical plasmonic LEDs, tuning the SP resonance wavelength and device development are crucial. We introduce a new, easily fabricated method that enables SP resonance tuning in the deep UV and near-IR wavelength regions. This method allows the development of highly efficient light-emitting devices across a wide range of wavelengths using plasmonics and nanophotonics.

One futuristic application of plasmonics is the development of high-efficiency light-emitting diodes (LEDs), which are anticipated to replace traditional fluorescent tubes as new sources of illumination. In 2004, we presented the first report demonstrating significant enhancements in photoluminescence (PL) for InGaN/GaN quantum well (QW) materials through the utilization of Ag thin films [1]. This method has garnered attention in the field of device applications and has been extensively studied by various research groups [2]. Recently, we have achieved enhancements in electroluminescence from a prototype plasmonic LED device structure that we fabricated [3].

Plasmonics offers significant enhancements in the blue emission efficiency of InGaN/GaN-based semiconductors. However, achieving high efficiency in the green wavelength range around 550 nm, which corresponds to the peak of human visual sensitivity, remains challenging using plasmonics and other existing methods. Green/yellow emissions from semiconductor LEDs suffer from a significant drop in efficiency, often referred to as the "green gap," which necessitates a solution. In this review, the author, who has been dedicated to addressing this issue since the early 2000s, presents a novel approach utilizing Ag nanoparticles and dielectric nanofilm structures to overcome this challenge and achieve highly efficient green light emission.

The next significant challenge lies in extending the surface plasmon (SP) resonance into the ultraviolet (UV) and infrared (IR) wavelength regions to enable broader applications. Through the utilization of aluminum, we have achieved a seven-fold enhancement of deep UV emissions at approximately 260 nm from AlGaIn/AlN quantum wells (QWs) [2]. Furthermore, we have successfully controlled the SP resonance by employing random metallic nanostructures on a mirror, allowing for the tuning of optical properties across the visible [4], deep UV [5], and near-IR [6] wavelength regions.

We have also introduced a new technique for enhancing the efficiency of InGaIn/GaN by combining metallic nanostructures with dielectric thin films [7], as well as depositing dielectric thin films instead of metals and utilizing UV laser irradiation [8]. Consequently, this technology paves the way for the development of advanced light-emitting devices, including highly efficient RGB LEDs and micro-LED displays.

The author would like to express gratitude to Mr. S. Kaito, Mr. Y. Kamei, Prof. T. Matsuyama, and Prof. K. Wada from Osaka Metropolitan University, Prof. K. Tamada from Kyushu University, and Prof. Y. Kawakami and Prof. M. Funato from Kyoto University for their valuable discussions and support. This work was made possible with the support of JSPS KAKENHI grants (B) (No. JP18H01903), (S) (No. JP19H05627), and (No. JP20H05622).

- [1] K. Okamoto, I. Niki, A. Shvarts, Y. Narukawa, T. Mukai, and A. Scherer, *Nat. Mater.*, 3, 601 (2004).
- [2] K. Okamoto, M. Funato, Y. Kawakami, and K. Tamada, *J. Photochem. Photobiol. C: Photochem. Rev.*, 32, 58 (2017).
- [3] N. Okada, N. Morishita, A. Mori, T. Tsukada, K. Tateishi, K. Okamoto, and K. Tadamoto, *J. Appl. Phys.*, 121, 153102 (2017).
- [4] K. Okamoto, K. Okura, P. Wang, S. Ryuzaki and K. Tamada, *Nanophotonics*, 9, 3409 (2020).
- [5] K. Shimano, S. Endo, T. Matsuyama, K. Wada and K. Okamoto, *Sci. Rep.*, 11, 5169 (2021).
- [6] K. Shimano, S. Endo, T. Matsuyama, K. Wada and K. Okamoto, *Appl. Phys. Exp.*, 14, 042007 (2021).
- [7] S. Kaito, T. Matsuyama, K. Wada, M. Funato, Y. Kawakami, K. Okamoto, *Appl. Phys. Lett.*, 122, 151110 (2023).
- [8] S. Kaito, T. Matsuyama, K. Wada, M. Funato, Y. Kawakami, K. Okamoto, *Research Square*, DOI: 10.21203/rs.3.rs-2515057/v1 (Patent Application No. 2022-014115).

Control of the photocurrent generation of 2D layered Materials

Thi Uyen Tran,¹ Wonkil Sakong,² Seong Chu Lim^{1,2*}

¹Department of Energy Science, Sungkyunkwan University, Suwon 16419, Republic of Korea

²Department of Smart Fab. Technology, Sungkyunkwan University, Suwon 16419, Republic of Korea

The bandgap determines the detection range of photodetectors. In this presentation, we discuss how we can extend this limit by controlling the electrical properties of sensing materials. In the case of MoS₂, the variation of the gate (V_{gs}) and source-drain (V_{ds}) bias can result in the metal-insulator transition, contributing to dramatic changes in photocurrent generation under laser irradiation. For instance, when MoS₂ exhibits metallic behavior, the mid-IR can be detected via intraband absorption from free carriers in the conduction band. In contrast, visible light can be sensed via interband transition when it becomes a semiconductor. In addition, we will discuss the control of the photocurrent generation mechanism from 2D Te/ReS₂ heterostructures from the photovoltaic to either photo-thermoelectric or the combined photovoltaic and photo-thermoelectric generation.

The correspondence should be addressed to: seonglim@skku.edu

Nonreciprocal second harmonic generation of 2D magnet

Shiwei Wu

*Fudan University, Shanghai, China
E-mail address: swwu@fudan.edu.cn*

Abstract:

Second harmonic generation is not only of technological importance for nonlinear optical devices, but also a powerful tool for the investigation of symmetry related physical phenomena that are otherwise challenging to probe. The power of this technique lies in its sensitivity to inversion-symmetry breaking, which is the prerequisite for non-vanishing SHG under the electric dipole approximation. While this SHG technique is usually used to study noncentrosymmetric crystallographic materials, the spin structure in magnetic materials may also break the space-inversion symmetry and lead to a nonreciprocal SHG signal. Recently we found the layered antiferromagnetism induced nonreciprocal SHG in CrI₃ bilayer is several orders of magnitude larger than that in bulk magnetic crystals. In this talk, I will report our latest studies on various two-dimensional magnetic materials and discuss the related technique issues with this novel SHG technique.

Brief biography:

Shiwei Wu is currently a professor of physics and the director of Key Laboratory of Micro- and Nano-Photonic Structures (Ministry of Education) at Fudan University. He got his B.S. degree at Fudan University in 2001 and his PhD degree at University of California, Irvine in 2007. Before he joined the faculty at Fudan in 2011, he did his postdoc research at Lawrence Berkeley National Laboratory. His research focuses on the development and application of scanning optical and electron microscopic techniques to explore emergent physics in low-dimensional quantum materials.

Enantioselective Sensing Using Collective Resonance on a 2D Chiral Plasmonic Lattice

Ji-Hyeok Huh¹, Ryeong Myeong Kim², Seokjae Yoo³, Q-Han Park^{4*}, Kitae Nam^{2*} and Seungwoo Lee^{1,5,6*}

¹KU-KIST Graduate School of Converging Science and Technology, Korea University, Seoul 02841, Republic of Korea

²Department of Materials Science and Engineering, Seoul National University, Seoul 08826, Republic of Korea

³Department of Physics, University of Inha University, Incheon 22212, Republic of Korea

⁴Department of Physics, Korea University, Seoul 02841, Republic of Korea

⁵Department of Biomicrosystem Technology, Korea University, Seoul 02841, Republic of Korea

⁶Department of Integrative Energy Engineering, Korea University, Seoul 02841, Republic of Korea

E-mail address: seungwoo@korea.ac.kr

Abstract: Chirality discrimination plays an essential role in various scientific disciplines such as biology, chemistry, and pharmaceuticals. We propose a novel theoretical concept of collective CD resonances (CRs), which exhibit much stronger optical chiral hotspots over a broad region than conventional methods. We also propose extending the traditional sensing theory called the chiral perturbation theory. As a result, we have successfully demonstrated the in situ determination of molecular chirality at the picomole level, with ultra-high sensitivity.

Determining the chirality of molecules is an essential task in various scientific fields, including biochemistry, pharmacology, and materials science. The concept of chirality refers to the property of molecules that have a non-superimposable mirror image, also known as enantiomers. This property is crucial as enantiomers can have different physicochemical and biological properties, which can lead to diverse biological activities or therapeutic efficacy. As such, the ability to accurately determine the chirality of a molecule is of utmost importance. Circular dichroism (CD) spectroscopy is a powerful tool for analyzing molecular chirality. This technique measures the differential absorption of left- and right-circularly polarized light (L/RCP) by a chiral molecule. However, CD spectroscopy has certain limitations. For instance, it requires high concentrations of the analyte and a long measurement time due to weak light-matter interactions caused by the size mismatch between the molecules and the probe light. Thanks to the concept of optical superchirality[1], various nanophotonic systems such as chiral plasmonic [2–4] and Mie resonance platforms [5] have been proposed to induce strong chiro-optical fields that can enhance their CD response. Despite these efforts, the confined nature of conventional chiral enhancement platforms that only generate chiral hotspots adjacent to the nanostructures still poses a challenge in detecting chiral molecules at low concentrations. To overcome this limitation, we propose an advanced traditional sensing theory called the chiral perturbation theory. As shown in **Fig 1.**, our approach aims to maximize the interaction between plane circularly polarized lights and chiral molecules by incorporating collective resonances on two-dimensional helicoid lattices [6]. Our methodology has exhibited ultra-high sensitivity at the pico-mole level and introduced a platform for real-time in-situ detection. This research has the potential to provide significant breakthroughs in various scientific fields, including pharmaceuticals, physiological diagnostics, pathogen detection, and beyond.

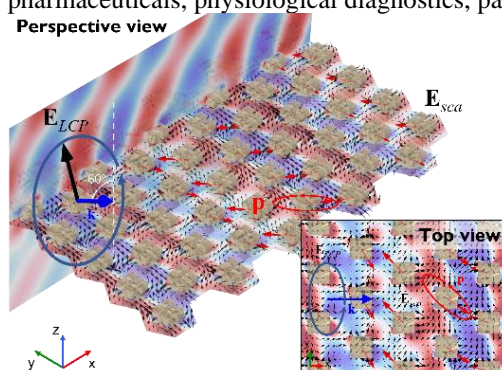


Fig. 1. Numerically retrieved collective spinning dipoles (\mathbf{p}) and scattered electric field (\mathbf{E}_{sca}) vectors on the 2D plasmonic chiral crystal. Perspective and top view of collectively rotating helicoid dipoles \mathbf{p} (red arrows on each helicoid) and scattered electric field (\mathbf{E}_{sca}) vectors (black arrows) at CR mode under 60° slanted incidence of left circularly polarized (LCP) light.

[1] Y. Tang and A. E. Cohen, Phys. Rev. Lett. **104**, 163901–163904 (2010)

[2] E. Hendry, T. Carpy, J. Johnston, M. Popland, R. V. Mikhaylovskiy, A. J. Lapthorn, S. M. Kelly, L. D. Barron, N. Gadegaard, and M. Kadodwala, Nat. Nanotechnol. **5**, 783–787 (2010)

[3] Y. Tang and A. E. Cohen, Science **332**, 6027, 333–336 (2011)

[4] J. M. Slocik, A. O. Govorov, and R. R. Naik, Nano Lett. **11**, 2, 701–705 (2011)

[5] M. L. Solomon, J. Hu, M. Lawrence, A. García-Etxarri, and J. A. Dionne, ACS Photonics **6**, 43–49 (2019)

[6] RM. Kim, J.-H. Huh, S. Yoo, T. Kim, C. Kim, H. Kim, JH. Han, NH. Cho, YaLim, SW. Im, E. Im, JR. Jeong, MH. Lee, T.-Y. Yoon, H.-Y. Lee, Q-H. Park, S. Lee, and KT. Nam, Nature **612**, 470–476 (2022)

Drift and funnel effects of trions in suspended MoSe₂ monolayer

Woo Hun Choi^{1,2†}, Seong Won Lee^{1,2†}, Su-Hyun Gong^{1,2*}

¹Departemnt of physics, Korea University, Seoul, Korea

²KU Photonics center, Korea University, Seoul, Korea

dngjs154@korea.ac.kr, atoum0712@korea.ac.kr, shgong@korea.ac.kr

Abstract: Charged excitons (trions) in transition metal dichalcogenides (TMDCs) are potential candidate of information carriers that can be controlled using electric fields analogous to conventional electronic devices. Also, like excitons, trion also preserve valley degree of freedom exhibiting intriguing physical properties. Here, we demonstrate drift and funnel effects of free trions in a suspended MoSe₂ monolayer by using a simple electromechanical device. We confirm that under the influence of electric force, locally excited trions were dragged and funneled toward the center of the stretched layer. Our research provides a direct way of controlling free trion motion and opens up the possibility for the application of trion-based optoelectronic devices.

Controlling the exciton transport in a transition metal dichalcogenides (TMDCs) layer are considered as a crucial step for developing TMD-based excitonic devices. Modulated potential landscapes are needed to deterministically manipulate the exciton's path, but their short recombination time hinders long-range transport. Thereby, interlayer excitons in TMDCs heterostructure have attracted attention to induce longer recombination lifetime. However, an electric field cannot affect the exciton's motion because of its charge-neutrality. In contrast, trions (i.e., charged excitons) carry a non-zero net charge, which provides great potential for their manipulation using externally applied electric fields as in conventional electronic devices. In this study, we achieved free-trion drift and funneling in a suspended MoSe₂ monolayer by exerting a gate-tunable electric field. The electric fields increase the trion density and pulls down the monolayer simultaneously. Drift effect of trions was directly analyzed by tracking the spatial shift of trion photoluminescence (PL) distribution under local excitation at various bottom gate voltage conditions. In numerical calculation, the electric force exerted on the trion was 2–4 orders of magnitude greater than the strain-induced force. We also successfully reproduced the observed drift behavior of the locally excited trions by using the drift-diffusion model.

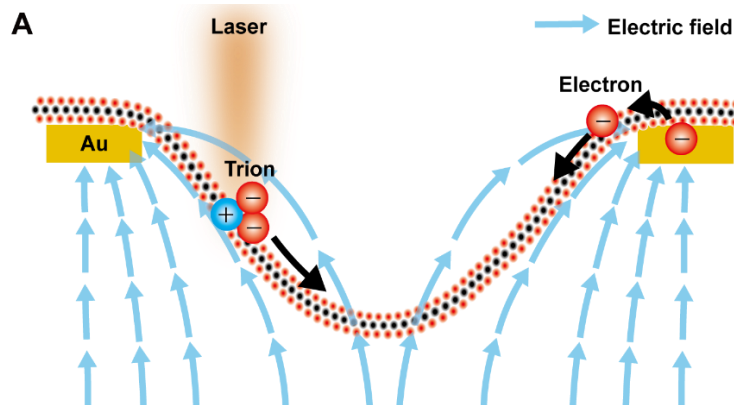


Fig1. A. Schematic diagram of the suspended MoSe₂ monolayer under the electric fields. The locally excited trions were drifted toward the center of monolayer.

Real-space Visualization of Spin Dynamics with Terahertz Polarimetric Imaging

Taewoo Ha

Center for Integrated Nanostructure Physics, Institute for Basic Science, Sungkyunkwan University, Suwon 16419, Republic of Korea
bspha77@gmail.com

Abstract: Terahertz (THz) time-domain spectroscopy offers a promising method for probing spin dynamics, characterized by an energy range of a few meV and picosecond response times. However, the long wavelength of THz waves restricts its suitability for microscopic imaging. In this talk, we introduce a near-field THz polarimetric method to visualize spin dynamics in real space, concentrating on planar spin Hall effects and spin precessing motion.

Spin dynamics, the study of how electron spins interact and evolve in various materials and systems [1,2], is fundamental to understanding and developing advanced data processing and storage technologies [3]. The behavior of electron spins, which are intrinsic angular momenta of electrons, is crucial in determining the magnetic and electronic properties of materials. Over the years, the trend in spin dynamics research has shifted towards exploiting the quantum nature of electron spins to achieve faster, more energy-efficient, and smaller-scale devices.

A range of methods have been devised to examine spin dynamics, with terahertz (THz) time-domain spectroscopy standing out as a promising approach due to its capacity to probe spin dynamics within an energy range of a few meV and response times in the picosecond regime [4,5]. Assessing spin dynamics in real space is of utmost importance, as it enables a deeper comprehension of the fundamental mechanisms and interactions, ultimately facilitating the design of more efficient and dependable devices. Although far-field THz spectroscopy has been employed to study magnetic systems, its long wavelength hinders its application in microscopic imaging. To tackle this challenge, we present a near-field THz method capable of visualizing spin dynamics in real space. Our technique centers on the planar spin Hall effect and spin precessing motion, offering new perspectives into spin dynamics and surpassing the limitations of traditional far-field THz spectroscopy.

[1] Boeglin, C. et al. Distinguishing the ultrafast dynamics of spin and orbital moments in solids. *Nature* **465**, 458–461 (2010).

[2] Radu, I. et al. Transient ferromagnetic-like state mediating ultrafast reversal of antiferromagnetically coupled spins. *Nature* **472**, 205–208 (2011).

[3] Ciornei, M.-C., Rubí, J. M. & Wegrowe, J.-E. Magnetization dynamics in the inertial regime: nutation predicted at short time scales. *Phys. Rev. B* **83**, 020410 (2011).

[4] Kampfrath, T., Tanaka, K. & Nelson, K. A. Resonant and nonresonant control over matter and light by intense terahertz transients. *Nat. Photon.* **7**, 680–690 (2013).

[5] Lee, H. et al. Terahertz spectroscopy of antiferromagnetic resonances in $\text{YFe}_{1-x}\text{Mn}_x\text{O}_3$ $0 \leq x \leq 0.4$ across a spin reorientation transition. *Appl. Phys. Lett.* **119**, 192903 (2021)

THz antennas for the application of photo-excited semiconductors

Geunchang Choi*,¹

¹*School of Electrical and Electronics Engineering, Chung-Ang University, South Korea*

*Email: nightsky@cau.ac.kr

Optical pump-terahertz probe technique based on femtosecond laser has been conducted in various semiconductor materials for measurements of carrier dynamics. As a probe beam, terahertz waves with low photon energy have many advantages such as being nondestructive and being far below the bandgap of the targeted semiconductor materials. On the one hand, terahertz nanoslot antennas have been studied for various applications, such as sensing and nonlinear effect, due to the advantage of background free, field enhancement, and field confinement [1]. Combined with semiconductor materials, terahertz nanoslot antennas enable various semiconductor materials to have unique properties such as characterization and an ultrafast terahertz device.

Here, we will present terahertz nanoslot antenna applications for photo-excited semiconductor materials. Our results were enabled by the strong field confinement of the antenna, which interacts with semiconductor materials effectively. First, we will discuss the measurement of surface carrier dynamics of the bulk semiconductor materials by using the nanoslot antennas fabricated onto the semiconductor materials [2]. After then, we will discuss the high on/off ratio and ultrafast terahertz modulation by the optical excitation of graphene/metal nanoslot antennas [3].

References

- [1] M. Seo, et al., Nat. Photonics 3 (3), 152-156 (2009)
- [2] G. Choi, et al., 6397-6401 (2017)
- [3] G. Choi, et al., Adv. Opt. Mater. 9 (16), 2100462 (2021)

Out-of-plane radiation of the topological metasurfaces

Ki Young Lee and Jae Woong Yoon

Department of Physics, Hanyang University, Seoul, 133-791, Korea

E-mail address: yoonyw@hanyang.ac.kr

Abstract: Photonic transports of In-plane topological states by intuitively emulating Hermitian electronic systems have received a lot of attention, but their out-of-plane radiation remain barely explored so far. By considering leakage radiation as non-Hermiticity, the extension of the topological notion to the resonant metasurfaces provides promising opportunities in terms of a new means for directly measuring topological bands as well as extra functionalities for free-space applications. In this talk, we discuss the fundamental mechanism of far-field radiation and resonant excitation in the topological junction metasurfaces consisting of thin film dielectric subwavelength gratings. These structures show complex valued Dirac-mass, Berry phase, and band structures represented by Fano spectral responses. We further discuss new optical functionalities found in the topological metasurfaces such as topological beam shaping and anomalous transmissive pure-phase-resonances.

1. Introduction

Topological interface states[1] between topologically distinct matters exhibit exotic physical properties such as the self-localization and the robustness against local environmental disturbances. Such states are mathematically treated as a Jackiw-Rebbi (JR) state which is zero-energy solution bound to the interface separating domains of opposite masses in the Dirac equation. With a mathematical analogy between the Dirac and optical wave equations, photonic topological natures have been actively investigated in versatile photonic platforms such as coupled microcavities, waveguide arrays, and photonic crystals.

Inherent open system natures of leaky photonic lattices or metasurfaces have triggered new fundamental ideas for non-Hermitian topology and offered exciting applications such as polarization-vortex beam generation and optical phase engineering. Thus, further investigations of such open topological natures provide a chance to achieve the stability and novel degrees of freedom for free-space optical devices. It has been reported that the leaky JR states [2] show a robust topological resonances in thin-film nanostructures, but the detailed role of leakage radiation induced non-Hermiticity in free-space optical devices has still remained unclear.

Here, we show efficient beaming of light as a unique characteristic of leaky JR states in topological junction metasurfaces. Far-field propagations of leakage radiation of JR states occur to a surface-normal direction with a small angular divergence from the localized resonance spot even confined to the subwavelength level. Such localized resonances also cause a light funneling that the excited electromagnetic energy flows predominantly toward the interface. This enables energy-efficient directional emission for light sources around the interface. We theoretically and numerically demonstrate such beaming phenomenon by presenting realistic device configurations.

2. Results

Figure 1a schematically illustrate a topological junction metasurface consisting of two different subwavelength gratings. The structure has total thickness $d = d_1 + d_2$ and refractive index n_1 covered by low index medium n_2 . The differences between the left and right side gratings are the period $a_{L,R}$ and the width of the grating ridge $W_{L,R}$. We assume the common structure parameters as $d_1 = 60$ nm, $d_2 = 40$ nm, $n_1 = 2.6$, and $n_2 = 1.45$. Each unit-cell is distinguished by the main parameters as $W_L = 90$ nm, $a_L = 360$ nm, $W_R = 227$ nm, and $a_R = 325$ nm. We focus on frequency regime near the second-order bandgap possessing fundamental transverse electric (TE_0) guided-mode resonances (GMR). In order to generate the leaky JR state, the two grating classes should satisfy the band inversion relation for photonic domain wall problem that means they are topologically distinct each other.

We show far-field radiation pattern $|E_y(x,z)|^2$ for the leaky JR state in Fig. 1b by a FEM simulation. Highly collimated surface-normal propagation occurs within the small radiation area around the interface $x = 0$. In this calculation, we assume the emitter array as an effective light sources for emulating fluorescent molecules or quantum dots. The light emitters are ideal point sources generating cylindrical waves for all directions at JR wavelength $\lambda_{JR} = 633$ nm. These sources are evenly placed inside the grating region from $x = -5$ to 5 μ m at the center of the guided-mode envelope as schematically depicted in Fig. 1b.

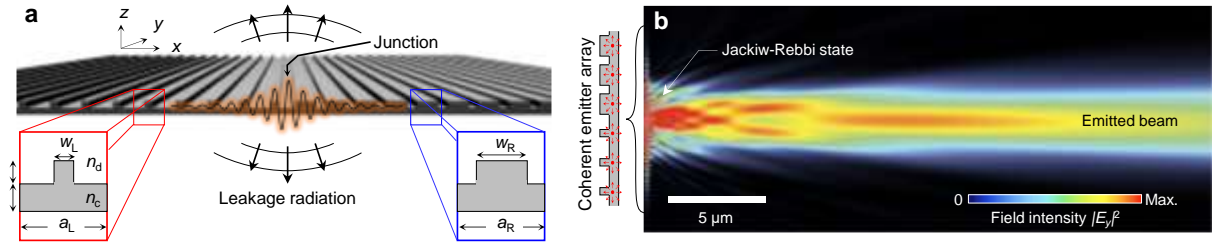


Fig.1. Far-field properties of the leaky Jackiw-Rebbi states. **a**, Schematics of topological junction super-cell configuration consisting of two different thin-film subwavelength gratings for generating the leaky Jackiw-Rebbi state at the interface. The red and blue boxes indicate unit-cell configurations of left and right side gratings, respectively. **b**, Far-field radiation pattern of electric field intensity $|E_y(x,z)|^2$. Array of point emitters is evenly placed inside the device region from $x = -5$ to $5 \mu\text{m}$ at $z = 0$.

Characteristic field distributions of a leaky JR state at the junction lead to efficient beaming of light from internal emitters with the help of the cavity-QED coupling and subsequent electromagnetic funneling effects. Intriguingly, this topological beaming effect allows direct beam shaping on the resonance state itself for any desired positive-definite profile by means of Dirac-mass control, which is readily obtainable with moderate fill factor variations in compatible manners with integrated optics architectures on a chip. Therefore, the proposed structure has great potential for creating efficient micro light emitters taking advantages of strong localization, narrow emission angle, high quantum efficiency, and adaptive beam shaping capability as well. These properties are highly desirable for numerous applications including display pixels, solid-state light detection and ranging, laser machining, optical interconnects and telecommunications.

The proposed method is also directly applicable for efficient optical detectors or absorption-based nanophotonic elements because they in-principle correspond to the time-reversed emitters that take all such advantages with identical constructions. In this respect, further study to produce two-dimensional topological beaming effect is important for the sake of practicality of the proposed concept. We consider that it should be made possible with two-dimensional Dirac-mass distributions or bi-grating designs that accommodate higher-order topological states. From a broader perspective, our result and associated follow-up study may motivate various research topics for the development of non-Hermitian topological nanophotonic elements in which interplay between topological states, internal gain or loss, and the external radiation continuum might create novel optical effects and concomitant device applications beyond the present limitations.

3. Conclusion

In conclusion, we propose a topological junction metasurface for an efficient beam generation through leakage radiation of the JR state. With the analytic expression of a leaky JR state and a FEM confirmation, we show their position-wavevector uncertainty relation corresponding to $\Delta x \Delta k_x = 1/2^{1/2}$, which allows their surface-normal far-field radiation to maintain the highly collimated beam profile from the tightly confined radiation area. Remarkably, we demonstrate the existence of the effective funneling boundary where the excited electromagnetic energy flow occurs unidirectionally toward the interface. Therefore, our findings may offer a promising scheme for new designs of nanophotonic antennas and provide a practical guidance of further experiments for fundamental natures of non-Hermitian topology.

4. References

- [1] Hasan, M. Z. & Kane, C. L. Colloquium: Topological insulators. *Rev. Mod. Phys.* **82**, 3045–3067 (2010)
- [2] Lee, K. Y. *et al.* Topological guided-mode resonances at non-Hermitian nanophotonic interfaces. *Nanophotonics* **10**, 1853–1860 (2021).

Understanding the Electronic Structures of Two-Dimensional Monolayer Materials via the Control of Spatial Resolution

Heesuk Rho

*Department of Physics, Jeonbuk National University, Jeonju, 54896, Republic of Korea
E-mail address: rho@jbnu.ac.kr*

Two-dimensional layered structures have distinct types of defects such as wrinkles and bubbles. Such defects are formed in various sizes from the microscale to the nanoscale. Therefore, a precise control of spatial resolution is required to explore the optical properties of two-dimensional materials in the presence of defects. In this talk, we present Raman results of two-dimensional materials with micrometer and nanometer resolutions. Micro-Raman imaging of bubbles identified the spatial changes in charge density in monolayer WS₂ under the influence of hexagonal boron nitride. Formation of wrinkles in WS₂ at the nanoscale resulted in the splitting of the in-plane optical phonon into two singlet modes. Furthermore, tip-enhance Raman spectroscopy resolved spatial distributions of electron density across the wrinkled WS₂ surface. Our study demonstrates that the control of spatial resolution is beneficial to understand the energy landscape of atomically thin defective materials. [This work was supported by the National Research Foundation of Korea (NRF) grants funded by the Korea government (MSIT) (Grant Nos. 2019R1A2C1003366 and 2022R1A4A1033358)]

Real-space mapping of ultra-confined ‘image’ phonon-polaritons

Sergey G. Menabde and Min Seok Jang

Korea Advanced Institute of Science and Technology (KAIST)

E-mail address: jang.minseok@kaist.ac.kr

Abstract: Hyperbolic phonon-polaritons in van der Waals crystals fundamentally have infinite number of the mode orders, however only the weakly confined first-order mode is typically accessible. We use near-field probing to map ultra-confined ‘image’ phonon-polaritons supported by the polaritonic material on gold substrate. These second-order hyperbolic modes possess significantly larger momentum yet similar lifetime compared to the first-order modes in a suspended material. Monocrystalline gold flakes provide scattering-free propagation and superior excitation mechanism for phonon-polaritons in our samples.

Polaritons – hybrid quasi-particles of light coupled to the collective oscillations of charges – provide an exceptionally high degree of field confinement and a capability for light manipulation at nanoscale. Very recently, a new class of ultra-compressed polaritonic modes in van der Waals crystals has been spotlighted as a superior platform for a strong light-matter interaction: the ‘image’ polaritons, supported by a polaritonic material in proximity to a metal when the polaritonic mode couples with its mirror image.

We use scanning scattering-type near-field optical microscope (s-SNOM) to study the hyperbolic ‘image’ phonon-polaritons in hexagonal boron nitride (hBN) [1] and orthorhombic molybdenum trioxide (α -MoO₃) [2] crystals at mid-infrared frequencies. Atomically-flat monocrystalline gold flakes are used as a substrate, practically eliminating the surface-mediated scattering of propagating polaritonic modes. Furthermore, ~20 μ m-long sharp gold edges efficiently launch polaritons with a planar wavefront. In such system, polariton properties can be accurately measured by the real-space mapping of their near-field interference with the excitation beam. Besides, gold substrate guarantees the maximum signal-to-noise ratio of the s-SNOM output signal, providing ideal conditions for near-field experiments at mid-infrared frequencies.

Our results are even more interesting in the context of earlier work on the experimental observation of the ultra-confined mid-infrared ‘image’ (also called ‘acoustic’) graphene plasmons that are twice as compressed and propagate 1.4 times more optical cycles compared to graphene surface plasmons under similar conditions [3].

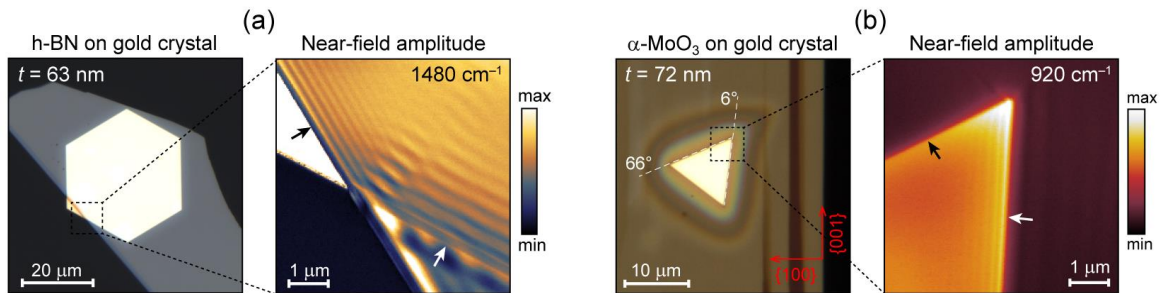


Figure 1. (a) Hyperbolic ‘image’ phonon-polaritons in h-BN on top of the monocrystalline gold flake. (b) In-plane anisotropic ‘image’ phonon-polaritons in α -MoO₃ on gold flake.

References

- [1] S. G. Menabde, S. Boroviks, J. Ahn, J. T. Heiden, K. Watanabe, T. Taniguchi, T. Low, D. K. Hwang, N. A. Mortensen, and M. S. Jang, *Sci. Adv.* **8**, eabn0627 (2022).
- [2] S. G. Menabde, J. Jahng, S. Boroviks, J. Ahn, J. T. Heiden, D. K. Hwang, E. S. Lee, N. A. Mortensen, and M. S. Jang, *Adv. Opt. Mater.* **10**, 2201492 (2022).
- [3] S. G. Menabde, I.-H. Lee, S. Lee, H. Ha, J. T. Heiden, D. Yoo, T.-T. Kim, T. Low, Y. H. Lee, S.-H. Oh, and M. S. Jang, *Nat. Commun.* **12**, 938 (2021).

Probing the Optical Near-field Using Scanning Thermal Microscopy

Kiin Nam¹, Hyuntae Kim³, Woongkyu Park², Jaeseung Im¹, Jae Sung Ahn^{2,†}, and Soobong Choi^{1,†}

¹ Department of Physics, Incheon National University, Incheon 22012, Republic of Korea

² Medical & Bio Photonics Research Center, Korea Photonics Technology Institute, Gwangju 61007, Republic of Korea

³ Park Systems Corporation, KANC 4F, Iui-Dong 906-10, Suwon, 16229, Republic of Korea

E-mail address: Jae Sung Ahn (jaesung.ahn@kopti.re.kr), Soobong Choi (sbchoi@inu.ac.kr)

Abstract:

Scanning thermal microscopy (SThM) enables to obtain thermal characteristic information such as temperature and thermal conductivity from the signals obtained by scanning a thermometer probe over a sample surface. Particularly, the precise control of the thermometer probe makes it possible to study near-field radiative heat transfer (NFRHT) by measuring the near-field thermal energy, which implies that when light is used as a local heat source, photothermal energy can be detected from the optical near-field by approaching the probe in the near-field region. Therefore, SThM can be utilised as a tool to generate the near-field optical images in spectral ranges where the photothermal interactions occur in the probe.

In this presentation, SThM-based near-field optical microscopy is introduced. To verify the photo response of the system, near-field optical images of a gold grating coupler were obtained while controlling the surface plasmon polariton (SPP) generation. The images have a spatial resolution of 40 nm and signal to noise ratio (SNR) of up to 19.8. In addition, graphene oxide (GO) is coated on the probe to improve optical contrast without significant degradation of spatial resolution. The coating of GO enhances the root-mean-square (RMS) contrast more than 2.56 times without significant loss of spatial resolution.

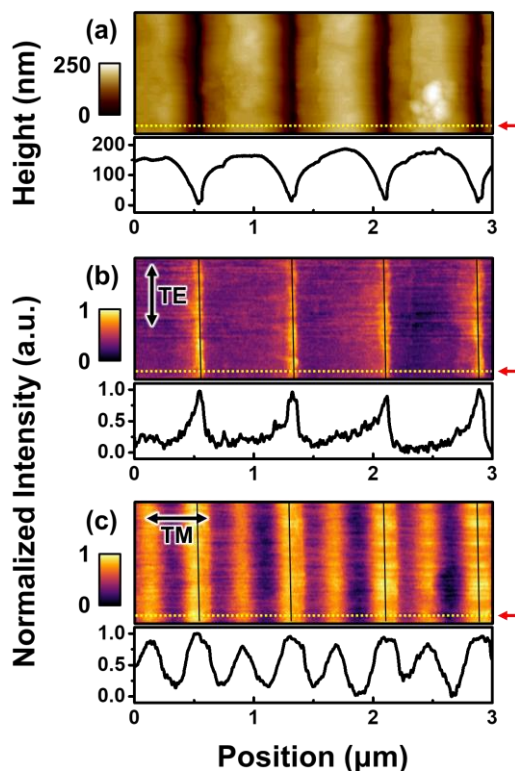


Figure 1. Polarization-dependent optical image in gold nano slit array. $3\mu\text{m}\times 1\mu\text{m}$ (a) topography image and temperature image for normal (b) TE and (c) TM incident condition with each line profile at dash line of the gold nanoslit array. Black solid lines in the image denote slit positions.

Atomic force microscope-guided nanoscale 3D printing of quantum dots and in situ Raman spectroscopy

Sangmin An

Department of Physics, Institute of Photonics and Information Technology, Jeonbuk National University
E-mail address: san@jbnu.ac.kr

Abstract: In this study, in order to successfully implement nanoscale 3D printing, nanonozzles come close to the surface with guidance of an atomic force microscope (AFM) within a few nm, effectively reducing the surface tension of the inner wall of the nanonozzle apex, and ejecting liquid to fabricate quantum dot-aggregated nanowires. And we in situ measured and analyzed characteristics of the fabricated wires by using optical apparatus (Raman spectroscopy) combined with AFM system.

1. Nanoscale 3D printing with guidance of AFM

3D printing technology is one of the keywords of the 4th industrial revolution, and its effectiveness has been recognized worldwide, and its applicability is expanding throughout wide area of science and industry [1-3]. One of the most important limitations of this 3D printing technology is that it is difficult to reduce the printing resolution of the printed object down to the nanoscale. This is because it is difficult to overcome the high surface tension acting at the inner surface of the nozzle apex in ambient conditions in order for the liquid to come out through the nanopore.

In this study, to overcome these limitations, nanoscale 3D printing technology was successfully implemented by facilitating a system of quartz tuning fork (QTF) – AFM combined with nanonozzle in Fig. 1(a) [4]. By attaching a nanonozzle to the end of one leg of the quartz tuning fork oscillator, even if it approaches the surface very stably by a few nm, while the tip is not damaged at all. It was configured so that liquid could be ejected through the nanopore. We used a Cadmium-Selenide (CdSe) quantum dot (QD) solution, and by immediately and very slowly (10 nm/s) retracting the nozzle in the opposite direction (upward) after the liquid was ejected on the surface, the water-soluble component of the solution evaporated in the air and only the QDs remained. It was possible to form a structure in the form of nanowires in which QDs are aggregated in Fig. 1(b).

2. In situ Raman spectroscopy of the fabricated Quantum dot nanowire

It is very important to investigate the physical properties by manufacturing nano shapes and measuring the spectroscopic characteristics of the manufactured objects. If we need to move the fabricated nanoscale objects to measure and analyze fluorescence characteristics or Raman spectroscopy after the nano-shaped object is manufactured (no on-site measurement), it takes a lot of effort and time to find the nano-shaped object for spectroscopic analysis because of its very small size as well as contamination of the nano-shaped object. In order to overcome this issue, in this study, we developed a system that can in situ measure and analyze the spectral characteristics immediately after manufacturing nano-shaped bodies, and measured and analyzed Raman spectroscopic characteristics immediately in the field without moving the prepared QD nanowires (Fig. 1c).

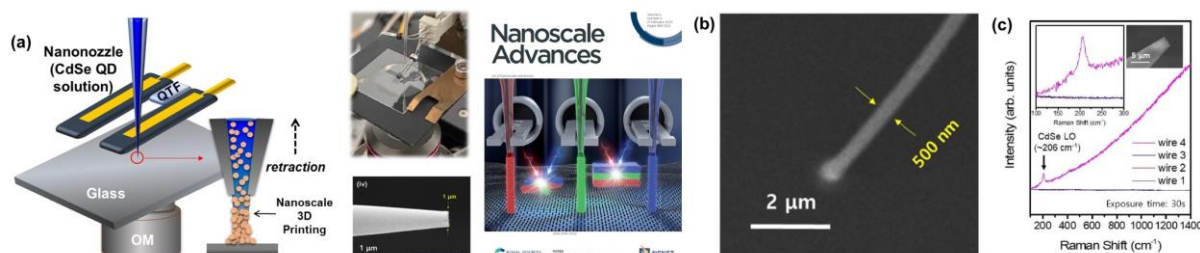


Figure 1. Experiments. (a) AFM-guided nanoscale 3D Printing technique (left). Schematic of QD-aggregated nanowire with different QD (right). (b) Fabricated QD-aggregated nanowire. (c) Raman spectroscopy of the fabricated nanowire.

References

- [1] H. Yang, D. Zhao, S. Chuwongin, J.-H. Seo, W. Yang, Y. Shuai, J. Berggren, M. Hammar, Z. Ma, and W. Zhou, "Transfer-printed stacked nanomembrane lasers on silicon", *Nat. Photon.*, **6**, 615–620 (2012).
- [2] D. Zhao, S. Liu, H. Yang, Z. Ma, C. Reuterskiöld-Hedlund, M. Hammar, and W. Zhou, "Printed Large-Area Single-Mode Photonic Crystal Bandedge Surface-Emitting Lasers on Silicon", *Sci. Rep.*, **6**, 18860 (2016).
- [3] M. Zastrow, "3D printing gets bigger, faster and stronger Research advances are changing the image of a once-niche technology", *Nature* **578**, 20-23 (2020).
- [4] Taesun Yun, Yong Bin Kim, Taegeon Lee, Heesuk Rho, Hyeongwoo Lee, Kyoung-Duck Park, Hong Seok Lee*, and Sangmin An*, "Direct 3D-printed CdSe quantum dots via scanning micropipette", *Nanoscale Adv.* **5**, 1070-1078 (2023).

Enhancing the quantum yield of Ultraviolet emissive Ti₂N MXene Quantum Dots by one-pot solvothermal synthesis

Anir S. Sharbirin¹, Dinh Loc Duong^{2,*} and Jeongyong Kim^{1,*}

¹Department of Energy Science, Sungkyunkwan University, Suwon 16419, Korea.

²Department of Physics, MonArk Foundry Scientist and Liaison, Montana State University, MT

E-mail address: j.kim@skku.edu

Abstract:

Nitride MXene-based quantum dots (MQDs) display photoluminescence (PL) with deep UV excitation [1] which suggest a better performance for light-emitting applications in the UV region. However, the emission is still in the visible region and the PL is relatively weaker compare to carbide MQDs. Furthermore, the quantum yield (QY) and the PL lifetime of Ti₂N MQDs displays drooping effect with high exciton density that would be unfavorable for practical applications. In this study, we synthesized titanium nitride (Ti₂N) MQDs by solvothermal synthesis. The Ti₂N MQDs exhibits UV emission centered around ~370 nm when illuminated with 240 nm excitation. We also observe an overall increase of QY with a maximum of 17.4%. Furthermore, we were able to decrease the QY drooping of the dispersed Ti₂N MQDs film when exposed with high exciton density. The reduction of PL lifetime with higher exciton density was also suppressed. Our studies help to better facilitate the applications of MQDs in UV optoelectronics.

References

[1] A.S. Sharbirin, S. Roy, T.T. Tran, S. Akhtar, J. Singh, D.L. Duong, J. Kim, J. Mater. Chem. C 10 6508–6514 (2022).

Elucidating the optical properties of light-emitting V₂N MXene quantum dots

Sophia Akhtar, Jaspal Singh, Trang Thu Tran, Shrawan Roy, Eunji Lee, Zarmeena Akhtar and Jeongyong Kim*

Department of Energy Science, Sungkyunkwan University, Suwon 16419, Republic of Korea.

E-mail address: * (j.kim@skku.edu)

Abstract

MXenes are 2D nanomaterials that serve as sources of MXene-derived quantum dots. MXenes are composed of early transition metal nitrides, carbides, or carbonitrides, and are fabricated by selective etching of the A layer from MAX phases[1]. The outstanding optical properties of MXene quantum dots (MQDs) have attracted significant attention in optoelectronic applications. MXene quantum dots (MQDs) are a plausible solution for PL enhancement owing to their prominent quantum confinement and edge effects [2] due to their small size. MQDs have an increased surface area [3] and retain the merits and properties of their 2D counterpart MXene, with the capability of surface functionalization for improved dispersion [4]. MQDs have been developed mostly from carbide MXenes, such as TiC₂ [5], Ti₃C₂ [6], V₂C [7], Nb₂C [8], and only recently light-emitting nitride MQDs based on Ti₂N MXene have been reported which showed superior UV absorption and light emission [9,10]. Expansion of the precursor choice for MQDs could provide diverse and advanced MQD characteristics facilitating their practical use.

In this study, we firstly report the synthesis of novel V₂N light-emitting MQDs. MQDs were prepared from a V₂N MXene precursor by using a hydrothermal process at 160 °C for 10 h. The structural and optical properties of the V₂AlN MAX phase, V₂N MXene, and MQDs were studied. Raman spectra of V₂N MAX phase and MXene were firstly provided in our work as shown in Figure 1 [11], facilitating their clear identification. Our V₂N MQDs are water-soluble and possess an average lateral diameter of 3.26 nm. The results of PL and PL excitation spectroscopy (PLE) indicate that our V₂N MQDs exhibit efficient light emission with deep UV absorption. The PL quantum yield was measured to be 11.8% which is highest value for the nitride based MQDs reported until now. Based upon the remarkable optical behavior and high quantum yield V₂N MQDs will expand the use of MQDs for various optoelectronic applications. Details will be presented.

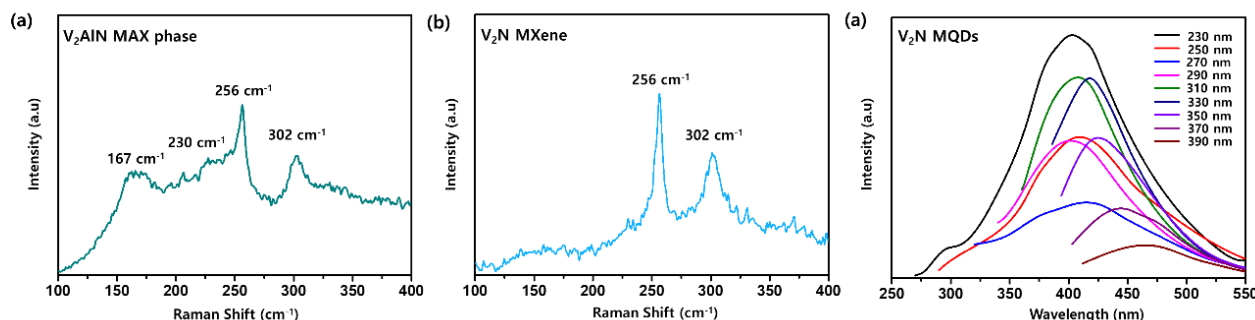


Fig. 1. Raman spectrum of as-synthesized (a) V₂AlN MAX phase (b) V₂N MXene. (c) Excitation wavelength-dependent PL spectra of the synthesized V₂N MQDs

References

- [1] P. Urbankowski, B. Anasori, K. Hantanasirisakul, L. Yang, L. Zhang, B. Haines, S. J. May, S. J. L. Billinge, and Y. Gogotsi, *Nanoscale*, **9**, 17722–17730, 2017.
- [2] D. Huang, Y. Xie, D. Lu, Z. Wang, J. Wang, H. Yu, H. Zhang, *Adv. Mater.*, **31**, 1901117, 2019.
- [3] A. Rafieerad, W. Yan, G. L. Sequiera, N. Sareen, E. Abu-El-Rub, M. Moudgil, and S. Dhingra, *Adv. Healthc. Mater.*, **8**, 1900569, 2019.
- [4] Q. Xu, J. Ma, W. Khan, X. Zeng, N. Li, Y. Cao, X. Zhao, and M. Xu, *Chem. Commun.*, **56**, 6648–6651, 2020.
- [5] J. Gou, L. Zhao, Y. Li, and J. Zhang, *ACS Appl. Nano Mater.*, **4**, 12308–12315, 2021.
- [6] F. Yan, J. Sun, Y. Zang, Z. Sun, H. Zhang, J. Xu, and X. Wang, *Dye. Pigment.*, **195**, 109720, 2021.
- [7] Y. Cao, T. Wu, K. Zhang, X. Meng, W. Dai, D. Wang, H. Dong, and X. Zhang, *ACS Nano*, **13**, 1499–1510, 2019.
- [8] G. Yang, J. Zhao, S. Yi, X. Wan, and J. Tang, *Sensors Actuators: B Chem.*, **309**, 127735, 2020.
- [9] S. Akhtar, S. Roy, T. T. Tran, J. Singh, A. S. Sharbirin, and J. Kim, *Appl. Sci.*, **12**, 4154, 2022.
- [10] A. S. Sharbirin, S. Roy, T. T. Tran, S. Akhtar, J. Singh, D. L. Duong, and J. Kim, *J. Mater. Chem. C*, **10**, 6508–6514, 2022.
- [11] S. Akhtar, J. Singh, T. T. Tran, S. Roy, E. Lee, and J. Kim, *Optical Materials*, **138**, 113660, 2023

Freestanding monolayer transition metal dichalcogenides on structured template

Hyun Jeong^{1*}, Hyung Chan Suh¹, Ga Hyun Cho¹, Gilles Lerondel^{2*}, Mun Seok Jeong^{1*}

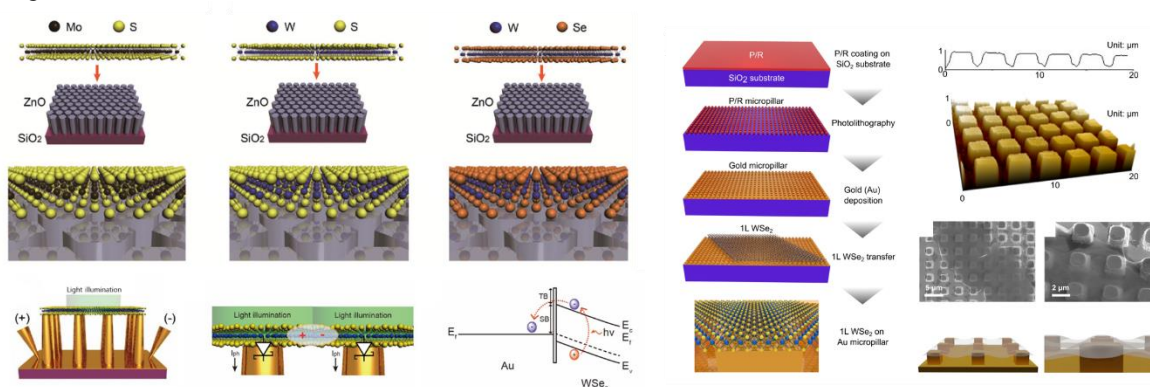
¹ Department of Physics, Hanyang University, Seoul 04763, Republic of Korea

² Laboratoire Lumière, nanomatériaux et nanotechnologie, CNRS-EMR 7004, Université de Technologie de Troyes, BP 2060, 10010 Troyes, France

E-mail address: hjeong6620@gmail.com, gilles.lerondel@utt.fr, mjeong@hanyang.ac.kr

Monolayer transition metal dichalcogenides (TMDs) are two-dimensional materials consisting of a transition metal sandwiched between two chalcogen atoms. Due to their thickness of only one atom, they are ideal for investigating fundamental properties at the nanoscale. Strain relaxation in monolayer TMDs can be well controlled, leading to potential applications in flexible electronics and optoelectronics. Their optical properties are of great interest, with strong light-matter interactions making them promising for photodetectors, light-emitting diodes, and solar cells. Monolayer WSe₂ is a particularly promising TMD material, with a direct bandgap making it an efficient light emitter and photodetector. [1]

This study discusses the integration of freestanding transition metal dichalcogenides (TMDs) onto ZnO nanorods (NRs) as a nanostructured substrate. [2] The photoluminescence (PL) spectra of monolayer TMDs on NRs show a significant enhancement compared to those on SiO₂, with a limited point of contact between the TMDs and the support. The absence of stress in the TMDs on NRs is confirmed by strong increases in Raman and PL intensities, along with characteristic peak shifts. In addition, the effect of charge transfer between the TMDs and ZnO NRs is found to be negligible. As for the device application of freestanding TMD on the nanostructure, the study proposes a new type of photodiode based on monolayer WSe₂, which can be transferred onto core-shell silicon-gold nanopillars, demonstrating a significantly high maximum photoresponsivity of 23.16 A/W. The paper concludes that such new point-cell photodiodes can resolve critical issues of 2D materials and improve device performance in monolayer transition metal dichalcogenide-based optoelectronics. In addition, dark excitons of 1-L WSe₂ were detected at room temperature by applying crystalline strain using a gold micropillar structure on a Si substrate. Local intense crystalline strain induced by the gold micropillar structure led to the detection of dark excitons in the high-stress region of the 1-L WSe₂. Furthermore, surface plasmon enhanced Raman scattering was observed as the distance between the 1-L WSe₂ and the gold micropillar surface decreased under the influence of the high strain.



References

- [1] Zou, Y., Zhang, Z., Yan, J. et al. *Nat. Commun.* **13**, 4372 (2022).
- [2] H. Jeong, H. M. Oh, A. Gokarna, H. Kim, S. J. Yun, G. H. Han, M. S. Jeong, Y. H. Lee, G. Lerondel, *Adv. Mater.* **29**, 1700308 (2017)

The preparation of transition metal dichalcogenides colloidal ink and its applications

Dae Young Park¹, Duc Anh Nguyen², Kang-Nyeoung Lee³, Jiseong Jang³, Geunchang Choi⁴, Heejun Yang⁵, Mun Seok Jeong^{1*}

¹Department of Physics, Hanyang University, Seoul 04763, Republic of Korea

²Division of Physics and Semiconductor Science, Dongguk University, Seoul 04620, Republic of Korea

³Department of Energy Science, Sungkyunkwan University, Suwon 16419, Republic of Korea

⁴School of Electrical and Electronics Engineering, Chung-Ang University, Seoul 06974, Republic of Korea

⁵Department of Physics, Korea Advanced Institute of Science and Technology, Daejeon 34141, Republic of Korea

E-mail address: mjeong@hanyang.ac.kr

Abstract: 2D transition metal dichalcogenides (TMDs) exhibit intriguing properties for applications in catalyst, optoelectronics, and electronics. Depending on the applications of TMDs, the favorite preparation methods can be varied. The colloidal ink of TMDs has advantages such as facile preparation, low synthetic temperature, and large scalability. However, it is commonly applied in hydrogen evolution reaction (HER) due to the high density of defects and organic impurities in colloidal TMDs ink. To expand the application of colloidal TMDs ink with its own advantage, the removal of defects and impurities or exploitation of applications must be conducted.

In this presentation, the two different applications of colloidal TMD inks are introduced. First, the memtransistor with large-area and high-quality molybdenum disulfide (MoS₂) thin films through a spray coating of ink with post sulfurization process was fabricated. Second, the bimetallic oxide nanoparticles from colloidal TMDs ink for the growth of carbon nanotubes are prepared via an intercalation and substitutional reduction reaction. This result proves the enough potential of colloidal TMDs ink for not only HER but also various applications.

Physical Implementation of Ant Colony Intelligence in Colloidal Particle and Phase-Change Material System

Bokusui Nakayama^a, Hikaru Nagase^a, Hiromori Takahashi^a, Yuta Saito^b, Shogo Hatayama^b,
Kotaro Makino^b, Eiji Yamamoto^a, and Toshiharu Saiki^a

^aKeio University and ^bNational Institute of Advanced Industrial Science and Technology
saiki@elec.keio.ac.jp

Abstract: Pheromone interactions were introduced into the colloidal particle system by using phase change material as a storage medium and near-field lens effect to mimic ant swarm intelligence. We demonstrated that it is possible to mimic organisms other than ants, such as bacteria, by controlling their self-propulsion and pheromone attraction abilities.

1. Introduction

In the collective behavior of organisms, some optimization is involved from the viewpoints of time, energy, and risk management. There have been studies to interpret and algorithmize their behavior using mathematical models and to utilize them as a solution search method for optimization problems. However, the current state of mathematical models is far from understanding the essence of biological behavior. For example, it is difficult to model the role of memory and internal states of behavior history based on biological observation alone. It would be useful to conduct research using a real physical system that can introduce various interaction mechanisms while simulating living organisms. In this study, we aim to construct a real physical system in which colloidal particles are regarded as individual organisms, and the interaction with the environment and the history of interactions between individuals are stored by phase-change materials to manifest purposive behaviors.

2. Method and main results

Colloidal particles with a diameter of 3 μm moving in water were used as ants to implement pheromone communication mechanism using a phase-change material and photothermal near-field lens effects [1]. The keys in implementation are (1) self-propelled ability of particles, (2) pheromone attracting ability, and (3) controllability of the relative ratio of these two abilities. Self-propulsion is obtained by using Janus particles (hemispherical surface of polystyrene particles is coated with gold), which are propelled under an alternating electric field. The pheromone attracting ability is implemented by using a chalcogenide phase change material (GeSbTe) as the substrate (the ground on which the ants move). When irradiated with a wide-area subnanosecond pulse of light from above, GeSbTe is heated directly beneath the particle by the lens-focusing effect, and changes from an amorphous phase to a crystalline phase. Since the crystallization occurs along the trajectory of the Janus particles, it is regarded as pheromone emission. Furthermore, the local formation of a highly conductive crystalline phase causes the AC electric field to be concentrated in the crystalline phase region, which eventually generates an electro-osmotic flow. Since this flow is always directed toward the crystalline phase region, it can be utilized as a pheromone attraction. Although both particle self-propulsion and pheromone attraction originate from the AC electric field, their relative ratios can be controlled depending on the frequency. When the pheromone attraction ability is enhanced, self-trapping occurs and bacterial colony formation can be mimicked. GeSbTe can also be used as a coating material for the particles themselves to implement memory functionality.

3. References

[1] B. Nakayama, H. Nagase, H. Takahashi, Y. Saito, S. Hatayama, K. Makino, E. Yamamoto, and T. Saiki, Proc. Natl. Acad. Sci. USA **120**, e2213713120 (2023).

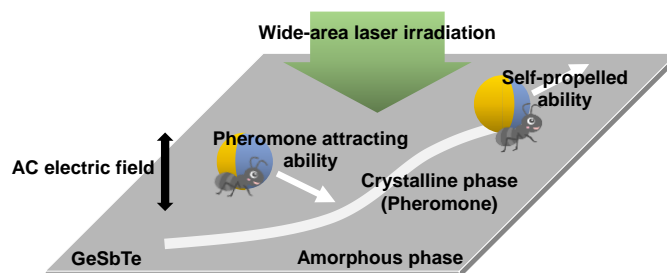


Fig. 1. Implementation of pheromone communication mechanism by using a phase-change material and photothermal near-field lens effect.

Resistive Memory Behavior of Defective Large-grain 2D Halide Perovskite Film

Hyeon Jun Jeong,¹ Taehoon Kim,¹ Dong Hyeon Kim,¹ Chan Kwon,¹ Jieun Jo,¹ Mun Seok Jeong^{1*}

¹Department of Physics, Hanyang University, Seoul, 04763, Republic of Korea

e-mail: mjeong@hanyang.ac.kr

Two-dimensional (2D) halide perovskites possess excellent photoelectric properties, making them promising candidates for optoelectronic applications such as solar cells, light-emitting diodes (LEDs), and photodetectors. In this study, we synthesized a 2D halide perovskite film using a binary ligand in an antisolvent solution. The film exhibited a periodic peak at a low angle and a strong exciton peak at approximately 410 nm, confirming the presence of two layers in the film. Photoluminescence spectra further revealed the existence of defects in the 2D halide perovskite due to the absence of cations, which provide important channels for the formation of conductive filaments inside the film. To investigate the switching behavior of the 2D halide perovskite film, we fabricated a simple memory device consisting of indium tin oxide (ITO)/2D halide perovskite/gold (Au). We verified the inhomogeneous switching behavior of the film inside the grain and at the boundaries using conductive atomic force microscopy (AFM). Our findings provide valuable insights into the potential applications of 2D halide perovskites for advanced memory devices.

Near-field modulation of single photon emitter with a novel plasmonic probe

Yunkun Wu*, Xifeng Ren

Key Laboratory of Quantum Information,
CAS, University of Science and Technology of China, Hefei
230026, China
*wuyk123@mail.ustc.edu.cn

Abstract: The interaction between surface plasmon polaritons (SPPs) and emitters has attracted increasing attention because of its potential to improve the quality of single-photon sources through stronger light-matter interactions. We introduce a hybrid plasmonic probe composed of a fiber taper and silver nanowire to controllably modulate the radiation properties of single photon emitters (SPEs) with different oriented polarization. After investigating the optical characters and SPP modes of this plasmonic probe, the polarization-dependent modulation results would be expected in theory and simulation. In the further research in experiment, the radiation lifetime is reduced by a factor as large as seven for out-of-plane oriented SPEs such as single CdSe quantum dots; while the average modulation amplitude varied from 0.69 to 1.23 for in-plane oriented SPEs such as hBN defect SPEs, depending on the position of the probe. The consistency between experiment and theory demonstrate that our work provides an efficient approach for optimizing the properties of SPEs for quantum photonic integration.

Over the past decades, single photon emitters (SPEs) have been the focus of intense research with the aim of obtaining brighter and purer sources as the basis of scalable quantum nanophotonics platforms. The ability to manipulate SPEs is essential for future quantum information processes and numerous methods have been proposed [1,2]. However, since the huge mismatch between the effective mode volumes of the SPE and conventional optical systems, the efficient manipulation of the radiation of SPEs still remains to be a challenge. Fortunately, surface plasmon polaritons (SPPs) offer a solution to significantly increase the coupling by confining the optical mode to nanometers and thus provide an enhanced SPE emission. It is known that the strength of the SPP–photon coupling highly depends on the relative orientation between the SPP mode and emitters [3], which is an important property that can be utilized to encode quantum information. Herein, our work is devoted to studying in detail the strong polarization-dependence of coherent modulation for SPEs.

In this work, we introduced a plasmonic probe, integrated by a suspended silver nanowire adhering to a fiber taper [4], to locally modulate the lifetime of SPEs with different orientations in the near field as shown in figure 1. We started the investigation from the basis optical characters of this novel plasmonic probe, and it was found that the radiation rate of the excited state in the SPE could be modulated efficiently and selectively when controlled the probe to the near field of the SPE. This change can be demonstrated by the measurements of lifetime in experiment and is strongly dependent on the polarized orientation of the SPEs. The experimental results were consistent with prior numerical simulations and theoretical analysis. Our work not only is a significant step toward on-demand regulation and practical application of SPE performance, but also provides a new scheme for analyzing the vectorial optical field based on a surface plasmonic probe.

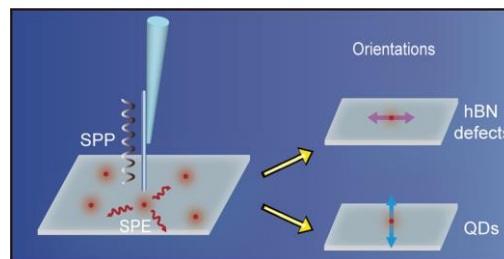


Fig. 1. Schematic of the modulation of SPEs with different orientations using a plasmonic probe in the near field.

- [1] Proscia, N. V.; Jayakumar, H.; Ge, X.; Lopez-Morales, G.; Shotan, Z.; Zhou, W.; Meriles, C. A.; Menon, V. M. *Nanophotonics* **9**, 2937–2944 (2020).
- [2] Palombo Blascetta, N.; Liebel, M.; Lu, X.; Taniguchi, T.; Watanabe, K.; Efetov, D. K.; van Hulst, N. F. *Nano Lett.* **20**, 1992–1999 (2020).
- [3] Wang, L.L.; Zou, C.L.; Ren, X.F.; Liu, A.P.; Lv, L.; Cai, Y.J.; Sun, F.W.; Guo, G.C.; Guo, G.P. *Appl. Phys. Lett.* **99**, 061103 (2011).
- [4] Wu, Y. K.; Lu, L.; Chen, Y.; Feng, L. T.; Qi, X. Z.; Ren, H. L.; Guo, G. C.; Ren, X. F. *Nanoscale* **11**, 22475–22481 (2019).

Plasmon-Enhanced Charge Transfer in Graphene/Au-Nanopillar-Arrays

Jungyoon Cho¹, Soyeong Kwon², Jungeun Song¹, Seoyoung Lim¹, Seawoo Moon¹, Jungtae Nam³,
Keun Soo Kim³, and Dong-Wook Kim^{1*}

(1) Department of Physics, Ewha Womans University, Seoul 03760, Korea

(2) Department of Mechanical and Aerospace Engineering, University of California Irvine, CA 92697, United States

(3) Department of Physics and Graphene Research Institute, Sejong University, Seoul 05006, Korea

**Email: dwkim@ewha.ac.kr*

Abstract: Graphene (Gr) is atomically thin material composed of pure carbon and has attracted great attention due to its outstanding electrical and optical properties. However, light-matter interaction is limited in Gr because it has extremely small volume. Thus, there have been numerous research efforts to fabricate and study Gr/metal nanostructures to boost optical absorption in Gr. Surface plasmon excitation in such hybrid systems can give rise to enhanced light-matter interactions in Gr. In this work, we investigated the electrical and optical characteristics of CVD-grown Gr monolayers transferred on Au-nanopillar (AuNP) arrays. The AuNP had a diameter of 300 nm, a height of 50 nm, and a period of 500 nm. The angle- and polarization-dependent reflectance spectra of Gr/AuNPs revealed the local minima in the visible and near-infrared range, which were originated from surface plasmon polaritons (SPPs) and localized surface plasmons (LSPs). The LSP-induced dips were observed near the wavelength of 570 nm, which were independent of the polarization and the incident angle of light. In contrast, the reflectance dips caused by the SPP excitation appeared only under illumination of the transverse magnetic mode light. Moreover, the SPP-induced dip positions strongly depended on the incident angle: the SPP-dip was found at 840 nm when the incident angle was 40°. The Gr monolayers on AuNPs exhibited up to a 20-fold increase in Raman intensity compared with those on flat Au thin films. The SPP- and LSP-induced charge transfer behaviors at the Gr/AuNP interfaces were studied using conducting atomic force microscope measurements. When the photocurrent of Gr/AuNP and Gr/flat-Au interfaces were compared, AuNP boosted the photocurrent by 40 and 2 times under SPP and LSP excitation wavelengths, respectively.

[1] X. Zhu, L. Shi, M. S. Schmidt, A. Boisen, O. Hansen, J. Zi, S. Xiao, and N. A. Mortensen, *Nano Lett.* **13**, 4690 (2013)

Vibrationally Hot Reactants in a Plasmon-Assisted Chemical Reaction

Hyun-Hang Shin¹ and Zee Hwan Kim^{1*}

¹Department of Chemistry, Seoul National University
E-mail address: zhkim@snu.ac.kr

Abstract: Recent studies on plasmon-assisted chemical reactions postulate that the hot electrons of plasmon-excited nanostructures may induce a non-thermal vibrational activation of metal-bound reactants [1,2]. However, the postulate has not been fully validated at the level of molecular quantum states. We directly and quantitatively prove that such activation occurs on plasmon-excited nanostructures: The anti-Stokes Raman spectra of reactants undergoing a plasmon-assisted reaction reveals that a particular vibrational mode of the reactant is selectively excited, such that the reactants possess >10 times more energy in the mode than is expected from the fully thermalized molecules at the given local temperature. Furthermore, a significant portion (~20 %) of the excited reactant is in vibrational overtone states with energies exceeding 0.5 eV. Such mode-selective multi-quantum excitation could be fully modeled by the resonant electron-molecule scattering theory [3,4]. The result validates the mechanism of plasmon-assisted chemical reactions and offers a new method to explore the vibrational reaction control on metal surfaces.

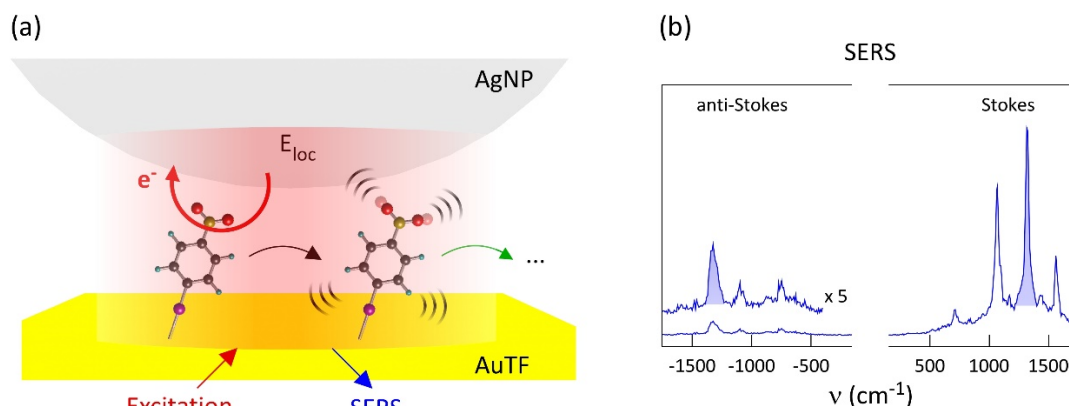


Fig. 1. (a) Scheme of hot-electron mediated vibrational excitation during plasmon-assisted reduction. Employing SERS, the reaction and vibrational energy are monitored simultaneously. (b) anti-Stokes / Stokes SERS spectrum of vibrationally excited reactant

- [1] P. Christopher, H. Xin and S. Linic, Nat. Chem. 3, 467-472 (2011).
- [2] P. Christopher, H. Xin, A. Marimuthu, S. Linic, Nat. Mater. 11, 1044-1050 (2012).
- [3] J. W. Gadzuk, Phys. Rev. B 44, 13466-13477 (1991)
- [4] J. W. Gadzuk, Phys. Rev. Lett. 76, 4234-4237 (1996)

Orientational change of gold nanorods with synthetic polymer brush by solvent exchange

Yu SEKIZAWA^{1*}, Hideyuki MITOMO², Yusuke YONAMINE², Takuya ISONO³, Kenji TAJIMA³, Hirofumi SATOH³, Kuniharu IJIRO²

⁽¹⁾ Grad. Sch. of Life. Sci., Hokkaido Univ., Hokkaido, Japan ⁽²⁾ RIES, Hokkaido Univ., Hokkaido, Japan ⁽³⁾ Grad. Sch. of Eng., Hokkaido Univ., Hokkaido, Japan)

E-mail address: sekizawa@poly.es.hokudai.ac.jp

Abstract: Rod-shaped gold nanoparticles (GNRs) have strong light absorbance depending on GNR orientation. Therefore, GNR orientation is important to control their characteristics. However, active orientation control of GNR is still challenging. In this research, we utilized synthetic polymer brush and its structural change to align and change GNRs' orientation. When mildly cationized GNRs are applied to poly(styrene sulfonate) (PSS) brushes, GNRs are adsorbed vertically in PSS polymer. When poor solvent for PSS or NaCl is applied to GNR-adsorbed PSS brush, GNR is drastically tilted. These phenomena occurred reversibly.

Gold nanoparticles have been applied in various fields because of their optical properties (Localized Surface Plasmon Resonance : LSPR). In particular, rod-shaped gold nanoparticles (gold nanorods: GNRs) have strong absorption of near infrared light due to their LSPR. Their absorption shows a significant dependence on the GNRs orientation toward incident light. However, dynamic orientation control of GNRs remains challenging despite of its importance. In our previous research, we have developed a method to adsorb cationic GNRs vertically on DNA-modified substrates[1]. Further, we demonstrated orientational change of GNRs on DNA-immobilized substrate by tuning DNA-GNR interaction strength[2]. However, adjustment of the interaction strength is difficult and the condition is quite limited, and DNA may not be suitable for further application due to their lack of variety as polymer. In this research, we utilized synthetic polymer brush, which have various types of properties, and its structural change to align and change GNRs' orientation for a broader potential for application. (Fig. 1).

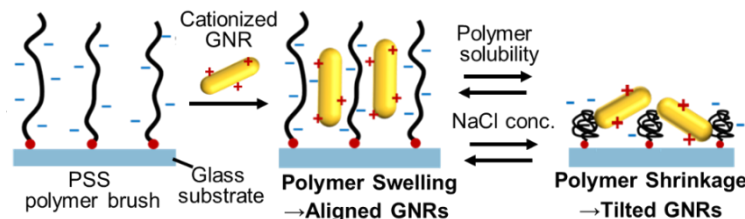


Fig 1. GNR alignment and orientation change on a polymer brush

PSS polymer brush was synthesized on glass substrate by atom-transfer radical polymerization. After the polymerization, cationized GNRs were adsorbed to the anionic polymer brush. The orientation of adsorbed GNR on the PSS brush was investigated by extinction spectra. The adsorbed GNRs showed low extinction peak in 800 nm compared to 500 nm peak, indicating vertical alignment of GNRs toward the substrate. As a next step, we demonstrated GNR orientational change by polymer structure change using NaCl and polymer solubility which is well-known factor to occur polymer shrinkage. When NaCl was added, the extinction peak around 800 nm increased depending on the NaCl concentration (Fig. 2, left). Furthermore, by adding organic solvent, the GNR orientation was gradually changed depending on PSS solubility (Fig. 2, right). These results indicate that the vertical GNRs on the polymer brush was tilted due to polymer shrinkage. These phenomena occurred reversibly.

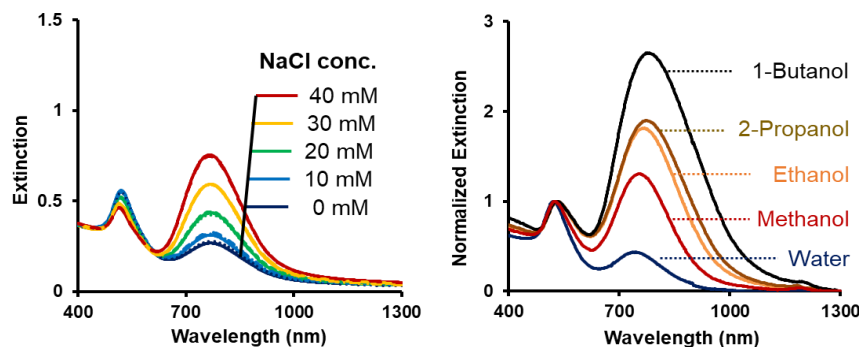


Fig 2. Spectral changes of GNRs on PSS polymer brush by NaCl concentration (left) and polymer solubility (right)

[1] Nakamura, S.; Mitomo, H.; Sekizawa, Y.; Higuchi, T.; Matsuo, Y.; Jinnai, H.; Ijiro, K., *Langmuir*, **36**, 3590–3599 (2020).

[2] Sekizawa, Y.; Mitomo, H.; Nihei, M.; Nakamura, S.; Yonamine, Y.; Kuzuya, A.; Wada, T.; Ijiro, K., *Nanoscale Adv.*, **2**, 3798–3803 (2020).

Discrete chiral gold nanorods with tunable chiroptical activities by pH and electric potential dual modulation

Han Lin¹, Hideyuki Mitomo², Yusuke Yonamine², Zhiyong Guo³, Kuniharu Ijro²

¹ Graduate School of Life Science, Hokkaido University, ² Research Institute for Electronic Science, Hokkaido University, ³ School of Material Science and Chemical Engineering, Ningbo University

E-mail address: han.lin.m2@elms.hokudai.ac.jp; mitomo@es.hokudai.ac.jp

Abstract: The emerging concept of tunable plasmonic chirality is mostly observed as a reconfigurable behavior or a feature of complex chiral plasmonic assemblies. For discrete colloidal particles, it is challenging to achieve reversible tunability or a transient response with regard to chiroptical activities. Herein, we demonstrate a core-gap-shell structure (gold nanorod-L/D cysteine-gold shell) coated with polyaniline (PANI) as a variable dielectric layer. By dual modulation from pH or electric potential to PANI structure, the dynamic adjustment of plasmonic and chiroptical activities was precisely obtained. This well-defined design provides an open platform for flexible and rational tailoring of plasmonic cores, chiral molecules, and variable dielectrics to chiroptical needs, which is important for realizing applications in chemical sensing, chiral nanocatalysis, enantioselective separations, and novel optical devices.

1. Introduction

Chirality as a term describing the geometric structure of an object could not be superimposed on its mirror image. Recent studies have demonstrated an interesting coupling between chiral molecules and metal nanoparticles, with new circular dichroism (CD) responses feeding back near the particle's localized surface plasmon resonance (LSPR). This is known as plasmon-induced chirality, or CD_{LSPR}. Most research on reconfigurable active chiral plasmons has so far concentrated on dimeric or three-dimensional assemblies. Tunable plasmonic chiroptical activities of discrete metal nanoparticles have rarely been reported.

Herein, we demonstrated an active plasmonic chiroptical system based on discrete chiral core-gap-shell structures@PANI (c-CGS Au NRs@PANI) with tunable CD_{LSPR} optical activities controlled by external pH and electric potential (Figure 1) [1].

2. Results and Discussion

The c-CGS Au NRs@PANI encapsulating L-cysteine molecules as shown in Figure 2A. The transverse LSPR-induced CD_{T-LSPR} was located at 601 nm, when the solution pH was 2. Adjusting the pH increase to 12, PANI had changed from the emeraldine base (ES) to the pernigraniline base (PB) state, and the CD_{T-LSPR} peak also completed a red-shift of about 60 nm due to the refractive index difference between the states (Figure 2B).

The electrical potential modulation was performed by applying voltages to the indium tin oxide surface loaded with c-CGS Au NRs@PANI monolayer films (Figure 2C). PANI was in the ES state under a higher voltage (0.4 V), and the CD_{T-LSPR} peak was located near 602 nm. As the voltage was reduced to -0.3 V, the ES state gradually transitioned to the leucoemeraldine base (LB) state and the CD_{T-LSPR} peak underwent the red shift to 616 nm, due to the increase in refractive index values (Figure 2D).

Satisfyingly, c-CGS Au NRs@PANI exhibited a wide wavelength range of CD_{T-LSPR} modulation (≈ 60 nm), stability (more than 100 cycles), accuracy (10 nm/V), and fast switching response (< 1 s), further enhancing their potential in fields such as chiral optical device fabrication.

4. Reference

[1] H. Lin, H. Mitomo, Y. Yonamine, Z. Guo and K. Ijro, Chem. Mater. **34**, 4062-4072 (2022).

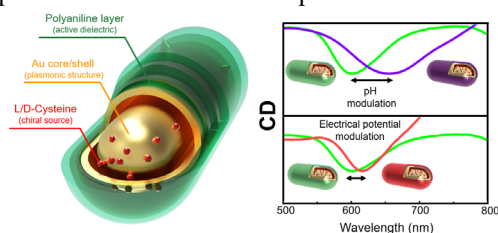


Figure 1. c-CGS Au NRs@PANI-based dual-modulable active plasmonic chiroptical system.

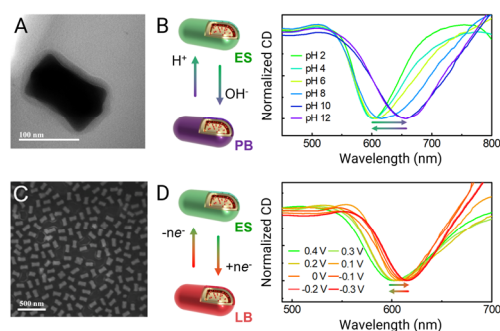


Figure 2. (A) TEM image of c-CGS Au NRs@PANI. (B) Schematic illustration of the dielectric environment switching by proton doping and de-doping, and CD spectra in response to different pH values. (C) SEM image of c-CGS Au NRs@PANI large-area monolayer films. (D) Schematic illustration of the dielectric environment switching by electrochemical redox, and CD spectra in response to different voltages.

Reflectance Spectroscopy of Optically Assembled Bio-nanoparticles with Plasmonic Nano-bowl Substrates

Masatoshi Kanoda^{1,2,3}, Kota Hayashi^{1,2,3}, Yumiko Takagi², Mamoru Tamura^{2,4},
Seiju Hasegawa⁵, Kohei Imura⁵, Shiho Tokonami^{2,3}, Takuya Iida^{1,2*}

1. Graduate School of Science, Osaka Metropolitan University, 1-2, Gakuencho, Nakaku, Sakai, Osaka, 599-8570, Japan

2. Research Institute for Light-induced Acceleration System (RILACS), Osaka Metropolitan University, 1-2, Gakuencho, Nakaku, Sakai, Osaka, 599-8570, Japan

3 Graduate School of Engineering, Osaka Metropolitan University, 1-2, Gakuencho, Nakaku, Sakai, Osaka, 599-8570, Japan

4 Graduate School of Engineering Science, Osaka University, 1-3 Machikaneyama, Toyonaka, Osaka, 560-8531, Japan

5 School of Advanced Science and Engineering, Waseda University, 3-4-1, Okubo, Shinjuku, Tokyo 169-8555, Japan

*Author e-mail address: t-iida@omu.ac.jp

Abstract: We investigated the mechanism of optical condensation detection of biological nanoparticles in plasmonic nano-bowl substrates (PNBS) with 500 nm periodic non-penetrating pores. Remarkably, we demonstrated that nanoparticles with spike proteins derived from SARS-CoV-2 on their surface were selectively optical condensation with a sensitivity two order higher than the number of viruses in the patient's saliva. This achievement is expected to revolutionize analytical techniques for various biological nanomaterials, including viruses.

Introduction:

There are many reports on the detection of biological samples with plasmonic substrates such as periodic nanohole arrays [1] because of their sensitivity to the refractive index of materials attached to their surfaces. Furthermore, it was theoretically proposed that an optical trapping using the light-induced force generated from localized surface plasmon (LSP) by having a metallic nanospoke structures in a nanohole array could improve the sensitivity of bioanalysis [2]. Rapid and highly sensitive detection of microparticles and bacteria were demonstrated by optical condensation of the target under the light-induced convection toward the trapping site (the stagnant area) between the bubble and the substrate [3]. However, when biological nanoparticles such as viruses, protein are targeted for detection, the efficiency of optical condensation of nanoscale objects must be improved. In this study, we develop a plasmonic substrate with nanoscale bowl-shaped periodic structures i.e., plasmonic nano-bowl substrate (PNBS) was developed for the detection of nanoparticles.

Method:

PNBS was produced by forming a layer of polymer on a glass substrate coated with a gold nanofilm, using self-assembled 500 nm particles as a template, removing the particles chemically, and then a gold film was coated on their top. After a sample dispersion liquid was dropped onto the PNBS, it was closed with a cover glass and target nanoparticles were assembled by optical condensation. At the first optical condensation, antibody-modified beads were assembled on the surface of PNBS. Next, the second optical condensation was used to selectively detect virus-mimetic nanoparticles (VMNPs) with the Spike protein of SARS-CoV-2 modified on the surface (two-step optical condensation method) [4]. After optical condensation, samples were detected by fluorescence imaging or reflectance spectroscopy. PNBS was also investigated by nonlinear optical microscopy.

Result and Discussion:

Fig. 1 shows developed PNBS with a periodic array of 500 nm nano-bowls, and the upper part of the substrate is coated with gold nanofilm. It was clarified that the reflection spectrum of PNBS exhibited a remarkable refractive index dependence. Moreover, the dependence of bubble generation efficiency on the laser power was investigated, and it was confirmed that a submillimeter bubble can be generated even under a laser power of only 2 mW. Our developed two-step optical condensation method enabled selective detection with a sensitivity two orders of magnitude higher than the concentration in saliva of patients with COVID-19 (10^{11} copies/mL) [5]. In addition, we reveal that several hundred nanoparticles can be detected with the peak shift of the reflection spectrum of PNBS before and after optical condensation. This achievement is expected to innovate the analytical technologies of various biological nanomaterials, such as viruses linked with next pandemic and harmful nanoparticles in the environment.

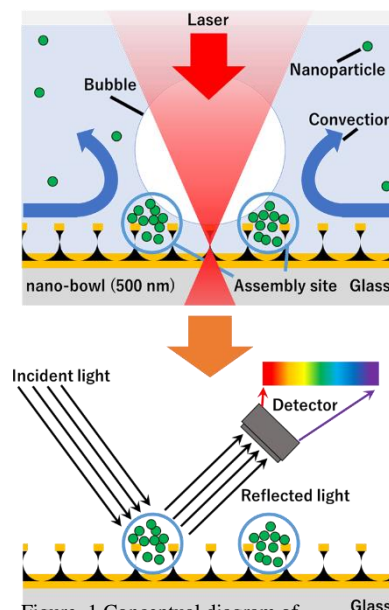


Figure. 1 Conceptual diagram of spectroscopic analysis of nanoparticles after optical condensation

References

- [1] A. Yanik, et al., *Nano Lett.*, **10**, 4962–4969 (2010). [2] T. Yoshikawa, M. Tamura, S. Tokonami, T. Iida, *J. Phys. Chem. Lett.*, **8**, 370 (2017). [3] K. Yamada, S. Tokonami, T. Iida, et al., *Jpn. J. Appl. Phys.*, **58**, SDDK08 (2019). [4] M. Kanoda, K. Hayashi, Y. Takagi, M. Tamura, Y. Takagi, S. Tokonami, T. Iida, submitted (2023). [5] N. H. L. Leung, et al., *Nat. Med.*, **26**, 676–680 (2020).

Large-scale Optical Condensation on the Solid-liquid Interface with an Optical Fiber Module

Kota Hayashi^{1,2,3}, Mamoru Tamura^{2,4}, Masazumi Fujiwara^{2,5}, Shiho Tokonami^{2,3}, Takuya Iida^{1,2*}

¹Department of Physical Science, Graduate School of Science, Osaka Metropolitan University

²Research institute for Light-induced Acceleration system, Osaka Metropolitan University

³Department of Applied Chemistry, Graduate School of Engineering, Osaka Metropolitan University

⁴Department of Material Engineering Science, Graduate School of Engineering Science, Osaka University

⁵Department of Chemistry, Graduate School of Natural Science and Technology, Okayama University

E-mail address: t-iida@omu.ac.jp

Abstract: We have developed a three-dimensional arbitrary optical condensation method with optical fiber module. Remarkably, it has been clarified that the dispersoids can be assembled linearly large scale on the substrate possibly mediated by the near-field light from the substrate irradiated by the laser from the optical fiber module.

1. Background and motivation

Since the invention of optical tweezers [1], optical manipulation of nano-micro objects has attracted attention in various fields. The driving force of the optical tweezers is the light-induced force, which is the electromagnetic interaction between light and matter. The light-induced force breaks down into the scattering force and gradient force. The former pushes the target objects toward the advancement of light due to light momentum transfer. The latter attracts the target objects to the laser spot. If the gradient force is dominant, the target objects can be trapped and manipulated on the laser spot. On the other hand, the objects can be assembled by the scattering force in the use of an interface [2]. Optical condensation was recently suggested to rapidly and high-densely assemble dispersoids by using light-induced force and light-induced convection based on the photothermal effect with laser irradiation on metallic nanostructures [3]. We developed optical fiber modules with metallic nano structures on their tip and suggested three-dimensional optical condensation with optical fiber modules [4]. In this contribution, we investigated optical condensation with the optical fiber module located on the substrate as shown in figure 1.

2. Method

The optical fiber module was prepared by coating metallic nanofilm on commercially available optical fiber by ion sputtering apparatus. The infrared continuous wave laser was introduced into the optical fiber module before optical condensation. The sample dispersion liquid was dropped onto the glass substrate. After that, the optical fiber module was inserted in the sample dispersion liquid and located on the substrate. Another glass substrate that has the space was sealed on the samples. Finally, the infrared continuous wave laser was introduced into the optical fiber module in the sample dispersion liquid.

3. Results and Discussion

When the laser was introduced into the optical fiber module, the dispersoids were transported by the light-induced force and light-induced convection and assembled in front of the optical fiber module. After a few minutes, a large number of dispersoids were assembled along the advancement of light, and its length was over several mm. The driving forces of this assembly phenomena may be the light-induced force of evanescent wave exited on the substrate and light-induced force and convection. This result leads to a near-field mediated assembly method of dispersoids for microfabrication and biological analysis.

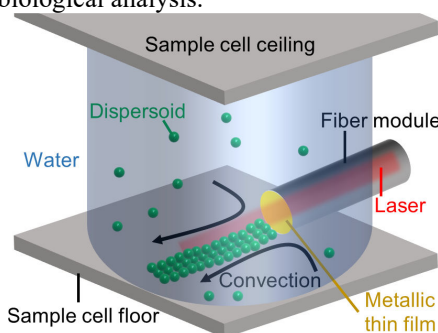


Figure 1. Schematic diagram of optical condensation with the optical fiber module.

[1] A. Ashkin, J. M. Dziedzic, and T. Yamane, *Nature* **330**, 769-771 (1987).

[2] T. Iida, S. Hamatani, Y. Takagi, K. Fujiwara, M. Tamura, and S. Tokonami, *Commun. Biol.* **5**, 1053 (2022).

[3] K. Hayashi, Y. Yamamoto, M. Tamura, S. Tokonami, and T. Iida, *Commun. Biol.* **4**, 385 (2021).

[4] K. Hayashi, M. Tamura, M. Fujiwara, S. Tokonami, and T. Iida, *Technical Digest of CLEO-PR 2023*, CTuA16D-04 (2023).

A barrier thickness effects study of photoluminescence and photoreflectance of InAs/GaSb Type-II MQW structures

Jae du Ha¹, Taein Kang¹, Jong Su Kim^{1*}, Sang Jun LEE²

¹Department of Physics, Yeungnam University, Gyeongsan 38541, South Korea

²Korea Research Institute of Standards and Science, Daejeon 34113, South Korea

-mail address: jongsukim@ynu.ac.kr

Abstract: We conducted a study using photoreflectance (PR) spectroscopy to investigate the impact of well thickness on the InAs/GaSb multi-quantum wells (MQWs). Type-II multi-quantum well structures composed of InAs and GaSb on GaSb substrates were grown by Molecular Beam Epitaxy (MBE). At a temperature of 20 K, when the thickness of the InAs layer is increased from 1 ML to 3 ML, the position of the photoluminescence (PL) peak is observed to shift to lower energies, 0.67 eV, 0.55 eV, and 0.37 eV, respectively. These observations suggest that as the thickness of the InAs layer increases, the quantum confinement effect weakens. The PR results at room temperature show GaSb E0 and E1 relate transition, respectively. We observed unknown transition between E0 and E1 transitions.

Electric Dipole Characteristics of Intermolecular Charge Transfer Excitons and Intramolecular Excitons in π -Conjugated Organic Materials

Sang-hun Lee¹⁾, Taek Joon Kim¹⁾, Jeongyong Kim²⁾, Jinsoo Joo^{1),*}

¹⁾ Department of Physics, Korea University

²⁾ Department of Energy Science, Sungkyunkwan University

E-mail address: dltkdgns5111@gmail.com, jjoo@korea.ac.kr

Exciton (electron-hole pair) is a fundamental quantum quasi-particle, which plays an important role for the performance of various optoelectronic devices. For π -conjugated organic materials, intramolecular exciton (Frenkel exciton, X_F) and intermolecular exciton (charge transfer exciton, IX) are electrically and/or optically generated and contributed to the realization of organic light-emitting diode (OLED) and organic solar cell (OSC). Although the OLED and OSC were successfully developed, the intrinsic characteristics of exciton dipole moments in organic have not been studied systematically.

In this study, m-MTDATA and T2T were used for electron donor (D) and acceptor (A), respectively, due to their planar molecule structure and high observability of IX by thermally activated delayed fluorescence (TADF). By mapping photoluminescence (PL) on back focal plane (BFP), we observed the perpendicular characteristics between exciton dipole moments of X_F and IX in heterojunction composed of m-MTDATA/T2T (D/A) molecules (Fig. 1). The characteristics of X_F and IX were analyzed through temperature-, incident excitation power (P_{in})-dependent PL, and time-resolved PL (tr-PL) spectra. The repulsive interaction between IXs induced the blue shift of PL spectra as temperature decreased or P_{in} increased, supporting the alignment of dipoles of IXs. Tr-PL decay curves showed considerably longer lifetime of IXs than that of X_F . In addition, electroluminescence spectra of IXs and X_F were investigated depending on the applied bias. From our results, we suggest the modulation of dipolar characteristics of exciton species in organic heterostructure as a promising candidate to advanced organic optoelectronics.

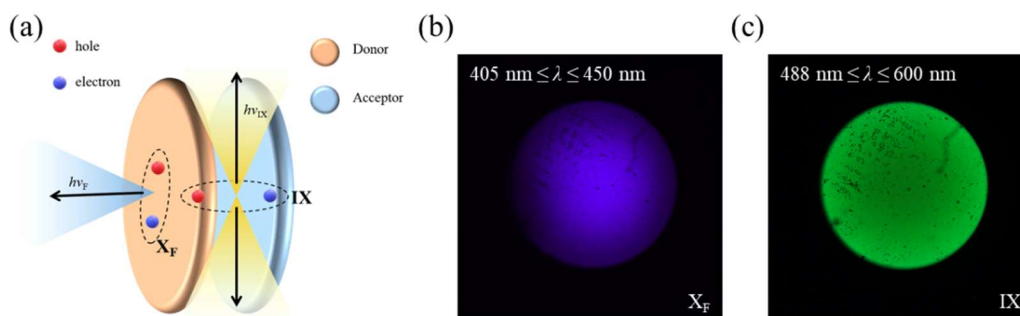


Fig. 1 (a) Schematic illustration of intramolecular Frenkel exciton (X_F) and intermolecular charge transfer exciton (IX) and corresponding direction of photon emission. (b) and (c) BFP PL images of T2T/m-MTDATA bi-layer captured by CCD camera filtered by optical long-pass filter for X_F ($405 \text{ nm} \leq \lambda \leq 450 \text{ nm}$) and IX ($488 \text{ nm} \leq \lambda \leq 600 \text{ nm}$), respectively.

A Variable-Focus Metalens with Continuous Adjustment Capability

Po-Sheng Huang^{1*}, Shih-Hsiu Huang¹, Cheng Hung Chu², Takuo Tanaka³, Pin Chieh Wu¹

¹Department of Photonics, National Cheng Kung University, Tainan 701, Taiwan

²YongLin Institute of Health, National Taiwan University, Taipei 10672, Taiwan

³RIKEN (The Institute of Physical and Chemical Research), Metamaterials Laboratory 2-1 Hirosawa, Wako, Saitama 351-0198, Japan

E-mail address: louis19950128@gmail.com

Abstract: Most metalenses have a fixed focal length after fabrication, but reconfigurable metalenses would be helpful for various applications, including scanning microscopy and 3D imaging. To address this issue, we innovated a metasurface optics design that allows dynamically-tunable metalenses with continuous focal length tunability within the visible range.

Introduction

The development of modern optical systems has become a hot topic for researchers, especially in the context of miniaturizing electronics and devices. Optical components, such as lenses, must keep pace with these changes. Metasurfaces comprising carefully engineered sub-wavelength meta-atoms allow for manipulating light properties at the nano-scale. With precise phase control of these meta-atoms, a lens-like phase distribution can be created. Metalenses created using this technology exhibit performance beyond the diffraction limit [1-3]. However, traditional metalenses lack tunability, as their optical properties are fixed at the time of fabrication. This lack of tunability limits their real-world applications [4]. This work reports an active all-dielectric varifocal metalens with GaN-based anisotropic meta-atoms (see Fig. 1a). By incorporating the overlapping of two intensity distributions from x - and y -polarizations, the superposition of the intensity paves a way to shift the focal spot in free space continuously. While the focal lengths of two linear states for the metalens are different, and the difference is below the tolerance of individual depth of focus, it can be continuously adjusted by rotating the polarization angle of the incident light. Figure 1b shows the images of the sample. A tunable varifocal metalens with a numerical aperture of 0.1 is numerically optimized and experimentally demonstrated to validate the concept, as shown in Figs. 1c and 1d. The proposed platform offers a promising opportunity for low-profile optical devices like 3D imaging systems.

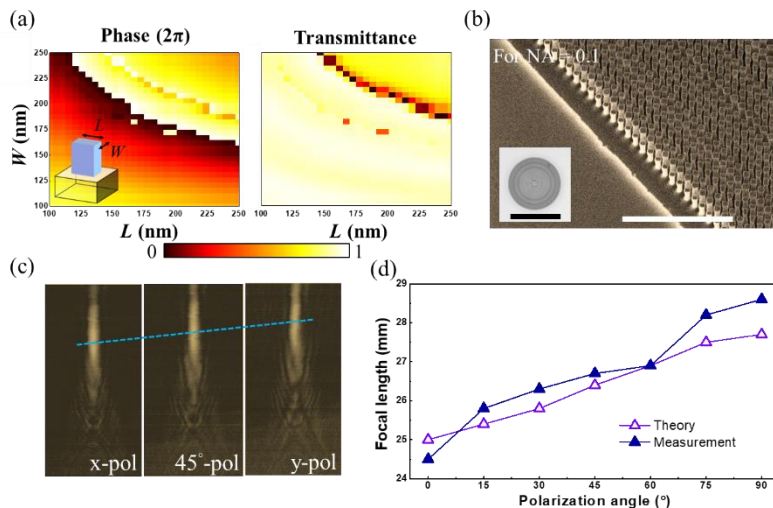


Fig. 1 (a) Database of the meta-unit phase and transmittance library for the variable-focus metalens, obtained through x -polarization incidence simulations. Inset: Schematic illustration for the GaN-based anisotropic meta-atom with L and W parameters (along x and y directions, respectively). (b) Tilted SEM image of the proposed metalens. The scale bar represents 3 μm . Inset: Optical microscope image of the metalens, with a scale bar of 500 μm . (c) Experimental cross-sectional results for three different polarization angles: x -polarization, 45° -polarization, and y -polarization. The cyan dash line shows the shifting of the focal length. (d) The comparison of measured and theoretical focal lengths as a function of polarization angle for NA = 0.1.

References

- [1] M. Shalaginov, S. An, Y. Zhang, F. Yang, P. Su, V. Liberman, J. Chou, C. Roberts, M. Kang, C. Rios, Q. Du, C. Fowler, A. Agarwal, K. Richardson, C. Rivero-Baleine, H. Zhang, J. Hu, T. Gu, *Nat. Commun.* 2021, **12**, 1225.
- [2] M. Khorasaninejad, W. Chen, R. Devlin, J. Oh, A. Zhu, F. Capasso, *Science* 2016, **352**, 6290.
- [3] H. Yang, G. Li, X. Su, G. Cao, Z. Zhao, X. Chen, *Sci. Rep.* 2017, **7**, 12632.
- [4] L. Kang, R. P. Jenkins, D. H. Werner, *Adv. Opt. Mater.* 2019, **7**, 1801813.

Non-Destructive Analysis of Thickness of Thin Films using home-built Spectroscopic Ellipsometry

Heewoo Lee¹, Jaejoon Kim¹ and Soobong Choi^{1*}

¹Department of Physics, Incheon National University, Incheon 22012, Republic of Korea
E-mail address: sbchoi@inu.ac.kr

Ellipsometry is a measurement tool that analyzes the change in the polarization state generated in the sample and can be used to determine the optical constants or thickness of film layers. This technique is widely used in various fields due to its high sensitivity and accuracy, as well as its non-contact and non-destructive properties [1].

Ellipsometry is an indirect measurement method that uses a model to calculate a theoretical value, which is then adjusted until it matches the measured value. Ellipsometry results are obtained by comparing measured and theoretical values, and wavelength-dependent measurements can provide a large number of data points, allowing for more comparisons and ultimately improving the reliability and accuracy of the results. Due to this advantage, Spectroscopic Ellipsometry (SE) has attracted significant attention, and various approaches have been developed. SE, due to the large amount of data it can generate, is particularly useful for analyzing multilayer films. Moreover, since it measures the optical spectrum, it can also be used for studying optoelectronic properties of materials such as band structures.

The Si sample and Si/SiO₂ sample were measured with a home-built rotating analyzer type spectroscopic ellipsometer, and the thickness of the native oxide layer and SiO₂ layer was obtained using the Tauc-Lorentz model.

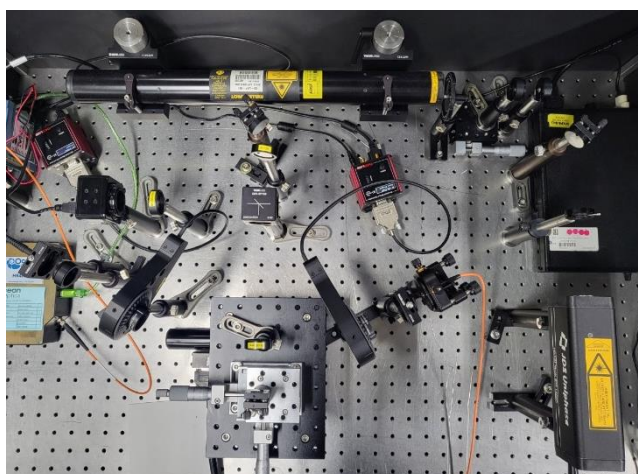


Fig. 1. Home-built spectroscopic ellipsometer setup.

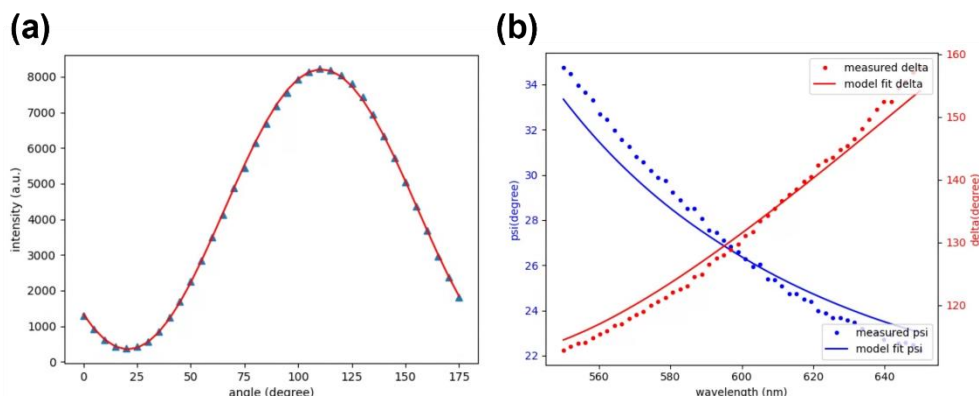


Fig. 2. (a) Graph of intensity versus analyzer angle. (b) Ellipsometric angle psi and delta spectrum.

[1] D.E. Aspnes, "Spectroscopic ellipsometry-past, present, and future.", *Thin Solid Films* **571** (2014), 334-344

Plasmon-assisted Spectroscopy of 1-, 2-, 3- Layer MoS₂

Kiin Nam¹, Jaeseung Im¹, Gan Hee Han¹, Jin Young Park¹, Hyuntae Kim², Sungjae Yoo³,
MohammadNavid Haddadnezhad³, Sungho Park³, Woongkyu Park⁴, Soobong Choi^{1*}

1. Department of Physics, Incheon National University, Incheon, 22012, Republic of Korea

2. Advanced Development Team 2, Park Systems Co.

3. Department of Chemistry, Sungkyunkwan University, Suwon, 16419, Republic of Korea

4. Medical and Bio Photonics Research Center, Korea Photonics Technology Institute (KOPTI), Gwangju, 61007, Republic of Korea

E-mail addresses: kinam@inu.ac.kr, sds1934@inu.ac.kr, ganghee@inu.ac.kr, jyp1234@inu.ac.kr, ht.kim@parksystems.com, sungjae826@skku.edu, m.n.haddad@skku.edu, spark72@skku.edu, wkpark@kopti.re.kr, sbchoi@inu.ac.kr*

Abstract: Enhancing optical response of low-dimension materials has attracted researcher's interest due to their poor response rate. In this regard, plasmon-assisted spectroscopy could be an appropriate tool for studying conventionally undetectable signals with resonant excitation. We investigated plasmon-assisted optical responses of a resonantly excited molybdenum disulfide (MoS₂) comprising of single-, bi- and tri- layers with gold nano-rings. The localized electromagnetic field near gold nano-ring which is fabricated by considering the energy of material photoluminescence enhances resonance Raman scattering (RRS) response.

The gold nano-rings cause slight changes in the peak position of E_{12g} and A_{1g} in monolayer MoS₂, with E_{12g} increasing and A_{1g} decreasing. However, in trilayer MoS₂, E_{12g} and A_{1g} peak positions are reversed. The changes of these main peak are affected by strain or doping effects [1]. The variation of E_{12g} peak could be explained by the strain effect dominate as layer number increasing. Meanwhile, the variation of A_{1g} peak is caused by screening of charge doping effect as layer number increasing. The decreasing feature of the differences of contact potential difference between MoS₂ and MoS₂ with gold nano-ring distinctively supports the results [2].

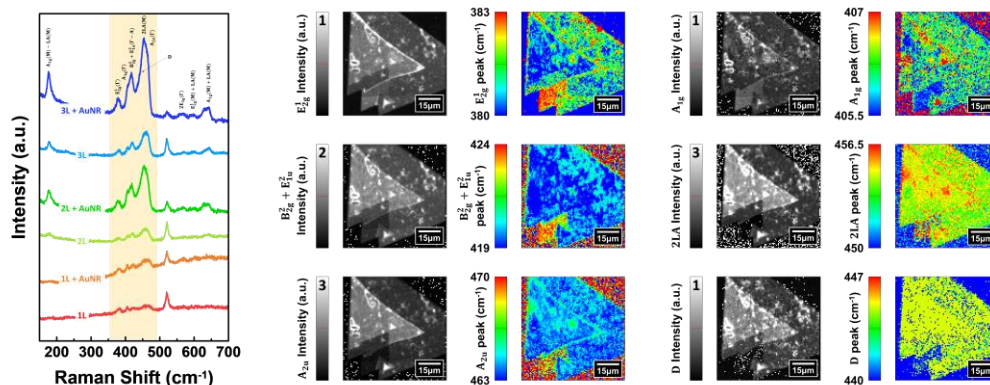


Figure 1. Resonance Raman spectra and plasmon-assisted Raman spectra of 1-, 2-, and 3- Layer MoS₂. The mapping data show intensity and peak position of plasmon-assisted Raman scattering.

[1] Jae-Ung Lee and Hyeonsik Cheong, J Raman Spectrosc. **49**(1), 66-75 (2018).

[2] Matěj Velický, Alvaro Rodriguez, Milan Bouša, Andrey V. Krayev, Martin Vondráček, Jan Honolka, Mahdi Ahmadi, Gavin E. Donnelly, Fumin Huang, Héctor D. Abruña, Kostya S. Novoselov, and Otakar Frank, J. Phys. Chem. Lett. **11**(15), 6112-6118 (2020).

Modulating Exciton States and Band Gap of ReS₂ by Oxygen Treatment

Krishna P. Dhakal^δ, Eunji Lee^δ, Tran Viet Anh,^{δ,⊥} Dinh Loc Duong,^{δ,⊥} Jeongyong Kim^{δ*}

Rhenium disulfide (ReS₂) is a 1T' phase direct gap layered semiconductor with intriguing in-plane anisotropic optical and electrical properties that has been extensively researched for polarization-sensitive optoelectronic applications of 2D layer crystals in the visible range. There are still many unanswered questions regarding the origin of the excitonic phenomena in the ReS₂ lattice, particularly regarding the defect states and their polarization characteristics. We investigated the exciton states of ReS₂ with the thicknesses from 1L to few layers and firstly identified the emergence of PL peak at ~1.4 eV (X₀) by the oxygen plasma treatment. The X₀ peak showed an isotropic polarization of PL emission, distinguished from the linearly polarized emission of other major PL peaks of ReS₂. DFT calculation predicted the narrowing of the bandgap by the bonding of Re and oxygen (O) atoms in the ReS₂ unit cell at the sulfur vacancy site where the reduction of bandgap was consistent with the observed peak position of X₀. Thus, we investigated the underlying excitonic phenomena of optically active impurity state (Re-O) in the 2D crystal of 1T'-ReS₂ lattice, which has exciton with isotropic light polarization, thereby expanding the utility of the anisotropic ReS₂ lattice in the suitable optoelectronic applications.

Keywords: ReS₂, defect, exciton, polarization,

1. Dhakal *et al.*; **Light: Science & Applications**, 7, 98 (2018).
2. Ghimire and Dhakal *et al.*; **ACS nano**, 15, 13770-13780 (2021).

Nonlinear polariton parametric oscillations in coupled microcavities

Hyeon-Seo Choi, Hyeonjong Jeong, and Chang-Hee Cho*

Department of Physics and Chemistry, Daegu Gyeongbuk Institute of Science and Technology (DGIST)

Daegu 42988, South Korea

E-mail address: chcho@dgist.ac.kr

Abstract: Exciton-polaritons composing light and matter have been intensively exploited in optical parametric oscillations since the nonlinearity in polariton possesses orders of magnitude stronger than pure photons and traditional nonlinear optical systems. Furthermore, S-shaped polariton dispersion can offer phase-matching parametric oscillation to be naturally achieved. However, the intra-branch parametric oscillation has several drawbacks to utilizing practical application because a resonant excitation is required at the inflection point of polariton dispersion and emitted idler wave at a large angle is precluding efficient collection due to weak coupling with light. In this work, we demonstrate the polariton parametric oscillations in coupled microcavities that provide two-level splitting of a lower polariton branch. The resonantly coupled microcavities increase the interaction between the inter-branches. By utilizing the increased interaction of polaritons, we observe the inter-branch scattering of polaritons under non-resonant excitation. Our results can offer a practical way toward the ability to realize nonlinear polaritonic devices.

Circular dichroism of valley-polarized excitons coupled with propagating waveguide modes

Jin-Woo Jung, Jiyeon Kim, Young-Jun Lee, and Chang-Hee Cho*

Department of Physics and Chemistry

Daegu Gyeongbuk Institute of Science and Technology (DGIST)

Daegu 42988, South Korea

E-mail address: chcho@dgist.ac.kr

The emergence of the inequivalent valley states in transition metal dichalcogenide monolayers has triggered intense attention toward the valleytronics since the inequivalent valleys can be generated and manipulated selectively using circularly polarized light. However, the valley depolarization leads to the strong degradation and fluctuation of the circular dichroism for the valley-polarized excitons, hindering application for development in practical valleytronic devices. In this work, we demonstrate that the circular polarization of the valley excitons is significantly increased at the end of the h-BN/WS₂/h-BN waveguide structures. By directly imaging far-field emission emitted from the waveguide structures, we show the circularly polarized exciton emission becomes spatially separated via the transport of the valley-polarized excitons coupled with the waveguide modes, thus enabling the enhancement of the circular dichroism at the end of the waveguide structures. The valley-dependent spatial separation reveals the chirality for the transport direction of the coupled emission propagating along the waveguide structures. This finding can open up a route to realizing practical valley-photon circuit devices.

Optical properties of anisotropic GeSe₂ nano flakes

Eunji Lee¹, Krishna Dhakal Prasad¹, Hwayoung Song², Heenang Choi³, Taek-Mo Chung³, Dinh Loc Duong^{1,4}, Saeyong Oh⁵, Hu Young Jeong⁵, Kibum Kang^{2,*}, Jeongyong Kim^{1,*}

¹ Department of Energy Science, Sungkyunkwan University, Suwon 16419, Republic of Korea

² Department of Materials Science and Engineering, Korea Advanced Institute of Science and Technology (KAIST)

³ Thin Film Materials Research Center, Korea Research Institute of Chemical Technology

⁴ Center for Integrated Nanostructure Physics, Institute for Basic Science

⁵ Graduate School of Semiconductor Materials and Devices Engineering, Ulsan National Institute of Science and Technology (UNIST)
E-mail address: eunjilee@g.skku.edu

Germanium diselenide (GeSe₂) is an emerging two-dimensional (2D) material demonstrating air stability, wide bandgap, and anisotropic absorption properties [1,2]. We investigated the photoluminescence (PL) of single-crystalline GeSe₂ grown by metal-organic chemical vapor deposition (MOCVD), focusing on its dependence on temperature and polarization. We found that two absorption bands around at 2.5 eV (A peak) and 1.5 eV (B peak) are present, separated by ~ 1 eV and both peaks were also observed in the PL spectra. The presence of both A and B bands in the PL spectrum shows that the origin of these peaks differs from prior 2D TMDs, where PL was found exclusively from the lower energy peak. [3] The temperature-dependent PL study (3 to 300 K) revealed a gradual decrease in A peak energy with increasing temperature, which is consistent with most semiconductor band edge emission due to phonon-induced gap renormalization [4], while the B peak energy gradually increased. We also studied the polarization dependent PL study and confirmed that the emission of the A peak was polarized along the crystal a-axis of the GeSe₂ while B peak is nearly unpolarized, indicating the defect induced mid-gap emission of B peak. Furthermore, excitation energy dependent PL study also suggest the fact of band edge emission of A peak which again support the defect induced origin of the B peak. Therefore, our comprehensive study of polarization, temperature and excitation energy dependent PL study provide important information on the origins of PL bands in the anisotropic GeSe₂, beneficial for many optoelectronic applications.

References

- [1] Yan, Y., Xiong, W. Q., Li, S. S., Zhao, K., Wang, X. T., Su, J., Song, X. H., Li, X. P., Zhang, S., Yang, H., Liu, X. F., Jiang, L., Zhai, T. Y., Xia, C. X., Li, J. B. and Wei, Z. M., *Adv. Opt. Mater.* **7**, 1900622 (2019).
- [2] Zhou, X., Hu, X. Z., Zhou, S. S., Zhang, Q., Li, H. Q. and Zhai, T. Y., *Adv. Funct. Mater.*, **27**, 1703858 (2017).
- [3] Dhakal, K. P., Duong, D. L., Lee J., Nam H., Kim M., Kan M., Lee Y. H. and Kim, J., *Nanoscale*, **6**, 13028-13035 (2014).
- [4] Zhao, W., Ribeiro, R. M., Toh, M., Carvalho, A., Kloc, C., Castro Neto, A. H. and Eda, G., *Nano Letters*, **13**, 5627-5634 (2013).

Spectroscopic visualization of photonic band structure of two-dimensional dielectric photonic crystals by using Fourier-plane scanning measurement

Changwon Seo¹, Eunji Lee², Jae Eon Shim¹, Siyul Lee¹, Sang Soon Oh³, Gi-Ra Yi⁴, Jeongyong Kim², and Teun-Teun Kim¹

¹Department of Physics and Energy Harvest-Storage Research Center (EHSRC), University of Ulsan, Ulsan, Republic of Korea.

²Department of Energy Science, Sungkyunkwan University, Suwon, 16419, Republic of Korea

³School of Physics and Astronomy, Cardiff University, Cardiff CF24 3AA, United Kingdom.

⁴Department of Chemical Engineering, Pohang University of Science and Technology (POSTECH), Pohang, Gyeongbuk 37673, Republic of Korea

E-mail address: cwseo323@ulsan.ac.kr

Abstract: Two-dimensional photonic crystals consisted with a lattice structure exhibit a photonic band structure due to the destructive interference of multiple reflections of light in the lattice media. Fourier-plane measurement is one of a method to obtain the photonic band structure of the photonic crystal. Here, we introduce a Fourier-plane measurement method with absorption peak dispersion images obtained from 2D photonic crystal arrayed by hexagonal lattice.

Introduction

Two-dimensional (2D) photonic crystals with honeycomb or hexagonal lattice have photonic band structure, thus, interesting wave-guiding characteristics can be achieved.[1,2] Recently, the honeycomb lattice has attracted attention for low-loss unidirectional waveguide platforms, because topological edge mode in the opened Dirac points can be easily obtained by geometrical perturbations.[3,4]

Fourier-plane analysis is a technique to measure the momentum space properties of light transmitted through a photonic crystal. By using a convex lens for optical Fourier transform, the diffraction patterns of the transmitted light are revealed at the Fourier plane. By staking the spectrum, light dispersions along a specific direction can be obtained. In this present, we introduce lab made Fourier-plane analysis method for measuring a photonic band structure of 2D photonic crystal. We fabricated 2D hexagonal lattice by using template imprinting method, and directly scanned optical Fourier plane by using pinhole scanning system. A part of photonic band structure can be clearly observed as shown in Figure 1. We expect that our Fourier-plane analysis method can help to understand optical properties of 2D photonic crystals.

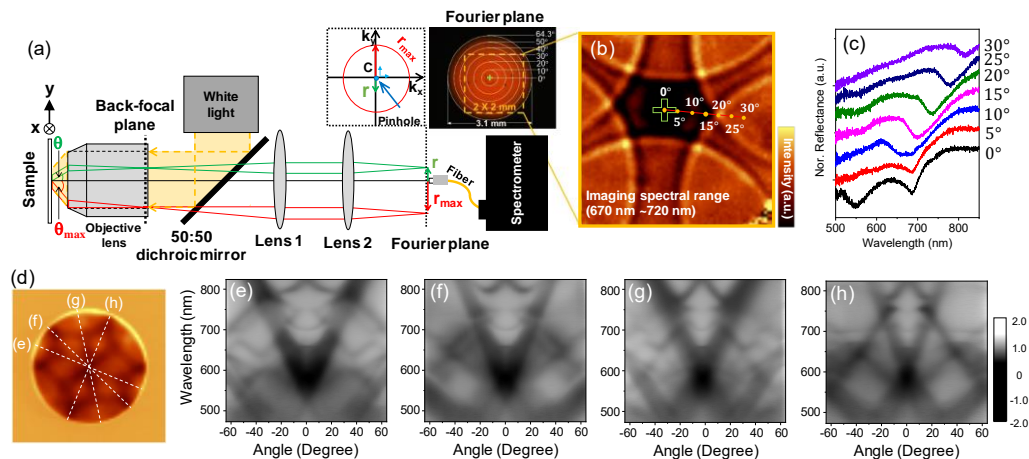


Figure 1. (a) Schematic of lab-made Fourier-plane measurement setup. (b) The reflectance mapping image obtained by scanning the yellow dashed box. The reflectance map is imaged by accumulating a wavelength range of 670 nm ~ 720 nm. (c) Angle-resolved white-light reflectance spectra at the yellow points along the red solid line in Fig. 1b. (d) Fourier-plane mapping image of a hexagonal lattice photonic crystal. (e)-(h) The absorption peak dispersion images along the white dashed line in Fig. 1d.

References

- [1] Mohammad Hafezi, et al., Nature Phys, 7, 907–912 (2011)
- [2] Ling Lu, et al., Nature Photon, 8, 821–829 (2014)
- [3] Yongkang Gong, et al., ACS Photonics, 7(8), 2089–2097 (2020)
- [4] Peter Lodahl, et al., Nature, 541, 473–480 (2017)

Transmittance of Layered Perovskite in Terahertz range

Junho Ryeom¹, Dae Young Park¹, Geunchang Choi², Mun Seok Jeong¹

¹*Department of Physics, Hanyang University, Seoul, Korea*

²*School of Electrical and Electronics Engineering, Chung-Ang University, Seoul, Korea*

E-mail address: mjeong@hanyang.ac.kr

The organic-inorganic halide perovskites have been receiving attention due to their intrinsic optical property of optoelectronic conversion to use solar cells, quantum dots, and light-emitting diodes [1-4]. However, the perovskites have stability issues in ambient conditions due to the heat, moisture, and light. To overcome the problem, 2D organic-inorganic halide perovskite has been suggested, which shows excellent stability because the hydrophobic properties of spacer prevent degradation. Furthermore, the band gap of 2D perovskite can be controlled by the composition of various components and species of spacer (large cation) [5,6].

In this work, we characterized 2D Ruddlesden-Popper(RP) phase perovskite by utilizing the terahertz time-domain spectroscopy (THz-TDS). The 2D RP-phase perovskite was synthesized with the chemical composition of $\text{BA}_2\text{MA}_{n-1}\text{Pb}_n\text{I}_{3n+1}$ ($n=1\sim3$) by controlling the composition of spacer. For THz transmission measurement, the 2D perovskite crystal was mechanically exfoliated with the tens of micrometer thickness, which shows several resonance absorption modes in the 0.5 ~ 2.5 THz range. Furthermore, we extracted terahertz conductivity of the 2D RP phase perovskite samples from the transmission data. Our result will give further understanding the basic physical properties of the 2D perovskite in various THz applications.

[1] Green, M., Ho-Baillie, A. & Snaith, H. The emergence of perovskite solar cells. *Nature Photon* 8, 506–514 (2014).

[2] Rong, Y., et al. Challenges for commercializing perovskite solar cells. *Science* 361(6408), (2018).

[3] Wang, H. C., Bao, Z., Tsai, H. Y., Tang, A. C., Liu, R. S., *Small* 2018, 14, 1702433.

[4] Lin, K., Xing, J., Quan, L.N. et al. Perovskite light-emitting diodes with external quantum efficiency exceeding 20 per cent. *Nature* 562, 245–248 (2018).

[5] C. C. Stoumpos, D. H. Cao, D. J. Clark, J. Young, J. M. Rondinelli, J. I. Jang, et al. *Chemistry of Materials* 28, 8, 2852-2867 (2016)

[6] Milot, R. L., et al. (2016). "Charge-Carrier Dynamics in 2D Hybrid Metal–Halide Perovskites." *Nano Letters* 16(11): 7001-7007.

Measurement of Optical Dispersion Relations for Transition Metal Dichalcogenides Nanostructures

Dong-Jin Shin, HyunHee Cho, Su-Hyun Gong

Korea University, Department of Physics
E-mail address: shgong@korea.ac.kr

Abstract: Polaritons are quasiparticles with a hybrid nature of matter and light. Exciton-Polaritons (EPs) in transition metal dichalcogenides (TMDCs) have been extensively explored due to their large exciton binding energies. Excitonic resonance in TMDCs is strong enough to realize inherent guided EPs in TMDCs membranes. Here, we report a direct measurement of optical dispersion relations for guided EPs in tungsten disulfide (WS_2) membrane via near-field coupling method and angle-resolved spectroscopy. We believe that our results pave a new way for nanophotonic applications.

Exciton-Polaritons (EPs) in transition metal dichalcogenides (TMDCs) have been extensively explored due to their strong excitonic behavior. EPs have been successfully demonstrated by integrating TMDCs monolayer with various microcavities. Meanwhile, excitonic resonance in TMDCs is strong enough to realize inherent guided EPs in TMDCs membranes. However, unlike cavity EPs, guided EPs have been far less studied because of their non-radiative nature which makes it hard to be detected using far-field microscope techniques. For this reason, recent studies on guided EPs have been accomplished only by near-field scanning optical microscope (NSOM). Here, we report a direct measurement of optical dispersion relations for guided EPs in tungsten disulfide (WS_2) multilayers via the near-field coupling method and angle-resolved spectroscopy. Using an oil-immersion microscope objective lens for the near-field coupling, we observed the anti-crossing behavior of the dispersion relation near the exciton resonance in freestanding WS_2 , which is a signature of polaritonic dispersion. We show that WS_2 multilayers are capable of supporting EPs at a nanometer-thickness limit. We also confirmed the pumping power dependence of polaritonic dispersions in WS_2 multilayers. Lastly, we first report the valley-polarized guided EPs in WS_2 layers at room temperature. This valley polarization originates from the strong coupling of photons with excitons in two different K and K' valleys. We believe that our findings will spark a new research direction for manipulating light or valley information in bare TMD layers.

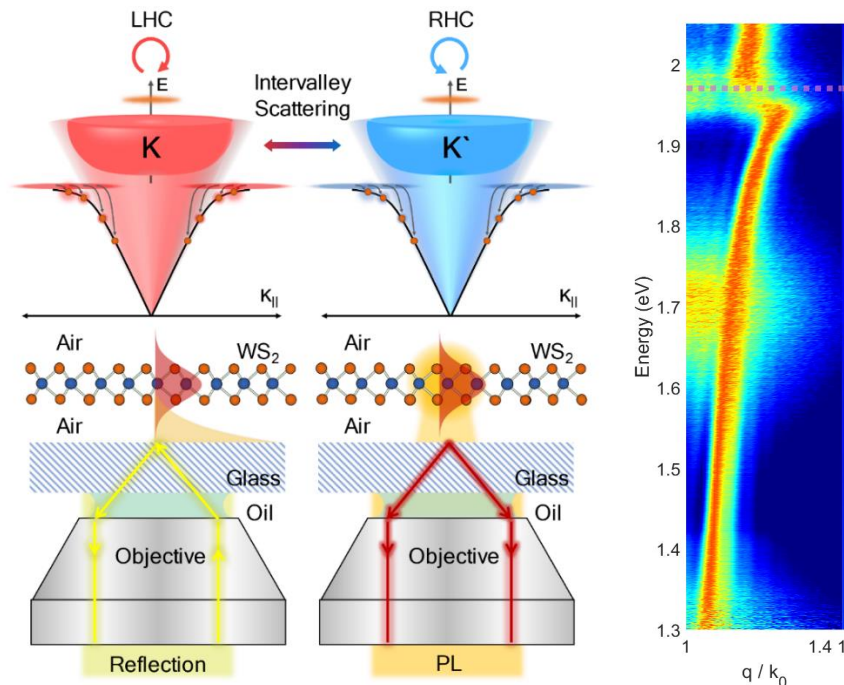


Fig. 1. Optical dispersion relations of exciton-polaritons detected by near-field coupling technique and their valley polarization.

References

[1] Shin, D.-J., Cho, H., Sung, J., Gong, S.-H., Direct Observation of Self-Hybridized Exciton-Polaritons and Their Valley Polarizations in a Bare WS_2 Layer. *Adv. Mater.* 2022, 34, 2207735.

The reduction of interfacial defect effect at 2D semiconductor/dielectric via low adhesive energy of perfluorinated polyether layer

Hyeong Chan Suh, Dae Young Park, Ju Chan Lee, DoHyeon Lee, Do Hyeong Kim, WooYeong Gang,
Mun Seok Jeong*

1 Department of Physics, Hanyang University, Seoul, 04763, Republic of Korea

** Corresponding Author: Mun Seok Jeong, e-mail: mjeong@hanyang.ac.kr*

The optical and electrical properties of transition metal dichalcogenides (TMDs) are sensitive to TMDs-dielectric interfaces. Silicon dioxide, a widely used dielectric substrate, contains various surface defects such as a charge puddle inducing the inhomogeneity of 2D materials. Thus, high-quality dielectric materials such as h-BN or Al_2O_3 have been applied for homogeneous and enhanced properties. The S10, one of the Perfluorinated Polyether (PFPE), is commercially used as a coating material for surface modification. It can alter the interface environment of TMDs-dielectric by passivating the dielectric surface. Here we report a facile way of passivation for surface charge puddle at SiO_2 substrate. The effect of surface passivation was confirmed by photoluminescence (PL) mapping of TMDs. The enhanced PL feature (six times in the case of MoS_2) with a uniform intensity was observed TMDs on S10 coated SiO_2 substrate..

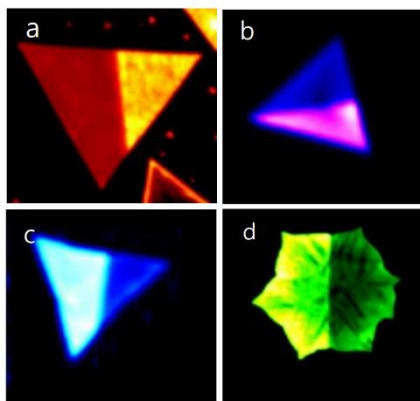


Fig 1. PL mapping data of (a) MoS_2 , (b) WS_2 , (c) MoSe_2 , and (d) WSe_2

Optical characterization of cubic and pyramidal MAPbBr₃ film formed by perovskite nano-seed

Taehoon Kim¹, Hyeon Jun Jeong¹, Kim yejin², Ko seoyeon², Yoon seokhyun², Mun Seok Jeong*

¹Department of Physics, Hanyang University, Seoul, 04763, Republic of Korea

²Department of Physics, Ewha Womans University, Seoul, 03760, Republic of Korea

*Corresponding Author: Mun Seok Jeong, e-mail: mjeong@hanyang.ac.kr

Halide perovskite materials have attracted attention as the next-generation materials for solar cells and displays due to their outstanding optical properties and long carrier lifetime. In this study, we fabricated the cubic and pyramidal MAPbBr₃ films with (100) and (111) planes (with facets) by using quantum dots as a nano-seed, respectively. Methylammonium bromide (MABr) and Lead (II) bromide (PbBr₂) were used to synthesize quantum dots based on MAPbBr₃. It was confirmed that pyramidal MAPbBr₃ films with the (111) plane have narrower optical band gap than MAPbBr₃ with the (100) plane on absorption and photoluminescence spectra. The influence of MA cation alignment direction as a polar substance, due to the electronegativity difference between Pb and Br, was confirmed using polarized Raman spectroscopy. Detailed analysis of the optical properties of these crystal planes is crucial for optoelectronic device applications. Further analysis of the optical and electrical characteristics of the (100) and (111) planes will be presented by measuring and analyzing them using techniques such as Kelvin probe force microscopy (KPFM), time-resolved photoluminescence (TRPL), and polarized Raman spectroscopy, highlighting potential applications in various directions for both structures.

Tip-induced nanoscale oxidation of graphene in aqueous media

Mingu Kang¹, Eunbeen Jeon², Meenakshi Rana³, Sunmin Ryu², Yung Doug Suh^{3,4,*}, and Kyoung-Duck Park^{1,*}

¹. Department of Physics, Pohang University of Science and Technology (POSTECH), Pohang 37673, Republic of Korea

². Department of Chemistry, Pohang University of Science and Technology (POSTECH), Pohang 37673, Republic of Korea

³. Department of Chemistry & School of Energy and Chemical Engineering, Ulsan National Institute of Science and Technology (UNIST), Ulsan 44919, Republic of Korea

⁴. Center for Multidimensional Carbon Materials (CMCM), Institute for Basic Science (IBS), Ulsan 44919, Republic of Korea

E-mail address: ydsuh@unist.ac.kr, parklab@postech.ac.kr

Abstract: Graphene oxide (GO) has unique optical and electrical properties with high stability. Here, we present tip-induced graphene oxidation in aqueous environment to produce GO with tip-enhanced Raman spectroscopy (TERS) approach. We observed local oxidation of graphene, changing into GO, when the graphene immersed in water and the laser-excited metallic tip approaches to the graphene.

1. Introduction

Carbon-based 2D materials have been extensively investigated due to their unique mechanical, electrical and optical properties [1,2]. In particular, chemically modified graphenes (i.e., graphene oxide) has great potential in optoelectronic applications as they exhibit enhanced stability, chemical reactivity, and electrical conductivity [3]. However, no alternative to producing GO from graphene is presented except large-scale chemically oxidizing graphite in acidic solutions. In this work, we demonstrate tip-induced oxidation of graphene under water to produce nanoscale graphene oxide (GO). The oxidation of graphene is confirmed by the increased Raman D-band intensity and reduced 2D-band intensity of the GO. We found that the oxidizing graphene into GO occurs only at the tip-approached region with the hyperspectral imaging of G, D, and 2D bands. We believe the oxidation process is based on the plasmon-induced chemical reactions of the metallic tip, liquid H₂O, and the graphene.

2. Results

As illustrated in Fig. 1a, we performed TERS of graphene under the aqueous environment. The excited Au tip induced the chemical reactions of water molecules and graphene, leading to the production of GO. The pristine graphene shows G-band (~1580 cm⁻¹) and 2D-band (~2590 cm⁻¹) intensity, as shown in Fig. 1b. On the other hand, oxidized graphene shows significant D-band (~1360 cm⁻¹) intensity with the reduced 2D-band intensity (Fig. 1c). We believe water molecule is necessary for oxidation of graphene since the graphene did not oxidize under ambient conditions, as shown in Fig. 1d. We also performed far-field hyperspectral imaging after we produce the nanoscale GO (Fig. 1e-g). We confirmed locally produced GO from the images since D-band peak is observed only at the tip-approached position where we indicated by the black dashed circles.

3. Figures

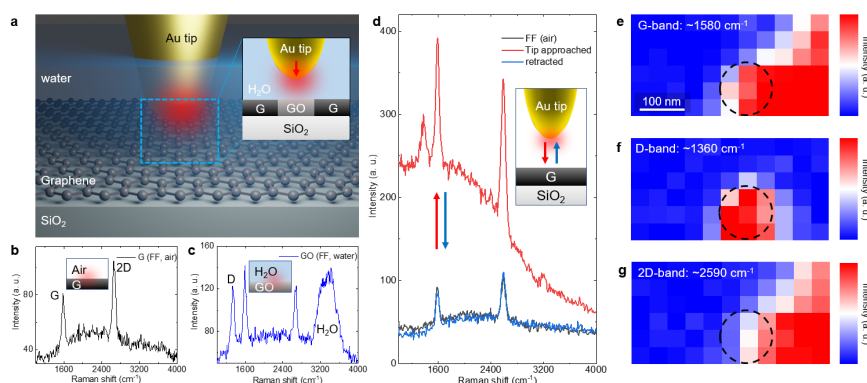


Fig. 1. (a) Schematic diagram of tip-enhanced Raman spectroscopy of graphene under water. Far-field spectra of pristine graphene under ambient conditions (b) and oxidized graphene under water (c). (d) tip-approached (TERS) and tip-retracted (far-field) spectra of pristine graphene. Hyperspectral imaging of locally oxidized graphene at the Raman shift of G-band (e), D-band (f), and 2D-band (g).

4. References

- [1] Y. Zhu, S. Murali, W. Cai, X. Li, J. W. Suk, J. R. Potts, and R. S. Ruoff, *Adv. Mat.* **22**, 3906-3924 (2010).
- [2] Z. Wei, D. Wang, S. Kim, S. Kim, Y. Hu, M. K. Yakes, A. R. Laracuenta, Z. Dai, S. R. Marder, C. Berger, W. P. King, W. A. de Heer, P. E. Sheehan, and E. Riedo. *Science*, **328**, 1373-1376 (2010).
- [3] A. C. Faucett, and J. M. Mativetsky, *Carbon*, **95**, 1069-1075, (2015)

Investigating Heterogeneous Defects in Single-Crystalline WS₂ via Tip-Enhanced Raman Spectroscopy

Sung Hyuk Kim^{1,2}, Chanwoo Lee², Byeong Geun Jeong², Dong Hyeon Kim^{1,2}, Seok Joon Yun^{2,3}, Wooseon Choi², Sung-Jin An², Dongki Lee⁴, Young-Min Kim^{2,3}, Ki Kang Kim^{2,3}, Seung Mi Lee^{5*}, Mun Seok Jeong^{1,6*}

¹*Department of Physics, Hanyang University*

²*Department of Energy Science, Sungkyunkwan University*

³*Center for Integrated Nanostructure Physics, Institute for Basic Science*

⁴*Department of Nanotechnology and Advanced Materials Engineering, Sejong University*

⁵*Surface Analysis Group, Korea Research Institute of Standards and Science*

⁶*Department of Energy Engineering, Hanyang University*

E-mail address: mjeong@hanyang.ac.kr

Abstract: Nanoscale defects in two-dimensional (2D) transition metal dichalcogenides (TMDs) alter their intrinsic optical and electronic properties, and such defects require investigation. Atomic-resolution techniques such as transmission electron microscopy detect nanoscale defects accurately but are limited in terms of clarifying precise chemical and optical characteristics. In this study, we investigated nanoscale heterogeneous defects in a single-crystalline hexagonal WS₂ monolayer using tip-enhanced Raman spectroscopy (TERS). Here we present the Raman properties of heterogeneous defects, which are indicated by the shifted A₁'(Γ) modes appearing on the W- and S-edge domains, respectively, with defect-induced Raman (D) mode. Also, quantum mechanical computations were performed for each majority defect and demonstrated the defect-induced variation in the vibrational phonon modes. TERS imaging promises to be a powerful technique for determining assorted nanoscale heterogeneous defects as well as for investigating the properties of other nanomaterials.

Topological waveguide gratings for compact coherent perfect absorbers

Chan Young Park, Ki Young Lee, Jae Woong Yoon

*Department of physics, Hanyang University, Seoul 04763, Korea
yoonjw@hanyang.ac.kr*

Abstract: We present coherent perfect absorbers based on topological guided-mode resonances. The proposed structure provides a fully confined resonance state in both vertical and lateral dimensions, creating a compact coherent absorber possibly operating at the critical coupling condition for the complete annihilation of certain optimized coherent incoming waves. We provide a promising Si-photonics design, incoming wave configuration, and theoretical performance for its operation as a compact coherent absorber in the integrated optics platform.

Controlling light absorption using resonant modes within nanophotonic structures in materials such as dielectrics, metals, and semiconductors plays a fundamental role in numerous application areas. In particular, research on leaky mode resonance such as surface plasmon resonance and guided-mode resonance (GMR) has shown extremely strong light absorption phenomena. When such leaky resonance modes are coupled with carefully prepared coherent input channels at the critical coupling condition, remarkably efficient phase-sensitive optical modulation is possible between two extreme states of coherent perfect absorption (CPA) and coherent total scattering (CTS) [1,2].

This study demonstrates the CPA-CTS phenomenon arising from leaky Jackiw-Rebbi (JR) state resonance at a topological junction of two GMR lattices. Using the diffractive-optical analogy of the one-dimensional Dirac equation and the temporal coupled-mode theory, we design a topological GMR CPA-CTS element where a critically-coupled JR state interacting with coherent radiations in the continuum. We analyze the singularity of the scattering matrix obtained from this model and derive the CPA condition for the JR state. We finally demonstrate rigorous numerical validation using the finite element method [3].

This device is designed to function as a complete absorber at a wavelength of 1500 nm, and optimal parameters that create a JR state resonance in this range were calculated using FEM. As shown in Figure 1, we designed a structure where the core consists of two layers within a slab structure with a lattice grid of uniform dielectric constants in the cladding. Parameters for such GMR nano-grid structures are defined by the period Λ , lattice width w , lattice layer thickness d_1 , and slab layer thickness d_2 . At the junction of two GMR lattices with different periods and lattice widths, strong leaky radiation occurs due to the formation of a JR state resonance at 1500 nm, which can be observed in the reflection spectrum. Such a single resonator can generally be described by TCMT in terms of radiation and internal decay rates, and the critical coupling condition representing a complete absorption state is satisfied when the internal decay rate due to direct scattering of the incident wave and the radiation decay rate due to coupling with the resonant mode are equal. Based on this condition, the amplitude of the incident wave at each port was determined, and when beams matched to each port were simultaneously vertically incident, the internal absorption rate was shown to depend on the phase difference between the two beams, as shown in Figure 3. The fully absorbed state at a phase difference of 0 and the complete scattering state at a phase difference of π can be clearly seen in the light intensity distribution shown in Figure 4.

We have demonstrated that complete absorption occurs using two beams that are matched by phase on a phase lattice. Therefore, based on the phase GMR, we propose the design of a silicon optical device that operates as an ultra-compact complete absorber within a photonic circuit platform.

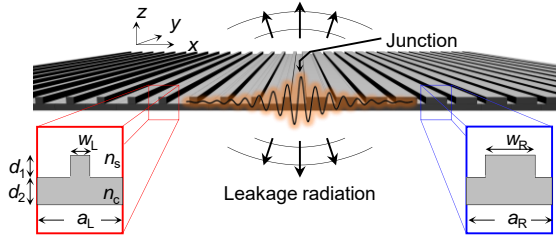


Fig. 1. Schematic of topological junction structure

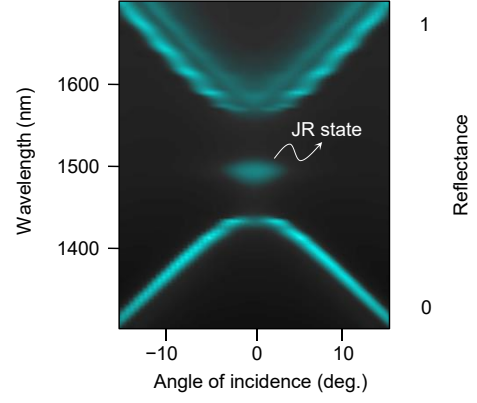


Fig. 2. Reflectance spectrum of Jakiw-Rebba resonance

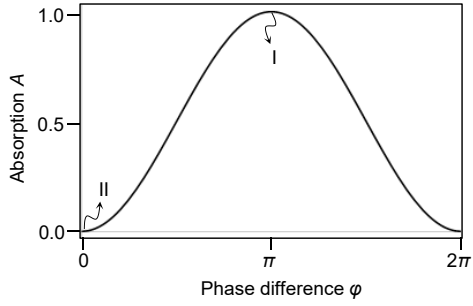


Fig. 3. Absorption for phase modulation

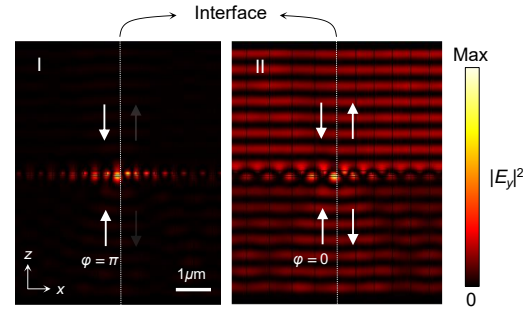


Fig. 4. Field distribution for two-beam interference

References

- [1] J Yoon, KH Seol, SH Song, R Magnusson, "Critical coupling in dissipative surface-plasmon resonators with multiple ports," *Optics express* 18 (25), 25702-25711.
- [2] JA Giese, JW Yoon, BR Wenner, JW Allen, MS Allen, R Magnusson, "Guided-mode resonant coherent light absorbers," *Optics Letters* 39 (3), 486-488.
- [3] KY Lee, KW Yoo, Y Choi, G Kim, S Cheon, JW Yoon, SH Song, "Topological guided-mode resonances at non-Hermitian nanophotonic interfaces," *Nanophotonics* 10 (7), 1853-1860.

Bright-Field and Edge-Enhanced Bioimaging using an Electrically Tunable Dual-mode Metalens

Hyemi Park¹, Inki Kim^{1,2*}

¹Department of Intelligent Precision Healthcare Convergence, Sungkyunkwan University, Suwon 16419, Republic of Korea

²Department of Biophysics, Institute of Quantum Biophysics, Sungkyunkwan University, Suwon 16419, Republic of Korea

E-mail address: inki.kim@skku.edu

Abstract: Due to their small feature sizes and low-amplitude contrast, microscopic biological samples present a variety of imaging challenges. A dual-mode metalens combined with a liquid crystal cell that can electronically switch between bright-field and edge-enhanced imaging in milliseconds is what we designed and experimentally realize. Using the ideas of geometric and propagation phase, the phase profiles of a normal metalens as well as one additional spiral phase with a topological charge are integrated. Because they are so small and compact, Metalens have shown great promise in bioimaging and have the potential to combine multiple functions into a single device. They can access completely complex information.

1. Introduction

Overall, bioimaging is critical tool for diagnosing and treating medical conditions, advancing scientific research and development, and improving the quality of healthcare for patients. But lenses used in conventional bioimaging have the disadvantage of being bulky and heavy. So we have been achieved using, 2D arrays of subwavelength structure known as meta-atoms, that have been developed to control the optical properties of light at will. We implement a method of introducing a spiral phase into a metalens to filter low-frequency components to produce edge-enhanced outputs while also focusing on light. Additionally, we developed and experimentally demonstrated an integrated metalens system that combines electrically programmable liquid crystal (LC) cells with multiplexed metalens to provide focus, imaging, and phase contrast imaging of bio cells.

2. Figures and tables

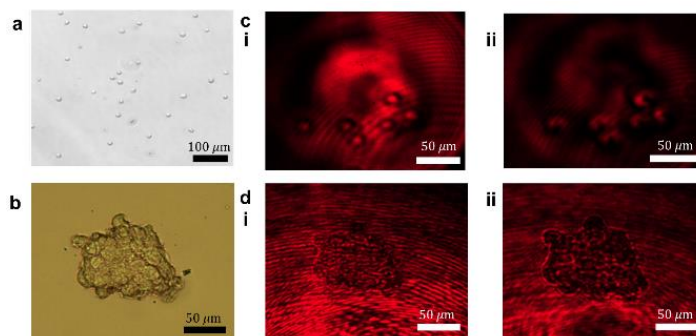


Figure 1: Biological imaging using the dual-mode metalens. Bright-field optical microscope images of (a) monocyte, (c) spheroid cells. Imaging using dual-mode metalens of (c) monocyte and (d) spheroid cells in (i) bright-field and (ii) edge-enhancement mode.

We experimented with monocytes from one of the phagocytes present in the blood that make up 2-8% of all white blood cell in the body. We observed 10-15μm single cells and 100-200 μm spheroid cells. Our dual-mode metalens, which has great potential for real-time monitoring of cell response and drug screening using spheroids, allows us to successfully observe small units of cells (Figure 1d i-ii).

3. References

- [1] Badloe, Trevon, et al. "Liquid crystal-powered Mie resonators for electrically tunable photorealistic color gradients and dark blacks." *Light: Science & Applications* 11.1 (2022): 118.
- [2] Chen, Wei Ting, Alexander Y. Zhu, and Federico Capasso. "Flat optics with dispersion-engineered metasurfaces." *Nature Reviews Materials* 5.8 (2020): 604-620.
- [3] Kim, Inki, et al. "Nanophotonics for light detection and ranging technology." *Nature nanotechnology* 16.5 (2021): 508-524.
- [4] Ren, Haoran, et al. "An achromatic metafiber for focusing and imaging across the entire telecommunication range." *nature communications* 13.1 (2022): 4183.

Ultrafast Photonic PCR with Metamaterial Perfect Absorber

Seho Lee^{1,2}, Inki Kim^{1,2*}

¹Department of Biophysics, Institute of Quantum Biophysics, Sungkyunkwan University, Suwon 16419, Republic of Korea

²Department of Intelligent Precision Healthcare Convergence, Sungkyunkwan University, Suwon 16419, Republic of Korea

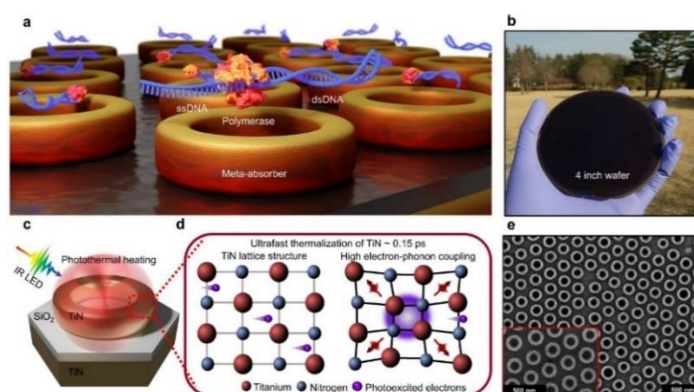
*E-mail address: (inki.kim@skku.edu)

Abstract: Polymerase chain reaction (PCR) is an essential technique in gene analysis and molecular diagnosis. There is a need for highly efficient chip-based portable PCR devices for point-of-care (POC) diagnostics due to the spread of infectious diseases. However, implementing a cost-effective chip-based PCR device remains challenging. We designed a ring-shaped titanium nitride perfect meta-absorber to achieve rapid heating and cooling cycling in the PCR process. We fabricated a large-area meta-absorber on a 4-inch wafer using multiple patterning of colloidal lithography in a cost-effective manner. We then performed 30 thermal cycles from the denaturation temperature of 95 °C to the annealing temperature of 65 °C, achieving a heating rate of 21.9 °C/s and a cooling rate of 7.8 °C/s in an ultrafast photonic reverse transcription PCR (RT-PCR). Overall, the low power consumption and highly efficient photothermal effect of our meta-absorber demonstrate the potential use of metasurfaces for ultrafast RT-PCR for POC molecular diagnostics.

1. Introduction

Research on PCR technology for rapid and accurate detection of pathogens is still actively being conducted. However, PCR amplification requires more than 30 cycles of thermal cycling and high power consumption, making it generally restricted to laboratory environments. Therefore, there is a need for portable and rapid nucleic acid-based diagnostic technologies that can be used outside of the laboratory. Recently, photonic PCR technology using low-power LEDs has garnered attention [1]. We implemented an efficient and low-cost metamaterial-based optical PCR using a broadband metamaterial absorber based on TiN. We performed DNA amplification within 6 minutes and 30 seconds using a 3.8W 940nm wavelength IR LED (Fig.1a). TiN ring-based metamaterial absorbers appear black in the visible spectrum due to their perfect absorption of all wavelength ranges from visible to near-infrared (Fig.1b). The ultrafast photothermal heating in the metamaterial absorber occurs when photons are absorbed by TiN (Fig.1c). When photons emitted from the light source reach the metamaterial absorber and are absorbed, electrons are no longer in equilibrium, and excited electrons exchange energy with TiN lattice phonons to generate heat. TiN has an ultrafast heating time of 0.15ps due to strong electron-phonon coupling, which is much faster than Au, which has a heating time of 5-10ps (Fig.1d) [2]. The metamaterial absorber was fabricated using a high-efficiency multi-patterning colloid lithography technique that enables mass production on 4-inch silicon wafers (Fig.1e).

2. Figures



“Fig. 1. TiN meta-absorber for DNA amplification”.

3. References

- [1] Kang, B.-H. et al. Ultrafast and Real-Time Nanoplasmonic On-Chip Polymerase Chain Reaction for Rapid and Quantitative Molecular Diagnostics. *ACS Nano* 15, 10194–10202 (2021).
- [2] Dal Forno, S. & Lischner, J. Electron-phonon coupling and hot electron thermalization in titanium nitride. *Phys. Rev. Materials* 3, 115203 (2019).

Metamaterial-assisted fluorescence correlation spectroscopy

Aleksandr Barulin¹, Hyemi Park², Inki Kim^{1,2*}

¹Department of Biophysics, Institute of Quantum Biophysics, Sungkyunkwan University, Suwon 16419, Republic of Korea

²Department of Intelligent Precision Healthcare Convergence, Sungkyunkwan University, Suwon 16419, Republic of Korea

*E-mail address: inki.kim@skku.edu

Abstract: Hyperlenses offer a unique opportunity to unlock bioimaging beyond the diffraction limit with conventional optics. Lateral scanning of nanoscale hindered diffusion of lipid analogues in live cell membrane structures has been accessible only using optical spatiotemporal super-resolution techniques. Here, we report a numerical study showing that gold/silicon multilayered hyperlens enables sub-diffraction fluorescence correlation spectroscopy (FCS). Thanks to high permittivity of silicon, the employed hyperlens enables nanoscale focusing of a Gaussian diffraction-limited beam below 40 nm even in the far-red spectral range. Despite the pronounced propagation losses, we quantify energy localization in the hyperlens inner surface to determine fluorescence correlation spectroscopy feasibility depending on hyperlens resolution and sub-diffraction field of view. We simulate the 3D diffusion FCS correlation function and observe the reduction of diffusion time of fluorescent molecules by nearly 50 times thanks to excitation energy confinement at the inner surface of the hyperlens. We numerically show that the hyperlens can effectively distinguish nanoscale transient trapping sites in simulated 2D lipid diffusion in cell membranes. Multilayered hyperlenses are experimentally fabricable platforms that display pertinent applicability for enhanced spatiotemporal resolution.

Two-dimensional dielectric metalenses provide unprecedented capabilities to focus light on a diffraction-limited spot and using a micrometer-thick nanostructure arrangements, as a compact analogue to conventional bulky objective lenses. Despite the metalens design solutions blossom toward imaging applications at several working wavelengths or even in a broadband wavelength range, single molecule fluorescence detection by a metalens has been elusive mainly due to strict requirements of high numerical aperture (NA), high focusing efficiency, and chromatic aberration correction. We investigate a metalens design that maintains dual-wavelength operation at 635 nm and 670 nm wavelengths, focusing efficiency above 50 %, and NA=0.6 to excite and collect single molecule fluorescence of diffusing Alexa 647N molecules and red light emitting nanoparticles. We demonstrate fluorescence excitation and collection by the metalens and optimize the experimental conditions to detect fast fluctuations of fluorescence intensity based on FCS. The proposed approach paves the way for a compact and, in the future, portable single-molecule detection system that could be applied for healthcare or monitoring environmental and industrial processes. Altogether, metamaterial-based structures provide promising platforms for the fundamental studies of nanoscale biomolecule dynamics and the compact detection systems of single molecules.

Metasurface-driven multiplexed nanospectroscopy via plasmonic resonance energy transfer

Yangkyu Kim¹, Inki Kim^{1,2*}

¹Department of Intelligent Precision Healthcare Convergence, Sungkyunkwan University, Suwon 16419, Republic of Korea

²Department of Biophysics, Institute of Quantum Biophysics, Sungkyunkwan University, Suwon 16419, Republic of Korea

*E-mail address : inki.kim@skku.edu

To understand dynamics in biomolecules and biological systems, a method is needed to continuously measure biomolecules in or out of cells in real time. Plasmon resonance energy transfer (PRET) is effective optical absorption spectroscopy method that can observe biomolecules in real time up to nanoscale units, and measured changes in cytochrome c in cells in real time while cells are dying [1]. The conventional PRET method was observed through the dark-field scattering spectrum by conjugating metal nanoparticles with chemical or biomolecules to transfer plasmon resonance energy [2]. However, this method can use only the limited scattering spectrum of nanoparticles and has multiplexing limitations for measurement samples.

We propose a metasurface-based sensing chip with a scattering spectrum suitable for targeted biomolecular absorption peak through nanostructure fabrication instead of nanoparticles. The grating effect formed by a cluster of cylindrical nanostructures and the gap plasmon resonance by metal-dielectric-metal multilayer form a dark-field scattering spectrum of an unlimited single peak in visible light. The developed metasurface sensing chip successfully obtained fingerprint imaging of each molecules from three different biomolecules (chlorophyll a, chlorophyll b, and cytochrome c). In addition, reactive oxygen specifications (ROS) of living cells were observed in real time through redox changes in cytochrome c.

This metasurface-based optical absorption spectroscopic method is noninvasive and can continuously measure multiple biomolecules in real time compared to previous nanoparticle-based PRET methods. We expect that his developed method will open a new chapter in the field of bio-sensing and imaging in the future.

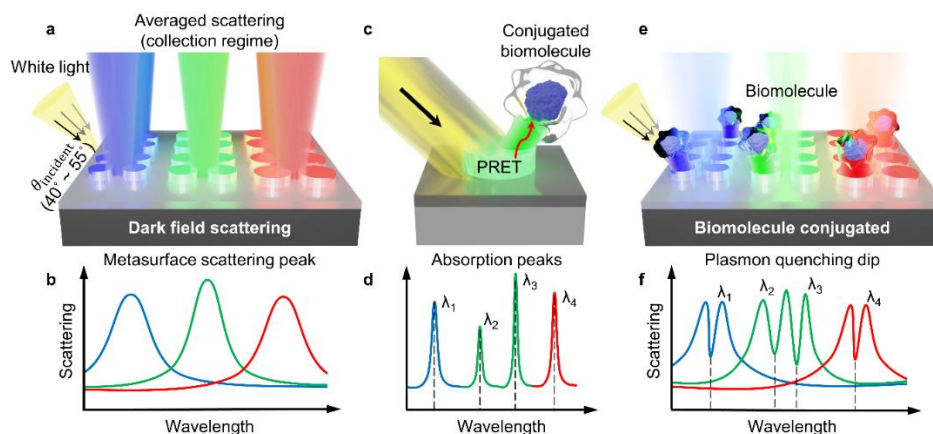


Fig. 1. Metasurface-based PRET method

- [1] Hongbao Xin, Wen Jing Sim, Bumseok Namgung, Yeonho Choi, Baojun Li, and Luke P Lee, Nature communications 10. 1, 3245 (2019)
[2] Gang Logan Liu, Yi-Tao Long, Yeonho Choi, Taewook Kang, and Luke P Lee, Nature Methods 4. 12, 1015-1017 (2007).

Advanced Tellurium/Graphene Heterostructures for Flexible IR Nanoscopy via CVD

Authors: Zhiyi Lyu and Dae Joon Kang*

Affiliation: Department of Physics, Sungkyunkwan University, 2066, Seobu-ro, Jangan-gu, Suwon, Gyeonggi-do 16419, Republic of Korea
**E-mail address: dj kang@skku.edu*

Abstract:

Integrating distinct two-dimensional (2D) materials can lead to groundbreaking electronic and optoelectronic functionalities. We introduce a low-temperature chemical vapor deposition (CVD) method for fabricating high-quality 2D tellurium (Te) on graphene (Gr) heterostructures, exhibiting superior structural and electrical characteristics. The Te/Gr heterostructure was thoroughly analyzed using scanning electron microscopy, Raman spectroscopy, and photoluminescence (PL) measurements. Our study demonstrates its applicability in flexible infrared (IR) nanoscopy detection, showcasing remarkable PL in the IR region. This research underscores the potential of CVD-grown 2D material heterostructures in advancing flexible electronic and optoelectronic devices.

.

Spectroscopic Characterization of Nanoplastics Using Photo-induced Force Microscopy

Sunho Lee^{1,2}, Seon Ae Hwangbo¹, Junghoon Jahng^{1*}, Tae Geol Lee^{1*} and Eun Seong Lee^{1*}

¹Korea Research Institute of Standards and Science (KRISS), Republic of Korea

²University of Illinois at Urbana-Champaign, United States

E-mail address: phyjjh@kriss.re.kr; tglee@kriss.re.kr; eslee@kriss.re.kr

The increasing evidence of the presence of nanoplastics in marine environments and aquatic organisms has engendered global research interests and public health concerns. Various toxicological studies have revealed the potential health hazards associated with nanosized plastics [1,2], highlighting the need for a comprehensive understanding of their behavior and environmental impact. While conventional approaches, such as electron microscopy and Raman/IR spectroscopy, have been extensively employed for nanoplastic analysis, their applications at nanoscale are constrained by sample damage from electron beams and the low spatial resolution of spectroscopic techniques. Herein, we present photo-induced force microscopy (PiFM) as a non-invasive approach to perform space-resolved spectroscopic analysis of nanoplastics. To mimic environmental degradation such as weathering and oxidation, nanoplastic samples were fabricated using a focused ultrasound system. Our results illustrate the versatility of PiFM as a method to probe the spatial distribution and chemical information of nanosized environmental plastics.

[1] L. Schröter and N. Ventura, *Small* **18**, 2201680 (2022).

[2] C. Jeong, H. Kang, Y. H. Lee, M. Kim, J. Lee, J. S. Seo, M. Wang and J. Lee, *Environ. Sci. Technol.* **52**, 11411 (2018).

Electrically tunable exciton-polaritons in 2D semiconductor-based microcavity

Young-Jun Lee, Jin-Woo Jung, Hyeon-Seo Choi and Chang-Hee Cho*

*Department of Physics and Chemistry
Daegu Gyeonbuk Institute of Science and Technology (DGIST)
Daegu 42988, South Korea
E-mail address: chcho@dgist.ac.kr*

Abstract: Exciton-polaritons are hybrid quasiparticles originating from the strong coupling between photons confined in an optical cavity and excitons in a semiconductor. They inherit the properties of both particles, such as half-light and half-matter, which make these quasiparticles promising in studying Bose-Einstein condensation and the non-linearities. Recently, the emergence of 2D transition metal dichalcogenides (TMD) has stimulated not only the challenge to realize Bosonic condensation of exciton-polariton at room temperature due to their large binding energy but also the control of the optical properties of exciton-polaritons possessing the unique character of TMD. However, although many studies have been conducted on exciton-polariton, Bosonic condensation of exciton-polaritons not using unintentional local traps and the manipulation of their optical properties still remain challenging. In this work, we suggest a simple way to enhance the interaction between polaritons by injecting carriers through the gate-tunable polariton device and present experimental results of electrically controlled optical properties of exciton-polaritons. Our work would be a great help to develop the exciton-polariton-based future devices.

Ultrafast melting of Au nanorods visualizing the localized surface plasmons

Eunyoung Park¹, Junha Hwang¹, Jaeyong Shin¹, Sung Yun Lee¹, Heemin Lee¹, Seung Phil Heo¹,
Daewoong Nam², Sangsoo Kim², Min Seok Kim², In Tae Eom², Do Young Noh³, Changyong Song¹

¹Department of Physics, POSTECH, Pohang, 37673, Korea.

²Pohang Accelerator Laboratory, Pohang, 37673, Korea.

³Department of Physics and Photon Science, GIST, Gwangju 61005, Korea.

eunyp@postech.ac.kr

Abstract: Ultrafast light-matter interaction invigorates research activities on light induced quantum control of materials properties by providing routes to explore new phases of matters in nonequilibrium states. With the exclusive excitations of electrons through femtosecond IR laser pulses, various physical processes can be accessed mode selectively, which enables the way to tackle fundamental science issues including the role of electrons in driving crystal phase changes. Au nanorod, are elongated gold single nanoparticle that has longitudinal localized surface plasmon (LSP). Understanding this surface plasmons in Au nanorod is essential, which enables to control optical properties in metal nanostructures. Despite the significance of surface plasmons in the light-matter interaction in metallic nanoparticles, the role of the localized surface plasmon in ultrafast melting has remained elusive. We studied the impact of surface plasmons dynamics in ultrafast phase transition of Au nanoparticle using femtosecond pump-probe X-ray imaging at PAL-XFEL. To study further, we directly imaged the reaction dynamics of photoinduced Au nanorod with femtosecond X-ray pulses. Shape distortion caused by LSP and further investigation of laser fluence and polarization direction dependence was carried out to result in various melting reaction in reaction in response to the surface plasmon excitations in metallic nanoparticles.

Figures

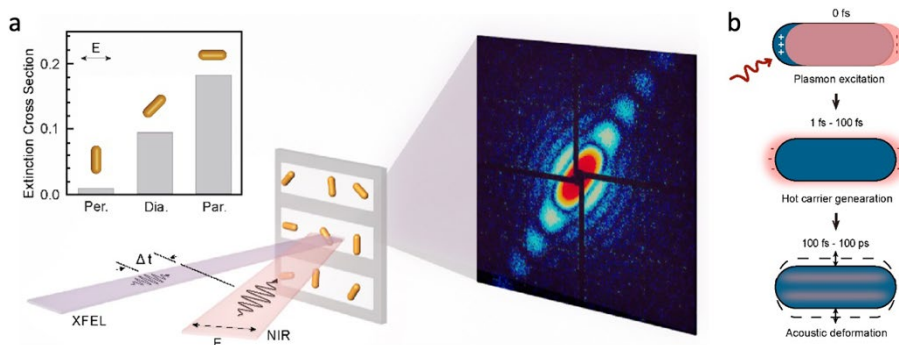


Fig 1. (a) Schematics of time-resolved single-pulse XFEL imaging experiments. Bar graph show the extinction cross section of the three groups with the laser polarization parallel (Par), diagonal (Dia) and perpendicular (Per) to the long axis of the nanorod. (b) Schematics of acoustic deformation due to localized surface plasmon.

Optical Condensation of Mixture of Plasmonic Nanoparticle and Microparticles via DNA Hybridization

Shuichi Toyouchi¹, Seiya Oomachi^{1,2,3}, Kota Hayashi^{1,2,3}, Yumiko Takagi¹,
Mamoru Tamura^{1,4}, Shiho Tokonami^{1,3}, Takuya Iida^{1,2}

Research Institute for Light-induced Acceleration System¹, Graduate School of Science², Graduate School of Engineering³, in Osaka Metropolitan University, Graduate School of Engineering Science in Osaka University⁴
E-mail address: t-iida@omu.ac.jp

Abstract: We have demonstrated the optical condensation of a mixture of plasmonic nanoparticles and microparticles via the light-induced acceleration of DNA hybridization. Using the method, a calibration curve showing high linearity was successfully obtained demonstrating the potential for quantitative analysis of DNA. The presenting results would open a new avenue allowing specific, rapid, and ultrasensitive quantitative DNA analysis.

1. Introduction

DNA is essential for life and used for various examinations in a wide range of fields such as medicine, pharmaceuticals, and food. Although it has become possible to quantitatively analyze DNA using digital PCR and next-generation sequencers in recent years, these conventional methods have problems with complicated processes, detection time, and accuracy. Thus, a new simple, rapid, and highly sensitive detection method of DNA is highly desired. To tackle the objective, we have proposed the principle of ‘light-induced acceleration’ of molecular recognition using synergetic effects between the light-induced force and the hydrodynamic interaction originating from the electromagnetic interaction of light in a solution containing probe particles modified with host molecules that molecularly recognize target molecules [1,2]. We develop a "heterogeneous probe optical condensation method" that enables rapid and highly sensitive DNA quantitative detection by applying this light-induced acceleration of DNA hybridization. A schematic illustration is shown in Figure 1. In the method, gold nanoparticles (Probe1, diameter 30 nm) and microparticles (Probe2, diameter 2 μm) functionalized with complementary probe DNA are employed as probe particles. On one hand, gold nanoparticles remarkably express the electric field enhancement and plasmonic heating of localized surface plasmons. On the other hand, strong light-induced force by Mie scattering exerts on the microparticle, resulting in light-induced convection. In a static fluid in a microwell, laser irradiation causes probe particles towards the solid-liquid interface and eventually assembles them. The target DNA is also condensed by hybridization between the probe particles. In this study, we evaluated the detection limit and demonstrated the possibility of DNA quantitative detection.

2. Methods

A mixed solution (approximately 7 μL) of fluorescent dye-labeled target DNA, Probe1, and Probe2 was enclosed in a homemade microwell. A near-infrared laser was irradiated from below onto the top solid-liquid interface of the microwell using an inverted microscope. Then fluorescence images of the light-induced assemblies were acquired when the target DNA concentration varied in the concentration range of 1 nM or less.

3. Results and Discussion

A positive correlation between the fluorescence intensity of the light-induced assembly and the target DNA concentration was confirmed, and a calibration curve showing high linearity was successfully obtained. The lower limit of detection is estimated to be around 200 pM of DNA concentration, suggesting that high-sensitivity detection equivalent to that of digital PCR can be achieved by light irradiation for only 3 minutes. We further examined the specificity of the method by introducing a few mismatch bases in the target DNA sequence. In the presentation, we will discuss the results from the viewpoint of plasmonic heating of the gold nanoparticles trapped in the light-induced assembly. The presenting results would open a new avenue for specific, rapid, and ultrasensitive quantitative DNA analysis.

4. References

- [1] T. Iida, Y. Nishimura, M. Tamura, K. Nishida, S. Ito, and S. Tokonami, *Sci. Rep.*, **6**, 37768 (2016)
- [2] T. Iida, S. Hamatani, Y. Takagi, K. Fujiwara, M. Tamura, S. Tokonami, *Commun. Biol.* **5**, 1053 (2022).
- [3] S. Toyouchi, S. Omachi, K. Hayashi, Y. Takagi, M. Tamura, S. Tokonami, T. Iida, et al., Paper in preparation (2023).

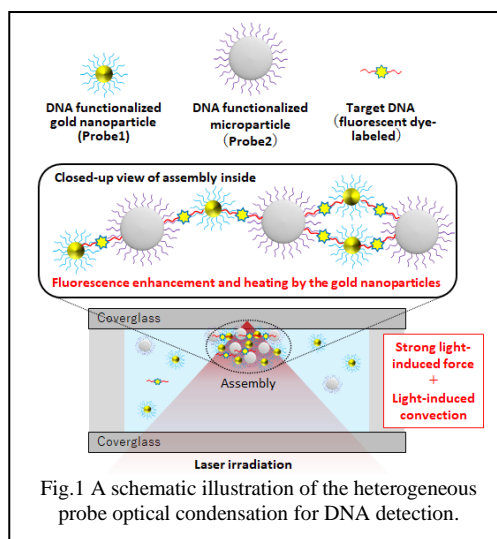


Fig.1 A schematic illustration of the heterogeneous probe optical condensation for DNA detection.

The TMDc fluorescence Lifetime image by pump-probe microscopy

Jin Yong Jeong¹, Jae Joon Kim¹, Soobong Choi^{1†*}

¹Department of Physics, Incheon National University, Incheon 22012, Republic of Korea

*sbchoi@inu.ac.kr

[†] Author contributions

Abstract: The transition-metal dichalcogenide (TMDc) MX₂, such as MoS₂, MoSe₂, WS₂ and WSe₂, has a layered structure [1]. Especially, the photoluminescence of MoS₂ and MoSe₂ is weakened by vacancies of chalcogen elements (S, Se), and PL intensity is enhanced by O-substitution at S vacancies or Se vacancies by heating a and b using a laser or hot plate [2,3,4]. In this study, Both pump and probe pulses were generated by a mode-locked Ti:Sapphire laser, with 80 MHz repetition rate and 800 nm central wavelength, and carrier lifetime was measure at room temperature in air. We will analyze the pI increase mechanism by measuring the carrier lifetimes of MoSe₂ upon O-substitution in Se vacancies using a pump-probe microscope.

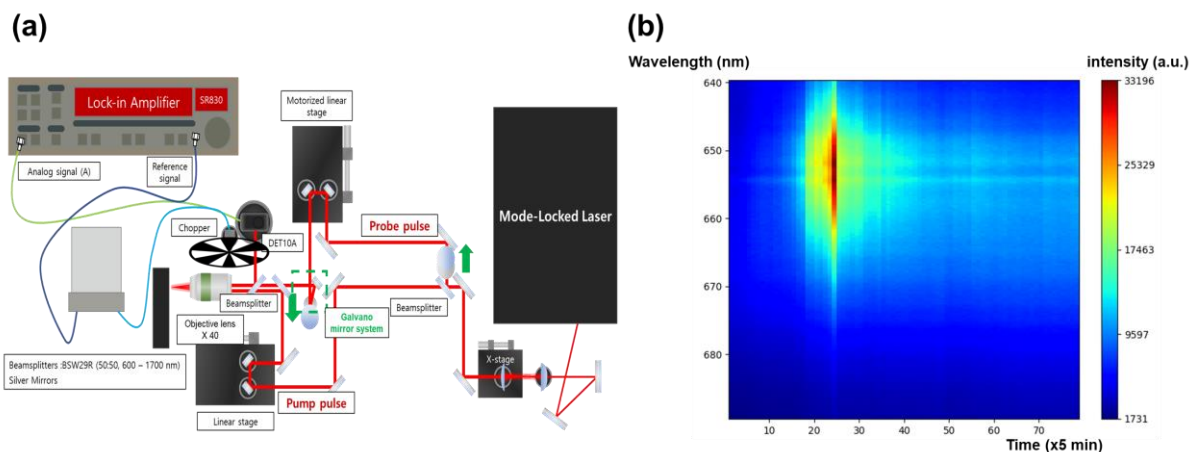


Figure 1. (a) The schematic diagram of an pump-probe microscopy (b) Graph of change in PL intensity of MoS₂ over time when irradiated with a laser at an output of 1mW (before lens) for 2 hours

- [1] Min Ju Shin et.al, "Photoluminescence Saturation and Exciton Decay Dynamics in Transition Metal Dichalcogenide Monolayers", (ournal of the Korean Physical Society 2014), pp 65 2077-2081
- [2] Hye Min Oh et.al, "Photochemical Reaction in Monolayer MoS₂ via Correlated Photoluminescence, Raman Spectroscopy, and Atomic Force Microscopy", (ACS Nano 2016), pp 10 5230-5236
- [3] "Laser Annealing Improves the Photoelectrochemical Activity of Ultrathin MoSe₂ Photoelectrodes", (ACS Appl. Mater. Interfaces 2019), pp 11 19207-19217

Scattering Dynamics of Two-dimensional Polaritons

Wonjae Choi, Q-Han Park

Department of Physics, Korea University, 145, Anam-ro, Seongbuk-gu, Seoul, Republic of Korea
E-mail address: chldnjswo01@korea.ac.kr

Abstract: We derive an analytic expression for the reflection and transmission coefficients of two-dimensional polaritons at the boundary using the Wiener-Hopf method. Scattering dynamics of polaritons are explained and compared with the plane wave case.

1. Introduction

Two-dimensional (2D) polaritons are propagating electromagnetic modes that are confined to 2D materials. When polaritons meet a boundary, they become reflected and transmitted but at the same time, unlike plane waves, scattered fields are generated because of the mode profile mismatch at the boundary. These scattered fields make the propagation of a polariton different from that of a plane wave. Since the scattered fields are an intrinsic property of the polaritonic systems, it is important to understand the effect of the scattered fields on polariton dynamics. However, due to the mathematical complexity, efforts mainly have been conducted for the graphene plasmon dynamics [1,2] which are relatively simple and offer promising applications. Although these works explained the graphene plasmon well, they are not sufficient to understand the scattering dynamics of a general polaritonic system. In this work, we obtain analytic expressions for the reflection and transmission coefficients of polaritons and study how the scattered fields change the dynamics of polaritons. Our analysis based on the exact solutions for scattering dynamics will help a fundamental understanding of polaritons.

2. Method and results

We consider a system depicted in Fig. 1(a) to analyze the effects of scattered fields on the dynamics of polaritons. In Fig. 1(a), two different 2D materials are sandwiched between two dielectric media. The Fourier-transformed time-harmonic Maxwell's equations ($e^{-i\omega t}$) can be decomposed into the TM and the TE part, and from the decomposed equations, we can derive exact solutions by using the Wiener-Hopf method [3,4].

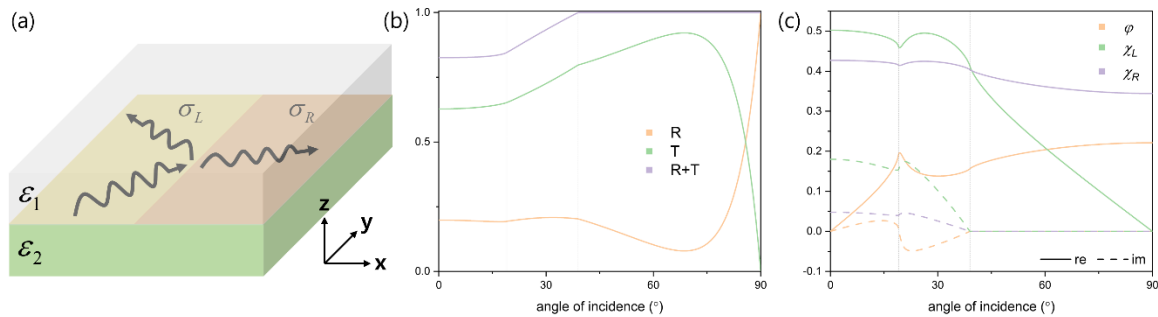


Fig. 1. The geometry of the system (a). All materials are lossless and nonmagnetic. Reflectance R , transmittance T , their sum $R+T$ (b), and the scattering coefficients φ and $\chi_{L,R}$ (c) are plotted against the angle of incidence.

The expressions for the reflection and transmission coefficients of polaritons include not only the ratio of the impedance or admittance like plane waves but also additional constants φ and $\chi_{L,R}$ resulting from the scattered fields. The reflectance R , transmittance T , and the scattering coefficients φ and $\chi_{L,R}$ are plotted in Fig. 1(b), (c). One of the prominent differences between the plane wave case and this polaritonic system is the existence of Brewster's angle. We can confirm that Brewster's angle does not exist in the polaritonic system, but only the Brewster-like effect exists. Our theory can quantitatively explain these phenomena and show vividly the effect of scattered fields on polariton dynamics which was not known previously.

3. References

- [1] Rejaei, Behzad, and Amin Khavasi. "Scattering of surface plasmons on graphene by a discontinuity in surface conductivity." *Journal of Optics* 17.7 (2015): 075002.
- [2] Siaber, S., S. Zonetti, and O. Sydoruk. "Junctions between two-dimensional plasmonic waveguides in the presence of retardation." *Journal of Optics* 21.10 (2019): 105002.
- [3] Margetis, Dionisios. "Edge plasmon-polaritons on isotropic semi-infinite conducting sheets." *Journal of Mathematical Physics* 61.6 (2020): 062901.
- [4] Daniele, Vito G., and Rodolfo Zich. *The Wiener-Hopf method in electromagnetics*. SciTech Publishing Incorporated, 2014.

Investigate of Moiré Excitons of Stacked WSe₂ Bilayer using by Near-Field Imaging

Youngbum Kim, K. P. Dhakal and Jeongyong Kim*

¹*Department of Energy Science, Sungkyunkwan University, Suwon 16419, Republic of Korea*

^{*}*E-mail address: j.kim@skku.edu*

The excitonic effects in two-dimensional transition metal dichalcogenides (TMDs) and their heterostructures have been extensively investigated. One such novel physical phenomenon is the emergence of interlayer excitons. It demonstrated that most TMD vdW heterostructures feature a type-II band alignment with the conduction band minimum (CBM) and valence band maximum (VBM) located in different monolayers. Additionally, the period of the moiré superlattice can be controlled by choosing materials with different lattice constants or adjusting the twist angle between the layers, leading to a new paradigm in engineering quantum materials [1]. However, the twisting angle dependence and the effect of the moiré pattern on the exciton state have not been fully understood in these twisted TMD structures. We will discuss about the near-field imaging of moiré excitons over high symmetry points in the Brillouin zone, which might show the interaction of excitons and moiré potentials. Near-field imaging techniques have not yet been used to investigate moiré exciton in 2D stacks. These results will open up new avenues for quantum optics.

References

- [1] Wu, F., Lovorn, T., & MacDonald, A. H., et al., Phys. Rev. Lett., **97**, 217403, (2018).

Manipulating the fluorescence contrast in liquid-gel phases

Jia-Ru Yu^{1,2}, He-Chun Chou¹, Wei-Ssu Liao², and Chi Chen¹

1. Research Center for Applied Sciences, Academia Sinica, Taipei, 115, Taiwan

2. Department of Chemistry, National Taiwan University, Taipei, 106, Taiwan
chenchi@gate.sinica.edu.tw

Abstract: Fluorescence tagging of supported lipid bilayers (SLBs) is an essential technique for imaging particular components of biological membranes. It is generally believed that tagged lipids would participate in the fluid phase rather than the gel phase. Such partition behavior of tagged lipids usually guides the interpretation of fluorescence bright or dark domains on the membrane. Here, we employed our homebuilt liquid-phase scanning near-field microscopy (SNOM) to study lipid bilayers [1] (Fig. 1 (a) and (b)). The liquid chamber was equipped with a heating circuit and temperature feedback to observe the movement and phase segregation of lipids under temperature control. Local lipid molecules can be manipulated from the gel phase to the fluid phase by the *a*-SNOM tip, which causes the reverse of the fluorescence contrast (Fig. 1 (c)). This demonstrates that there is no preferable partition of the fluorescence tag in the fluid or gel phases. The packing type of the lipids affected the quantum yield of the fluorophore and led to a distinct fluorescence contrast between the gel and fluid phases. Our results not only reveal the fundamental issue of fluorescence tag partitioning, but also offer a practical guide for interpreting fluorescence contrast.

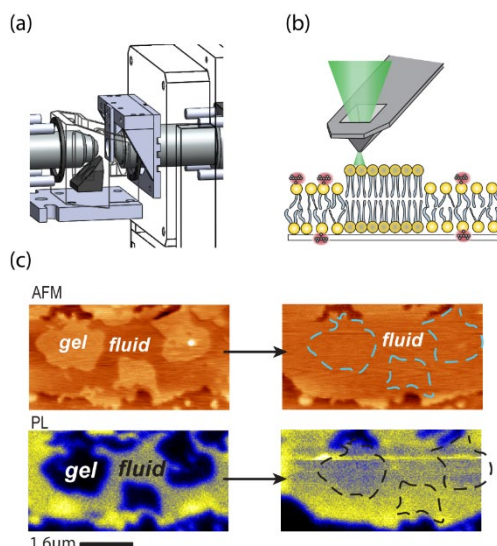


Fig. 1 (a) Schematic illustration of the homebuilt liquid-phase SNOM system. (b) Schematic illustration of a *a*-SNOM tip to scan lipid bilayers. (c) The sequential *a*-SNOM images of the DPPC:DOPC = 1:1 SLB with 3% Texas red-DHPE fluorescence probe. Top row is the *a*-SNOM topography and the bottom row is the simultaneous recorded *a*-SNOM fluorescence intensity map.

References

[1] Yu, J.R.; Chou, H.C.; Yang, C. W.; Liao, W. S.; Hwang, I. S.; Chen, C 2020, *Rev. Sci. Instrum.* 910, 73703.

Optical and electrical control of nanoscale metal-semiconductor tunnel junction

Huitae Joo¹, Hyeonwoo Lee¹, Sujeong Kim¹ and Kyoung-Duck Park^{1*}

¹Department of Physics, Pohang University of Science and Technology (POSTECH), Pohang 37673, Republic of Korea.
E-mail address: parklab@postech.ac.kr

Abstract: Electron density of 2D transition-metal dichalcogenides (TMDs), a key metric determining optoelectronic performance, significantly influences their optical characteristics, such as radiative emission rate and valley polarization. However, precise modulation of the doping density in 2D TMDs at the nanoscale remains a challenge. Here, we present a nanomechanical engineering of metal-semiconductor tunnel junction through conductive tip-enhanced photoluminescence (c-TEPL) spectroscopy. Moreover, we facilitate the doping-dependent switching of TEPL intensity and valley polarization, induced by the tip-induced local electric field. This allows us to induce and probe nanoscale optical heterogeneities in TMD monolayers, opening a pathway toward ultrathin optoelectronic device applications.

1. Introduction

The electromechanical control of the 2D monolayer transition metal dichalcogenides (TMDs) has been widely studied to manipulate its optical properties. However, overcoming the extremely low room-temperature photoluminescence quantum yield (QY) of 2D TMDs such as MoS₂ remains challenging. Recently, electrostatically doped MoS₂ ML showed highly enhanced room-temperature quantum yield (QY) of photoluminescence [1]. Therefore, modulation of the charge concentration of the MoS₂ leads to manipulate radiative recombination of neutral excitons in MoS₂ ML.

Here, we present tip-induced nanomechanical control of metal-semiconductor tunnel junction. The geometry of MoS₂ ML and Au substrate forms a metal-semiconductor tunnel junction, and its electrical coupling strength is precisely modulated using shear force atomic force microscopy (AFM) technique. By exploiting its <0.2 nm vertical precision, we systematically control the level of metal-semiconductor interaction. The decreased gap between the MoS₂ ML and the Au substrate allows electrons to travel from MoS₂ ML to the Au substrate. This enables the local manipulation of the doping density of the MoS₂ monolayer at the nanoscale region, confirmed with <15 nm spatial resolution of tip-enhanced photoluminescence (TEPL) spectroscopy. Furthermore, we employ c-TEPL spectroscopy technique to dynamically control the doping density and corresponding photoluminescence intensity and valley polarization from tip-induced local electric field.

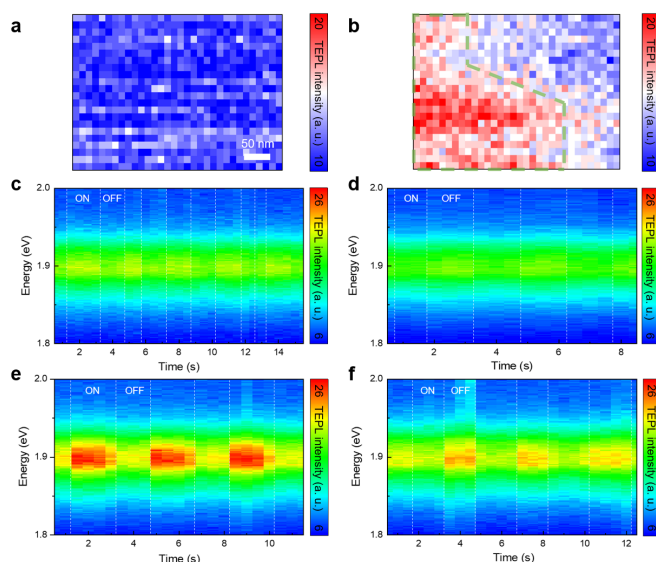


Fig. 1. Hyperspectral image of TEPL intensity of weakly coupled region (a) and intermediately coupled region (b). Green dashed line indicates the intermediately coupled region. Homogeneous TEPL intensity in weakly coupled region according to external negative electric field (c) and positive electric field (d). TEPL intensity changes in intermediately coupled region corresponding to external negative electric field (e) and positive electric field (f).

2. References

- [1] Lien, D. H. et al. “Electrical suppression of all nonradiative recombination pathways in monolayer semiconductors”, *Science*. **364**(6439), 468–471 (2019).

The Bacterial Flagellar Motor through Torque Spectroscopy

Vincent Manning, Maddison Beahm, Julia Kalynchuk, and Ilyong Jung

Monmouth University
E-mail address: ijung@monmouth.edu

Abstract

At low *Reynolds* number, bacteria such as *Escherichia coli* propel themselves by rotating a set of flagella driven by 40 nm transmembrane molecular machines- that are known as the bacterial flagellar motors [Fig. 1]. When those motors exert torques in counterclockwise fashion, a cell forms a bundle of flagellar filaments and swims forward. However, if one of the filaments switches clockwise, the bundle is broken and the cell tumbles to navigate towards a new favorable direction in response to chemical gradients. However, despite extensive studies, we lack sufficient understanding of the underlying torque generating mechanisms that are responsible for cell locomotion. Here, I investigate the motor dependence on external torque using exciting novel techniques, the magnetic torque wrench, to rapidly apply variable loads on cells and broadly scan torque-speed spectrum in real time [Fig. 2]. In addition, we investigate the relationship between the motor speed and the number of torque generating protein unit, stators. Our results indicate that single a proton can generate torque for a discrete angular step in the rotation of the bacterial flagellar motors.

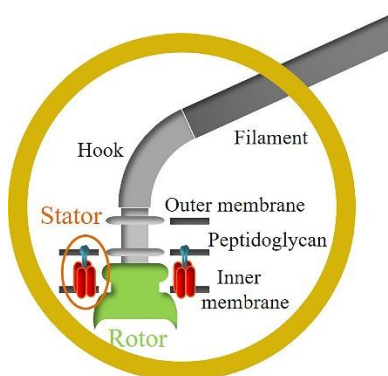


Fig. 1. Side view of *E.coli* BFM showing overall structure including filament, hook, stators, rotor, and membranes.

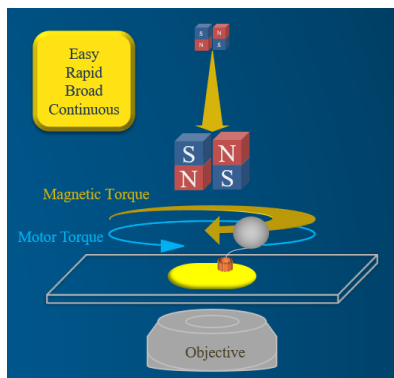


Fig. 2. The magnetic tweezers (MT) presents an ability to readily and rapidly exert a broad range of torques on cells to measure torque-speed spectrum. It is possible to investigate the BFM activities under full load, partial load, zero load, and even negative load.

Near-field Raman spectroscopy with multipolar Hamiltonian and real-time-TDDFT

Takeshi Iwasa,^{1,2} Masato Takenaka,¹ Tetsuya Taketsugu¹

¹Hokkaido University, Sapporo Japan, ²JST-PRESTO, Saitama, Japan
E-mail address: tiwasa@sci.hokudai.ac.jp

Abstract: Raman spectroscopy with near-field achieves sub-molecular spatial resolution when using a scanning tunneling microscopy. To fully understand the selection rule of near-field Raman spectroscopy and imaging, we developed a theoretical method based on the multipolar Hamiltonian that allows us to go beyond the dipole approximation by considering the full spatial distribution of the electric near-field. Furthermore, under the framework of real-time time-dependent density functional theory, both on- and off-resonance Raman scattering can be calculated in the same manner. For demonstration, the on- and off-resonance near-field Raman spectra of benzene were calculated and the selection rule was analyzed in terms of the spatial distribution of the near-field and molecular vibrational coordinates.

The optical near-field refers to a non-propagating light field localized around an emitter or scatterer, such as metallic nanostructures. The interaction between the near-field and molecules can overcome the diffraction limit of propagating light, induce non-dipolar excitations, and enable nanoscale chemical analysis down to single molecules even at sub-molecular resolutions. Recent experiments utilizing scanning tunneling microscopy offer a unique platform for nanoscale spectroscopy, microscopy [1], and photochemistry [2]. From a theoretical perspective, the optical near-field excitation of molecules requires us to go beyond the dipole approximation, which is not possible with the available ab initio codes. To study the interaction between the near-field and molecule, we developed first-principles methods based on the multipolar Hamiltonian for electronic excitations [3-4] and vibrational excitations [5-6]. By combining these techniques, we developed a theoretical approach to near-field Raman spectroscopy. In this paper, we explain our theoretical method that is based on the multipolar Hamiltonian and real-time time-dependent density functional theory (RT-RS-TDDFT) that enable the computation of on- and off-resonance Raman in the same framework.[7]

In the multipolar Hamiltonian, the interaction between the near field and molecule is described by the spatial integration of the inner product of the molecular polarization field and electric field, both of which can depend on the position as follows:

$$H_{\text{int}}(\mathbf{r}, t) = - \int \hat{\mathbf{P}}(\mathbf{r}', t) \cdot \mathbf{E}(\mathbf{r}', t) d\mathbf{r}'$$

where $\hat{\mathbf{P}}$ is the electric polarization field operator, whose explicit form is

$$\hat{\mathbf{P}}(\mathbf{r}) = \sum_{\alpha} e_{\alpha} (\hat{\mathbf{q}}_{\alpha} - \mathbf{R}) \int_0^1 \delta[\mathbf{r} - \mathbf{R} - \lambda(\hat{\mathbf{q}}_{\alpha} - \mathbf{R})] d\lambda$$

where e_{α} and $\hat{\mathbf{q}}_{\alpha}$ are the charge and position operator of the α th electron in the molecule, respectively. While the Taylor expansion of this electric polarization field gives multipoles such as dipoles, quadrupoles, and octapoles, our method uses the original form of the polarization field without any approximation.

Using this interaction Hamiltonian, near-field-induced electronic excitations were calculated with the RT-RS-TDDFT program Octopus. For the Raman spectra, the near-field-induced dipole moments of a target molecule are calculated for slightly distorted geometries from its optimized geometry and then the normal coordinate derivatives of the induced dipole moment of the molecule are obtained.

The near-field Raman spectrum of benzene is shown as a demonstration. Under the off-resonance condition, the selection rule of the Raman spectra is well understood by considering both the spatial structure of the near field and molecular vibration. Under the on-resonance condition, the Raman spectra are strongly affected by the nature of the selected excited state. Interestingly, on-resonance Raman spectroscopy can be activated even when the near field forbids the π - π^* transition at equilibrium because of vibronic couplings originating from structural distortions.

4. References

- [1] R. B. Jaculbia, T. Iwasa et al., Nat. Nanotechnol. 15, 105 (2020).
- [2] E. Kazuma et al., Science, 360, 521 (2018).
- [3] T. Iwasa and K. Nobusada, Phys. Rev. A, 80, 043409 (2009).
- [4] T. Iwasa and K. Nobusada, Phys. Rev. A, 82, 043411 (2010).
- [5] T. Iwasa, M. Takenaka, T. Taketsugu, J. Chem. Phys., 144, 124116 (2016).
- [6] M. Takenaka, T. Taketsugu, T. Iwasa, J. Chem. Phys., 152, 164103 (2020).
- [7] M. Takenaka, T. Taketsugu, T. Iwasa, J. Chem. Phys., 154, 024104 (2021).

Rough-Cut End Surface Effect on Signal-to-Noise Ratio in Fiber-Optic SERS Detection

Seonung Kim, Minkyung Shin, Kyunghun Kim, Dae Hong Jeong
Department of Chemistry Education, Seoul National University, Seoul, Republic of Korea
E-mail address: jeongdh@snu.ac.kr

Fiber-optics based surface-enhanced Raman scattering (FO-SERS) can remotely detect analyte molecules by adjusting the fiber length. [1-3] However, the strong Raman signal of the fiber-optic material limits its application for remote SERS sensing. [4] We reduced the background noise signal by *ca.* 32 % using fiber-optics with a roughened surface cut instead of a flat one. (Fig. 1) We also attached silver nanoparticles labeled with 4-fluorobenzenethiol to the end surface of an optical fiber to create a SERS-signaling substrate. The SERS intensity and signal-to-noise ratio (SNR) values were significantly higher for the fiber-optics with a roughened surface than for those with a flat surface. (Fig. 2) This suggests that the fiber-optics with a roughened surface could be an efficient FO-SERS sensing platform.

Acknowledgement: This work was supported by the National Research Foundation of Korea (NRF) grant funded by the Korea government (MSIT) (No. NRF-2021M3C1C3097205).

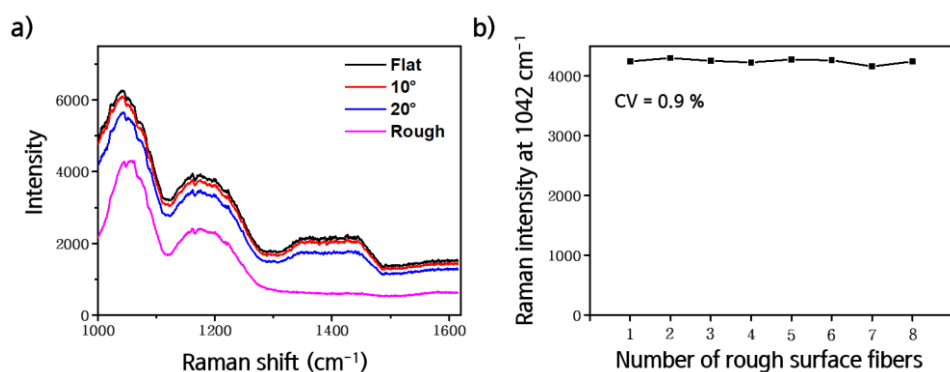


Fig. 1. Raman signals from the optical fiber itself under an excitation of 785 nm. (a) Raman spectra of optical fibers with different end surfaces. (b) Signal reproducibility of rough-surface fiber fabrication.

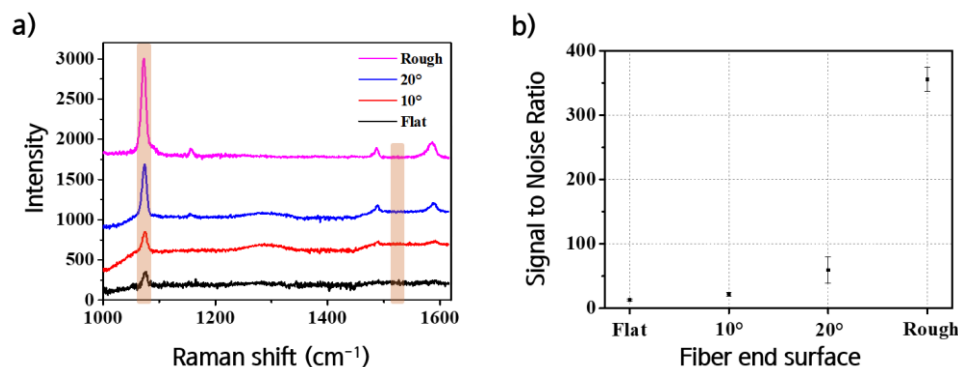


Fig. 2. Signal-to-Noise Ratio (SNR) comparison of fiber optics with different end shapes. (a) SERS spectra of different end-shaped optical fibers after subtracting each bare fiber signal. (b) Scatter plot of the SNR of different end-shaped optical fibers. (SERS signal was based on the 1072 cm⁻¹ peak in Fig. 2 (a), and the noise was calculated as the standard deviation in a range from 1515 to 1535 cm⁻¹, which was a flat section in all sample spectra in Fig. 2 (a).)

- [1] L.Li, S. Deng, H. Wang, R. Zhang, K. Zhu, Y. Lu, Z. Wang, S. Zong, Z. Wang, and Y.Cui, *Nanotechnology* **30** (2019).
- [2] Z. Chen, Z. Dai, N. Chen, S. Liu, F. Pang, B. Lu, and T. Wang, *IEEE Photon. Technol. Lett.* **26**, 777-780 (2014).
- [3] G. F. Andrade, M. Fan, and A. G. Brolo, *Biosens. Bioelectron.* **25**, 2270-2275 (2010).
- [4] J. May and Y.-S. Li, *Appl. Opt.* **35**, 2527-2533 (1996).

Photoreflectance Study of InGaAs/InAsPSb Multiquantum Well Structure: Investigation of Optical Properties

Behnam Zeinalvand Farzin¹, Jong Su Kim¹, Tae In Kang¹, Jaedu Ha¹, Sang Jun Lee²

¹Department of Physics, Yeungnam University, Gyeongsan 38541, Korea

²Korea Research Institute of Standards and Science, Daejeon 34113, Korea

E-mail address: jongsukim@ynu.ac.kr

Abstract: This study investigates the photoreflectance properties of a semiconductor device based on an InGaAs/InAsPSb multi-quantum well (MQW) structure. The extended InGaAs LED structures composed of different numbers of the multi-quantum wells (6 and 9) were grown by the MBE method. The study reveals the sensitivity of photoreflectance spectra to changes in excitation intensity and temperature and provides valuable insights into the confinement effects on the optical properties of the MQWs. This research contributes to understanding semiconductor device physics and could inform the design and optimization of high-performance optoelectronic devices.

1. Introduction

InGaAs/InAsPSb multi-quantum well (MQW) light-emitting diodes (LEDs) are a promising optoelectronic device class that has gained significant attention in recent years [1]. These devices are based on a heterostructure design that incorporates thin layers of InGaAs and InAsPSb, which create a quantum well structure that enables efficient radiative recombination and light emission. Using InAsPSb as a barrier material offers numerous advantages, including a wide range of energy bandgaps, high carrier mobility, and reduced Auger recombination. Furthermore, incorporating strain-balanced heterostructures can improve the device performance by reducing nonradiative recombination and increasing carrier lifetime. InGaAs/InAsPSb MQW LEDs have been successfully applied in various optoelectronic applications, such as high-speed communication, sensing, and imaging. This technology is still under active research and development as efforts continue to optimize the device design, fabrication process, and material properties for further efficiency, power output, and spectral range improvements [2,3].

2. Figures and tables

The sample under investigation is shown in figure 1.

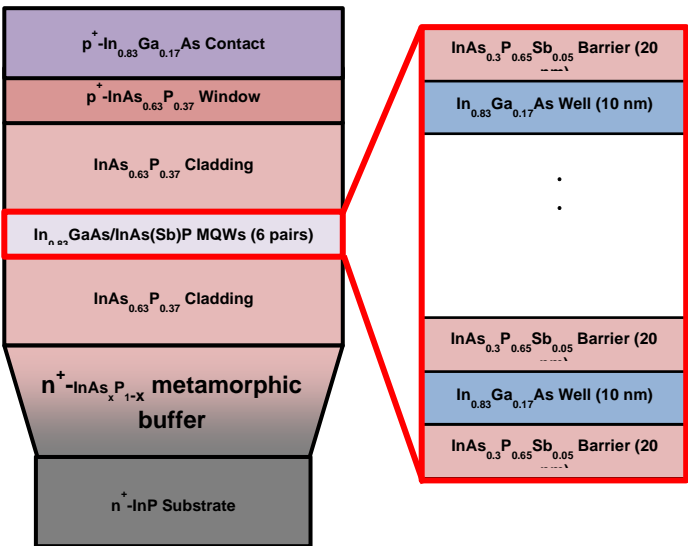


Fig.1) The structure of the InGaAs/InAsPSb MQW LED.

4. References

- [1] Buffolo M, Magri A, De Santi C, Meneghesso G, Zanoni E and Meneghini M 2021 Gradual Degradation of InGaAs LEDs: Impact on Non-Radiative Lifetime and Extraction of Defect Characteristics *Materials* 14 1114
- [2] Lee H-J, Jang I-K, An W-C, Kwac L K, Kim H-G and Kwak J S 2017 Enhanced output power of InGaAs/GaAs infrared light-emitting diode with GaIn1-xP tensile strain barrier *Current Applied Physics* 17 1582–8
- [3] Phillips A F, Sweeney S J, Adams A R and Thijs P J A 1999 The temperature dependence of 1.3- and 1.5- μm compressively strained InGaAs (P) MQW semiconductor lasers *IEEE Journal of selected topics in quantum electronics* 5 401–12

Electrically active controllable graphene metasurface phase retarder

Hyunwoo Park¹⁾, Sodam Jeong¹⁾, Hyeongi Park¹⁾, Soojung Baek²⁾, Teun-Teun Kim¹⁾

¹⁾University of Ulsan, Daehak-ro, Nam-gu, Ulsan, 93, Republic of Korea

²⁾Korea Advanced Institute of Science and Technology (KAIST), Daehak-ro, Yuseong-gu, Daejeon, 291, Republic of Korea

E-mail address: tkim@ulsan.ac.kr

Abstract: Anisotropic materials with chirality or birefringence can be used to manipulate the polarization state of electromagnetic waves, but these materials are lacking in the terahertz region. In this study, an active graphene metasurface phase retarder capable of actively controlling anisotropy was implemented in the THz region by combining graphene with an isotropic artificial metasurface. Maximum phase retardation of 90° through a metasurface with bilayer graphene suggests its use as a tunable quarter-wave plate. Continuous control from linear- to circular-polarization states may provide a wide range of opportunities for the development of compact THz polarization devices and polarization-sensitive THz technology.

1. Introduction

The polarization of electromagnetic waves plays an essential role in a wide range of fields because the electromagnetic responses of materials and devices typically depend on the polarization states of the incident electromagnetic waves. Sophisticated manipulation of polarization states is critical for the organization of complicated optical systems. Birefringence distinct refractive indices along orthogonal principal axes has been widely employed to manipulate the polarization states of electromagnetic waves. However, naturally occurring birefringence is extremely weak and requires a substantially long propagation length to obtain adequate phase retardation. Particularly in the THz regime, the lack of natural materials with strong birefringence is an obstacle to the realization of practical polarization components or devices.

For practical applications at THz frequencies, metasurfaces (the two-dimensional counterpart of metamaterials, composed of a two-dimensional array of planar structures) are among the most promising platforms due to the versatility of their design. For the realization of active metasurfaces, it becomes necessary to incorporate a tunable medium, of which the optical properties can be modulated in real-time under external stimuli. Among various tunable media, graphene is considered a versatile platform because it exhibits gate-controllable light-matter interactions through the Fermi level shift.

Here, we describe electrically controlled graphene metasurfaces (GMs) that can preferentially modulate the polarization states of THz waves. An active metasurface is formed by integrating mono- or bilayer of graphene micro-ribbons with isotropic metasurfaces. The effective refractive index along one axis can be efficiently modulated by varying the optical conductivity of the graphene micro-ribbons, thereby weakening the capacitive coupling between adjacent meta-atoms in an anisotropic manner [1]. As a result, the polarization states of an incident linearly polarized THz wave can be efficiently changed to a circularly polarized state at the output. This approach will provide a facile way of constructing ultra-compact active polarization modulators and imaging devices [1].

2. Figures

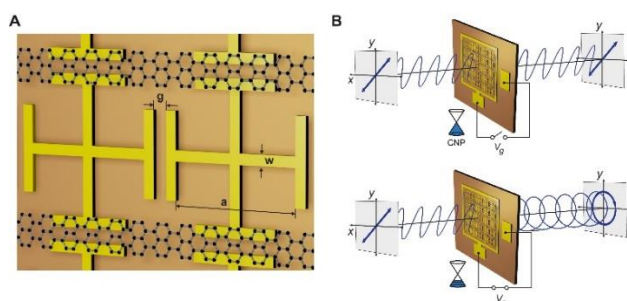


Fig. 1. Graphene metasurface for the electrical control of polarization states

3. References

- [1] Kim, T.-T. et al. Electrical access to critical coupling of circularly polarized waves in graphene chiral metamaterials. *Sci Adv* **3**, e1701377 (2017).
- [2] Park, H. et al. Electrically tunable THz graphene metasurface wave retarders. *Nanophotonics* doi.org/10.1515/nanoph-2022-0812 (2023)

Tunable THz graphene metasurface beam splitter

Hyeonggi Park¹, Sodam Jeong¹, Hyunwoo Park¹, Soojeong Baek² and Teun-Teun Kim^{1*}

¹Department of Physics, University of Ulsan 44610, Republic of Korea

²Department of Mechanical Engineering, Korea Advanced Institute of Science and Technology (KAIST)

*ttkim@ulsan.ac.kr

Abstract: We experimentally demonstrated electrically tunable Terahertz (THz) beam splitter based on graphene metasurfaces. The proposed beam splitter can significantly control the ratio of transmission and reflection of incident THz wave through modulation of graphene's conductivity by gating. The electrically tunable THz metamaterial beam splitter can be applied to various optical systems such as spectrometers, interferometers, imaging systems and THz communications.

Introduction

Beam splitter is essential devices in optics because it plays a pivotal role in optical systems such as interferometer that can measure various physical characteristics. Nevertheless, conventional beam splitters have limitations owing to bulky and heavy, which makes them unsuitable for integrated use of optical devices. In particular, the etalon effect of thick beam splitters induce time domain distortion of THz pulse due to multiple internal reflection. It is still challenging to make thin, easy integrating and high efficient beam splitter. To overcome this, we experimentally demonstrated electrically tunable transmission and reflection ratio of THz wave by varying the graphene's optical conductivity. Recently, gate-induced switching and linear modulation of THz wave can be achieved in a hybrid material system consisting of artificially constructed meta-atoms and atomically thin graphene layers [1]. The proposed metasurface beam splitter is formed by integrating graphene layer with square shaped thin file type metasurfaces (Fig. 1. (a)). Fig. 1. (c) shows that measured transmission and reflection, and it clearly shows that the etalon effect can be significantly reduced. It is also shown that the consistency of experimental and numerical results. Benefitting from the highly efficient tunable THz graphene metasurface beam splitter, the proposed beam splitter can be applied to reconfigurable intelligent surface for THz wireless communications and advanced imaging systems.

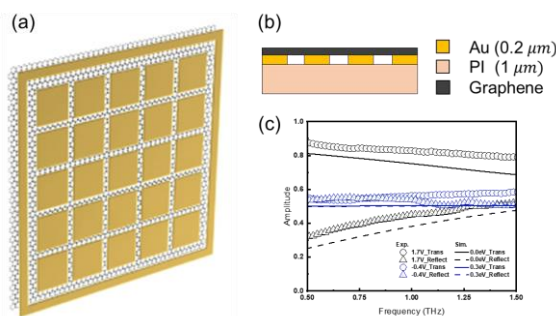


Fig. 1. (a, b) Schematic illustration of graphene metasurfaces for active beam-splitter. (c) Experimental and simulation results

References

- [1] S.Lee, *et. al.*, "Metamaterials for enhanced optical responses and their application to active control of terahertz waves" *Adv Mat.*, **32**, 2000250 (2020).

Plasmonic Contribution of Ag Nanowires Electrodes on Photovoltaic Performance of ZnO/NiO Heterojunctions

**Jungeun Song¹, Malkeshkumar Patel², Sara Evelyn Johannesson^{1,3}, Kayoung Cho⁴, Jaehong Park⁴,
Joondong Kim² and Dong-Wook Kim^{1,*}**

Department of Physics, Ewha Womans University, Seoul 03760, Korea¹

Department of Electrical Engineering, Incheon National University, Incheon 22012, Korea²

Department of Chemistry, University of Edinburgh, Edinburgh 46124, United Kingdom³

Department of Chemistry, Ewha Womans University, Seoul 03760, Korea⁴

E-mail address: dwkim@ewha.ac.kr

Transparent photovoltaic (TPV) devices have attracted growing research interest due to their high visible transmittance and the ability to selectively absorb short-wavelength sunlight [1]. TPV devices can be used in windows of buildings and vehicles, which can supply electric energy in highly populated areas. In this work, we investigated the electrical and optical properties of ZnO/NiO-heterojunction-based TPV devices. ZnO(10 nm)-coated Ag nanowires (AgNWs) were prepared as the top electrodes of our devices. The ZnO/AgNW electrodes are known to exhibit high electrical conductivity and optical transparency. Numerical calculations as well as experimental measurements were carried out to characterize the optical properties of our TPV devices. The local current-voltage spectra of the TPV devices were obtained by conductive atomic force microscopy (C-AFM). In particular, we paid attention to the photovoltaic performance of the devices with and without ZnO/AgNW electrodes. The C-AFM results showed that the photocurrent strongly depended on the wavelength and polarization direction of the incident light. When the polarization of the incident light was perpendicular to the AgNW axes, the larger photocurrent was measured. This suggested that the localized surface plasmon excitation in AgNWs could raise the optical absorption and resulting photocurrent of our solar cells [2,3]. The plasmonic contribution of the AgNWs was strongly supported by the optical spectra. Kelvin probe force microscopy measurements are also carried out to explain the plasmon-enhanced surface potential changes in our TPV devices under light illumination.

[1] M. Patel, J. Song, D. Kim, J. Kim, Appl. Mater. Today, **26**, 101344 (2022).

[2] X. Liu, B. Wu, Q. Zhang, J. N. Yip, G. Yu, Q. Xiong, N. Mathews, T. C. Sum, ACS Nano, **8**, 10, 10101-10110 (2014).

[3] I. I. Zamkoye, J. Boucle, N. Leclerc, B. Lucas, S. Vedraïne, Sol. RRL, **7**, 2200756 (2023).

Optical Characterizations of WS₂/Au and WS₂/Ag Structures Prepared by Metal-Assisted Exfoliation

Eunseo Cho, Nahyun Kim, Anh Thi Nguyen, Seoyoung Lim, Jungeun Song, Jungyoon Cho, and Dong-Wook Kim*

Department of Physics, Ewha Womans University, Seoul 03760, Korea

*Email: dwkim@ewha.ac.kr

Abstract: Transition metal dichalcogenides (TMDs) have attracted attention due to their intriguing physical properties, such as sizable bandgap energies, large exciton binding energy, and high electron mobility. TMD/metal structure fabrication and characterization are important for both material research and device applications. In this work, WS₂ flakes were prepared directly on template-stripped Au and Ag layers, instead of using polymer-based exfoliation and transfer processes.^[1] WS₂/Au and WS₂/Ag structures with a number of layers (N_{WS_2}) ranging from 1 to 10 were obtained and their optical properties were investigated. The samples' apparent colors were influenced by N_{WS_2} and the underlying metal layers. To confirm N_{WS_2} for each flake, the measured and calculated optical reflectance spectra were compared. Numerical calculations suggested that the optical absorption in the WS₂ flake (A_{WS_2}) for WS₂/Ag could be almost two times larger than that for WS₂/Au. Local maxima of A_{WS_2} were found close to the exciton resonance wavelengths of the WS₂ flakes. The peak positions of A_{WS_2} of WS₂/Ag, in particular, appeared close to the C exciton resonance and exhibited a redshift with increasing N_{WS_2} . Due to the exceptionally high refractive indices of WS₂, the optical phase shift at the WS₂/metal was quite considerable even though the flakes were much thinner than the visible wavelengths. As a result, optical resonance modes can be anticipated in WS₂/Au and WS₂/Ag with $N_{\text{WS}_2} \sim 10$. WS₂ flakes' thickness- and underlying-metal-dependent optical characteristics were also studied using micro-Raman and PL measurements.^[2] These results can help us to propose optimal WS₂/metal structures for optoelectronic devices.

[1] Heyl et. al., Adv. Mater. Interfaces 9, 2200362 (2022)

[2] Sohn et. al., J. Phys. Chem. C 121, 22517 (2017).

Energy and Charge Transfer between Monolayer WS₂ and Ti₂N MXene Quantum Dots

Wendy B. Mato, Rebekah E. Kong, Anir S. Sharbirin, Jolene W. P. Khor and Jeongyong Kim*

Department of Energy Science, Sungkyunkwan University, Suwon 16419, Korea
E-mail address: j.kim@skku.edu

MXene quantum dots (MQDs) has been proven to demonstrate excellent light-emitting properties manifesting efficient photoluminescence (PL) with various color and high quantum yield [1]. Transition metal dichalcogenides (TMDs) which are semiconductors of atomically thickness have also been extensively studied for the optoelectronic applications [2,3]. In this work, we studied the energy and charge transfer behavior of monolayer TMDs transferred on MQDs by forming the heterostructure (HS) between monolayer tungsten disulfide (WS₂) with titanium nitride (Ti₂N) MQDs. Through this fabrication, we observed the enhancement in PL in heterostructure of monolayer WS₂ and Ti₂N MQDs due to energy transfer [4]. The larger band gap energy (~3.0 eV) of Ti₂N MQDs relative to monolayer WS₂ (~2.0 eV) suggests the energy transfer of electron from MQDs to monolayer WS₂ when illuminated with 375 nm wavelength excitation. Furthermore, the PL spectral weights of the HS show larger trion distribution compared to monolayer WS₂ due to the charge transfer. We expect that by understanding the PL behavior of the HS, they could be applied to the optoelectronic applications such as imaging and sensing while expanding the use of MQDs and monolayer TMDs.

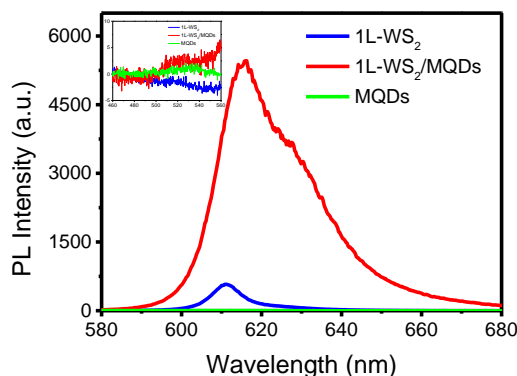


Fig. 1. PL spectra of monolayer WS₂ (blue), WS₂/Ti₂N MQDs (red), Ti₂N MQDs (green) showing the PL enhancement in the heterostructure.

References

- [1] A.S. Sharbirin et al., Opto-Electron. Adv. **4**, 200077 (2021).
- [2] S. Roy et al., J. Phys. Chem. C. **121**, 1997 (2017).
- [3] G. Wang et al., Rev. Mod. Phys. **90**, 021001 (2018)
- [4] Ebe, Hinako et al., ACS applied materials & interfaces vol. **14**,15 (2022)

Anomalous interlayer coupling depending on the twist angle of ReS₂ bilayers

Trang Thu Tran¹, Taegeon Lee², Krishna P. Dhakal^{1*}, Heesuk Rho^{2*}, Jeongyong Kim^{1,*}

¹Department of Energy Science, Sungkyunkwan University, Suwon 16419, Republic of Korea

²Department of Physics, Research Institute of Physics and Chemistry, Jeonbuk National University, Jeonju 54896, Republic of Korea

*E-mail address: dhakal@skku.edu, rho@jbnu.ac.kr, j.kim@skku.edu

Twisted lattices formed by stacking two layers of Van der Waals heterostructures (vdWHs) based on transition metal dichalcogenides (TMDs) materials have gained many interesting correlated electronic phases and optical properties.[1–3] Here, we created systems of twisted bilayer (tBL) rhenium disulfide (ReS₂) with varying twist angles using stepwise dry transfer methods. ReS₂ is a distorted (1T') phase 2D semiconductor with a direct gap at the Γ point, which is famous material of in-plane anisotropic optical and electrical properties [4], however the twisting angle dependence electronic properties such as band gap change or phonon renormalizations have not yet been investigated in this type of 1T'-2D system. We investigated the low frequency Raman modes in the twisted bilayer systems with twist angles ranging from 1° to 145° and found the presence of an interlayer breathing mode, confirming the interlayer interaction. In addition, the PL measurement showed that the band gap at the Γ point was changed by twisting angle in comparison to the naturally exfoliated bilayer. Interestingly, a 1° and 3° twisted sample mimic the exfoliated bi-layer systems in terms of the observed PL and Raman spectra while with other higher twist angles, a scenario of weaker interlayer coupling was observed over 9°. Unlike the 2H TMDs that are rigid to change the direct band gap for any of the twist angles [4] our result of PL peak position of tBL ReS₂ changed by twisting angle emphasizing interesting structural or optical phenomena in the twisted ReS₂. The possible modification of ReS₂'s flat band structure at the Γ point due to varying interlayer coupling and/or moiré potential in twisted lattices could cause the observed anomaly, which will be discussed in the presentation. Our work provides an effective and versatile means to engineer band structure of 1T'-phase ReS₂ for further applications in optoelectronic devices.

References

- [1] Quan, J.; Linhart, L.; Lin, M.-L.; Lee, D.; Zhu, J.; Wang, C.-Y.; Hsu, W.-T.; Choi, J.; Embley, J.; Young, C.; Taniguchi, T.; Watanabe, K.; Shih, C.-K.; Lai, K.; MacDonald, A. H.; Tan, P.-H.; Libisch, F.; Li, X. Phonon Renormalization in Reconstructed MoS₂ Moiré Superlattices. *Nat. Mater.* **2021**, *20* (8), 1100–1105.
- [2] Park, S.; Kim, M. S.; Kim, H.; Lee, J.; Han, G. H.; Jung, J.; Kim, J. Spectroscopic Visualization of Grain Boundaries of Monolayer Molybdenum Disulfide by Stacking Bilayers. *ACS Nano* **2015**, *9* (11), 11042–11048.
- [3] Park, S.; Kim, H.; Kim, M. S.; Han, G. H.; Kim, J. Dependence of Raman and Absorption Spectra of Stacked Bilayer MoS₂ on the Stacking Orientation. *Opt. Express* **2016**, *24* (19), 21551.
- [4] Ghimire, G.; Dhakal, K. P.; Choi, W.; Esthete, Y. A.; Kim, S. J.; Tran, T. T.; Lee, H.; Yang, H.; Duong, D. L.; Kim, Y. M.; Kim, J. Doping-Mediated Lattice Engineering of Monolayer ReS₂ for Modulating In-Plane Anisotropy of Optical and Transport Properties. *ACS Nano* **2021**, *15* (8), 13770–13780.

Deterministic control of electron density in atomically thin semiconductor

Sujeong Kim,¹ Hyeonwoo Lee,¹ Seonhye Eom,² Gangseon Ji,² Huitae Joo,¹ Soo Ho Choi,³
Ki Kang Kim,³ Hyeon-Ryeol Park,² and Kyoung-Duck Park,^{1*}

¹Department of Physics, Pohang University of Science and Technology (POSTECH), Pohang 37673, Korea

²Department of Physics, Ulsan National Institute of Science and Technology (UNIST), Ulsan 44919, Korea

³Center for Integrated Nanostructure Physics, Suwon 16419, Korea

*E-mail address: parklab@postech.ac.kr

Abstract: Electron density plays an important role in determining optical and electrical characteristics of two-dimensional (2D) transition metal dichalcogenide (TMDs), leading to versatile applications of optoelectronic devices. Here, we present a nanoscale electric pulse generator induced by the plasmonic metallic tip, enabling spatial modification of the electron density at the nanoscale region in a reversible manner. We demonstrate the frequency-dependent modulation of photoluminescence (PL) intensity, confirming the nanoscale modification of the electron depletion region.

1. Introduction

Controlling the electron density of two-dimensional (2D) transition metal dichalcogenide (TMDs) plays an important role in optoelectronics devices, determining optical and electrical characteristics of devices. A recent study has shown that the electrostatic doping of TMDs monolayer enhances photoluminescence (PL) quantum yield [1]. Here, we present a tip-induced nanoscale electric pulse generator to regulate the local electron density, which consequently enhances PL quantum yield at the nanoscale region. Specifically, we manipulate the electron depletion region to control the PL quantum yield of TMDs monolayer at the nanoscale. Quantitative analysis of the obtained PL intensity with a theoretical model confirms the dynamic controllability of electron depletion region in our experiment. We envision that this modality paves the way toward the electrically tunable nano-optoelectronic devices.

2. Results

We apply DC electric field by the metallic tip at the quantum tunneling regime to control the electron density of MoS₂ monolayer. By applying positive gate voltage, electrons move from MoS₂ monolayer to the metallic tip, as shown in Fig. 1a. It leads to the formation of the electron depletion region at the vicinity of the tip and correspondingly enhanced PL intensity, as shown in Fig. 1b. We then manipulate the frequency of the electric pulse. Increasing the frequency of electric pulse indicates the decreased effective time of electron transport, which consequently reduces the electron travel range and limits the electron depletion region. Fig. 1c shows the resultant deterministic control of electron depletion region by frequency modulation of nanoscale electric pulse. Indeed, we confirm the reduction of the electron flow from MoS₂ monolayer to the metallic tip, by increasing the frequency of electric pulse, as shown in Fig. 1d. By applying high frequency electric pulse to the MoS₂ monolayer, the current from MoS₂ monolayer to the metallic tip is instantaneously saturated, implicating the deterministic electron depletion region with the high frequency electric pulse.

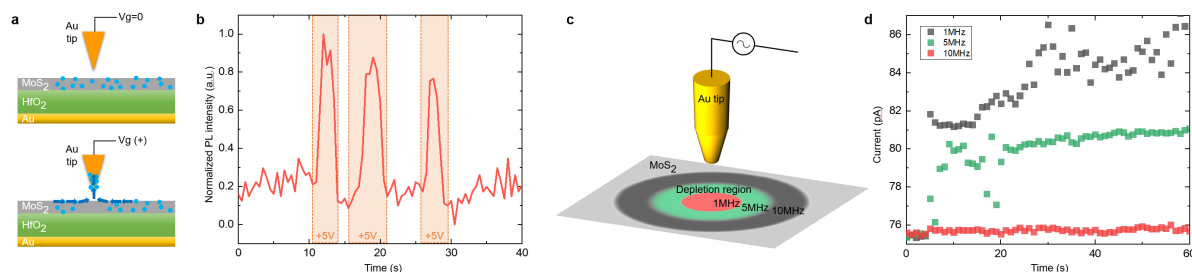


Fig. 1. (a) Schematic illustrations of the electron population control by the metallic tip at the quantum tunneling regime. (b) PL intensity switching of MoS₂ Monolayer applying dc electric field. (c) The illustration of manipulating the frequency of nanoscale electric pulse and corresponding electron depletion region. (d) The frequency-dependent electron flow of MoS₂ Monolayer.

3. References

[1] Der-Hsien Lien., Shiekh Zia Uddin, Matthew Yeh, Matin Amani, Hyung Jin Kim, Joel W. Ager III, Eli Yablonovitch and Ali Javey, Science. **364**, 6439 (2019).

Prediction of Quantum Yields of 2D-Transition Metal Dichalcogenides by Machine Learning

Jolene W. P. Khor, Trang Thu Tran, Anir S. Sharbirin and Jeongyong Kim*

Department of Energy Science, Sungkyunkwan University, Suwon 16419, Korea

*j.kim@skku.edu

Transition metal dichalcogenide (TMD), a two-dimensional (2D) semiconducting material, have recently attracted the interests of many research due to its advantages compared to the bulk materials, especially in optoelectronic applications originating from its strong light emissive properties in visible range. Photoluminescence quantum yield (PLQY) is an important factor in characterizing the optical properties of monolayer TMDs (1L-TMDs). PLQY is used to measure the efficiency of light emission of a material, which is important for various optoelectronics applications such as light-emitting diodes, photovoltaics, and lasers [1]. Although there are existing experimental methods for PLQY measurement of 1L-TMD, the PLQY heavily depends on PL spectra, indicating that PLQY can be conveniently predicted by analyzing the spectral shape of PL spectra and the experimental conditions used to obtain the PL spectra [1-3]. QYs of organic fluorescent materials was previously predicted using molecular descriptors by employing data-driven technique [4], however the prediction of PLQYs of 1L-TMDs was not explored so far.

Machine learning (ML), a subset of artificial intelligence, has drawn a lot of attention because of its outstanding ability to recognize and understand massive amounts of data efficiently [5], and ML-driven methodologies has been employed effectively in 2D materials researches [6,7].

In this study, we conducted PLQY measurements on exfoliated 1L-TMDs and more than 1,200 experimental PL spectra and their corresponding PLQY values, were used as our database for ML model development. A total of 11 features extracted from PL spectra and the experimental conditions, were used as the input variables, and the absolute PLQY values as the output variables, to train the model using the Extreme Gradient Boosting (XGBoost) ML algorithm. The result showed a strong linear correlation between experimental PLQY and XGBoost-predicted PLQY, suggesting the high accuracy of the model's prediction. Utilizing the Shapley additive explanation (SHAP), we also found that generation rate is essential in PLQY prediction of 1L-TMD.

[1] S. Roy, A.S. Sharbirin, Y. Lee, W.B. Kim, T.S. Kim, K. Cho, K. Kang, H.S. Jung, J. Kim, *Nanomaterials* **10**, 1032 (2020).

[2] G. Weber, F.W. Teale, *Trans. Faraday Soc.* **53**, 646 (1957).

[3] J.C. de Mello, H.F. Wittmann, R.H. Friend, *Adv. Mater.* **9**, 230–232 (1997).

[4] C.-W. Ju, H. Bai, B. Li, R. Liu, *J. Chem. Inf. Model.* **61**, 1053–1065 (2021).

[5] Y. LeCun, Y. Bengio, G. Hinton, *Nature* **521**, 436–444 (2015).

[6] A.C. Rajan, A. Mishra, S. Satsangi, R. Vaish, H. Mizuseki, K.-R. Lee, A.K. Singh, *Chem. Mater.* **30**, 4031–4038 (2018).

[7] A.Y. Lu, L.G. Martins, P.C. Shen, Z. Chen, J.H. Park, M. Xue, J. Han, N. Mao, M.H. Chiu, T. Palacios, V. Tung, J. Kong, *Adv. Mater.* **34**, 2202911 (2022).

Prediction of Quantum Yields of MXene Quantum Dots by Machine Learning

Shamima Afroz, Jolene W. P. Khor, and Jeongyong Kim*

Department of Energy Science, Sungkyunkwan University, Suwon 16419, Korea

*j.kim@skku.edu

MXene ($M_{n+1}X_n$) is an emerging class of layered two-dimensional (2D) materials, which are derived from their bulk-state MAX phase ($M_{n+1}AX_n$, where M: early transition metal, A: group element 13 and 14, and X: carbon and/or nitrogen). MXenes have found wide-ranging applications in energy storage devices, sensors and catalysis owing to their high electronic conductivity and wide range of optical absorption. Research has shown that quantum dots (QDs) derived from MXene (MQDs) not only retain the properties of the parent MXene but also demonstrate significant improvement on light emission and quantum yield (QY). Recently, work on light-emitting MQDs has shown good progress, and MQDs exhibiting multi-color PL emission along with high QY have been fabricated [1]. MXene-based quantum dots (MQDs), which are obtained by fragmenting MXenes into a nanometer scale, can display photoluminescence (PL), suggesting light-emitting applications for bandgap-less MXenes [2]. Photoluminescence quantum yield (PLQY) is an important factor to identify the optical properties of MQDs. PLQY is used to measure the light emission efficiency of a material, which is important for various optoelectronics function such as lasers, photodiodes, and optical fiber communications [3]. Although there are existing experimental methods for PLQY measurement of MQDs, the PLQY mainly depends on PL spectra. Therefore, by analyzing the spectral shape of PL spectra and the experimental conditions used to obtain the PL spectra, PLQY can be predicted [3-5]. Based on past research, QYs of carbon dots was predicted using alkaline catalysts by utilizing data-based methodology [6], however the prediction of PLQYs of MQDs was not studied so far.

A subset of artificial intelligence, machine learning (ML) has attracted much attention due to its outstanding ability to efficiently recognize and understand large amounts of data [7]. ML-driven methods are being effectively employed in various scientific research areas of optics and photonics where it can serve as a powerful tool for the on-demand design of photonic devices [8].

Using ML-techniques we investigated PLQYs prediction of MQDs. In this study, we conducted PLQY measurements on synthesized MQDs and used the obtained results of PL spectra and their corresponding PLQY values to develop the ML model for prediction. To train the model using ML algorithm, features extracted from PL spectra and the experimental conditions were used as the input variables, and the absolute PLQY values were used as the output variables.

- [1] Sharbirin, Anir S., Sophia Akhtar, and Jeongyong Kim. "Light-emitting MXene quantum dots." *Opto-Electronic Advances* 4, no. 200077-1. 3, (2021).
- [2] Sharbirin, Anir S., Shrawan Roy, Trang Thu Tran, Sophia Akhtar, Jaspal Singh, Dinh Loc Duong, and Jeongyong Kim. "Light-emitting Ti 2 N (MXene) quantum dots: synthesis, characterization and theoretical calculations." *Journal of Materials Chemistry C* 10, no. 16: 6508-6514, (2022).
- [3] S. Roy, A.S. Sharbirin, Y. Lee, W.B. Kim, T.S. Kim, K. Cho, K. Kang, H.S. Jung, J. Kim, *Nanomaterials* **10**, 1032, (2020).
- [4] G. Weber, F.W. Teale, *Trans. Faraday Soc.* **53**, 646, (1957).
- [5] J.C. de Mello, H.F. Wittmann, R.H. Friend, *Adv. Mater.* **9**, 230-232, (1997).
- [6] Han, Y., Tang, B., Wang, L., Bao, H., Lu, Y., Guan, C., Zhang, L., Le, M., Liu, Z. and Wu, M. Machine-learning-driven synthesis of carbon dots with enhanced quantum yields. *ACS nano*, *14*(11), pp.14761-14768, (2020).
- [7] Y. LeCun, Y. Bengio, G. Hinton, *Nature* **521**, 436-444, (2015).
- [8] Duan, B., Wu, B., Chen, J.H., Chen, H. and Yang, D.Q. Deep learning for photonic design and analysis: Principles and applications. *Frontiers in Materials*, p.592, (2022).

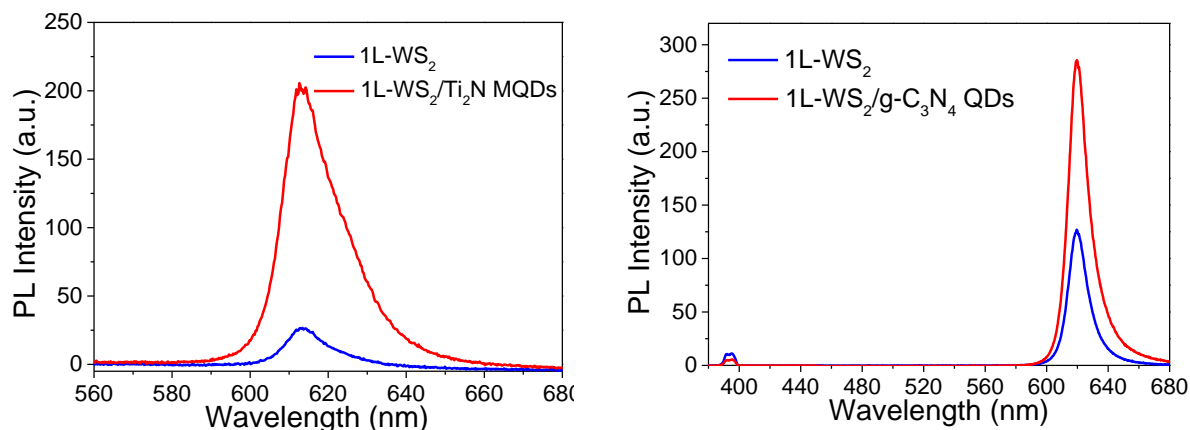
UV-excited Photoluminescence of 0D-2D Heterostructures

Rebekah E. Kong, Wendy B. Mato, Anir S. Sharbirin, Jolene W. P. Khor, and Jeongyong Kim*

Department of Energy Science, Sungkyunkwan University, Suwon, 16419, Republic of Korea

*Email: j.kim@skku.edu

Transition Metal Dichalcogenides (TMDs), are atomically thin two-dimensional (2D) semiconducting materials with a direct optical band gap when thinned to the monolayer limit [1]. Thus far, significant research efforts have been devoted to the properties of 2D TMDs in diverse fields which have been widely publicized in various applications. Recent achievements of quantum dots (QDs) derived from 2D materials have affirmed their auspicious applications in the bio imaging, batteries, optoelectronic devices, electrochemical water splitting as well as sensors industries thanks to their fascinating optical, electrical, catalytic and electrochemical characteristics [2]. Herein, we explore the PL behavior in 2D TMDs monolayers (1L-TMDs) interfaced with QDs derived from different 2D materials, particularly MXene and graphitic carbon nitride. The PL emission of 1L WS₂ from QDs on-region was considerably enhanced when irradiated with a 375nm laser regardless of the QDs used. These results indicate the exciting potential of 2D-QDs in tuning the luminescent properties of single-layer TMDs via UV excitation (3.31 eV). We believe these 0D/2D heterostructures could have promising applications in quantum optoelectronics or light-emitting technologies.



References

- [1] A. Boulesbaa et al., *J. Am. Chem. Soc.*, **138**, 14713 (2016)
- [2] A. Manikandan et al., *Progress in Quantum Electronics*, **68**, 100226 (2019)

Patternable MXene (Ti_3C_2) electrodes for flexible optoelectronic devices

Jiseong Jang¹, Dae Young Park², Hyeon Jung Park², and Mun Seok Jeong^{2,*}

¹Department of Energy Science, Sungkyunkwan University

²Department of Physics, Hanyang University

E-mail address: mjeong@hanyang.ac.kr

Abstract: MXenes are two-dimensional transition metal carbides, nitrides, and carbonitrides that have attractive properties such as high specific surface area, large interlayer spacing, active surface site, and high electrical conductivity [1,2]. Among them, titanium carbide (Ti_3C_2) has been widely researched for energy storage devices and flexible electrodes with its noteworthy high electrical conductivity ($\sim 11,670$ S/cm) [3,4]. The MXene electrodes are generally coated by a simple spin-coating process. However, spin-coating has a limit for patterned electrodes.

In this work, we used spray-coating for MXene electrode fabrication. MXene was successfully prepared from Ti_3AlC_2 by HF-based etching solution. 2D Te film with MXene electrode exhibited comparable device performance with metal electrodes such as on-off ratio of $\sim 10^2$, and maximum mobility of ~ 0.5 $\text{cm}^2/\text{V}\cdot\text{s}$. Also, MXene electrodes are well fabricated on a flexible substrate and stable for the bending cycle. The results provide a guideline for patternable MXene electrodes for optoelectronic devices.

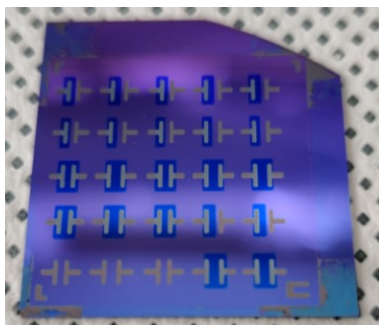


Fig. 1. Spray coated MXene electrode



Fig. 2. Flexibility of MXene electrode

[1] Y. Gogotsi, and B. Anasori, ACS Nano **13**, 8491-8494 (2019).

[2] S. K. Hwang, S. M. Kang, M. Rethinasabapathy, C. Roh, and Y. S. Huh, Chem. Eng. J. **397**, 125428 (2020).

[3] S. Ahn, T. H. Han, K. Maleski, J. Song, Y. H. Kim, M. H. Park, H. Zhou, S. Yoo, Y. Gogotsi, and T. W. Lee, Adv. Mater. **32**, 2000919 (2020).

[4] B. Lyu, M. Kim, H. Jing, J. Kang, C. Qian, S. Lee, and J. H. Cho, ACS Nano **13**, 11392 (2019).

The variation of optical properties in the hydrothermally synthesized 2D Tellurium by laser treatment

**In Cheol Choi^{1,2}, Dae Young Park², Kang-Nyeong Lee³, Dong Hyeon Kim^{2,3}, Chae Won Lee²,
Hyung Mo Jeong^{1,4*}, Mun Seok Jeong^{2*}**

¹Department of Smart Fab. Technology, Sungkyunkwan University, Korea

²Department of Physics, Hanyang University, Korea

³Department of Energy Science, Sungkyunkwan University, Korea

⁴School of Mechanical Engineering, Sungkyunkwan University, Korea

E-mail address: incheolu@naver.com, mjeong@hanyang.ac.kr

The 2-dimensional (2D) semiconductors such as graphene, transition dichalcogenides (TMDCs) and black phosphorus (BP) have great potential, and they are next-generation semiconductor channel after silicon.

The field effect transistor with hydrothermally synthesized 2D Tellurium which is one of the 2D materials have been reported in 2018[1]. The 2D Tellurium demonstrated high field effect mobility ($\sim 500 \text{ cm}^2/\text{Vs}$) with p-type semiconducting property ($E_g \sim 0.4 \text{ eV}$), comparing with BP, it also showed outstanding stability under ambient. Many reported 2D Tellurium papers used hydrothermally synthesized 2D Tellurium since mechanical exfoliation is impossible due to the narrow interlayer distance.

The PVP, which is widely used as a capping ligand in the synthesis of nanomaterials, is known to give an n-doping effect due to the electron donating group of long carbon chain. In the case of 2D Tellurium synthesized by hydrothermal method, PVP is used as capping ligand, indicating the interaction of PVP and 2D Tellurium existed. In this work, the unique Photoluminescence (PL) in hydrothermally synthesized 2D Tellurium was observed at different position of pure PVP. The newly observed PL peak was confirmed as charge transfer exciton between LUMO of PVP and valence band of 2D Tellurium via Raman scattering, IR nanoscopy, and AFM.

[1] Yixiu Wang, Gang Qiu, Ruoxing Wang, Shouyuan Huang, Qingxiao Wang, Yuanyue Liu, Yuchen Du, William A. Goddard III, Moon J. Kim, Xianfan Xu, Peide D. Ye and Wenzhuo Wu, " Field-effect transistors made from solution-grown two-dimensional tellurene", Nat. Electron., 1 (2018), 228–236.

MAPbBr₃ Perovskite Quantum Dots Size Effect with Polarity of Solvent

SeongOn Park^{1,2}, DoKyum Kim², Clare C. Byeon^{1*}, Chang-Lyoul Lee^{2*}

Department of Mechanical Engineering, Kyungpook National University, Dague 41566, Republic of Korea.¹

Advanced Photonics Research Institute (APRI), Gwangju Institute of Science and Technology (GIST), Gwangju 61005, Republic of Korea.²

byeon@knu.ac.kr^{1*}, vespr@gist.ac.kr^{2*}

Abstract: Methylammonium lead perovskite (MAPbX₃) shows the excellent optoelectronic properties such as being color tunable over entire visible range. There are several ways to change the emitting wavelength such as combination of the halides, changing synthesis temperature, control the growth conditions by ligand engineering. However, halide combination may undergo ion migration in electronic field and temperature control during synthesis limits the choice of solvent. We propose the size control of MAPbBr₃ Perovskite quantum dots (PQDs) by varying the polarity of solvent to change the emission wavelength without changing synthesis temperature or halide composition. As a result, the size of our MAPbBr₃ PQDs decreased from ~10.1 nm to 3.1 nm, showing the PL spectrum blue-shifted from ~ 511 nm to ~ 478 nm depending on the polarity of the solvent.

Keywords: Perovskite Quantum Dots, Blue perovskite, Solvent polarity, Wavelength tunable perovskite

Elimination of Unavoidable Doping Effects by Passivation Layers in InSe FET via CYTOP/TFSI Composite Treatment

Chan Kwon, Hyeon Jung Park, Ji eun Jo, Dae Young Park, and Mun Seok Jeong*

Department of Physics, Hanyang University, Seoul, 04763, Republic of Korea
chan940319@hanyang.ac.kr

The recent interest in post-transition metal chalcogenides (PTMCs) has led to the investigation of indium selenide (InSe), a III-VI semiconductor compound with excellent electrical properties. However, previous study reports that InSe FETs degrade their performance in ambient air because of their vulnerability to moisture and oxygen. Recent studies attempted to passivate InSe FETs using Poly methyl methacrylate (PMMA) and CYTOP. However, the polymer passivation layer induces unavoidable doping effects and causes the device to lose its intrinsic property.

In this study, The n-type doping effect of CYTOP used as a passivation layer was effectively controlled by Bis (trifluoromethane) sulfonimide (TFSI) compositing. This CYTOP/TFSI composites spin-coated on the surface of InSe FETs and analyzed their stability and electrical properties according to the concentration of TFSI.

The n-type doping effect of CYTOP in the device was successfully offset by TFSI, which has a p-type doping effect. The doping effect was completely canceled when the concentration of TFSI/CYTOP was 15 mg/ml, which can protect the device from ambient air while maintaining intrinsic device performance. This work can contribute to the development of InSe devices with air stability and various device applications using 2D semiconductors with intrinsic properties.

Investigating the Influence of Surface Schottky Barriers on Localized Optoelectronic Properties of MoS₂

Deogkyu Choi¹, Juchan Lee¹, Chaewon Lee¹, Chan Kwon¹, Jieun Jo¹, Seungho Bang¹, Hyeon Jung Park¹,
Dae Young Park¹, Yo Seob Won², Soo Ho Choi², Ki Kang Kim², and Mun Seok Jeong^{1,*}

¹Department of Physics, Hanyang University (HYU), Seoul 04763, Republic of Korea

²Department of Energy Science, Sungkyunkwan University (SKKU), Suwon 16419, Republic of Korea

Presenter: ejrrb379@hanyang.ac.kr (Deogkyu Choi)

corresponding author: mjeong@hanyang.ac.kr (Mun Seok Jeong)

The use of ultrathin materials has been attractive as a new type of electronics and optoelectronics due to their remarkable performances and promising applicability. However, their reliability is still a challenge due to unexpected degrading factors up to the present. Herein, the influence of Schottky barrier height (SBH) on optoelectronics based on monolayer molybdenum disulfide is explored. A significant reduction of photocurrent in the contact area is observed by measuring the localized photocurrent as a function of device location. The oppositely induced space charge region (OI-SCR) caused by a negative SBH attracts localized metal-insulator transition and interrupts the photo-excited carrier recombination process. The responsivity and detectivity of the channel region are simultaneously higher than the OI-SCR. In the case of the recombination process, the dominant trap states could act as recombination centers or deep-level traps, depending on the position. The deep trap states in the OI-SCR caused a slower response time, resulting in two times slow-respond than the channel region. Our study provides novel insights into the effects caused by the metal-semiconductor interface states on optoelectronic devices and its essential role in designing 2D material-based optoelectronics.

Key words: Schottky barrier height, optoelectronics, localized photocurrent, oppositely induced space charge region

2023 APNFO abstract

The Stability Investigation of Polymer-Dopant Composite-coated Post-Transition Metal Chalcogenide

Ji Eun Jo, Dae Young Park, Chan Kwon, Hyeon Jung Park, and Mun Seok Jeong*

Department of Physics, Hanyang University, Seoul, Republic of Korea

Post-transition metal chalcogenides (PTMCs), which consist of layered structures formed by combining post-transition metals (Group III) and chalcogenides (Group VI), exhibit excellent electrical properties and an adjustable bandgap, making them promising candidates for next-generation materials. In particular, InSe has attracted attention due to its outstanding features, including high carrier mobility ($\sim 300\text{cm}^2/\text{Vs}$ at RT) and unique thickness-dependent behavior with an indirect band gap for few layers while a direct band gap for bulk layers when exceeding a critical thickness [1]. Despite the advantages of InSe, it is difficult to utilize due to its instability in air. InSe is sensitive to moisture, and oxidation occurs spontaneously when exposed to air.

To address this issue, a polymer-dopant composite was developed to protect the surface of InSe from oxygen and water. The composite was fabricated by mixing PMMA and Benzyl viologen (BV) for n-type doping and spin-coated onto the InSe surface. Raman spectroscopy and electrical measurements were performed to investigate the effect of dopant concentration on the InSe surface. It was found that using PMMA polymer alone is insufficient for preventing oxidation, and that changes in the Raman peak position and electrical properties occur after composite coating.

In this work, Raman spectroscopy and electrical measurements effectively revealed the oxidation tendency and doping effect of InSe. Furthermore, this result provides a potential solution for fabricating InSe devices that exhibit improved stability and performance in atmospheric environments.

[1] *InfoMat* 2021, 3 (6) , 662-693.

[2] *ACS Nano* 2017, 11, 7, 7362–7370

Dark Excitons from WSe₂ Monolayer on the Au Micro-pillar Structures

Ga Hyun Cho, Hyun Jeong, Hyeong Chan Suh, Mun Seok Jeong

Department of Physics, Hanyang University

E-mail address: physicscho@naver.com

WSe₂ monolayer is a direct bandgap semiconductor whose optical properties are dominated by the presence of bound electron-hole pairs, namely excitons. WSe₂, a member of the larger class of semiconducting transition metal dichalcogenides (TMDs), has an attractive property: its monolayer has an optically dark exciton. Dark excitons have much longer radiative lifetimes than bright excitons. Therefore, these dark excitons are appealing candidates for quantum computing and optoelectronics.

However, the process of generating dark excitons in WSe₂, which is currently being studied, is complicated. Most experiments are performed at cryogenic temperatures and use difficult methods, such as applying magnetic fields. Here, we report a method for generating dark excitons in WSe₂ through micro-pillar structures very easily, without the complexity of other physical or chemical methods. We show a ~40 meV intravalley energy splitting between the dark and bright exciton. We also show that significantly enhanced PL intensity was observed in WSe₂ on Au micro-pillars as compared to that on SiO₂ plate and on Au plate, respectively. WSe₂ has a PL lifetime of 146 ps on Al₂O₃ and 270 ps on Au MPs, respectively. These values indicate that the dark exciton is observable when there is strong crystalline strain and gold surface plasmon interaction. Note that the monolayer WSe₂ intrinsic radiative decay time is only a few ps.

Through our research, the dark excitons, which play an important role in optically controlled information processing, can be generated from the WSe₂ monolayer in a simple way, bringing us one step closer to the commercialization of dark excitons.

The band gap widening of 2D Tellurium via the formation of TeO₂

Chaewon Lee¹, Dae Young Park¹, In Cheol Choi², Mun Seok Jeong^{1*}

1 Department of Physics, Hanyang University, Seoul 04763, Republic of Korea

2 Department of Smart Fab. Technology, Sungkyunkwan University, Suwon 16419, Republic of Korea

Presenter: leech5424@hanyang.ac.kr (Chaewon Lee)

Corresponding Author: mjeong@hanyang.ac.kr (Mun Seok Jeong)

Two-dimensional (2D) semiconductors have been intensively studied due to excellent optical and electrical properties with high flexibility. In the electronics, both p- and n-type semiconductor are essential components to fabricate various logic circuits. However, a few p-type semiconductors have been applied although numerous n-type semiconductors have been studied. Black phosphorous, representative p-type semiconductor have attracted the interest of scientists, however its instability under ambient conditions is the main drawback in the fields of fundamental study and practical application. To solve this problem, 2D tellurium with high stability and field effect mobility is recently reported. However, high off current of BP and Te originating from the narrow band gap energy (~ 0.4 eV) is still challenging issue in p-type semiconductor. In this study, we prepared 2D TeO₂, p-type semiconductor with a wide bandgap (3.28 eV) using the oxidation of hydrothermally synthesized 2D Te to solve the narrow bandgap problem. The β -TeO₂ phase was successfully formed by two different oxidation process using UV-O₃ and thermal treatment. This work can be contributed to the exploit of electronics with 2D semiconductors by addressing the p-type semiconductor issues.

Optical characterization of GaSb buffer for growth of InAs/GaSb superlattice

Jong Won Cha¹, Tae In Kang¹, JaeDu Ha¹, Gyoung Du Park¹, Jong Su Kim^{1*}, Sang Jun Lee²

¹Department of Physics, Yeungnam University, Gyeongsan 712-749, Korea

²Nano Materials Evaluation Center, Korea Research Institute of Standards and Science, Daejeon 305-340, Korea

E-mail address: jongsukim@ynu.ac.kr

Abstract: We conducted optical characterization of GaSb buffer layers grown by MBE on n-type GaSb substrates at various growth temperatures (485, 515, 540, and 570 °C) using PL and PR measurements in order to grow an InAs/GaSb superlattice type-II structure. PL results showed that at 17K, Ga-antisite and Ga-vacancy defects were observed around 0.70 eV and 0.72 eV in the 480 °C and 515 °C samples, respectively. In addition, Ga-rich defects were clearly observed in the signal at 0.771 eV for the 515 °C growth temperature. The signal for the acceptor-bound exciton transition was observed at 0.79 eV for all growth temperatures. Based on this, we compared the emission coefficient k by varying the power of the excitation source at low temperatures. PR results showed a comparison of internal electric fields through the FKO signal.

1. Introduction to main text format and page layout

InAs/GaSb superlattice type-II structure has received significant attention in the fields of electrical engineering and material science due to its excellent electrical properties, such as high electrical conductivity. It has various applications in fields such as infrared detectors, quantum infrared lasers, photovoltaic devices, and high-speed transistors, and has been successfully applied as a detector element.[1-3] To successfully grow the InAs/GaSb superlattice structure, the quality of the GaSb buffer must be considered. In particular, for GaSb buffers grown using Molecular Beam Epitaxy (MBE), complex defects such as Ga-antisite and Ga-vacancy, as well as compensation by acceptors and donors, are important factors that can affect the electrical, optical, and magnetic properties of the device. We analyzed and evaluated the optical properties using Photoluminescence(PL) and Photoreflectance (PR) experiments by varying the growth temperature of GaSb on the substrate.

2. Figures and tables

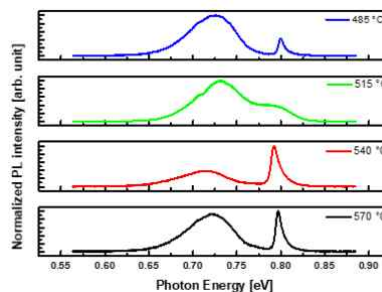


Fig. 1. PL result at 17K

3. Equations

$$f = \frac{2}{3\pi} \sqrt{2\mu} \left(\frac{1}{e\hbar F} \right) \quad (1)$$

4. References

- [1] ALTARELLI, M. Electronic structure and semiconductor-semimetal transition in InAs-GaSb superlattices. Physical review B, 1983, 28:2: 842.
- [2] WEI, Yajun; RAZEGHI, Manijeh. Modeling of type-II InAs/GaSb superlattices using an empirical tight-binding method and interface engineering. Physical Review B, 2004, 69:8: 085316.
- [3] RODRIGUEZ, J. B., et al. MBE growth and characterization of type-II InAs/GaSb superlattices for mid-infrared detection. Journal of Crystal Growth, 2005, 274.1-2: 6-13.

A study on the defect density of InAsP metamorphic buffer structure using photoreflectance spectroscopy

Gyoung Du Park¹, Jae Du ha¹, Tae In Kang¹, Jong Su Kim^{1,*}, Sang Jun Lee²

¹Department of Physics, Yeungnam University, Gyengsan, Korea

²Korea Research Institute of Standards and Science, Daejeon, Korea

E-mail address: jongsukim@ynu.ac.kr

Abstract: The metamorphic buffers with progressively modified compositions relieve strain caused by lattice mismatch in the active layer of III-V devices and reduce the density of crystalline defects and threading dislocations, improving device quality. Therefore, we focus on the careful design and high-quality, optical and internal electrical properties of modified buffer structures for InAs_xP_{1-x} composition grade buffers on InP substrates by metal-organic chemical vapor deposition (MOCVD). The electric field (F) is characterized through photoreflectance (PR) measurements. Comparing the PR spectrum at 300K based on the overshoot layer result with the PR spectrum, it can be seen that the As composition is in a similar position to the main oscillation signal at around 0.81eV, 0.72eV, and 0.61eV. $x = 0.5, 0.55$, and 0.7 , respectively. In addition, a Franz-Keldysh oscillation (FKO) signal was observed in the energy region above the optical bandgap. The FKO signal can be analyzed by Fast-Fourier Transform (FFT) method to calculate the F value of the sample interface. FFT results The FFT frequency values of $15.79 \text{ eV}^{-3/2}$, $46.32 \text{ eV}^{-3/2}$, $78.14 \text{ eV}^{-3/2}$ are InAs_{0.7}P_{0.3} samples, $29.81 \text{ eV}^{-3/2}$, $77.89 \text{ eV}^{-3/2}$ and $131.29 \text{ eV}^{-3/2}$ (InAs_{0.55}P_{0.45} samples), $14.58 \text{ eV}^{-3/2}$, $41.89 \text{ eV}^{-3/2}$ and $80.39 \text{ eV}^{-3/2}$ InAs_{0.5}P_{0.5} samples. As a result of calculating these FFT frequency values as F values, it was confirmed that the InAs_{0.55}P_{0.45} samples had lower F values up to 70 kV/cm compared to other samples. This result suggests that the InAs_{0.55}P_{0.45} sample has a lower defect density than the other samples. In general, if a photoelectric charge continuously occurs in a sample, the intensity of F may decrease because a charge electric field is accumulated near the electric field and shields the electric field. Known as the field screening effect, this effect causes the photovoltaic effect. At this time, the defect caused photo-generated carrier trapping and was consumed by a non-radiative recombination process. Therefore, a decrease in defects leads to an increase in the field screening effect of reducing F. In conclusion, from the F values calculated through the PR spectrum, when using the InAs_{0.55}P_{0.45} sample in the metamorphic buffer, the defects such as crystallographic defect density and threading dislocation in the active layer of the device are expected to decrease and improve efficiency.

Investigate the optical and electrical properties of InGaAs, and InAsP extended SWIR detector

Jiseong Go¹, Taein Kang¹, Jaedu Ha¹, Jongsu Kim^{1*}, Youngho Kim², Jieun Kang, and Sangjun Lee²

¹Department of physics, Yeungnam university, Gyengsan 38541, Korea

²Korea Research Institute of Standard and Science, Daejeon 34113, Korea
jongsukim@ynu.ac.kr

Abstract— InAs_{0.85}P_{0.15} and In_{0.63}Ga_{0.17}As active layers are on n+-InAs_xP_{1-x} denatured buffer grown by Metal-Organic Chemical Vapor Deposition (MOCVD). Photoluminescence (PL) measurement was performed at room temperature to understand the optical properties of the two samples. The PL peaks of InAs_{0.85}P_{0.15} and In_{0.83}Ga_{0.17}As were 0.496 eV and 0.486 eV, respectively. To measure the electrical characteristics of the two samples, I-V measurement, and Time-resolved photocurrent (TRPC) measurement were performed.

Keywords—Photoluminescence; Time-resolved photocurrent; I-V; SWIR

I. INTRODUCTION

The short-wavelength infrared (SWIR) detectors are being extensively studied for applications in related technologies such as non-destructive, non-contact infrared spectroscopy, pharmaceutical, and agricultural quality screening [1], air and hazardous substance detection [2], and medical diagnostic device development [3]. Therefore, it is necessary to fabricate a faster and more sensitive detector device and to evaluate the optical and electrical properties of the device. Here, InAs_{0.85}P_{0.15}/InP and In_{0.83}Ga_{0.17}As/InP are introduced as extended SWIR devices that measure longer wavelengths (up to 3.4 μ m). the two samples were grown through MOCVD, and the buffer of the metamorphic structure was grown in consideration of the difference between the substrate and the lattice constant.

Figure. 1 shows the result of PL measurement at room temperature using a 532 nm Continuous Wave laser to investigate the optical characteristics of the two samples. As a result of PL measurement, the PL peak of InAs_{0.85}P_{0.15} at room temperature was 0.496 eV, and the PL peak of In_{0.83}Ga_{0.17}As was 0.486 eV. This means that the In_{0.83}Ga_{0.17}As detector reacts at longer wavelengths than the InAs_{0.85}P_{0.15} detector. This is thought to be a difference in quality.

Figure. 2 compares the attenuation time of the photoelectric current formed by light through TRPC measurement without bias of the two samples. In Figure 2, the carrier lifetime of the In_{0.83}Ga_{0.17}As sample was shorter 10 μ s than that of the InAs_{0.85}P_{0.15} sample. Therefore, since the In_{0.83}Ga_{0.17}As response speed is faster, it is more suitable than InAs_{0.85}P_{0.15} as a detector.

Figure. 3 shows the results of analyzing the dark currents of the two samples through I-V measurement. The measured unit cell was consistent with the unit cell measured by TRPC, the In_{0.83}Ga_{0.17}As sample reacted more sensitively to the bias voltage than InAs_{0.85}P_{0.15}, and the response according to the magnitude of the reverse dark current was consistent with the trend of the photoelectric current attenuation time measured by TRPC. The optical and electrical properties of two samples In_{0.83}Ga_{0.17}As and InAs_{0.85}P_{0.15} grown with MOCVD for use as SWIR detectors were investigated.

1. HP Hansen et al., Proceedings Volume 6939, Thermosense XXX; 693901 (2008)

2. LH Matthies et al., Proceedings Volume 5083, Unmanned Ground Vehicle Technology V; (2003)

3. MP Edgar et al., Scientific Reports 5, Article number: 10669 (2015)

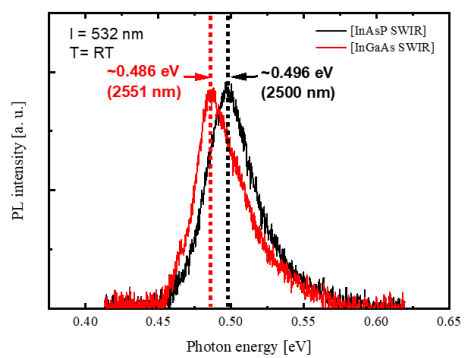


Fig. 1. PL results at room temperature for both samples.

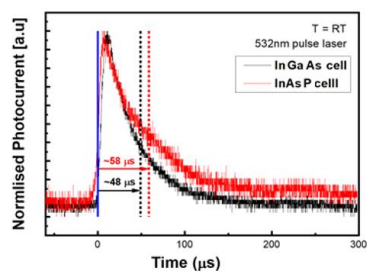


Fig. 2. The result of TRPC at room temperature

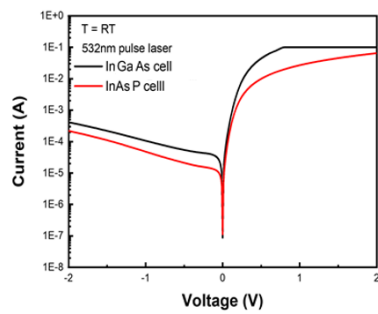


Fig. 3. The result of I-V measurement at room temperature

Eight-Band k.p Theory for GaAs/Ga_{0.75}Al_{0.25}As Superlattice

S. Bahareh Seyedein Ardebili, Jong Su Kim*

Department of Physics, Yeungnam University, Gyeongsan 38541, Republic of Korea

E-mail address: (jongsukim@ynu.ac.kr)

Abstract: This theoretical work investigates the first transition energy for GaAs/Ga_{0.75}Al_{0.25}As superlattices at room temperature and examines the effects of well width. Using Kane's 8-band k.p model with Luttinger parameters, a numerical simulation is employed based on the central difference approximation for the discretization procedure. Varying the well width between 5 and 15 nm, the study determines the optimal well width for the highest first transition energy. The results show an increase in the first transition energy with increasing well width, attributed to increased confinement of electrons and holes within the quantum well region. The findings provide insights for designing and optimizing GaAs/Ga_{0.75}Al_{0.25}As superlattices for optoelectronics and semiconductor devices, utilizing the 8-band k.p theory as a theoretical framework.

1. Introduction

Semiconductor superlattices, consisting of alternating layers of different semiconductors, have gained significant interest due to their unique electronic and optical properties, making them promising candidates for various optoelectronic applications [1]. The 8-band k.p theory provides a theoretical framework for calculating the electronic band structure and optical properties of semiconductors, including quantum wells and superlattices [2]. The first transition energy of the superlattice is an important property that affects the device's performance and can be studied using the 8-band k.p theory [2]. In this context, this study aims to investigate the effects of well width on the first transition energy of GaAs/Ga_{0.75}Al_{0.25}As superlattices using the 8-band k.p theory at room temperature. The findings of this study can offer insights into optimizing the design and performance of semiconductor superlattices for various applications.

2. Equations

The Schrödinger equation can be employed to calculate the energy levels of electrons:

$$\hat{H} = E\psi_j(\mathbf{k}, r), \quad (1)$$

where \hat{H} is the total Hamiltonian operator, and E is the corresponding energy. The SL wave function $\psi_j(\mathbf{k}, r)$ ($j = 1, 2, \dots, 8$) can be expanded as a linear combination of the basis states $u_v(r)$ and envelope function $F_j(\mathbf{k}, r)$ as follows [3]:

$$\psi_j(\mathbf{k}, r) = \sum_{v=1}^8 u_v(r)F_j(\mathbf{k}, r), \quad (2)$$

where the wave vector \mathbf{k} is defined as (k_{\parallel}, k_z) and $k_{\parallel} = k_x^2 + k_y^2$, of which k_x and k_y are the wave vector components in the plane of SL, j is the subband (basis) index, k_z is the SL wave vector along the growth direction (z-axis), $u_v(r)$ are the zone-center basis states, r is the in-plane position vector and $F_j(\mathbf{k}, r)$ is the v th component of the j th subband envelope function along the z-axis. By applying equations 1 and 2 and utilizing the finite difference discretization technique, the eigenvalues of the Schrödinger equation can be solved for every point in the structure, ultimately resulting in the attainment of the eigenvalues.

3. References

- [1] V. Čížas, L. Subačius, N. V. Alexeeva, D. Seliuta, T. Hyart, K. Köhler, ... and G. Valušis, Physical Review Letters. **128**, 236802 (2022).
- [2] R. Eppenga, M. F. H. Schuurmans, and S. Colak, Physical Review B. **36**, 1554 (1987).
- [3] M. Rygała et al., Physical Review B. **104**, 085410 (2021).

Comparison of transient photovoltage decay on recombination process for p-i-n and nBn photodetector

Taein Kang¹, Jiseong Go¹, Jaedu Ha¹, Jongsu Kim^{1*}, Jieun Kang², and Sangjun Lee²

¹Department of physics, Yeungnam university, Gyengsan 38541, Korea

²Korea Research Institute of Standard and Science, Daejeon 34113, Korea

E-mail address: (8-point type, centered, italicized)

Abstract: Transient photovoltage (TPV) decay measurements are performed with the infrared photodetectors, which have p-i-n and nBn device structures. TPV decay having a different behavior for photodetector structures is observed by employing a nanosecond pulsed laser with a 1024 nm wavelength without any background illumination. As the laser power and cell area of the p-i-n photodetector were increased, the decay time gradually decreased in relation to trap-assisted recombination, and it was observed that the steady state was maintained in the nBn structure in relation to the saturation of the minority carrier lifetime.

1. Introduction

In the heterojunction infrared (IR) photodetector device, it should be a main concern to define the proper cell size to reduce dark current, power consumption, and high-temperature operation for the ranges of atmospheric windows 1-3, 3-5, 8-12 μm . Understanding the photocarrier recombination process in such IR photodetector devices should be useful for further improvement [1]. Among these devices, the IR photodetector structure, in which the barrier is implemented, has been studied to reduce unwanted dark current components without impeding photogenerated carriers at the same time [2].

The purpose of this study is to examine the influence of carrier traps and recombination on TPV with p-i-n and nBn IR photodetectors and to understand the play role of the barrier and the absorber region in nBn IR photodetector better. Also, it can be assumed to have nearly a lack of the depletion region, so the generation-recombination (GR) to the net dark current from the absorber layer is limited. Thus, it is capable of high-temperature operation for IR detection [3].

2. Figures

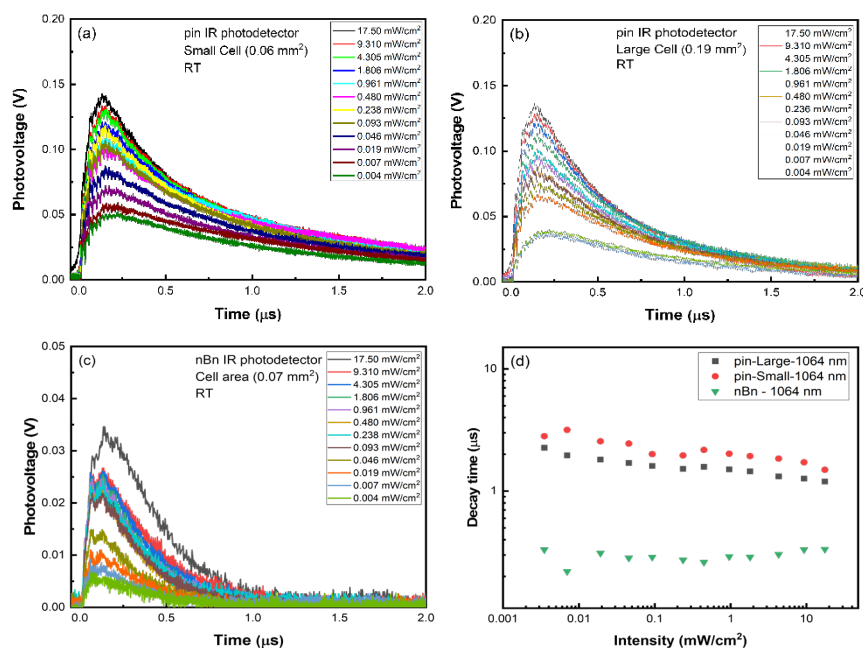


Fig. 1. Power dependent of TPV measurements on (a) small cell of p-i-n IR photodetector, (b) large cell of p-i-n IR photodetector, (c) nBn photodetector, and (d) compared photovoltage decay time with increasing intensity of the pulsed laser.

3. References

- [1] Cui, H.Y., Zeng, J.D., Tang, N.Y., and Tang, Z, Opt. Quant. Electron. **45**, 629-634 (2013).
- [2] Klipstein, P., " XBn barrier photodetectors for high sensitivity operating temperature infrared sensors", In Proceedings of SPIE, (Orlando, USA), 69402U-1-11 (2008)
- [3] Martyniuk, P., Kopytko, M., and Rogalski, A., Opto-electronics review. **22**, 127-146 (2014)

High-Performance and Lithography-Free WS₂-based Vertical Heterostructures Photovoltaic Devices

Anh Thi Nguyen, Eunseo Cho, Seoyoung Lim, Jungeun Song and Dong-Wook Kim*

**Department of Physics, Ewha Womans University, Seoul 03760, Korea*

**Email: dwkim@ewha.ac.kr*

There have been intensive research efforts to investigate intriguing physical phenomena of transition metal dichalcogenides (TMDs). TMDs have emerged as promising materials in photovoltaic-device applications due to their unique electronic and optical properties. However, TMD-based photovoltaic devices remain limited by challenges such as low-efficiency and high fabrication costs. In this work, we fabricated vertically stacked metal/semiconductor/metal heterostructures using WS₂ multilayers by a simple fabrication and studied their physical properties. The WS₂ multilayer flakes were exfoliated on template-stripped ultra-flat Ag layers, which were evaporated on SiO₂/Si wafers and then peeled off from the wafers using UV-curable epoxy. In order to investigate the transport properties of the flakes, we prepared 2-micron-sized Au top electrodes evaporated on the WS₂ flakes using a shadow mask consisting of holey carbon films. The current-voltage (*I*-*V*) characteristics of the Au/WS₂/Ag structures were obtained from current-sensing atomic force microscope measurements. Under the illumination of white LEDs, not only the *V*_{OC} and *J*_{SC} relationship, but also the polarization-dependence of the device characteristics were investigated. Optical measurements and simulations of the Au/WS₂/Ag device were also performed to understand the photocurrent characteristics. All of these results allow us to evaluate the photovoltaic performance of the Au/WS₂/Ag vertical heterostructures fabricated by the newly proposed lithography-free processes.

Studies of Exciton-Plasmon Coupling in WS₂/Au-Nanogratings

Seoyoung Lim, Anh Thi Nguyen, Eunseo Cho, Jungyoon Cho, Jungeun Song, and Dong-Wook Kim*

Department of Physics, Ewha Womans University, Seoul 03760, Korea

*Email: dwkim@ewha.ac.kr

Transition metal dichalcogenides (TMDs) have attracted a lot of attention for both device applications and basic science. TMDs have unique optical properties because of their extraordinarily high real and imaginary refractive indices. However, the light-matter interaction in TMD layers is limited by their exceedingly limited physical volume. Thus, there have been intensive research efforts to fabricate TMD/metal nanostructures. In such hybrid systems, surface plasmons can couple with exciton and give rise to enhanced light-matter interactions. In this work, multilayer WS₂ flakes were directly exfoliated on 320-nm-period Au-nanogratings (AuNGs). AuNGs were fabricated by simply evaporating Au thin films on blue-ray disc templates. Angle- and polarization-dependent reflectance spectra of AuNGs convincingly demonstrated the excitation of propagating surface plasmon polaritons (SPPs). Moreover, the SPP excitation wavelengths are close to those of exciton resonance in WS₂ layers. We prepared electrodes on top of WS/AuNG structures using shadow masks and studied their transport characteristics using current-sensing atomic force microscope (C-AFM). C-AFM measurements allowed us to study how the SPP-exciton coupling could affect the photocurrent behaviors of WS₂/AuNG structures. While carrying out the C-AFM measurements, we illuminated the samples using light sources with various incident angles and wavelengths. The flake thickness dependence further enabled us to tune the spectral responses of WS₂/AuNG structures. In this presentation, we will discuss possible optoelectronic device applications of TMD/metal hybrid nanostructures.

Investigating the Influence of Temperature-dependent Anti-Solvent Treatment and Turbidity Point on Perovskite Solar Cell Efficiency

Hyojung Kim^a, Jaegwan Sin^b, Mijoung Kim^a, Moonhoe Kim^b, Jeonghun Shin^c, Jinpyo Hong^c, JungYup Yang^{a,b,*}

^a The Institute of Basic Science, Kunsan National University, Gunsan, 54150, Republic of Korea

^b Department of Physics, Kunsan National University, Gunsan, 54150, Republic of Korea

^c Department of Physics, Hanyang University, Seoul, 04763, Republic of Korea

E-mail address: jungyup.yang@kunsan.ac.kr

Organic-inorganic halide perovskites possess exceptional optical and electrical characteristics for next-generation photovoltaic cells. The performance of perovskite solar cells is influenced by the fabrication conditions of the perovskite light absorber layer. This study determined the optimal anti-solvent treatment (AST) time for synthesizing the perovskite light absorber layer in relation to the turbidity point (TP) of the precursor solution during spin coating. The TP was found to depend on various conditions such as temperature and substrate. Anti-solvent engineering was a crucial factor in augmenting the efficiency of perovskite. It is imperative to ascertain the effects of the anti-solvent and temperature in the synthesis of perovskite within a glovebox and to meticulously control them for obtaining high-crystallinity perovskite films with uniform properties for future applications. The AST time and internal temperature of the glovebox significantly impacted the crystallinity and device performance of the perovskite. Optimal device performance of 18.9% for a methylammonium lead iodide (MAPbI₃) solar cell with n-i-p normal planar structure was achieved by applying an AST time of 9.5 s at 25 °C. This optimal AST time yielded a minimum trap density of $2.1 \times 10^{15}/\text{cm}^3$, which was related to the trap states of MAPbI₃.

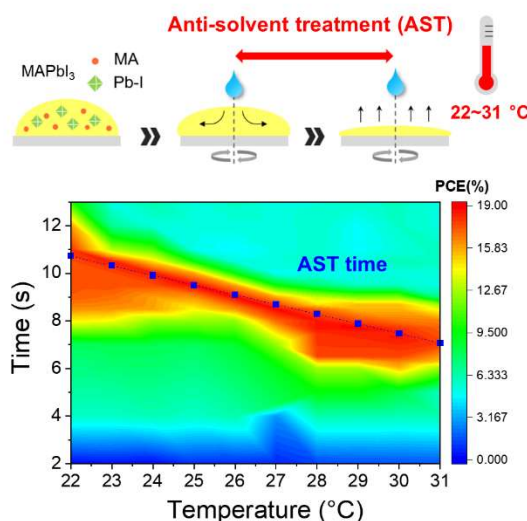


Fig. 1. Schematic of AST procedure and outcomes showing relationship between AST time, internal temperature, and device efficiency [1]

References

- [1] J. Sin, H. Kim, M. Kim, M. Kim, J. Shin, J. Hong, and J. Yang, Solar Energy Mater. Solar Cells. **250**, 112054 (2023).

Enhancing Efficiency and Stability of Triple-Cation Perovskite Solar Cells with the 1,3,7-Trimethylxanthine Additive

MiJoung Kim, Hyojung Kim, Jaegwan Sin, MoonHoe Kim, Jaeho Kim, Hana Kang, JungYup Yang*

The Institute of Basic Science, Department of Physics, Kunsan National University

E-mail address: kmj0602@kunsan.ac.kr, jungyup.yang@kunsan.ac.kr

Abstract: Perovskite polycrystalline films typically contain numerous intrinsic and interfacial defects resulting from the solution preparation process, which can significantly impact both the photovoltaic performance and the reliability of perovskite solar cells (PSCs). In this study, we investigate the use of 1,3,7-trimethylxanthine ($C_8H_{11}N_4O_2$), also known as caffeine, as an additive in the perovskite film to improve its quality. Caffeine, as a Lewis base with two carbonyl groups, interacts coordinatively with Pb^{2+} ions of the perovskite through its carbonyl ($C=O$) groups. The caffeine as an additive in the perovskite film promotes crystal growth and enhances the grain size of the perovskite thin films. This, in turn, leads to simultaneous improvement of the power conversion efficiency (PCE) and long-term stability of PSCs. Our results show that the addition of 0.75 wt% caffeine results in a maximum PCE of 21.07%, and better stability, maintaining over 85% of its initial PCE after 1000 hours under ambient air conditions.

Incorporation of UV-enhanced MXene quantum dots in photodetectors

Zarmeena Akhtar, Sophia Akhtar, Anir S. Sharbirin, Wendy B. Mato, Rebekah Esther, Jeongyong Kim*

Department of Energy Science, Sungkyunkwan University, Suwon 16419, Republic of Korea.

*E-mail address: * (j.kim@skku.edu)*

Abstract

MXenes are 2D materials which are comprised of early transition metal carbides, nitrides, or carbo-nitrides [1, 2]. Owing to their unique properties including high carrier mobility, hydrophilicity, optical transmittance, metal-like conductivity, and adjustable surface group, they are widely being applied in electrical and optical devices [3]. Photodetectors (PDs) have generated great interest and are investigated in fields such as imaging, sensing, detection, and monitoring [4]. Photodetectors based on quantum dots (QDs) offer numerous advantages, such as low cost, a tunable spectral response range, potential for multiple-exciton generation, and outstanding detective performance[5].

The incorporation of $\text{Ti}_3\text{C}_2\text{T}_x$ in CsPbBr_3 QD thin films improved the stability and photocurrent [6]. Enhanced responsivity, defectivity and external quantum efficiency were observed for the Ga_2O_3 – $\text{Ti}_3\text{C}_2\text{T}_x$ based PDs owing to the enhanced contact for photoelectron transfer [3]. A MXene-GaN-MXene based multiple quantum well photodetector showed improved responsivity and reduction in dark current as compared to the traditional Metal-Semiconductor-Metal PDs [7]. MXenes are employed in photodetectors but so far there is no report for the incorporation of MXene quantum dots (MQDs) in photodetection applications. The desirable features of 2D MXenes are inherited by MQDs [8, 9]. This study focuses on incorporation of MQDs into opto-electronic devices like photodetectors (PD).

In this study, the MQDs will be incorporated into the active layer of the PD and the basic characterization parameters determining the quality of PD performance will be evaluated by executing relevant experiments. The light-absorption ability of the active layer will be determined by responsivity and external quantum efficiency. The incorporation of MQDs in PDs can potentially enhance the photodetection performance with an increased responsivity, defectivity and external quantum efficiency and a reduction in dark current. Details will be presented.

References

- [1] S. Akhtar, S. Roy, T. T. Tran, J. Singh, A. S. Sharbirin, and J. Kim, Appl. Sci., **12**, 4154, 2022.
- [2] A. S. Sharbirin, S. Roy, T. T. Tran, S. Akhtar, J. Singh, D. L. Duong, and J. Kim, J. Mater. Chem. C, **10**, 6508–6514, 2022.
- [3] X. Zhu, Y. Wu, G. Li, K. Zhang, S. Feng, and W. Lu, ACS Appl. Nano Mater. **6**, 2048–2062, 2023.
- [4] L. Gao, Y. Zhao, X. Chang, J. Zhang, Y. Li, S. Wageh, O. A. Al-Hartomy, A. G. Al-Sehemi, H. Zhang, and H. Ågren, Materials today, **61**, 169-190, 2022.
- [5] R. Guo, M. Zhang, J. Ding, A. Liu, F. Huang and M. Sheng, J. Mater. Chem. C, **10**, 7404-7422, 2022.
- [6] H. Li, Z. Li, S. Liu, M. Li, X. Wen, J. Lee, S. Lin, Ming-Yu Li, and H. Lu, Jr. of Alloys and Compounds, 895, 162570, 2022.
- [7] L. Luo, Y. Huang, K. Cheng, A. Alhassan, M. Alqahtani, L. Tang, Z. Wang and J. Wu, Light Sci Appl, **10**, 177, 2021.
- [8] S. Akhtar, J. Singh, T. T. Tran, S. Roy, E. Lee, and J. Kim, Optical Materials, **138**, 113660, 2023
- [9] A. S. Sharbirin, S. Akhtar, and J. Y. Kim, Opto-Electronic Adv., **4**, 200077, 2021.